

Dialysis technology in Australian Aboriginal Desert Communities

A Forward-Osmosis design and qualitative analysis

Michael C. Smith
MBiomedE, B.E. (Elec)

07/02/2016

Version 20160207c
Flinders University
Faculty of Science and Engineering
School of Computer Science, Engineering and Mathematics
Medical Device Research Institute

Supervisors:
Professor Karen Reynolds, PhD
Professor Mark Shephard, PhD, OAM

Contents

1. Introduction	7
1.1. About this project	7
1.2. The desert context	8
1.2.1. The problem of relocation	8
1.2.2. Aboriginal community dialysis clinics	10
1.2.3. Dialysis water demand	11
1.2.4. Dialysate production in the desert: Kintore NT	13
1.2.5. The need for innovation	20
1.3. Forward osmosis dialysate production in the desert	20
1.3.1. Design principles	21
1.3.2. Choice of membrane	22
1.3.3. Technical focus of this project	22
1.3.4. Technology in context	23
2. Dialysate production theory	25
2.1. Introduction and background	25
2.1.1. RO and FO processes	25
2.1.2. Critical design questions	27
2.2. Theory	28
2.2.1. Design principles	28
2.2.2. Analytical model	30
2.2.3. Dialysate production	33
2.2.4. Backwashing and Recovery	34
2.3. Evaluation	35
2.3.1. System parameters	36
2.3.2. Production	38
2.3.3. Recovery	44
2.4. Pilot experiments	46
2.4.1. Parameters	46
2.4.2. Apparatus	47
2.4.3. Method	48
2.4.4. Results	49
2.5. Discussion	53
2.5.1. General comments	53

2.5.2.	Choice of parameters	54
2.5.3.	Production	56
2.5.4.	Recovery	57
2.6.	Conclusions	57
2.6.1.	Answers to initial questions	57
2.6.2.	Future work	58
3.	Dialysate production control	61
3.1.	Introduction and background	61
3.1.1.	Ideal production profile	62
3.1.2.	Single-variable controller principles	63
3.1.3.	Multi-variable and fuzzy control	64
3.2.	Materials and Methods	69
3.2.1.	Apparatus	69
3.2.2.	Osmotic backwashing	73
3.2.3.	Injection protocols	73
3.2.4.	Control protocols	74
3.2.5.	Output management protocols	76
3.2.6.	Experimental methods	78
3.3.	Results and discussion	79
3.3.1.	Experiment one: Fixed injection, PI recirculation, alternating output	79
3.3.2.	Experiment two: Two-stage injection, PI recirculation, altern- ating output	80
3.3.3.	Experiment three: Fuzzy-logic control, alternating output	81
3.3.4.	Experiment four: Fuzzy-logic control, free-flow output	82
3.3.5.	Experiment five: Fuzzy-logic control, recirculation chopping	83
3.3.6.	Experiment six: Fuzzy-logic control, free-flow output, batch output	84
3.3.7.	Paradoxical conductivity response	85
3.4.	Conclusions	88
4.	Dialysate production limitations	89
4.1.	Introduction and background	89
4.1.1.	Considerations when using an RO membrane in FO mode	89
4.2.	Materials and Methods	92
4.2.1.	Apparatus	92
4.2.2.	Dialysate production	92
4.3.	Results and discussion	94
4.3.1.	Dialysate production	94
4.3.2.	Production limits	98
4.3.3.	Practical considerations	100
4.4.	Conclusions	102

5. Osmotic backwashing: a computational model	105
5.1. Introduction and background	105
5.1.1. Osmotic backwashing	105
5.1.2. Computational modelling	107
5.2. Model development	109
5.2.1. Membrane modelling	109
5.2.2. Surface mass-flow	114
5.2.3. Model parameter estimates	116
5.2.4. Program structure	118
5.3. Materials and method	124
5.3.1. Experimental setup	124
5.3.2. Production stage	124
5.3.3. Backwashing stage	124
5.3.4. ECP and ICP model tuning	125
5.3.5. Backwashing and production analysis	125
5.4. Results and discussion	126
5.4.1. ECP and ICP estimates	126
5.4.2. Backwashing mechanism	127
5.4.3. Production optimisation	129
5.5. Conclusions	132
5.5.1. Significant findings	132
5.5.2. Summary	133
6. Design for remote Aboriginal health: a methodology	135
6.1. Introduction and background	135
6.1.1. The need for a context-sensitive design methodology	135
6.1.2. The challenges of social research in engineering design for re- remote communities	136
6.1.3. Methodology requirements	140
6.2. Methodology	141
6.2.1. Identifying the <i>user</i>	141
6.2.2. Exploring context	142
6.2.3. Encoding context	145
6.2.4. Assessing outcomes	146
6.2.5. Methodological summary	146
7. Design for remote Aboriginal health: application	149
7.1. Introduction	149
7.2. Method	149
7.2.1. Research preparation	150
7.2.2. Engineering ethnography	151
7.2.3. Data encoding and modelling	154
7.2.4. Model simulation	157

7.3.	Results and discussion	158
7.3.1.	Model analysis	159
7.3.2.	Constraints as data	167
7.3.3.	Simulation output	168
7.3.4.	Ethnographic preference frequencies	170
7.4.	Conclusions	174
7.4.1.	Significance of design variations	174
7.4.2.	Other design variations	175
7.4.3.	Limitations of the method	175
7.5.	Methodology validation	177
7.5.1.	External criteria	177
7.5.2.	Assessment summary	183
7.6.	General use of the methodology	184
8.	Conclusion	185
8.1.	Introduction	185
8.2.	Major findings	186
8.2.1.	Theoretical analysis	186
8.2.2.	Control optimisation	186
8.2.3.	Production optimisation	187
8.2.4.	Computational methods and Osmotic backwashing	187
8.2.5.	Technical summary	188
8.2.6.	Technology in context	189
8.2.7.	Comments on water consumption	190
8.3.	Future work	190
8.3.1.	Ethnographic iteration	190
8.3.2.	Membrane disinfection	191
8.3.3.	Membrane failure monitoring	191
8.3.4.	Reverse salt-leak	192
8.3.5.	Excess use of dialysate concentrate	192
8.3.6.	Use of FO membrane elements	192
8.3.7.	Large dialysis centres	193
8.3.8.	Summary	193
Appendix A.	Derivations for chapter 2	197
A.1.	General principles	197
A.2.	Non-ideal properties	198
A.3.	Approximating bulk values from local values	199
A.4.	Trans-membrane concentration difference and stability:	200
A.5.	Input priming rate and <i>overprime</i> factor	204
A.6.	Effective production time	204
A.7.	Backwashing and recovery compensation	206
A.8.	Production with non-constant flow	206

Appendix B. Notes for chapter 5	209
B.1. Well-mixed membrane cell compartments	209
B.2. Diffusion considerations	210
B.3. Matrix inversion considerations	210
B.4. Numerical methods	211
Appendix C. Symbols and parameters	213
C.1. Symbols	214
C.2. Symbols for derivations	216
C.3. Symbols for modelling	217
C.4. Model parameters	220
Appendix D. Patent document	221
Appendix E. Ethics documents	225
Appendix F. Fieldwork documents	231
Appendix G. QRM scenario and model fragments	245
References	259

Abstract

A brief analysis of the provision of dialysis services in Australian Aboriginal desert communities showed that improvements in dialysis system design may provide greater opportunity for return-to-country for Aboriginal patients. The need for a robust, desert-suitable dialysis system with greater water and energy efficiency than existing reverse-osmosis (RO) based systems was identified. Forward-osmosis (FO) based innovations were considered for this application due to their inherent advantages in water and energy efficiency. The use of standard, spiral-wound RO membrane elements for FO was also explored, due to their proven suitability to desert conditions. The need to evaluate any design changes in terms of their impacts on remote Aboriginal dialysis services and their communities in a culturally safe way was also identified.

A theoretical analysis of a suitable FO membrane process was completed by developing a one-dimensional analytical model. The process was based on the use of dialysate concentrate as a draw-solution and groundwater as a feed-solution. Approximations were made for external and internal membrane polarisation. Theoretical predictions were used to design and experimentally validate various strategies for controlling the output fluid concentration and flow-rate to meet the requirements for a typical medical treatment. Batch-mode production was found to be the most simple and efficient method in terms of total dialysate volume production.

Due to the use of RO elements in the design, the need for the backwashing of accumulated salt from the feed-side of the membrane was identified. This was accomplished by an extended application of osmotic backwashing, which was optimised by computational modelling and experimental analysis. It was found that the backwashing process was relatively slow, yet was a major determinant of the apparent dialysate output flow-rate of the process.

Experiments and analysis showed that there was little to be gained in terms of water efficiency by the use of this FO-based design when compared with an RO-based equivalent. Instead, a significant gain in energy efficiency was found for the FO-based design, but at the cost of an increase in system size due to the need for extra membrane area.

A culturally-safe methodology was developed for the evaluation of these design changes in the context of Aboriginal desert communities. Increases in system energy efficiency and size were passed to a qualitative reasoning and modelling (QRM) engine, the model for which was developed from a brief and purposive ethnography of the remote context. It was found that the advantages of increased energy efficiency were likely to be small compared with the disadvantages associated with any loss of working space due to increased dialysis system size.

Declaration

I certify that this thesis does not incorporate without acknowledgement any material previously submitted for a degree or diploma in any university; and that to the best of my knowledge and belief it does not contain any material previously published or written by another person except where due reference is made in the text.

Michael C. Smith

Acknowledgements

Thanks to: Professor Karen Reynolds, who has provided steadfast support and supervision over the last four years; Professor Mark Shephard for wisdom and support for the qualitative part; Dr Mark McEwen, Nathan Little and FBE Pty Ltd for funding and supporting the project from its very inception; Sarah Brown and the non-profit Aboriginal corporation, *Western Desert Nganampa Walytja Palyantjaku Tjutaku* (WDN-WPT) Aboriginal Corporation for in-kind support and for helping make things happen on the desert side; Hamid Kooshanfar for spending a year on the instrumentation and control system for the prototype; Karl, Brian and all at Flinders Medical Centre's biomedical engineering department for putting up with the prototypes in the wet-room; Dr Olivia Lockwood and Dr Mark McEwen at Flinders Medical Centre's biomedical engineering research group for supporting the development of the project with tools, parts and test equipment; Associate Professor Murk Bottema for help with numerical methods; The remote communities of the Western Desert region; Dr Robert Nordon of UNSW who planted the seed for the idea of this project in 2002; The Membrane Society of Australasia for their perspective and of course Xavia, Lucien and Matthea, my daily support, my home, my light and my gift.

Funding disclosure

This project was partly funded by FBE Pty Ltd and supported by the Medical Device Research Institute at Flinders University. Its author was the recipient of an Australian Postgraduate Award scholarship. Thanks also to the biomedical engineering department at Flinders Medical Centre, South Australia, who provided research and laboratory facilities. The project also received in-kind support from the non-profit Aboriginal corporation, *Western Desert Nganampa Walytja Palyantjaku Tjutaku* (WDNWPT) Aboriginal Corporation.

Dedication

To those who have lived and died at Topsy Smith's Hostel.

Notes

- Fieldwork for this project was carried out with ethics approval from the Central Australian Human Research Ethics Committee (CAHREC: 13-13) and Flinders University's Social and Behavioural Research Ethics Committee (SBREC: 5789) with input from Yunggoendi Mande First Nations Centre (see appendix E).
- The prototype concept for output conductivity control by recirculation of draw-side fluid was protected by an Australian Provisional patent, #2013903865 (See appendix D).
- This thesis document was typeset using MiKTeX 2.9, which is an implementation of L^AT_EX2e – a program that formats documents, layouts and text to optimise readability. Its algorithms occasionally place images and tables on separate pages to avoid inconvenient breaks in the flow of text.
- The digital version of this document includes hyperlinks at cross-references and citations. There is also a video of dialysate production and backwashing simulation embedded in figure 5.4.4. The *Garp3* model fragments in appendix G are included as embedded post-script (.eps) figures and are zoom-able in digital readers¹.

Je n'ai fait celle-ci plus longue que parce que je n'ai pas eu le loisir de la faire plus courte.

– Blaise Pascal, 1657

¹*This is version 20160207*

Preface

This is a biomedical engineering thesis. It is concerned not only with the creative application of scientific principles to specific medical and healthcare technology problems, but with the impact of design changes on the health and wellbeing of the communities who use the technology. In particular, this thesis is concerned with the efficient production of medical dialysate fluid, with the hope that it may facilitate better access to dialysis treatment for Australian Aboriginal people in remote desert regions, where there is a growing rate of kidney failure and associated need for treatment (see chapter 1).

This thesis explores a novel method of dialysate production that exploits the principles of forward-osmosis (FO) but uses inexpensive and robust reverse-osmosis (RO) membrane elements (chapter 2). In collaboration with others, hundreds of hours of effort were put into the development of a prototype system capable of controlling the quality of dialysate fluid to within medical tolerances (chapter 3), only to discover that the proposed method of control was problematic, and that a simple batch-control method produced far better control and yield (chapter 4).

The use of RO membranes for FO is considered to be unconventional due to various reasons, including the geometry of their construction - a problem that may be overcome by the use of osmotic backwashing – an approach that has been thoroughly explored by both experimentation and numerical modelling (chapter 5).

Having shown the technical limitations of the design, the potential impact of its implementation was evaluated through an ethnographic analysis of the context for which it was designed, so as to test its suitability and limit the risk of cultural injury to the Aboriginal communities and patients for whom the design improvements were originally intended (chapters 6 and 7). The general relevance and impact of improvements in the context of remote desert Aboriginal healthcare, and potential directions for future development are summarised in chapter 8.

In general, the project has been a success, both in proving its main technical concept and in examining its relevance in-context. It would have been more rewarding in some ways if it had generated a major breakthrough in the field, or caused a major impact on remote water and/or energy consumption or healthcare practices. Instead, the project's achievements have been modest: the technology may yet have some application in dialysis treatment in low-energy applications or a similar field. The ethnographic methodology developed to explore the context was, in itself, a major undertaking and may be used for design in other remote and/or culturally sensitive contexts. Its application here was useful in showing the limitations on the relevance of the design improvements - a process that helped to keep the author humble and grounded.

1. Introduction

1.1. About this project

Dialysis¹ is a medical treatment used in place of human kidney function in patients with varying degrees of kidney disease or failure. Its basic operation involves the exchange of fluid and solutes across a semi-permeable membrane that separates a patient's blood from a prepared fluid called *dialysate* (Levy et al., 2009). This fluid is prepared within a dialysis machine by injecting dialysate concentrate solutions into a stream of clean water from a separate reverse-osmosis (RO) machine². Treatments last about five hours and must be undertaken three times per week (Farrington and Greenwood, 2011) – a protocol that requires patients either to have machinery installed in their home or to relocate to housing near to dialysis centres, most of which are located in cities or major centres.

For relocation to be avoided, dialysis treatment must be made available where people normally live. For Aboriginal dialysis patients, whose homelands are close to remote communities, they may have the opportunity of returning-to-country without missing their regular treatments. There are an ever-growing number of small, remote-community dialysis clinics, each with two to four dialysis chairs³. With the recent advent of mobile dialysis trucks, the capacity of these remote dialysis clinics can be temporarily expanded during major community events.

Mobile dialysis treatment places additional technical demands on equipment: it needs to be energy and water efficient, lightweight, compact, robust and easy to operate and maintain; it needs to be able to handle water extracted from remote bores, which may be hot, hard, chlorinated or brackish; it must be able to operate on intermittent and low-quality power from diesel generators.

¹The term “Dialysis” is used throughout as short-hand for a set of medical treatments, of which *Hae-modialysis* is the most typical example. Here, this discussion is largely concerned with dialysis treatment for chronic kidney failure. Patients undergoing dialysis in this context will typically receive treatment several times a week on an ongoing basis.

²Typical treatment methods are based on those use by Fresenius 4008 and 5008 series dialysis machines and associated technology, accessories and treatment functions. At the time of writing, the Fresenius corporation was responsible for the provision of dialysis technology throughout Australia's Northern Territory, including most of the Western Desert region and its communities.

³Dialysis treatment clinic capacities are measured in “chairs” - each of which is attached to one dialysis machine. A chair can usually treat two patients in a 12-hour shift, provided that sufficient nursing capacity is available.

This project has focused on a specific technical innovation: the efficient production of dialysate from groundwater using forward-osmosis (FO). This is a low-energy alternative to the existing RO process used to treat water for remote dialysis. By re-configuring existing RO membrane elements for this FO application, the proven robust suitability to desert conditions of such elements may be exploited.

Unlike other FO applications, dialysate production naturally lends itself to an FO modality, as pre-packaged dialysate concentrate makes a convenient draw-solution, which can be used directly for treatment without the need for recovery that is typical of other FO technologies. Instead, here the design focus is on the challenge of controlling the dilution of the dialysate output, and the requirement for backwashing of accumulated salt from the closed feed-side membrane envelopes.

When it comes to designing equipment for the desert, variables such as water and energy consumption may be significant, as may the ease of maintenance, the level of modularity, the system's reliability and overall cost. Each of these has an impact on the operation of a dialysis service, and in turn on the perspectives of patients, nurses, service providers community members and others.

To examine the impact of these and other inter-related and competing priorities, an ethnographic design methodology has been developed and implemented, through which the impact of design variations can be traced and visualised through their effects on other variables, and evaluated against the competing priorities of various stakeholders. This has helped not only to keep the project in perspective, but also to ensure that any innovations minimise any negative impact while designing in this culturally sensitive context.

1.2. The desert context

This section begins by describing the background to this design project, including the hazards of patient relocation, the challenges of providing dialysis locally in the desert context and its associated water and energy demands. It includes an examination of the technical detail of the current method of dialysate production in desert communities, using the an established desert dialysis clinic as a case-study. This is followed by a brief description of the FO innovation that is the major focus of this project, and an introduction to the ethnographic methodology that has been used to explore the desert context and evaluate the chosen design trajectory.

1.2.1. The problem of relocation

Compulsory relocation and its subsequent difficulties are one consequence of renal failure for Aboriginal people in Central Australia. Many patients'

current living conditions, including their diets, were contributing not to health improvements but to further deterioration; yet these patients had been uprooted from their homes for the sole purpose of improving their health.

(Devitt and McMasters, 1998, pg.67)

For Aboriginal Australians, deprivation from native lands can cause grief, and relocation to major centres for dialysis treatment has a history of being both stressful and counterproductive (Devitt and McMasters, 1998). Elsewhere, it has been established that the health of rural dwellers is often directly affected by location and access to healthcare centres (Baum et al., 2008). There are several reasons why relocation is particularly problematic: firstly, to live in an Australian regional centre or city is to live very much in a white⁴ person's world, with its documents, police, literacy, money, alcohol and other realities of daily life that may carry different significance in remote Aboriginal communities⁵. Secondly, conflict may arise between cultural groups, family members or individuals who for one reason or another should not be sharing a space, as commonly occurs in urban dialysis centres and their associated accommodation. Thirdly, with most communities being *dry*⁶, the sudden availability of alcohol can be a temptation for patients, whose kidneys can't process the extra fluid, and for their family members on whose support they may depend. A common anecdote describes dialysis patients being sent to Alice Springs for treatment, together with a few disinterested family members who soon get bored and disappear into the local community, returning drunk to make trouble at the hostels where patients are staying (for similar examples, see Devitt and McMasters, 1998, chp 3). Fourthly, accommodation is expensive in major centres and often needs to be obtained temporarily and urgently for patients and their supporting family members. There are plenty of anecdotes describing patients being evacuated to Alice Springs and attending dialysis sessions every other day, while sleeping in the dry bed of the Todd River at night. Finally, patients get homesick; they miss *bush tucker*; they miss their family members and their land. Relocation for dialysis treatment is depressing, lonely, expensive and fraught with trouble and temptation, none of which are healthy for patients. Where possible, it is better for chronic dialysis patients to return to their home lands or country for treatment.

To facilitate this need for return-to-country, dialysis clinics have been built in remote communities, with patients being managed centrally (usually out of Alice Springs) and rotated through their remote communities according to their general health and

⁴Terms like "white" are used throughout to refer to those cultural characteristics described in *whiteness theory* (Thompson, 2004) which includes a set of behaviours and signs of status that are independent of skin-colour or ethnic background. See Kowal (2006) for a thorough description of whiteness in Australian Aboriginal interactions with white culture.

⁵The term "community" is used throughout this work to refer to Australian Aboriginal-controlled communities which typically have a population of less than 1000 persons and are remote from major cities.

⁶The term "dry" means the possession and consumption of alcohol is banned.

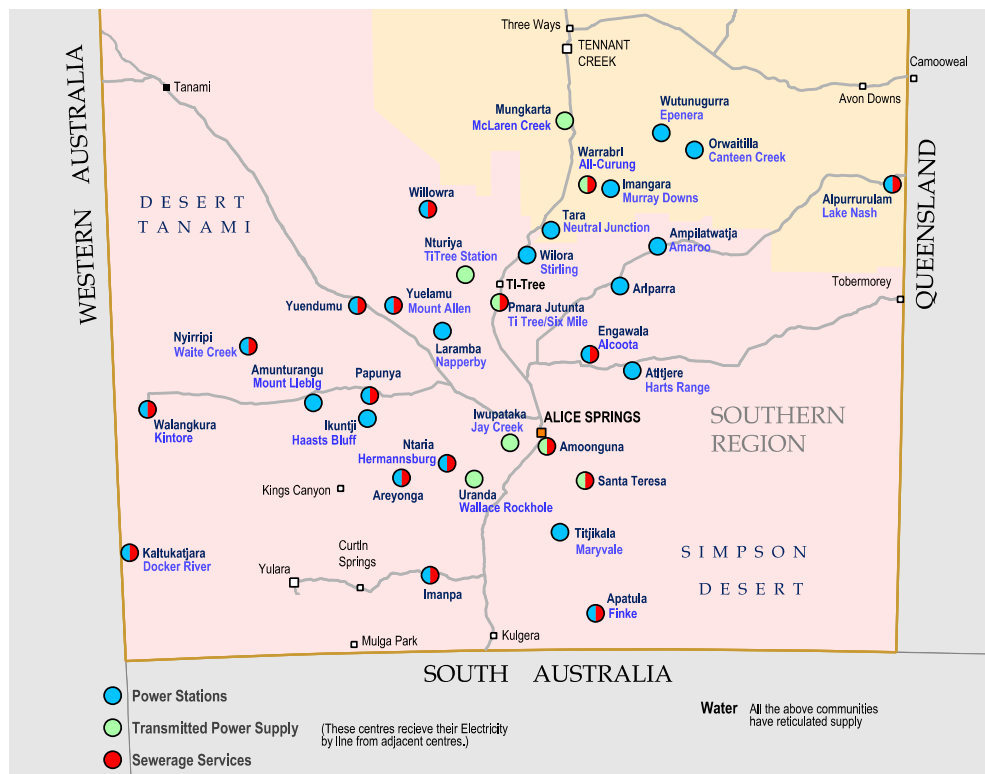


Figure 1.2.1.: Indigenous communities of the Southern region of the Northern Territory. (Image courtesy of Power and Water Corporation (PowerWater, 2009b))

wellbeing, the opinion of their nephrologists and the availability of remote treatment spaces. When a mobile dialysis clinic (or “dialysis truck”) is available, extra patients can have temporary access to treatment in remote communities, with the extra treatment spaces being provided on-board the truck.

1.2.2. Aboriginal community dialysis clinics

The Kintore dialysis clinic was established in 2004 and was the first remote renal dialysis clinic in Central Australia (Brown, 2011). It is located in the Gibson Desert, 500 km west of Alice Springs, in Australia’s Northern Territory (see map in figure 1.2.1). Access for all vehicles, including dialysis trucks and those that transport fuel, food and equipment is via an unsealed road, which is impassable when wet and somewhat corrugated when dry.

A dialysis unit like Kintore’s with two chairs and one nurse can support up to two patients each day (see image in figure 1.2.2). With patients receiving treatment three times per week on alternating days, the unit can cater for up to four patients. When two



Figure 1.2.2.: Two dialysis chairs at Kintore (July, 2011)

renal nurses are available, each chair can be operated for up to two treatments each day (Monday to Saturday), so that up to eight patients can be provided for, at a maximum of 24 treatments per week. In practice, this level of service is rarely desired or available due to the challenges of managing and transporting patients and the difficulties associated with staffing the clinic for two shifts-worth of nurses. Nevertheless, when considering any innovation in dialysis equipment, it is worth assessing its impact on the maximum demand for water and energy consumption in any remote community where it is likely to be used.

1.2.3. Dialysis water demand

Providing dialysis treatments at a maximum of rate of 24 per week corresponds to an extra demand on a town's water supply about 7.2 kL per week⁷. Compared with Kintore's average weekly water consumption of 1212 kL (PowerWater, 2009c), this represents an additional demand of 0.59 % of the town's total consumption: a relatively

⁷The demand for town-water for each dialysis treatment should not be confused with the demand for dialysate fluid. The amount of treated dialysate fluid available from each kL of supplied town water depends on the recovery rate, r , of the desalination process. For this analysis, a rate of $r = 50\%$ was used (See table 1.2.2).

Community name	Population	Total (kL/week)	Dialysis %
Haast's Bluff	165	519	1.39 %
Hermannsburg	160	3076	0.23 %
Kintore	350	1212	0.59 %
Mt Liebig	252	942	0.76 %
Nyirrippi	320	1096	0.66 %
Papunya	342	2135	0.34 %

Table 1.2.1.: Dialysis burden on community bulk water consumption.

(Data from (PowerWater, 2009c))

small environmental impact. Other Aboriginal desert communities have similar levels of water consumption, and would feel the impact of a dialysis unit to varying degrees (see table 1.2.1). The worst hit in the Western Desert region would be the community at Haast's Bluff, which would feel the impact of a 1.39 % increase in water demand during peak dialysis times. In general, it would appear that the relative demand of dialysis on community water supplies is insignificant compared with other community needs. This does not mean that water conservation has *no* value in these places: water is still seen by many as relatively scarce, and any increase or reduction in demand due to technical innovation may affect how such technology is received and used (see section 1.3.4).

For most of the year, surface water is scarce in Australian deserts (see figure 1.2.3). Groundwater is available all year, although domestic consumption is relatively high (Brown, 2001). At Kintore, three bores produce an annual discharge of 74 ML (about 1400 kL/week). A sustainable yield from the aquifer at Kintore was estimated to be 235 kL/day (about 1650 kL/week) - a limit that seems to have been frequently exceeded (Brown, 2001; PowerWater, 2009c). For other communities in the Western Desert region, it seems likely that most of their extracted water is *old* water, perhaps up to 80,000 years old, extracted at a rate much higher than it can be recharged (Cresswell et al., 1999). The uses of water in remote communities are highly varied and may include irrigation of parks, gardens, ovals, use in community activities and businesses as well as domestic use (PowerWater, 2009c). It has been suggested that water is frequently wasted in remote communities (Henderson and Abrahams, 2010).

The value and perception of water depends on who uses it: for community members, its meaning is tied up with local history and culture (Pearce et al., 2010), while researchers see it as scarce, salty and in need of a lot of energy to purify (Brown, 2001). Australians in general think of it as expensive and its purification as energy intensive (Dolnicar and Schäfer, 2009), but when these priorities are competing, the need for water usually trumps the need to conserve energy - a perspective that is echoed wherever water is desalinated around the world (Dawoud, 2005).

While the environmental impact of water conservation in dialysis treatment is relatively



Figure 1.2.3.: Kintore's main street after rain (July 2011)

small (as shown above in table 1.2.1), the *value* of any water conservation effort (or lack thereof) may be much more significant. The impact of any technical innovation in dialysis on this and other competing values is of major concern, and is handled in this project by the ethnographic design methodology described in chapter 6. A case study in remote Aboriginal community dialysate generation is presented here to facilitate understanding of the *technical* context of any innovation.

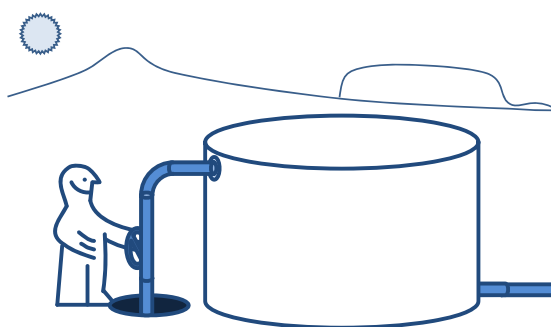
1.2.4. Dialysate production in the desert: Kintore NT

Dialysis equipment is generally designed for use in urban, surface-water-fed, air-conditioned medical centres. In desert installations, dialysis water pre-treatment systems must be able to handle groundwater that may be hot, brackish, and/or heavily chlorinated. For dialysis treatment, the water must be highly purified, as small amounts of impurities can be dangerous to patients (Pislor et al., 2011). Water treatment for dialysis in Kintore proceeds through several stages, beginning with extraction of water from the aquifer and ending with the delivery of a high-purity RO stream to each dialysis machine.

1.2.4.1. Groundwater quality

Kintore's water quality is typical of that in the Western Desert region. Its typical Total Dissolved Solids (TDS) measurements of around 851 mg/L are above the limit specified in Australia's safe drinking water guidelines (PowerWater, 2009a)⁸. Its calcium-carbonate levels are also dangerously high at 472 mg/L, which is more than twice the acceptable limit (ibid.). Like many remote communities, this water is the only available town-supply, is generally unpalatable and has a tendency to form obnoxious calcium-carbonate crystals on anything it touches, including household taps, washing machines and evaporative air-conditioners. The town-water's overall salinity and tendency to form calcium-scale are the major considerations in the performance of any desalination process for the desert context.

1.2.4.2. Extraction, storage and pressure



Water recharges into the South Arunta aquifer system and fills three bores at Kintore. Pumps in each bore alternate in raising water to a 250 kL tank on a hill, 24 metres above the town. The tank stores water under-capacity at 187 kL at a level set by a float-switch. From the tank, water is piped down the hill, through a UV treatment system and then delivered to the town.

Town water is delivered to the dialysis clinic⁹, where it is stored in a 9.0 kL tank, with its level maintained at its maximum capacity by a float-valve. A tank of this size was selected in order that the centre would have at least a week's supply close to hand (Brown, 2001).

The water pressure developed by the tank's height is relatively low, at around 85 kPa, and must be raised above the minimum 200 kPa required to operate dialysis machines.

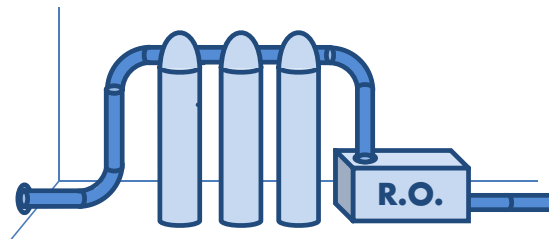
⁸This reference (PowerWater, 2009a) contains details of groundwater supplies for all remote communities within Australia's Northern Territory.

⁹The dialysis clinic is well-known and affectionately referred to as the "Purple House" and is painted accordingly.

1.2 The desert context

A *Grundfos* pump with an attached accumulator and pressure vessel cycles periodically to maintain the building supply pressure at 600 to 700 kPa. The water is then delivered to a refrigerating “chiller-package”, which can provide cooling for this water during the warmer seasons. As of July, 2011, the chiller was permanently shunted out of the water supply system and left unused.

1.2.4.3. Pre-treatment



Once inside the building, the water passes through an in-line filter, which has been known to become clogged with calcium carbonate, or *scale*. Although multimedia or sand/gravel filtering is common in dialysis pre-treatment systems (Eldridge, 2006), this process is absent at Kintore, due to the low turbidity of the bore water. The water passes directly into an activated-charcoal tank which serves to remove any free chlorine, chloramines and any organic matter.

After carbon treatment, the water is softened to remove calcium and magnesium ions. The softening resin is recharged periodically from a nearby store of saturated (NaCl) “brine”. The process of recharging is usually automated and scheduled to occur late at night, and is not usually done while dialysis treatment is in progress.

After softening, the water passes through a pair of cartridge filters with pore-sizes of five-microns and one-micron each. These remove any particles of resin or carbon that may have escaped from their tanks. By this stage, the water should be very clean: free of particles, chlorine, chloramines, organic matter and instead contain only large quantities of dissolved Na^+ and Cl^- ions. This stream must be desalinated before it can be used for dialysis (Belkacem et al., 2007).

1.2.4.4. RO desalination

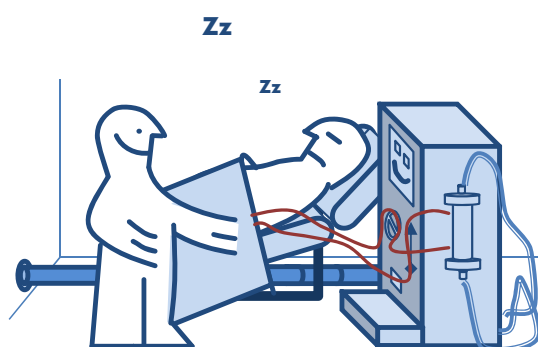
RO is a common method of desalinating pre-treated groundwater for various applications both in Australia (Werner and Schafer, 2007) and overseas (Dawoud, 2005). The process typically involves applying a pressurised feedwater stream, containing dissolved salts, to one side of a semi-permeable membrane. The membrane rejects most

of the dissolved solute molecules, allowing water to pass through to form a permeate stream. The osmotic pressure-difference between the feedwater and permeate streams must be overcome by hydrostatic pressure applied to the feedwater stream, in order for any amount of permeate to flow. A flow-pump is typically used to pressurise the feedwater, and it is this pump that consumes most of the operating energy of an RO process.

The centre at Kintore operates using a single, dedicated Fresenius™ *AquaUNO*™ RO unit for each dialysis machine. This RO unit works by recirculating excess permeate to dilute the incoming feedwater, resulting in a recovery rate of about 50 %. It has a maximum specified permeate output of 833 ml/min, which may only be achieved in desert clinics when the unit's RO membrane is at its newest. This has been a source of frustration for the local nursing staff, as a desired demand setting on dialysate machines is for dialysate flow at 800 ml/min - a flow-rate that is close to the RO unit's operating limit. To cope with this limitation, treatment and cleaning-cycle flow-rate settings are typically set at a lower rate of 500 ml/min. At 50 % recovery, this corresponds to a demand for feedwater at approximately 1.0 L/min: equivalent to about 300 L of feedwater that must be extracted and processed for each five-hour patient treatment.

Typical RO membranes in-use in the Australian desert context are typically thin-film-composite, polyamide, brackish-water spiral-wound elements sized according to their equipment. A major treatment unit in Alice Springs has an array of 4.0× 40 inch RO elements; the Fresenius™ *AquaUNO*™ RO units that are typically attached to remote dialysis equipment use 4.6× 11 inch compact elements. Similar elements were evaluated in the theoretical analysis in chapter 2 (see table 2.3.1).

1.2.4.5. Dialysis treatment



The working principle of dialysis involves a controlled interaction between a patient's blood and dialysate fluid, where fluids and solutes are allowed to pass between the blood and dialysate compartments. On a Fresenius dialysis machine, this is done by

managing separate blood and dialysate fluid circuits, allowing them to meet only in a *dialyser* module – a single-use, membrane separation device containing a large surface area spread over the lumens of hundreds of sterile hollow-fibres.

Access to a patient's blood is typically achieved by maintaining sterile connections to a surgically-created *arterio-venous* fistula within a patient's arm. These are connected to the tubing of a single-use blood circuit, which includes a machine-driven blood-pump segment, a heparin injection point and dialyser connections.

The details of medical dialysis treatment are beyond the scope of this thesis. However, the basic function of the dialyser includes allowing the diffusion of desirable solute molecules from the dialysate fluid into the blood, and diffusion of waste-products from the blood into the dialysate stream, the outgoing branch of which is directed into a waste stream and discarded.

Dialysate fluid is typically generated within a dialysis machine by the injection of dialysate concentrate (*Part A*) and a buffering agent (*Part B*) into a heated, degassed RO permeate stream (Fresenius, 2007). The dilution rate is such that 1.0 part of *Part A* is normally combined with 1.225 parts of *Part B* and 32.775 parts of RO water (Fresenius, 2014). Over the course of each treatment, about 150 L of dialysate fluid is generated within a dialysis machine, which is delivered by a flow-pump at a prescribed rate to the dialyser module.

1.2.4.6. Production costs

To evaluate any technical innovation in dialysis water or energy efficiency in terms of its economic benefit, it is worth briefly examining the operational costs of water treatment for dialysis. By examining the specifications for the installed dialysis equipment, the cost in terms of both consumed energy can be estimated at less than \$1.00 per treatment (see tables 1.2.3 and 1.2.2). By comparison, the operational cost of a two-chair remote dialysis clinic is about \$1,100 per treatment¹⁰ (fieldnotes, 16/05/2013). This is not to say that innovation in water or energy efficiency would not result in any significant benefit: dependency on energy consumption becomes particularly significant in mobile dialysis trucks, where patients, nurses and equipment must function in a relatively confined space, and where power is delivered by a noisy under-floor diesel generator.

1.2.4.7. Mobile dialysis treatment

Australia's Northern Territory (NT) and state of South Australia (SA) have recently moved towards providing mobile dialysis trucks, that carry water treatment and dialysis equipment to communities in order to provide dialysis for patients on short,

¹⁰Compare this with the cost of in-hospital dialysis at approx. \$500 per treatment, or in-home dialysis at approx. \$300 per treatment (Fortnum et al., 2012).

Typical permeate design requirement per machine	500 ml/min
Typical recovery rate (r) for R.O. unit	$r = 0.50$
Feedwater requirement per machine	1.0 L/min
Typical feedwater salinity (TDS) (PowerWater, 2009a)	851 mg/L
Hourly feedwater requirement	60 L/hr
Typical treatment time	5 hours
Total water consumption per treatment	5 hr \times 60 L/hr = 0.3 kL per treatment
Retail price of water (PowerWater, 2011)	\$1.30 per kL
Water cost per patient treatment	= \$0.39/treatment

Table 1.2.2.: Basic dialysis water consumption data (Data derived from Eldridge, 2006)

No. of dialysis chairs at Kintore Clinic demand pump	Two chairs, one machine each 800 W average = 400 W per machine
R.O. unit power consumption	+ 400 W per machine
Water treatment power total	= 800 W per machine
Typical patient treatment time	5 hrs
Energy per patient treatment	5hrs \times 800 W = 4.0 kWh
Retail price of energy (Jacana, 2014)	\$0.30 per kWh
Energy cost per patient treatment	= \$0.80/treatment

Table 1.2.3.: Basic dialysis energy consumption data



Figure 1.2.4.: The Purple Truck mobile dialysis unit, parked at a remote community (May, 2013)

return-to-country trips. One truck is operated by the non-profit organisation, non-profit Aboriginal corporation, *Western Desert Nganampa Walytja Palyantjaku Tjutaku* (WD-NWPT), and is instantly recognisable by its purple cab and adornment with paintings by artists from the Western Desert region (see image in figure 1.2.4). The affectionately named, “Purple Truck,” visits Western Desert communities such as Kintore at times of peak demand, such as during major community events.

The Purple Truck takes its electricity from an on-board diesel generator which has a maximum electrical capacity of 8.8 kW. The peak operating demand of the mobile service approaches 8 kW. The use of diesel fuel for conversion to electricity is a relatively expensive way to power a medical service, costing about \$1.00 per kWh, compared with \$0.20 per kWh if the truck is able to be connected to the town supply. Nevertheless, the economic cost of generator power per treatment is still relatively small when compared with the operating costs of a mobile dialysis unit. However, the *electrical* burden of water treatment, at approximately 0.8 kW, is much more significant at about 10 % of the typical generator load.

1.2.5. The need for innovation

From this brief analysis of the desert dialysis context, there is an identifiable need for an inexpensive, robust, desert-suitable dialysis system that is more water and energy efficient than the existing RO-based dialysate production process. The need for efficiency is neither economic nor environmental: the need to conserve water is driven by the way water is *valued* by various stakeholders, while the need to conserve energy is driven by the *practical* limitations of mobile treatment. There are many other potential design improvements that may be made, such as improving the existing system's compactness, modularity, ease of maintenance, weight, tolerance of hard water, and other parameters. It is worth noting that innovation anywhere in the system is likely to affect *all* of these variables to some degree, and these, in turn, are likely to have impacts on other equipment, people and operations within dialysis services and the communities they serve.

The most important need of any dialysis innovation is for the increased facilitation of the return-to-country of Aboriginal patients. As discussed in section 1.2.1, the opportunity to return-to-country is valued very highly by patients, their families and their communities. It is not immediately obvious whether any specific technical innovation will result in increased rates of return-to-country: the causal relations between technical innovation and healthcare service availability must be separately mapped out and evaluated. However, without such a systematic assessment of the context, there is the risk that the benefits of any innovation will be lost, or may result in negative outcomes for the people for whom the benefits are intended.

1.3. Forward osmosis dialysate production in the desert

A specific technical innovation was chosen: that of FO-based dialysate production using standard RO membrane elements. This was chosen because of the convenience of using dialysate concentrate as a draw-solution, combined with the potential of exploiting the reported energy and water efficiency of benefits of FO processes (see Zhao et al., 2012; Cath et al., 2006) while keeping the proven, desert-suitability of inexpensive, off-the-shelf RO membrane elements¹¹. At the same time, an ethnographic methodology was developed specifically to explore and document the real-life context

¹¹Details and literature describing the state of membrane technology relevant to this application can be found in section 2.1.1. Literature reviews were separated for each major section to improve clarity and readability due to the multidisciplinary nature of this work. Literature for fuzzy-logic controllers is reviewed in section 3.1.3; literature for osmotic backwashing and computational modelling is discussed in 5.1; each aspect of the proposed design-for-context methodology is justified through literature in chapter 6.

in which the existing RO-based dialysis technology is used. After establishing the theoretical feasibility and practical limitations of various technical prototypes, the effects of the most-likely design variations were then able to be evaluated against the priorities of the various stakeholders identified by the ethnographic analysis.

1.3.1. Design principles

Producing dialysate by using energy to separate salt from clean water via an RO system, then immediately injecting dialysate concentrate salts into the clean-water stream seems wasteful. The energy spent on RO desalination of water for dialysis could, in principle, be reduced by using the dialysate concentrate as a draw-solution as part of an FO process. There are several reasons why this is an attractive application for FO technology: firstly, unlike many other FO applications (see examples in Zhao et al., 2012), there would be no need to recover or re-use the draw solution: if the dilution rate could be appropriately controlled, the diluted draw solution would instead become the finished dialysate product. Secondly, the issue of reverse salt-leak would become a minor adjustment for the dialysate product, while the concentrated feed-side solution could simply be discarded, similar to that of the brine of existing RO systems. Thirdly, the concentration of dialysate concentrate solution is approximately 500 times that of a typical desert groundwater source. This concentrated solution is normally diluted by an RO stream so as to leave the dialysate product at approximately 20 times the concentration of the groundwater source. These high concentration differences should allow a suitably designed FO process to produce dialysate at a high rate, preferably at a rate comparable to that demanded by medical treatment, without needing an enormous amount of membrane surface area. While the specific use of FO for dialysate production has been proposed by others (Talaat, 2009; Talaat et al., 2010), their focus is on the limitations of using spent dialysate rather than desert groundwater as a feed-solution.

There is a significant safety issue to be concerned with here: the usual RO process produces a clean permeate stream from a single-membrane stage. The quality of the permeate stream is monitored by continuous conductivity measurement (typically $< 30 \mu\text{S}/\text{cm}$) is monitored in order to evaluate the effectiveness of the membrane's rejection of ions. When using a draw-solution opposite the feedwater in an FO process, there is no chance to monitor the salt-flux through the membrane, as any draw-side conductivity measurements will be thousands of times greater than any variation due to trace ions leaking through the membrane. Since small quantities of certain ions can be dangerous to patients (Arias et al., 2011; Pislors et al., 2011), an alternative system of evaluating the membrane's working integrity must be implemented. The design of such a monitoring system was beyond the scope of this project.

1.3.2. Choice of membrane

As FO has yet to become mainstream technology, FO membrane packages are still relatively expensive and exclusive (see, for example, Porifera, 2014; HTI, 2014). By comparison, RO elements are inexpensive, abundant and more compact than their FO equivalents (Lee et al., 2011; Ettiari et al., 2011). Furthermore, a 4040-size¹² RO element may have twice the active membrane area compared with an FO package of the same size (Kim and Park, 2011). RO elements are also relatively robust, being built to withstand high pressures on their active membrane surfaces. They are currently in widespread use in dialysate production in the relatively harsh environments of remote desert communities, and as such, are available through established purchasing and distribution channels. They are also well-established in their use in medical-grade applications such as in the preparation of dialysate fluid from groundwater sources. In this project, an FO prototype using an RO membrane element was developed and evaluated in order to take advantage of these properties.

1.3.3. Technical focus of this project

The FO production of dialysate using RO membrane elements presents two fundamental challenges. The first is the need to produce dialysate at a flow-rate sufficient for medical treatment, while maintaining its concentration at a prescribed value. The second is the need to backwash the closed feed-side membrane envelopes that are typical of spiral-wound RO element packages. These two challenges demand a cyclic production modality, where controlled dialysate output is produced for a period of time, followed by a brief, non-productive backwashing and membrane recovery period. The apparent dialysate output over any cycle therefore needs to be optimised in terms of maximising the dialysate quality and volume during the production stage, and minimising the non-productive time spent backwashing the element.

A thorough theoretical analysis of the proposed FO production process is presented in chapter 2. The theory suggests that this cyclic arrangement is feasible, provided that excess concentrate is able to be injected to compensate for the accumulation of salt on the closed feed-side of the membrane within the RO element and that the output concentration is able to be controlled independently of the total salt stored within the element itself.

Various output concentration control methods were tested, including proportional-integral (PI), fuzzy-logic control (FLC) and batch control. The details of each method and corresponding experimental results are described in chapter 3. The simplest and most effective control strategy was found to be that of collecting the output from each production cycle in a controlled batch. This approach was tested further so that the

¹²The standard size designation of “4040” refers to an tubular element package that is 40 inches long by 4.0 inches in diameter.

practical limitations on production could be identified and compared against typical medical dialysate production targets (see chapter 4).

The technique of osmotic backwashing is not usually applied to RO membranes in the direction or to the extent to which it is used in this particular application. As such, its performance under these circumstances is largely unstudied. To understand the workings and limitations of this application, a computational model of the entire membrane element and production/backwash cycle was developed and used to visualise various production and backwash scenarios. The structure of the model, together with its tuning and evaluation against experimental data, is described in chapter 5.

1.3.4. Technology in context

The consideration of context in engineering design is not simply an abstract idea or matter of cultural sensitivity: historical evidence shows that it is *necessary* to consider context carefully in order for design projects to be successful (Love, 1998; Oates et al., 2004; Leys, 2003; Dawson et al., 2003). Part of this necessity stems from the realisation that a designed system consists of both social and technical subsystems:

...an engineering system can be conceived as a socially constructed, purposeful, open system that consists of interacting components spanning the social, functional, technical, and process domains and changing over time.

(Bartolomei, 2007, pg 7)

A dialysis service can be thought of as a system of inter-related technologies, people and physical entities such as dialysis equipment, spare parts, technicians, buildings, vehicles, patients, nurses, administrators and community members. If the intention of a technical design is to facilitate valuable social outcomes, such as the rate of return-to-country for Aboriginal patients, then designers can no longer be said to be simply designing a technical *device* - they are participating in the design of a healthcare *service*. This suggests the need to work closely with an existing organisation, and to fulfil the ethical obligation of healthcare service designers to include in the design process those whom the service seeks to serve, particularly when designing for vulnerable people. The health philosophy of *Primary Health Care* describes it as follows:

The people have the right and duty to participate individually and collectively in the planning and implementation of their health care.

(Article IV from the 1978 declaration of Alma Ata: WHO, 2005)

This right is echoed in current approaches to Indigenous health research in Australia, both in the attitude of Australia's National Health and Medical Research Council (NHMRC) and in the Aboriginal cultural principle of *reciprocity*:

Reciprocity requires the researcher to demonstrate a return (or benefit) to the community that is valued by the community and which contributes to

cohesion and survival... Aboriginal and Torres Strait Islander communities have the right to define the benefits according to their own values and priorities.

(NHMRC, 2003, pg 10)

A methodology was developed and is presented here that incorporates these three principles: the understanding that healthcare technology functions as part of a complex socio-technical *system*; the right of people to *participate* in the implementation of their own healthcare services; and the right of Aboriginal communities to set their own *priorities*.

The methodology is based around a quick ethnographic analysis of a given remote community dialysis context. From collected ethnographic data, a model of identified causal relations is produced, so that dependencies between relevant variables may be easily visualised. By passing the causal model to a qualitative reasoning and modelling engine, outcomes from design variations can be easily identified, compared against values and presented to community members and interested stakeholders before further design iteration.

The implementation of such an invasive and personal methodology at the interface between the culture of an engineering design team and that of any remote Aboriginal desert community carries with it the risk of causing cultural injury. This risk has been studied in trans-cultural healthcare at the interface between nurses and the Maori people of New Zealand (Papps and Ramsden, 1996). To mitigate this risk, the methodology incorporates cultural safety principles, together with its other ethical priorities, in order to facilitate the safe and ethical design of dialysis equipment at this cross-cultural interface. The complete methodology, including its rationale, its ethnographic and qualitative methods and an evaluation against external criteria, is described in chapter 6.

The methodology was applied to the needs of this project, to evaluate outcomes due to variations in dialysis system energy efficiency and compactness. This was done by carrying out a brief ethnography in a remote Aboriginal community similar to Kintore, where the dialysis truck was in operation for a two-week period. By carrying out interviews with patients, nurses administrators and community members, enough data¹³ was collected to enable a qualitative model of the remote dialysis service to be generated and simulated. Outcome variations due to design changes were then able to be evaluated against the priorities and values expressed by research participants at the remote site. The results from this approach, together with any identified limitations of the methodology, are also discussed in chapter 7.

¹³A note on usage: The word *data* has been used throughout as a singular mass-noun, similar to words like *information*, rather than as a plural of the noun *datum*.

2. Dialysate production theory

This chapter is adapted from a paper published as: Smith, M. C., & Reynolds, K. J. (2014). Forward osmosis dialysate production using spiral-wound reverse-osmosis membrane elements. Journal of Membrane Science, 469, 95-111.

2.1. Introduction and background

As discussed in chapter 1, there is a large and ever-growing need for dialysis treatment in remote and regional Australia – a need that may be somewhat addressed by improving the suitability of dialysis equipment for use in remote desert regions where dialysis clinics are becoming more common. The main technical innovation in this project is based on the exploitation of the energy and water efficiency advantages of FO, by using dialysate concentrate as a draw-solution and pre-treated groundwater as a feed-solution. In this chapter, the theoretical feasibility of using a standard spiral-wound RO membrane element in FO mode for dialysate production is examined, together with the feasibility of production at a rate sufficient to facilitate medical treatment.

2.1.1. RO and FO processes

As discussed in section 1.2.4.5, dialysis treatment uses an RO permeate stream to dilute concentrated dialysate fluids. The generation of this RO stream requires the energy-intensive use of a flow pump to overcome the osmotic pressure of supplied feedwater. Unlike RO, FO processes can take advantage of an osmotic pressure gradient and use it as a source of energy to drive the desalination of feedwater. This is typically done by supplying a draw-solution of far greater osmolarity than that of the feedwater to one side of a membrane, while supplying feedwater to the other. With no external pressure applied, water molecules will naturally diffuse across the membrane from the feedwater to dilute the draw-solution.

2.1.1.1. Current FO applications

Current FO processes include those concerned with power generation (Han et al., 2015; Klaysom et al., 2013), impaired water treatment (Lutchmiah et al., 2014), desalination

(Li et al., 2013a; Zhao et al., 2012), fertiliser production (Phuntsho et al., 2014) food and pharmaceutical concentration (Klaysom et al., 2013; Chung et al., 2012b) and various other niche applications. Many others have expressed a vision of FO as part of a global solution to shortages of energy and freshwater (Chung et al., 2012a; Ge et al., 2013; Oh et al., 2014; Klaysom et al., 2013; Han et al., 2015) although for most applications FO is only a primary processing stage (Lutchmiah et al., 2014; Li et al., 2013a) after which a second separation must take place to recover the draw solute (Chung et al., 2012a; Lutchmiah et al., 2014; Shaffer et al., 2015). For power generation and water treatment, designs are focused on membrane flux and draw-solute recovery (Zhao et al., 2012), with the energy used by any recovery process largely negating the low-energy gains of the primary FO stage (Shaffer et al., 2015). The main advantage of FO as an RO substitute is that FO membranes and processes are better suited to handling complex feed solutions such as wastewater or seawater (Oh et al., 2014; Lutchmiah et al., 2014).

To truly enjoy the advantages of FO, a process must use its diluted draw-solution for some direct purpose, rather than pass it through a secondary separation process. In the application to dialysate production proposed in this project, the high-energy RO separation step is replaced by a FO process that dilutes and mixes a dialysate concentrate precursor. For this application, the choice of draw-solution is limited to the dialysate concentrate options available for patient treatment.

2.1.1.2. Draw solution considerations

Draw solution selection has a large impact on the effectiveness of an FO process (Shaffer et al., 2015). The ideal draw solution is inexpensive, non-toxic, highly soluble, easily recovered, compatible with the selected membrane and with a molecular size large enough to limit reverse-solute flux yet small enough to have enough diffusivity to mitigate internal concentration polarisation (ICP) (Ge et al., 2013; Holloway et al., 2015; Li et al., 2013a; Shaffer et al., 2015; Chung et al., 2012b). This demanding list leaves very few suitable solutes for FO. Nevertheless, in our dialysate-production application, there is no need to recover the solute, and furthermore, the dialysate concentrate is mostly made up of NaCl, with a little sodium bicarbonate (NaHCO_3) and small portions of other organic and inorganic salts. This gives it the draw-solution advantages shown by monovalent inorganic salts (Ge et al., 2013; Shaffer et al., 2015). Dialysate concentrate is thus fairly ideal draw solution, with its principal disadvantage being its tendency to lose solute to the feedwater via reverse solute flux. Since the lost dialysate salts are easily replaced and non-toxic, this is a minor issue in practice.

2.1.1.3. Using an RO element for FO

A primary consideration when choosing a membrane for FO is the design of the membrane support layer. An ideal membrane is thin, highly porous and minimally tortuous (Shaffer et al., 2015; Lutchmiah et al., 2014). These three aspects of membrane design are defined in its structural parameter S_{me} : a published value that can be used to compare the FO suitability of various membranes (Shaffer et al., 2015). It is this parameter that determines the severity of ICP, hence much of recent FO membrane research has focused on improving the structural parameter and reducing ICP (Lutchmiah et al., 2014). The thickness and tortuosity of conventional RO membrane support-layers has caused RO-type membranes to be avoided in FO applications (McCutcheon and Elimelech, 2007; Lutchmiah et al., 2014).

A second obstacle to the use of RO membranes for FO is the geometry of their commercial packaging (Cath et al., 2006). A major obstacle to their use in this manner lies in their geometry: their membrane sheets are formed into envelopes that are closed on three sides, leaving the support side of the membrane relatively inaccessible and thus prone to salt accumulation due to reverse solute-leak and the presence of non-zero concentrations of dissolved salts in the feedwater (Xiao et al., 2011). This geometry forces any FO process to be carried out in AL-DS mode, as there is no way to inject draw-solution into the closed envelopes of the support layer of off-the-shelf RO modules. This arrangement may cause increased flux (Lutchmiah et al., 2014) but with the consequence of increased fouling and ICP due to the inflow of salt towards the support layer (Chung et al., 2012a). While the effects of fouling may be ameliorated by frequent backwashing (Shaffer et al., 2015), the effects of ICP may be severe¹.

Specialised, spiral-wound FO membranes are similar in price to RO elements of the same package size yet contain only half the functional membrane area (Kim and Park, 2011). By comparison, medical-grade RO elements are inexpensive, compact, lightweight and abundant (Lee et al., 2011; Etori et al., 2011). It is desirable, therefore, to be able to exploit these advantages of spiral-wound RO elements for FO applications, provided that the problems of salt accumulation and increased ICP can be overcome.

2.1.2. Critical design questions

This analysis aims to test the theoretical feasibility of using an RO element element in FO mode to produce un-buffered² dialysate. The method involves supplying a concentrated draw-solution to the active-layer side of the membrane while supplying feed-water to the support-layer side within the membrane envelope. Dialysate fluid may

¹The severity of ICP in this context is shown in-detail in section 2.4.4.2

²The term *dialysate* is used hereafter to refer to un-buffered dialysate solution, to which a sodium-bicarbonate buffering solution would normally be added before its use in medical applications.

then be generated from the draw-side at a fixed flow-rate and at a prescribed concentration³, sustained over a period time equivalent to a five-hour treatment. To achieve these aims, the following questions must be addressed:

1. What size and/or number of membrane elements would be necessary for sufficient dialysate to be continuously produced?
2. How much production time can be expected before the feed-side envelopes accumulate excessive salt?
3. How can the system be recovered so that production can continue?

2.2. Theory

To answer these questions, a basic membrane process design was conceived, from which an analytical model was developed.

2.2.1. Design principles

The following basic principles were used to model the process:

1. An RO element membrane is to be used in FO mode with Active-Layer-Draw-Solution (AL-DS⁴) orientation.
2. The draw-side is to be supplied with dialysate concentrate *part A*, which is to be injected into the proximal end of the element.
3. Feedwater is to be delivered to the element's central tube and allowed to flow across the feed-side of the membrane.
4. Water is to be drawn across the membrane from feed-side to draw-side according to local osmotic pressures.
5. Salt is to be expected to diffuse in reverse across the membrane from the draw-solution to the feed-solution and accumulate in the membrane envelope.
6. Any salt delivered by the feedwater is to be expected to accumulate in the feed-side membrane envelope.
7. Dialysate is to be collected from the output at the distal end of the draw-side.

This arrangement is shown in figure 2.2.1.

³The term *concentration* is used throughout this article to refer to the *osmolarity* of a fluid, which is a quantity more relevant to osmotic processes than the *molarity* to which the term is usually applied.

⁴Other authors (Achilli et al., 2009) have distinguished between FO mode and Pressure-Retarded Osmosis (PRO) mode. Here an asymmetric membrane is used in AL-DS mode, sometimes referred to as PRO mode. As this process is designed to operate with neutral system pressure, the term FO is preferred as it describes the *type* of process, rather than the *orientation* of the membrane.

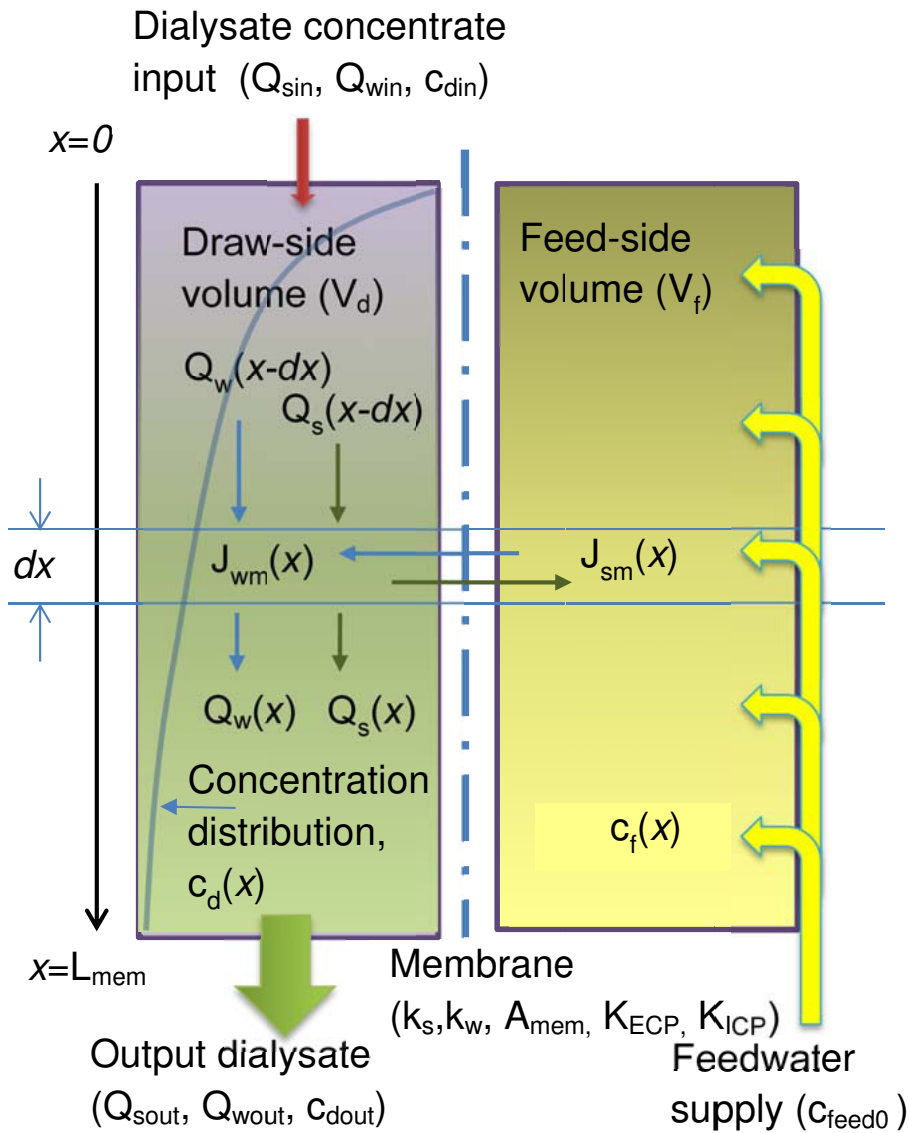


Figure 2.2.1.: An FO dialysate production model based on distributed strips of an RO membrane element.

2.2.2. Analytical model

2.2.2.1. General model

A general mathematical model of the FO mechanism was developed to describe the movement of salt and fluid across any small area of the membrane. The membrane was treated as a series of differential strips so that Morse' law could be applied locally to each strip. This enabled the relationship between trans-membrane water flux, $J_{wm}(x)$, concentration difference, $\Delta c(x)$, and hydrostatic pressure, $\Delta P(x)$, to be modelled at any distance, x , from the input to the system. Firstly, the absolute concentration difference, $\Delta c(x)$, was defined in terms of the local draw- and feed-side concentrations, $c_d(x)$ and $c_f(x)$:

$$\Delta c(x) = c_d(x) - c_f(x) \quad (2.2.1)$$

This allowed a basic model for water flux, $J_{wm}(x)$, to be written, using Morse' law and the membrane water flux constant, A . The van 't Hoff constant, i , universal gas constant, R and temperature, T were used to convert between concentration and pressure:

$$J_{wm}(x) = A (iRT\Delta c(x) - \Delta P(x)) \quad (2.2.2)$$

This model has limited application to practical processes, which must cope with significant external and internal concentration polarisation (ECP and ICP), which have been known to cause substantial losses of flux in other FO processes (Lay et al., 2012; Zhao et al., 2012). ECP and ICP effects were included in the model by modifying the *absolute* local concentration difference, $\Delta c(x)$ to become an *apparent* difference, $\Delta c^*(x)$:

$$\Delta c^*(x) = (c_d \cdot f)(x) - (c_f \cdot g)(x) \quad (2.2.3)$$

Here, f and g are functions that modify c_d and c_f to accommodate ECP and ICP effects. Since the type of membrane element under discussion here is of a type originally designed for RO applications, its membrane support layer and corresponding ICP effects are found on the feed-side of the process, while ECP effects are found on the draw-side of the membrane. Both f and g are functions of the water flux, $J_{wm}(x)$, which is itself a function of x . They are written here in a form borrowed from Lay et al. (2012):

$$\begin{aligned} f(J_{wm}) &= e^{-\frac{J_{wm}}{K_{ECP}}} \\ g(J_{wm}) &= e^{\frac{J_{wm}}{K_{ICP}}} \end{aligned} \quad (2.2.4)$$

Here, K_{ECP} and K_{ICP} are the mass transfer coefficients for ECP and ICP⁵. A general, one-dimensional model for membrane fluid flux was therefore able to be written as

⁵The convention in Lay et al. (2012) has been followed here of writing the mass transfer coefficient $K_{ICP} = \frac{D}{S_{me}}$ in terms of its diffusion coefficient (D) and structural parameter (S_{me}) rather than its inverse, the resistance to solute diffusion ($K = \frac{S_{me}}{D}$).

follows:

$$J_{wm}(x) = A \left(iRT \left(c_d(x) e^{-\frac{J_{wm}(x)}{k_{ECP}}} - c_f(x) e^{\frac{J_{wm}(x)}{k_{ICP}}} \right) - \Delta P(x) \right) \quad (2.2.5)$$

2.2.2.2. Simple model

Unfortunately, equations like those found in the general model above are very difficult to simplify or integrate without resorting to numerical methods (McCutcheon and Elimelech, 2007). To continue with the analysis, f and g were approximated as constant-valued functions. Furthermore, as hydrostatic pressure is usually very low for FO processes (unlike the significant back-pressures found in pressure-retarded osmotic systems), ΔP was able to be omitted⁶. To simplify the notation, constants k_w and k_s were used to denote the membrane water and salt permeability constants, instead of the traditional symbols for hydraulic permeability of water, A , and reverse solute flux constant, B .

$$\begin{aligned} \Delta P &= 0 \\ f(J_{wm}) &= \mu \\ g(J_{wm}) &= \lambda \\ k_w &= A \cdot iRT \\ k_s &= B \end{aligned} \quad (2.2.6)$$

The appropriate choice of the constants, μ and λ , is discussed further in section 2.4.4.2, and compared with output from the pilot numerical model. Using these constants, the modified formula for $\Delta c^*(x)$ was able to be written in terms of $\Delta c(x)$:

$$\begin{aligned} \Delta c^*(x) &= c_d(x)\mu - c_f(x) \cdot \lambda \\ &= \Delta c(x) + c_d(x)(\mu - 1) - c_f(x)(\lambda - 1) \end{aligned} \quad (2.2.7)$$

The simplifications in 2.2.6 allowed a simpler but more useful model to be written:

$$\begin{aligned} J_{wm}(x) &= k_w \Delta c^*(x) \\ &= k_w (c_d(x)\mu - c_f(x)\lambda) \end{aligned} \quad (2.2.8)$$

A similar formula was developed for trans-membrane salt-flux, J_{sm} :

$$\begin{aligned} J_{sm}(x) &= k_s \Delta c^*(x) \\ &= k_s (c_d(x)\mu - c_f(x)\lambda) \end{aligned} \quad (2.2.9)$$

⁶This assumption was later found to be incorrect (see section 3.3.7): there was significant hydrostatic pressure generated over the longitudinal resistance of the membrane's draw-side during stages with high draw-side recirculation rates. This non-ideal property was included in the computational model.

By integrating this simple model over the length of the element, it can be shown that the bulk, trans-membrane fluid and salt fluxes⁷ are proportional to the apparent bulk trans-membrane concentration difference, and therefore largely independent of the distributions of salt on each side of the membrane (see A.3):

$$\begin{aligned} J_{wm} &= k_w \Delta c^* \\ J_{sm} &= k_s \Delta c^* \end{aligned} \quad (2.2.10)$$

2.2.2.3. Compensation for salt leakage and accumulation

It is clear from examination of this simple model that the size of the apparent trans-membrane salt difference, Δc^* , determines the membrane fluid flux, J_{wm} , which ultimately results in output flow from the system. During production, this difference must be kept at a level high enough to maintain adequate output flow as salt accumulates in the feed-side envelopes. To compensate for this, excess salt must be added to the draw-side. To estimate the rate of compensation, a comparison of ideal and practical membrane properties is needed.

For an *ideal* element with no reverse-salt leak, the salt mass-flow at the output, Q_{sout} , must eventually rise to match the input injection rate, Q_{sin} , as no salt is lost from the system. When commercial dialysate concentrates are used, the input concentration, c_{din} , can be known, which allows the ideal input concentrate volume injection rate, Q_{win0} , to be estimated from the desired outputs, $Q_{wtarget}$ and $c_{dtarget}$:

$$Q_{win0} \cdot c_{din} = Q_{wtarget} \cdot c_{dtarget} \quad (2.2.11)$$

For *practical* elements however, the salt injection rate, Q_{win} , must be set higher than the ideal input rate, Q_{win0} , in order to provide excess salt to offset the feed-side accumulation and to compensate for ECP and ICP. The compensating *overprime* factor, $F_{OP} = \frac{Q_{win}}{Q_{win0}}$, can be calculated from the basic parameters of the system:

$$F_{OP} = \frac{\frac{\lambda}{V_f} \left(\frac{k_s}{k_w} + c_{feed0} \right) + \frac{\mu}{V_d} \left(\frac{k_s}{k_w} + c_{dtarget} \right)}{\frac{\lambda}{V_f} \left(\frac{k_s}{k_w} + c_{feed0} \right) + \frac{\mu}{V_d} \cdot \left(\frac{k_s}{k_w} + c_{din} \right)} \cdot \frac{c_{din}}{c_{dtarget}} \quad (2.2.12)$$

Here, the feed-water concentration is c_{feed0} , and the bulk draw- and feed-side compartment volumes are V_d and V_f . By adding excess input salt at a controlled rate, the problem of feed-side salt accumulation may be somewhat ameliorated, provided that

⁷Distributed quantities, such as trans-membrane flux $J_{wm}(x)$ or concentration difference $\Delta c^*(x)$ are written here as functions of their position in space (x). When integrated, J_{wm} , Δc^* and others become bulk quantities and variables in their own right, and are notated here without parentheses.

the draw-side output concentration can be controlled at the target value, $c_{dout} = c_{dtarget}$. The problem of dialysate output control has medical significance and is a major challenge of this design.

2.2.3. Dialysate production

2.2.3.1. Output concentration control

It is proposed here that dialysate concentration control may be achieved by recirculating the draw-side fluid from the output end to the input, using a flow pump whose rate may be continually adjusted to keep the output concentration constant (see figure 3.2.1 and experiments in section 3.2.1). This method has the advantage of varying the draw-side concentration distribution, $c_d(x)$, without changing the bulk concentration c_d .

To maintain a stable output concentration at the target value, $c_{dout} = c_{dtarget}$, the speed of the recirculation pump must continuously decrease as salt accumulates in the system. Early in the production cycle, when there is little salt in the element, the pump should run at a high speed, flattening the salt distribution along the length of the element. As salt accumulates in the system, the pump speed must slow, causing more salt to be retained near the input-end. This should continue to the point of saturation, where the accumulation of salt is such that the element cannot produce sufficient dilution along its length to reduce the output concentration to the target value. The time over which production can be effectively controlled is the *effective production time*.

2.2.3.2. Initial state

The beginning of effective production is at the time, t_0 , when the system first reaches stability, with both output concentration, c_{dout} , and flow-rate, Q_{wout} , reaching their target levels. To reach this state, the system must first be primed with sufficient salt to form a distribution, $c_{dt0}(x)$, that has the target concentration value, $c_{dtarget}$, at its output end, where the distance from the injection point, x , is equal to the full length of the element, L_m :

$$c_{dt0}(x = L_m) = c_{dtarget} \quad (2.2.13)$$

2.2.3.3. Final state and effective production time

The end of effective production is at the time of draw-side saturation, t_s , when the draw-side concentration everywhere will be greater than or equal to the target output concentration. If the bulk concentration, c_{dts} , at this time can be known, the effective

production time, $t_{eff} = t_s - t_0$, can be estimated (see A.6):

$$t_{eff} = \frac{\mu (c_{dts} - c_{dt0}) \cdot \left(\frac{V_d}{\mu} + \frac{V_f}{\lambda} \right)}{\left(F_{OP} \cdot \left(1 - \frac{c_{feed0}}{c_{din}} \right) + \frac{c_{feed0}}{c_{dtarget}} - 1 \right) Q_{wtarget} \cdot c_{dtarget}} \quad (2.2.14)$$

2.2.3.4. Useful volume

It is trivial to calculate the useful dialysate volume, V_{cycle} , from the set flow rate, $Q_{wtarget}$, and the effective production time, t_{eff} :

$$V_{cycle} = Q_{wtarget} \cdot t_{eff} \quad (2.2.15)$$

A considerable portion of useful output may be wasted while waiting for the system to first stabilise. If the salt injection rate, Q_{win} , can be varied instead of maintaining it at a constant rate, the total useful output volume may be increased. The maximum limit to this increase, V_{max} , may be estimated by examining salt concentration on the feed-side at both the beginning of effective production, c_{ft0} , and at the point of saturation, c_{fts} :

$$\begin{aligned} V_{cycle} &\leq \frac{(c_{fts} - c_{ft0}) V_f}{\frac{k_s}{k_w} + c_{feed0}} \\ &= V_{max} \end{aligned} \quad (2.2.16)$$

2.2.4. Backwashing and Recovery

Once the effective production limit has been reached, production cannot continue without first removing the accumulated salt from the feed-side of the membrane. It is suggested here that osmotic backwashing, as described by Sagiv and Semiat (2010); Ramon et al. (2010); Werner et al. (2013) and others, may be a suitable approach⁸. To achieve this, the draw-side fluid must be temporarily displaced by a low-osmolarity backwash solution, such as free water, diluted dialysate or treated feedwater. The FO mechanism would then work in reverse to flush the accumulated solutes from the closed envelopes of the feed-side compartment. A thorough exploration of this method is described in chapter 5.

⁸The reasoning behind the choice of RO-type membrane elements is described in section 1.3.2. The need for backwashing is a consequence of this choice, explored in detail in chapter 5. It would have been an interesting study to explore the use of off-the-shelf FO membrane elements in this application, as backwashing may not have been needed. However the question of whether inexpensive, robust and proven RO elements can be used in this medical FO application is of great significance to remote health equipment design, despite the known limitations of RO elements for use in FO mode. It is this question that underlies the entire thesis, which attempts to evaluate both the practical and social suitability of the use RO elements in FO-mode in the desert context. See chapter 1 for details.

2.3 Evaluation

During this stage there can be no production, and excess dialysate must be generated during the preceding production stage and briefly stored to cover the non-productive backwashing and recovery time, t_{bf} . This excess production requires an artificial increase in the set target output flow rate, $Q_{wtarget}$. The average, or *apparent* flow rate over a complete production/recovery cycle is designated here as $Q_{wtarget}^*$. If an apparent dialysate flow-rate is specified for a dialysis treatment, the corresponding flow-rate target setting can be specified:

$$Q_{wtarget} = \frac{V_{cycle} \cdot Q_{wtarget}^*}{V_{cycle} - Q_{wtarget}^* \cdot t_{bf}} \quad (2.2.17)$$

Alternatively, this equation can be rearranged to show the flow rate that will appear for a given set flow target:

$$Q_{wtarget}^* = \frac{V_{cycle} \cdot Q_{wtarget}}{V_{cycle} + Q_{wtarget} \cdot t_{bf}} \quad (2.2.18)$$

Due to this backwashing time, there is an upper limit to the apparent production rate, even if the set rate can be made infinitely large. That is, as $Q_{wtarget} \rightarrow \infty$:

$$Q_{wtarget}^* \rightarrow \frac{V_{cycle}}{t_{bf}} \quad (2.2.19)$$

This upper limit may be useful to know, yet is unlikely to be achieved in practice, as the necessary high set value of $Q_{wtarget}$ would result in severe ECP and ICP, which would in turn reduce the size of V_{cycle} . The estimation of a practical limit to $Q_{wtarget}^*$ is discussed below (see section 2.3.3.1).

2.3. Evaluation

The analytical model described above was evaluated with the aim of finding answers to the questions listed in section 2.1.1. Practical parameter values were selected from values taken from measurements and publications. Critical design parameters, such as membrane and feedwater quality, were varied through typical ranges to assess the system's sensitivity to variations in those parameters. The sensitivity of the system to ECP and ICP was also evaluated to help establish the likely validity of the model's simple ECP and ICP approximations.

2.3.1. System parameters

2.3.1.1. Production targets

The system was developed with medical applications in mind⁹. A typical dialysis treatment may be specified at 14.0 mS/cm conductivity, for which the concentrate and buffering delivery proportioning system would then be automatically adjusted. Dialysate flow-rates on Fresenius™ machines can be set to 300, 500 or 800 ml/min, according to the direction of a nephrologist (Fresenius, 2007). The analysis here is concerned with dialysate production for treatment at 500 ml/min. However, the proposed system uses only dialysate concentrate *Part A* as a draw-solution. This changes the target setpoints to equivalent *Part A* only settings of, $Q_{wtarget} = 484$ ml/min, and $\sigma_{target} = 11.6$ mS/cm. If this dialysate precursor can be generated according to these targets, the complete dialysate mixture will be able to be produced at the medical rate by simply adding the usual proportion of *Part B* bicarbonate buffer. Furthermore, for some experiments and analyses it was found useful to model dialysate production at lower flow-rates or half-rates, hence the appearance of the lower target, $Q_{wtarget} = 242$ ml/min in various calculations. For instance, a relatively low target production rate was chosen for this evaluation in order to minimise calculation errors due to the simple approximation of ECP and ICP.

2.3.1.2. Permeability constants

Two of the more critical membrane parameters are the hydraulic permeability of water, A (m/Pa·s)¹⁰, and reverse solute flux constant, B (m/s). These factors relate trans-membrane pressure to water flux and trans-membrane concentration to reverse solute flux and are usually published as membrane characteristics for RO operation. Some authors have referred instead to the combination, $\frac{B}{A}$, as it reflects the overall quality of the membrane (Lee et al., 2011). A high-quality membrane, therefore, has high water permeability, low reverse solute flux and therefore low $\frac{B}{A}$. A list of published membranes and their characteristics is shown in table 2.3.1.

For the analysis above (see section 2.2) it was convenient to use a single constant, k_w , to describe the relationship between trans-membrane concentration difference and water flux, rather than A , which relates osmotic pressure and flux. Using the van 't Hoff constant for free, dissociated ions, $i \approx 1$, the ideal gas constant, $R = 8.314 \times$

⁹A note on the units: As this is primarily an engineering study of the production of dialysate by an unconventional method, units appropriate to dialysis (ml/min and mS/cm) have been preferred when assessing the usable production of the designed system.

¹⁰A note on the units: The first reference (Arias et al., 2011) cited in table 2.3.1 uses (m/Pa·s) for permeability and (m/s) for flux. As this thesis covers multiple technical disciplines (including membranes, dialysis and computational modelling), SI units have been preferred throughout.

2.3 Evaluation

Membrane	A (m/Pa·s)	B (m/s)	$\frac{B}{A}$, (Pa)
Hydranautics ESPA2-4040 ^a	1.56×10^{-11}	4.00×10^{-8}	2.56×10^3
Toray TM70 ^a	1.03×10^{-11}	7.00×10^{-8}	6.36×10^3
Typical polyamide ^b	5.56×10^{-12}	5.56×10^{-8}	1.00×10^4
Dow Filmtec BW30-4040 ^a	7.70×10^{-12}	1.50×10^{-7}	1.95×10^4
Oasys TFC ^c	1.03×10^{-11}	3.33×10^{-7}	3.24×10^4
Hand cast TFC ^c	3.42×10^{-12}	5.56×10^{-7}	1.63×10^5
Brackish water polyamide ^d	1.19×10^{-12}	-	-

Sources: ^aArias et al. (2011); ^bLay et al. (2012); ^cTirafferri et al. (2013);
^dMasse et al. (2010)

Table 2.3.1.: Membrane characteristics for a range of membranes described in current literature.

$10^{-3} \text{ L} \cdot \text{kPa} \cdot \text{K}^{-1} \text{mmol}^{-1}$, and the standard temperature, $T = 298 \text{ K}$, conversions were able to be made between the two forms:

$$\begin{aligned} k_w &= i \cdot A \cdot R \cdot T \\ k_s &= B \end{aligned} \quad (2.3.1)$$

For this evaluation, a spread of B and A values was taken from the range of values shown in table 2.3.1.

2.3.1.3. Concentration polarisation

For membranes in the orientation AL-DS, water flows from the membrane-support layer through to the active layer adjacent to the draw-solution. In this orientation, the effect of ECP at the active-layer surface is small compared with the effect of ICP (You et al., 2012). To adjust for ICP, values for the membrane structural parameter, S_{me} , and solute diffusivity, D , were taken from literature (see table 2.3.2). The parameter $K_{ICP} = \frac{D}{S_{me}}$ was calculated from these values, while the parameter K_{ECP} was estimated to be an order of magnitude larger than K_{ICP} (Lay et al., 2012).

$$K_{ECP} = 10 \times K_{ICP} \quad (2.3.2)$$

These parameters were used to choose values for μ and λ which were then used to approximate the apparent bulk trans-membrane water flux, J_{wm} , under ECP and ICP conditions (see sections 2.4.1.2, 2.4.4.2 and discussion at 2.5.2.3).

2.3.1.4. Geometry

To estimate values for membrane element geometry, a common, 4.0 inch by 40 inch, spiral-wound RO membrane element (Hydranautics ESPA1-4040) was autopsied and measured. Elements of this type are common in large-scale dialysis RO systems in Australia and are easy to obtain. Measurements and published values are shown in table 2.3.2.

2.3.1.5. Environment

A typical total-dissolved solids (TDS) value for local tapwater (SA Water, 2013) was used to estimate c_{feed0} . The concentration of dialysate *Part A* was estimated from labelled values for ingredients on a concentrate package (Fresenius, 2014). Variations in feedwater supply concentration were estimated from a typical spread of groundwater solute concentrations from $c_{feed0} = 0 \rightarrow 20.0$ mosm ($0 \rightarrow 470$ mg/L TDS), derived from published data (PowerWater, 2009a). These and other system and environmental parameters are shown in table 2.3.2.

2.3.1.6. System inputs

There is a need to compensate for the non-ideal properties of this process by over-priming the draw-side with excess concentrate by a factor of $F_{OP} = \frac{Q_{win}}{Q_{win0}}$, as shown in equation 4.1.2. For practical membranes with qualities in the range $\frac{B}{A} = 2.5 \times 10^3 \rightarrow 1.5 \times 10^5$ Pa, this overprime factor varies linearly between $F_{OP} = 1.19 \rightarrow 2.43$ (see figure 2.3.1, a). If a high-quality element, with $\frac{B}{A} = 2.56 \times 10^3$ Pa (see table 2.3.1) was to be used, the compensation for salt-leak due to membrane quality would be small, and instead, F_{OP} would become largely determined by feedwater quality.

For brackish feedwater concentrations in the target range of $c_{feed0} = 0 \rightarrow 20.0$ mosm/L ($0 \rightarrow 470$ mg/L TDS - see section 2.3.1.5), the overprime factor varies linearly between $F_{OP} = 1.43 \rightarrow 1.76$ (see figure 2.3.1, b). At the selected default groundwater concentration of $c_{feed0} = 11.0$ mosm/L (259 mg/L), using the adjusted element parameters (see table 2.3.2), the overprime factor was estimated at $F_{OP} = 1.61$.

2.3.2. Production

2.3.2.1. Initial state

As described in section 2.3.2.1, the system must first be primed with salt until the output concentration, c_{dout} , reaches its target value, $c_{dtarget}$, before dialysate production can begin. Meanwhile, the feed-side salt concentration, c_f , must be allowed to rise

2.3 Evaluation

Parameter	Symbol	Value	Units
Membrane hydraulic permeability ^a	A	7.70×10^{-12}	m/Pa·s
Reverse solute flux constant ^a	B	3.75×10^{-7}	m/s
Membrane structural parameter ^b	S_{me}	5.89×10^{-4}	m
Solute diffusivity ^h	D	1.35×10^{-9}	m^2/s
Mass transfer coefficient ^b	K_{ICP}	2.29×10^{-6}	$kL \cdot m^{-2} \cdot s^{-1}$
Mass transfer coefficient ^b	K_{ECP}	2.29×10^{-5}	$kL \cdot m^{-2} \cdot s^{-1}$
Membrane area ^c	A_m	7.9	m^2
Membrane length ^c	L_m	0.93	m
Membrane total width ^c	W_m	8.49	m
Membrane thickness ^d	-	0.14	mm
Draw-side spacer thickness ^d	$2 \cdot w_d$	0.66	mm
Draw-side fluid volume fraction ^d	ϵ_d	0.9	$\frac{m^3}{m^3}$
Feed-side spacer thickness ^d	$2 \cdot w_f$	0.25	mm
Feed-side spacer volume fraction ^d	ϵ_f	0.68	$\frac{m^3}{m^3}$
Draw-side total volume ^d	V_d	2.35	L
Feed-side total volume ^d	V_f	0.67	L
Feedwater osmolarity ^e	c_{feed0}	11 (259)	mosm/L (mg/L)
Draw-side concentrate input ^f	c_{din}	8000	mosm/L
Target conductivity ^g	σ_{target}	11.6	mS/cm
Equivalent target concentration ^g	$c_{dtarget}$	247	mosm/L
Target flow rate ^g	$Q_{wtarget}$	242	ml/min

Values derived from these sources: ^aArias et al. (2011); ^bTiraferri et al. (2013); ^cHydranautics (2011); ^dElement autopsy; ^eSA Water (2013); ^fFresenius (2014); ^gFresenius (2007); ^h(Lynch, 1974).

Table 2.3.2.: The system, membrane element and environmental parameters used to evaluate the analytical model.

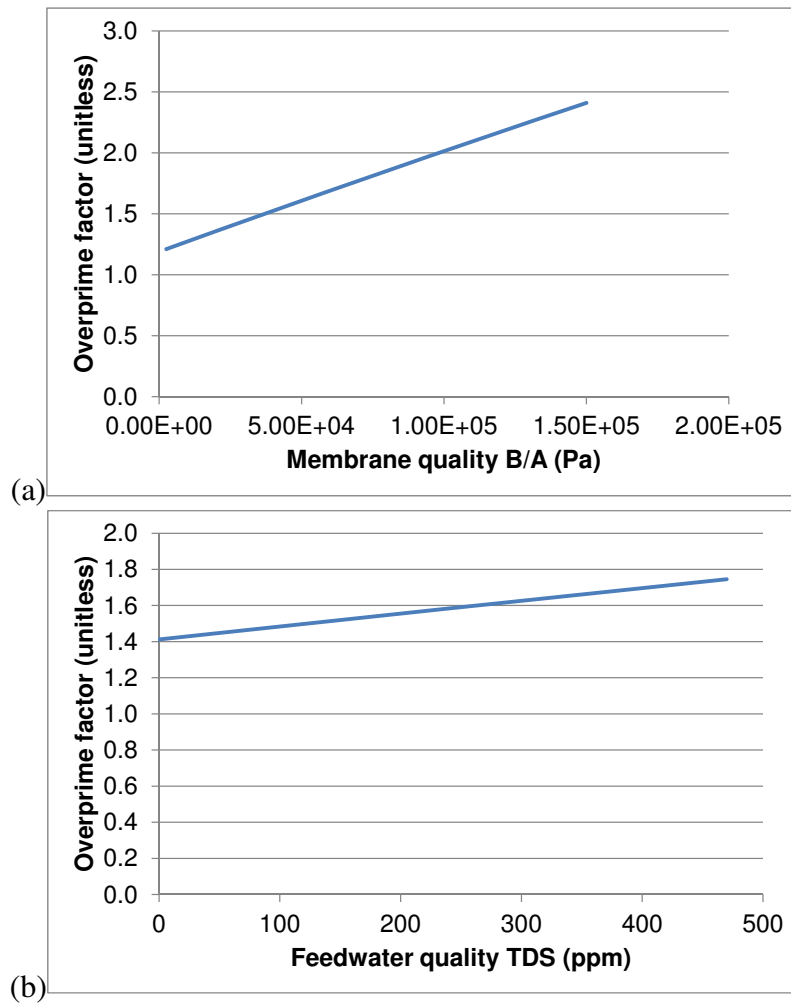


Figure 2.3.1.: The need to overprime with excess salt depends on membrane quality (a) and feed-water quality (b).

2.3 Evaluation

until the apparent concentration difference, Δc^* , has decreased to the level required to produce the target flow rate, by $Q_{wtarget} = k_w A_m \Delta c^*$. A recirculation pump capable of very high speed would be able to maintain a flat distribution of salt along the length of the draw-side compartment during this priming phase. If this were possible, at t_0 the distribution would be almost constant, with $c_d(x) = c_{dtarget} = 247$ mosm/L everywhere.

For practical systems, the draw-side salt distribution, $c_d(x)$, can never be flat, but instead must decrease along the element length. By the time the target output concentration, $c_{dtarget}$, is reached, some extra salt will have already accumulated in the draw-side, and some production capacity will have been lost. Results from the pilot experiment showed that by the time a stable output concentration is obtained, plenty of volume will have already been produced (see section 2.4.4.1). This experiment was simulated using the prototype computational model¹¹, which estimated the initial state, bulk, draw-side concentration at $c_{dt0} = 370$ mosm/L. This value is much higher than the ideal estimate of $c_{dt0} = c_{dtarget} = 247$ mosm/L, which shows that at that point in the simulated experiment, a significant portion of the potentially useful production capacity of the system had already been lost.

2.3.2.2. Final state

Numerical estimates of effective production time depend on knowledge of the distribution of salt throughout the draw-side, $c_{dts}(x)$, at the point of saturation. Although it is difficult to determine this distribution analytically, numerical modelling or experiment (see sections 2.4.2.1 and 2.4.2.1) can help provide useful values with which the dependency of production time on other design parameters may be evaluated. For this analysis, a value of $c_{dts} = 522$ mosm/L was estimated from numerical modelling of the distribution at saturation (see figure 2.3.2).

2.3.2.3. Effective production time

Effective production time, t_{eff} , is perhaps the most important system characteristic, as it determines the total useful volume produced, the frequency of backwashing and the set target output flow-rate. The effective production time is very sensitive to membrane quality¹², varying by nearly 25 min over the selected range of membrane qualities (see figure 2.3.3, b). For high-quality membranes, the production time may be up to $t_{eff} = 30$ min when fed with feedwater at the default value of $c_{feed0} = 11.0$ mosm/L (259 mg/L).

With the chosen system values of membrane quality and feedwater, effective production time was estimated to be $t_{eff} \approx 11.4$ min. If the initial stabilisation time were

¹¹The full model is described in chapter 5

¹²The conclusions stated here were later found to be incorrect: The predicted dependency on membrane quality was later shown to be dwarfed by a dependency on ECP and ICP (see chapter 5).

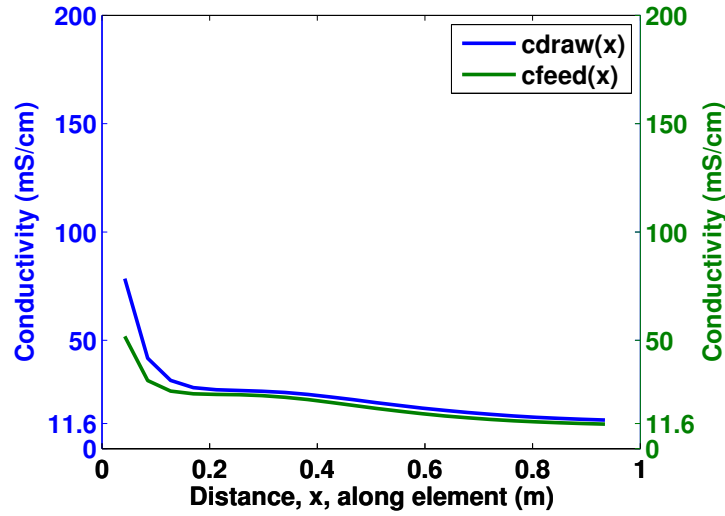


Figure 2.3.2.: Modelled salt distributions on the draw- and feed-side of the membrane at the limit of effective production.

able to be optimised, the ideal value of $c_{dt0} = 247$ mosm/L may be obtainable, which would give a maximum effective production time of $t_{eff} \approx 20.7$ min with all other parameters remaining unchanged. If the same ideal initialisation were combined with a high-quality membrane, a further improved maximum effective production time of $t_{eff} \approx 52.16$ min may be possible.

2.3.2.4. Effect of ECP and ICP

As discussed in section 2.2.2.2, a suitable value for trans-membrane water flux (J_{wm}) must be chosen in order to approximate μ and λ to accommodate ECP and ICP effects. While μ varies little over the range of water flux that appears in the modelled system (see figure 2.4.2), the dominance of λ means that J_{wm} must be carefully chosen. Although most bulk approximations to flux give a value between $\lambda = 1 \rightarrow 2$ (see section 2.4.4.2), local flux values may be very high, producing a high ICP effect at $\lambda = 5$. The effective production time of the system decreases rapidly with increasing λ and decreasing μ (see figure 2.3.3 and discussion in section 2.5.2.3).

2.3.2.5. Effective production volume

Using the estimated maximum effective production time of $t_{eff} \approx 21$ min (see section 2.5.3.1), and a target flow-rate, $Q_{wtarget} = 242$ ml/min, the expected cycle production

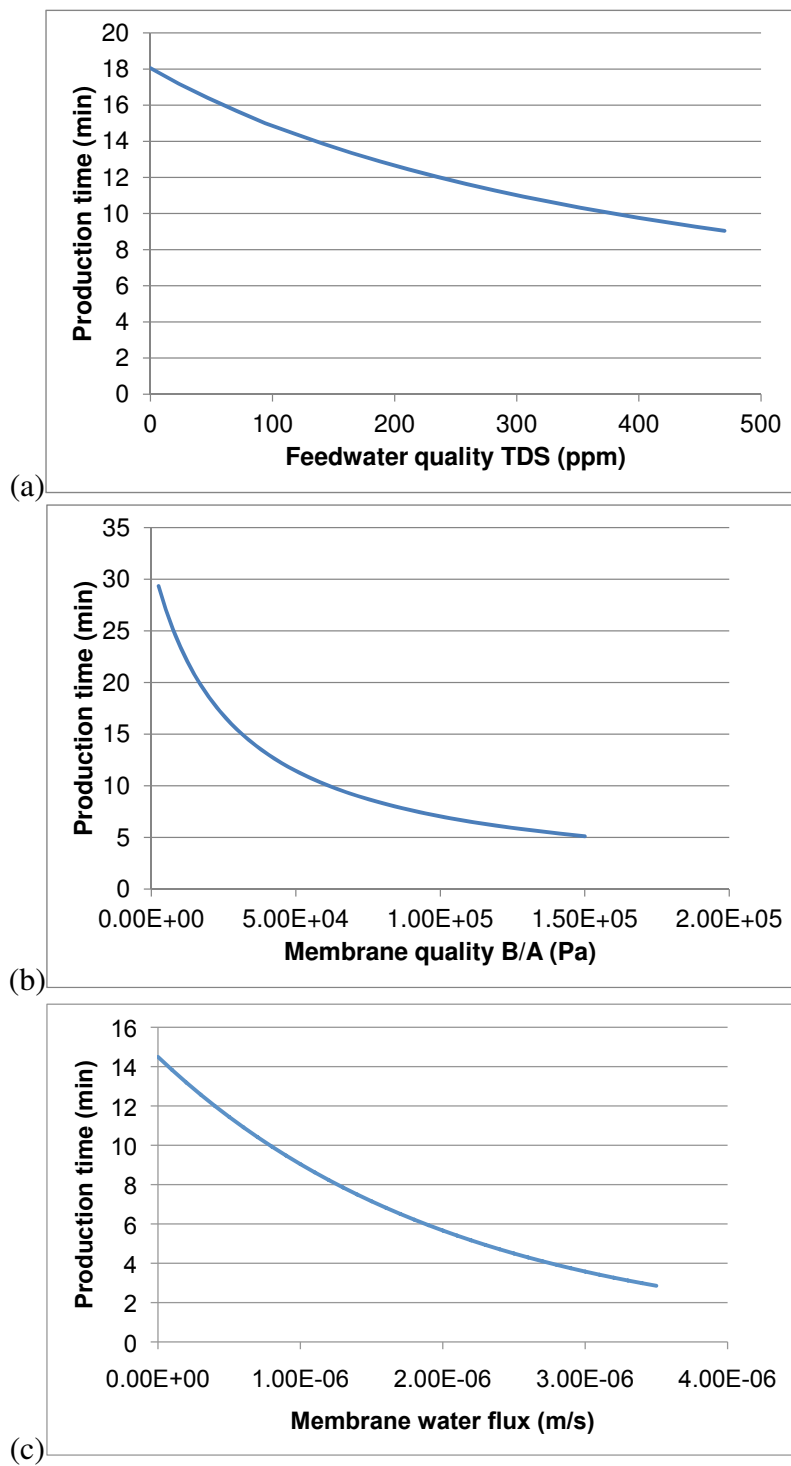


Figure 2.3.3.: The effective production time depends on feed-water quality (a), membrane quality (b) and on membrane water flux, (c).

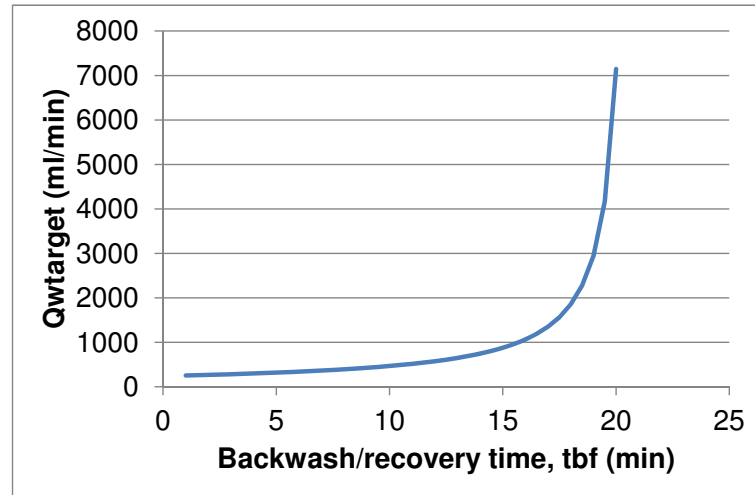


Figure 2.3.4.: The set target production flow-rate ($Q_{wtarget}$) must be increased to compensate for time lost during osmotic backwashing.

volume, V_{cycle} , can be estimated using equation 2.2.15:

$$\begin{aligned} V_{cycle} &= Q_{wtarget} \cdot t_{eff} \\ &= 5010 \text{ ml} \end{aligned} \quad (2.3.3)$$

The parameter, t_{eff} , is itself a function of $Q_{wtarget}$, as it varies due to the effects of ECP and ICP, which are themselves amplified by increased flow-rates. For instance, at an increased set flow-rate of $Q_{wtarget} = 484 \text{ ml/min}$, the net production can be predicted to be $V_{cycle} = 3.9 \text{ L}$ - a dramatic decrease in useful output compared with the $\sim 5.0 \text{ L}$ for the lower flow-rate calculated above in equation 2.3.3. This loss of efficiency is a key determinant of the maximum apparent production rate, as discussed below (see section 2.3.3.2).

2.3.3. Recovery

2.3.3.1. Recovery time and apparent production

The backwash/recovery time, t_{bf} , can be used to include the entire non-productive time in each production cycle. By passing a range of values for t_{bf} to equation 2.2.17, the corresponding adjustments to target flow rate settings can be estimated (see figure 2.3.4).

From this figure, it is clear that there is a hard, theoretical limit to the allowable recovery time at around 20 minutes for this system. For a typical recovery time of around six minutes (see figure 2.4.4 in section 2.4.4.3), the apparent production rate cannot

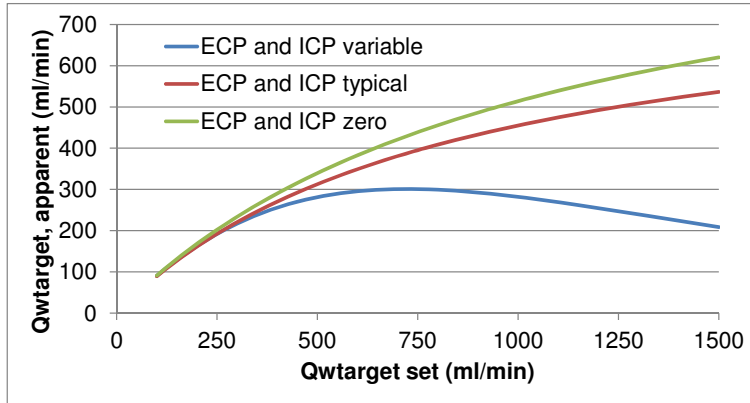


Figure 2.3.5.: The apparent production flow rate is limited by ECP and ICP effects

increase above a certain, calculable limit:

$$\begin{aligned}
 Q_{wtarget}^* &= \frac{V_{cycle}}{t_{bf}} \\
 &= 835 \text{ ml/min}
 \end{aligned}
 \tag{2.3.4}$$

In practice, this limit may be unattainable, as it depends on achieving an impossibly large production flow rate, $Q_{wtarget}$, and ignoring ECP and ICP. By evaluating equation 2.2.18 over a range of set flow rates, $Q_{wtarget}$, and calculating the net production, V_{cycle} , for ECP and ICP for each, the limiting value of $Q_{wtarget}^*$ for this system appears to be about 300 ml/min (see figure 2.3.5).

2.3.3.2. Maximum production volume

The discussion above only counts effective production from the time when the system's output flow and concentration have stabilised. If, instead, useful output could be collected during the early stabilisation phase, the total useful production volume could be increased, up to a maximum value of V_{max} . This limit can be evaluated by setting the initial system state at the point when the bulk feed-side concentration matches the feed-water concentration, $c_{ft0} = c_{feed0} = 11 \text{ mosm/L}$, and defining its final, saturated state at $c_{fts} = 522 \text{ mosm/L}$:

$$\begin{aligned}
 V_{cycle} &\leq \frac{(c_{fts} - c_{ft0}) V_f}{\frac{k_s}{k_w} + c_{feed0}} \\
 &= V_{max} \\
 &= 11.25 \text{ L}
 \end{aligned}
 \tag{2.3.5}$$

This is almost double the ~ 5.0 L output estimated from the stable, ideal production time calculated in 2.3.3. The incorporation of this excess output into the total useful dialysate output is explored further in chapters 3 and 4.

2.4. Pilot experiments

A pilot experiment was carried out in order to test the analytical theory described above. The tested scenario was also imitated with the use of a pilot, two-dimensional computational model. The results of both are presented together.

2.4.1. Parameters

2.4.1.1. Membrane and environmental characteristics

A used membrane element (Filmtec BW30-4040) was available for this experiment. The element had been in use for various prototyping experiments for more than 12 months and had appeared to have suffered increased membrane solute permeability¹³. Several preliminary tests and simulations were carried out to estimate the level of decay, which was found to be well matched by a value of $B \approx 2.29$ m/s, which was 2.5 times greater than the published value for this element (compare values published for the element in table 2.3.1, with those used for evaluation and experimentation in table 2.3.2). All other environmental values were the same as those used for the evaluation in section 2.3.

2.4.1.2. Choice of μ , λ and F_{OP}

To keep the experimental design simple, μ and λ were estimated from a value for trans-membrane flux, J_{wmAVG} , calculated by averaging the target output flow over the whole membrane area:

$$J_{wmAVG} = \frac{Q_{wtarget} - Q_{win}}{A_m}$$

$$\lambda = e^{\frac{J_{wmAVG}}{K_{ICP}}} \approx 1.25 \quad (2.4.1)$$

$$\mu = e^{-\frac{J_{wmAVG}}{K_{ECP}}} \approx 0.98 \quad (2.4.2)$$

¹³This presumption was later shown to be unlikely by computational modelling. The apparent degradation was able to be explained in terms of increased ECP and ICP, combined with an underestimation of longitudinal membrane resistance (see 5.4.1.1).

These were then used together with other parameters to derive a value for the overprime factor, using the equation in 4.1.2:

$$F_{OP} \approx 1.61 \quad (2.4.3)$$

2.4.2. Apparatus

2.4.2.1. Experimental system

The test element was placed in a suitable pressure vessel with connections at top and bottom for both draw- and feed-side compartments. Dialysate concentrate *Part A* was drawn from a container and delivered to the top of the active-layer/draw-side compartment using a diaphragm-piston dosing pump with a stroke volume of 1.125 ml. Draw-side fluid was recirculated by a speed-controlled gear-pump with a maximum flow-rate of 1.4 L/min under load. Output fluid was sampled and collected in a vessel on a weighing scale. Conductivity was continuously measured at the draw-side output using a cell recovered from a decommissioned dialysis machine. Tapwater with an estimated TDS of 259 mg/L was pretreated to remove particles and chlorine then continuously supplied to the membrane element's feed-side central tube. Between production cycles, the element was osmotically backwashed by using the recirculation pump to displace the draw-side fluid with treated tapwater. Process timing, valves, pumps and other hardware were controlled and managed by a custom-built interface on a laptop running National Instruments LabVIEW™ ver. 9.0. A process diagram showing a similar experimental setup is shown in figure 3.2.1 in 3.

2.4.2.2. Computational model

A pilot computational model of the system was implemented using MATLAB™ ver. 7.12.0 (R2011a). The full details of the model are presented in chapter 5. The membrane was modelled as a sheet divided into a number of small, square segments, each separating a small draw-side volume from a corresponding feed-side volume. The general analytical model described above (see equations 2.2.5), including ECP and ICP effects was then solved for each segment by an iterative numerical method. Calculated salt and fluid flows between compartments were then used to update matrices of pressure and salt concentration for each compartment. By injecting salt into the modelled input-end of the sheet and supplying feedwater to the feed-side envelope edge, output flow-rates and concentrations were able to be updated and recorded every 10 ms of simulated time.

Variations in the experimental and evaluation parameters presented here (see table 2.3.2) were able to be simulated in the numerical model. The experimental scenario

described below was simulated and is presented in parallel with the experimental results (see section 2.4.4), and its initial and final values for c_{dt0} and c_{dts} were used for estimations of t_{eff} (see section 2.4.3.2).

2.4.3. Method

To initialise the membrane, the element draw-side was first continuously flushed with low-osmolarity feedwater for at least six minutes, to backwash any residual salt from previous experiments that may have remained in the feed-side compartment. The target output flow-rate was set to half of a typical production rate ($Q_{wtarget} = 242$ ml/min) to minimise ECP and ICP effects, and the target concentration was set to the adjusted $c_{dtarget} = 11.6$ mS/cm.

2.4.3.1. Input

At $t = 0$ minutes, the metering pump was activated so as to deliver pulses of *Part A* concentrate at a net rate corresponding to $Q_{win} = 13.8$ ml/min. Pulses were initialised cyclically, once every 4.89 seconds, to meet this rate. The draw-side output concentration, c_{dout} , was allowed to rise at its natural rate towards $c_{dtarget}$, at which point the production stage was considered to have begun.

2.4.3.2. Production

During each pulse-cycle, output fluid was collected in a vessel placed on a weighing scale. The time of arrival of each 100 g of output was recorded manually. This accumulating-mass signal was differentiated with respect to time to form a flow-rate signal that was continuously recorded (hence its step-wise nature as shown in figure 2.4.1). The output conductivity was automatically and continuously recorded.

For one-quarter of the time of each pulse-cycle, the output valve was closed, allowing the recirculating pump to draw fluid from the output-end of the draw-side compartment and deliver it to the input end, to facilitate control of the output fluid conductivity. The pump-speed was controlled by a proportional-integral controller implemented in software.

2.4.3.3. Recovery

The conductivity threshold for the end of the production phase was set at 13.0 mS/cm. As soon as output at this level was detected, the system was automatically triggered to begin its osmotic backwash phase.

A backwash time of 6.0 min., as predicted by the numerical model (see section 2.4.4.3), was used as a setting to backwash the membrane between production cycles. This was achieved by using valves to allow the recirculation pump to backwash fluid from a supply and pump it into the lower-end of the draw-side of the membrane element, displacing the entire draw-side solution and providing excess fluid to replace the volume lost to the feed-side through the membrane. After the backwashing time, the system was returned to its production settings and allowed to fill with salt again before beginning its next production phase.

2.4.4. Results

2.4.4.1. Production

The system experienced a long stabilisation phase due to having a low set target flow rate. Once adequate salt had accumulated in the system, useful dialysate was produced at the draw-side output for approximately 10 min before the system became saturated with salt. Both the target concentration and flow-rate were maintained at $\sim \pm 5\%$ throughout this period (see figure 2.4.1).

2.4.4.2. Modelling ECP and ICP

While the aim of this analysis was not necessarily to validate the experimental and numerical models against each other, the similarity between the output of the two models helps provide more information about the internal behaviour of the experimental system and the choice of parameters, particularly the use of simple approximations for μ and λ in modelling ECP and ICP.

Figure 2.4.3 shows that the spread of flux during peak production is reasonably broad, and that the maximum effect of ICP on apparent bulk, feed-side concentration, $c_f(x)$, may be as much as 4.5 times greater than that seen in an ideal element, while the effect of ECP is relatively small. The choice of an appropriate design point flux, J_{wm} , is therefore dominated by its impact on ICP effects and the value of λ ¹⁴.

Despite the wide range of values for J_{wm} , very little fluid is actually delivered at a high rate of flux, as such high flows are typically isolated to a small area of the membrane sheet (see figure 2.4.3, b). Instead, 90% of the net membrane flux falls within

¹⁴For readers interested in membrane characterisation, flux values varied widely over the membrane area due to the non-uniform distribution of salt concentration over the sheet. Chapter 5 examines this in depth, including comparison with membranes from other studies. For reference, typical flux values estimated over the area of the sheet during peak production varied between 0.5 and 1.0×10^{-6} (m/s) (see figures 2.4.2 and 2.4.3). FO processes described by Tiraferri et al. (2013) show fluxes in the range of 10 to 20 L/m²/hr (2.8 to 5.6 m/s). These are $5\times$ to $10\times$ higher than the fluxes typical of the process described here. This is to be expected, as the RO element used in this study is especially prone to ICP. See further discussion in chapter 5.

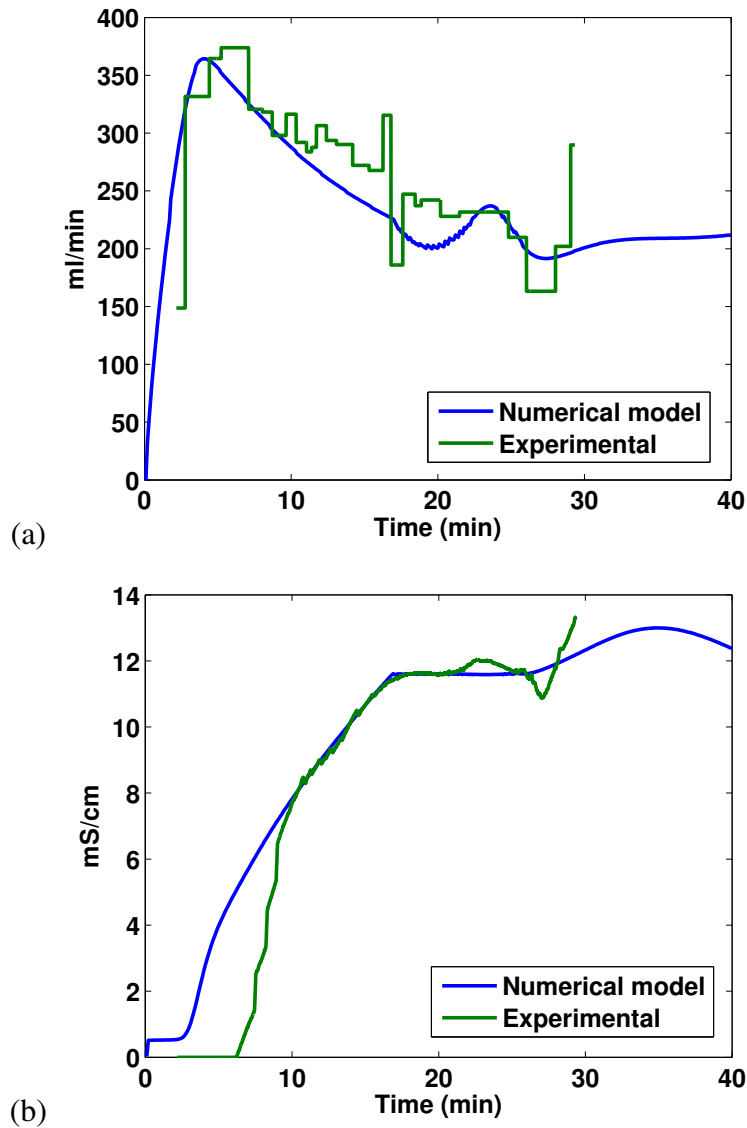


Figure 2.4.1.: Graphs of dialysate production output vs time from experiments and numerical modelling at 242 ml/min show reasonable agreement for both flow (a) and conductivity (b) responses.

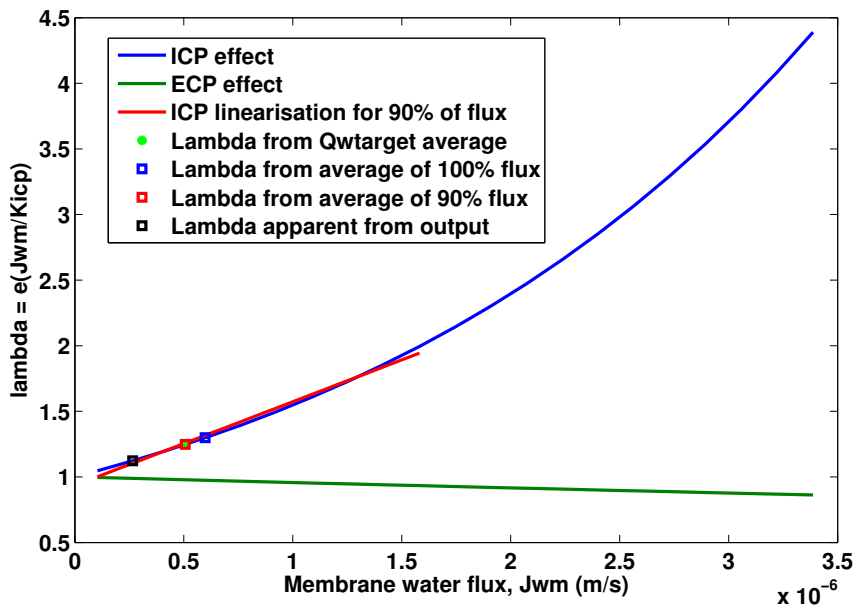


Figure 2.4.2.: ECP and ICP effects due to variations in J_{wm}

a much smaller flux range (see 2.4.3, a). The average over that range is close to the simple value calculated by $J_{wmAVG} = \frac{Q_{wtarget} - Q_{win}}{A_m}$ (see section 2.4.1.2). The various approximations for λ are shown superimposed on the plot in figure 2.4.2.

2.4.4.3. Recovery modelling

A graph of the behaviour of the bulk values of c_d and c_f during osmotic backwashing was generated using the numerical model and is shown in figure 2.4.4. The point where the whole volume of draw-solution has been displaced can be seen as an elbow in the plot of the c_d response soon after the initiation of the backwash process. After this time, the draw-side¹⁵ concentration slowly rises as it accumulates salt, while fluid is lost through the membrane to the feed-side. The bulk, feed-side concentration, c_f , continued to fall throughout the backwashing phase, with the two bulk values approaching each other after nearly six minutes¹⁶.

¹⁵At this time, the “draw-side” is temporarily feeding water across the membrane to the “feed-side”, which temporarily has a higher osmolarity, and is therefore drawing fluid across the membrane.

¹⁶Later experiments showed this to be an underestimate of the necessary backwash time (see section 5.4.3.2).

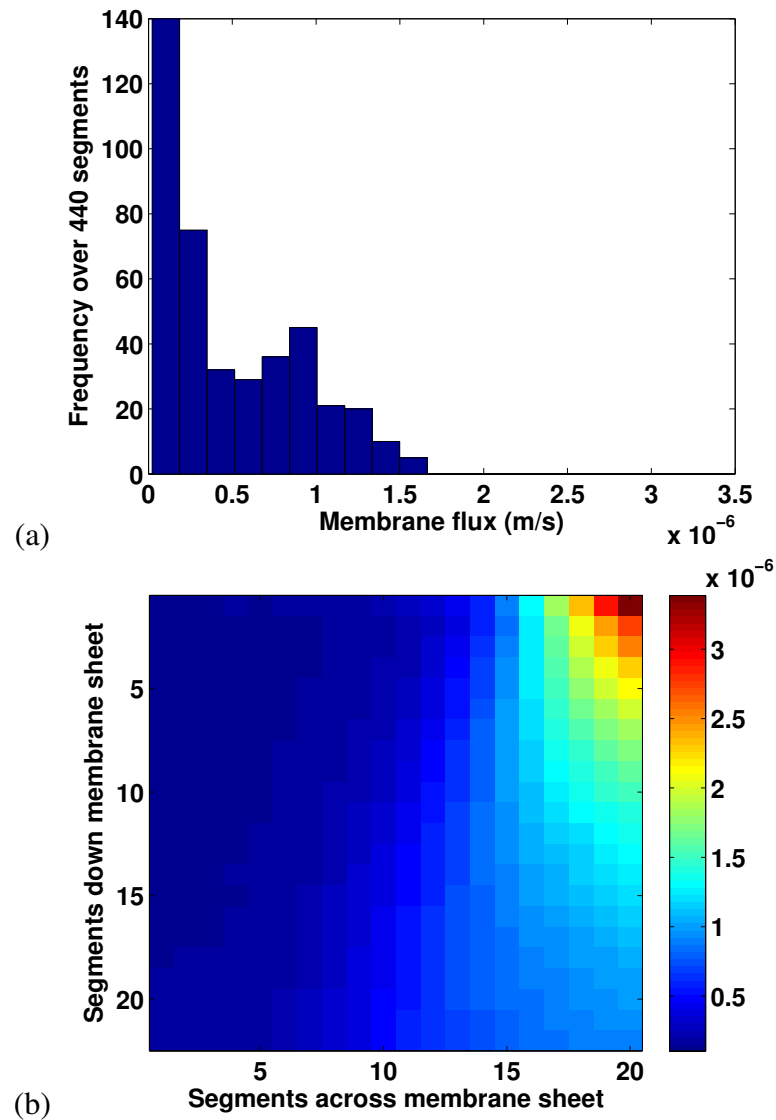


Figure 2.4.3.: Histograms of numerical modelling of trans-membrane flux show a wide range of variation over the membrane sheet. However, 90% of the fluid flow occurs over a small range (a) of flux values. Peak flows are shown to be isolated to small areas of sheet (b).

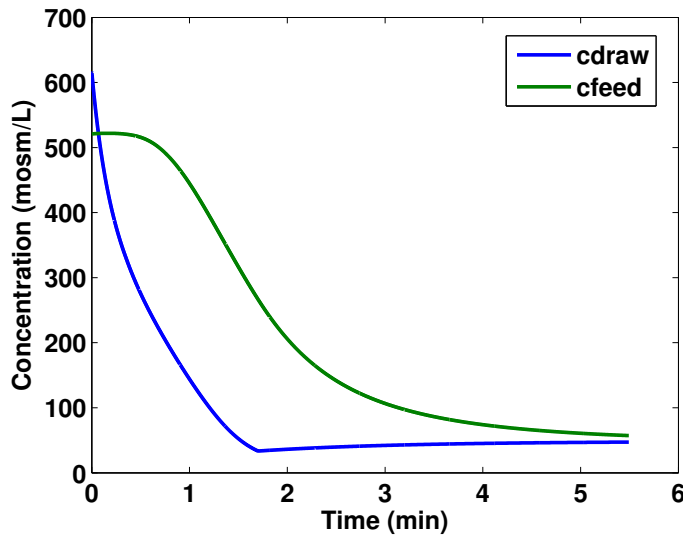


Figure 2.4.4.: Bulk draw- and feed-side concentrations approach each other during osmotic backwashing. The numerical model shows an initial phase where draw-side fluid is displaced from the element, followed by a soaking time where the draw- and feed-side bulk concentrations approach each other. In this figure, $c_d = c_{draw}$ and $c_f = c_{feed}$.

2.4.4.4. Recovery experiment

Production and backwash stages were alternated to demonstrate the recoverability of the backwash phase (see figure 2.4.5). Some oscillation is present during the conductivity-controlled production stage. Discussion of controller oscillation is explored in chapter 3.

2.5. Discussion

2.5.1. General comments

The analysis, pilot experiment and numerical modelling showed that the method proposed here has potential for use in remote dialysate production applications. The pilot experiment and modelling appeared to hold a reasonable correspondence with the theory: for most of the production stage, both conductivity and flow-rate fell within $\pm 5\%$ of their target values (see figures in 2.4.1). Nevertheless, performance must be improved further, as the tolerance on medical grade dialysate conductivity is $< \pm 2\%$ (Fresenius, 2007).

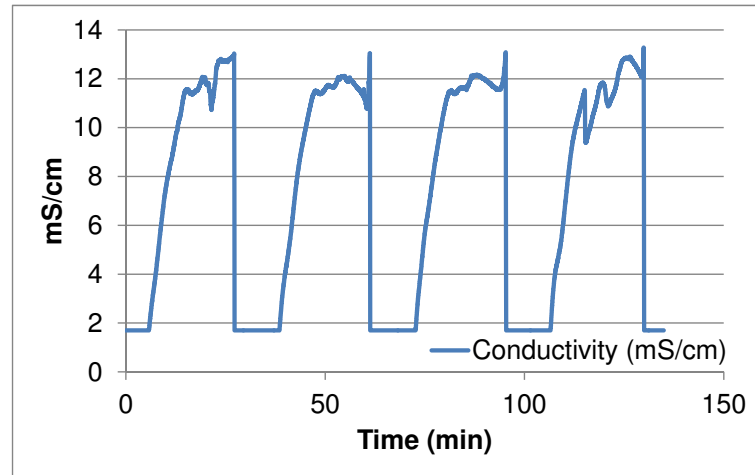


Figure 2.4.5.: Repeated experimental production and backwash cycles show occasional instability in conductivity regulation.

2.5.2. Choice of parameters

2.5.2.1. Variations in membrane element geometry

This analysis was based around a combination of the geometry of a Hydranautics™ ESPA1-4040 element and the published parameters for the Filmtec™ BW30 element used in the pilot experiments. The ESPA1 is a relatively common element used in regional dialysis applications, and one was freely available for autopsy and measurement. However, not all membrane elements use the same internal geometry as the ESPA1; there are variations in glue boundaries, active surface areas, spacer thicknesses and number of spiral-wound envelope-leaves. Nevertheless, this analysis is indicative in general of the behaviour of similar elements. To test the performance of specific elements, further experimental analysis will be necessary.

The analytical model presented in chapter 2 is one-dimensional and treats each membrane strip of length dx as a divider of compartments that are well-mixed along their width. The pilot computational model instead segments the membrane in two dimensions. Neither model has a third-dimension: both ignore interplay between adjacent sections of the spirally wrapped sheets, although others have attempted to model spiral-wrapped membranes in this way (Gu et al., 2011). Although this pilot experiment shows a degree of agreement with the numerical model, it remains to be seen whether one- or two-dimensional modelling is adequate for spiral-wound packages.

2.5.2.2. Choice of overprime factor

An overprime factor was calculated to compensate for salt leakage, salt accumulation, ECP and ICP. Since the output conductivity was controlled, the output flow was allowed to stabilise without direct intervention. In the pilot experiment, the output flow rate was observed to stabilise within 5 % of the target flow rate during a 10 min production phase, indicating that the value of the calculated overprime rate was reasonable for this system.

A major consideration in overpriming the system is the cost of dialysate concentrate, as any non-unity overpriming rate will necessarily consume more concentrate than would otherwise be consumed by an RO-based dialysate production method. Any advantages in water and energy efficiency associated with the FO method proposed here may be negated by the increased cost of the consumption of excess concentrate.

2.5.2.3. Overestimation of λ

While the simple estimate of λ used here did enable useful output to be generated by the pilot experiment, it did not quite match the actual or apparent λ value that was estimated post-hoc by running and observing numerical models. Choosing λ by taking an average of all fluxes clearly produced an overestimate (see figure 2.4.2) The simple estimate and the average over 90% of flux values were both adequate, but it remains to be seen whether there exists a more reliable method for estimating λ through modelling or experiment.

In one sense, neither μ nor λ are real process parameters, but are generalised approximations to the effects of ECP and ICP over the whole membrane sheet, and over the whole production process. It is convenient to use such values to estimate the various performance characteristics of a proposed system, such as effective production time and the necessary overprime rate, but the values do not actually reflect any real intrinsic process quantity or parameter.

2.5.2.4. Other process characteristics

All salt in the analysis and modelling was treated as completely dissociated sodium-chloride (NaCl). In practice, dialysate concentrate is made from multiple ions of various sizes, concentrations and temperature-dependent dissociation constants. If these were to be calculated more precisely, a small adjustment for the effective osmolality and membrane permeability, B , would have to be made. It is the opinion of the author that, for this analysis, these variations are likely to be insignificant compared with measurement error.

2.5.3. Production

2.5.3.1. Effective production time

The experimental production time was consistent with the value predicted by the numerical and analytical models. However, its relatively short 10 min would be inadequate for a practical system. If the stabilisation phase could be optimised, it might be possible to obtain close to the maximum theoretical production time of 21 min for the tested element, or even up to 53 minutes if a high-quality membrane was used¹⁷.

2.5.3.2. Practical flow rates

As shown in section 2.2.4, production must be paused while osmotic backwashing and recovery are carried out. The set flow-rate must therefore be raised to cover this downtime and to further compensate for the corresponding increase in ECP and ICP effects. As shown in figure 2.3.5, these effects can be severe at higher flow-rates, so much so that raising the set production target will eventually be counter-productive and will cause a decrease in apparent flow. The turning point is near the maximum apparent production value of $Q_{wtarget}^* \approx 300$ ml/min, where the system would be running at a high set flow target of $Q_{wtarget} = 730$ ml/min.

Operating at this limit would be inefficient, as the useful production volume would be significantly diminished to $V_{cycle} \approx 3.1$ L. At this rate, compared with $V_{cycle} \approx 5.5$ L for a system running at an apparent output of $Q_{wtarget}^* = 150$ ml/min. Operating the system at lower flow-rates presents a significant advantage in terms of production efficiency.

2.5.3.3. Stabilisation time

The calculations of effective production above apply only to circumstances where the process has reached a stable state of concentration output and flow-rate. Before this time, the bulk trans-membrane salt difference, Δc^* , is much larger than it normally would be during production, causing a dramatic increase in output flow-rate (see figure 2.4.1). This corresponds to rapid dilution of the draw-side fluid and corresponding loss of salt. There is a reasonable chance of greatly increasing the total useful output *volume* by injecting extra salt during this priming stage, so that the initial output flow-rate be used to produce useful dialysate.

¹⁷These predictions were based on estimates of high quality membranes and were later proven to be incorrect by experiment (see section 5.4.3.2). Computer modelling also showed that the severe effects of ECP and ICP were likely to be more significant than membrane quality (see section 5.4.1.2).

2.5.4. Recovery

2.5.4.1. Osmotic backwashing

These experiments showed that a fairly efficient backwash time for a single 4040 element may be ~ 6 min (see section 2.4.4.3), which allows about 15 min to then return the element to a state of effective production (see hard limits in evaluation section 2.3.3). This total of 21 min for backwashing and recovery should be minimised as much as possible to reduce the need for large values of $Q_{wtarget}$ and their associated ICP-related inefficiencies. The experimental analysis above shows a recovery time of $16 + 6 = 22$ min (see figure 2.4.1) which is not realistic for practical systems, as it would require an impossibly high target flow-rate (see figure 2.3.4) to produce a useful apparent flow.

2.5.4.2. Choice of backwashing fluids

During backwashing, both the draw- and feed-side fluid concentrations approach a bulk concentration value that sits somewhere between them both (see figure 2.4.4). Since the draw-side volume is much greater than that of the feed-side in this case, the final end-backwash concentration will be much closer to the initial backwash fluid concentration than to that of the saturated feed-side solution.

As discussed in section 2.3.2.1, effective production can only begin when the draw-side has been primed to a state where its output conductivity meets the target $c_{dout} = c_{dtarget}$. The state required for maximum effective production time is one where the draw-side fluid has uniform concentration at the target level along its length, that is, $c_d(x) = c_{dtarget}$ (see section 2.4.3.2). This may be achieved slowly by using the dosing pump, or may be achieved rapidly by using dialysate fluid as the backwash fluid, as this fluid is essentially a large quantity, uniformly mixed at $c_{dtarget}$. It remains to be seen exactly how much fluid volume is needed to complete each backwash, and whether backwashing with dialysate fluid is a practical approach. The compensation for large quantities of lost dialysate fluid through backwashing would greatly increase the needed target flow-rate and decrease the overall efficiency of the system. Clearly the nature, time and volume of the backwashing and recovery process is critical, and is the subject of chapter 5.

2.6. Conclusions

2.6.1. Answers to initial questions

1. What size and/or number of membrane elements would be necessary for sufficient dialysate to be continuously produced?

In general, this analysis suggests that production is maximised by having a high-quality membrane with low $\frac{B}{A}$, a low set flow-rate, $Q_{wtarget}$ and a short backwash/recovery time, t_{bf} . To facilitate adequate dialysis treatment, a practical system would need to produce dialysate at 484 ml/min. As shown in figure 2.3.5, to achieve this target would be difficult using the method described here, with a single, low-quality 4040 element. The data suggests that to achieve this flow-rate target would require an impractically short backwashing/recovery time, high peak output flows and the elimination of ECP and ICP effects. Instead, the analysis shows that an element operating at half the desired flow-rate would be much more practical as its ICP effects would be minimal and its ECP effects would be negligible. If two such elements were connected in parallel, each producing at this rate of 242 ml/min, enough dialysate would be generated for patient treatment.

2. How much production time can be expected before the feed-side envelopes fill with solute?

This analysis also shows that the effective production *time* is not as critical as the production *volume* in each cycle. This volume is a good indicator of system efficiency and is reduced by ECP and ICP effects. An efficient system with a low-quality membrane should be able to produce a useful volume of $V_{cycle} \approx 5.0$ L. This is about half the theoretical maximum volume able to be extracted from the system, $V_{max} \approx 11.3$ L. If the initial stabilisation phase can be exploited, the useful output may be greatly increased. Nevertheless, with a complete dialysis treatment requiring ~ 150 L, this will still require at least 13 production/backwash cycles.

3. How can the system be recovered so that production can continue?

The process of osmotic backwashing seems to be a reasonable approach for this system, being relatively fast and efficient. At present, the greatest delay is in the process of membrane recovery. In the experiments shown above, backwashing was done using treated, low-osmolarity tapwater: an approach that greatly reduces the total element salt, which then needs to be replaced before production can continue. This time should be made as short as possible. If the element can be backwashed using a small quantity of previously produced dialysate, this would be ideal, provided that the net loss to V_{cycle} could be tolerated.

2.6.2. Future work

There are three areas of this study that have only been examined to a basic level: the limitations of the system control arrangement, the effect of the quality of the membrane and the optimisation of an effective osmotic backwashing process.

2.6.2.1. Controller improvement

One interesting outcome of this work was the observation that the theoretical maximum production volume, $V_{max} \approx 11.3$ L, was much greater than the calculated controlled limit of $V_{cycle} \approx 5.0$ L. As discussed, this is largely due to the high flow-rate of low-osmolarity fluid that would normally be discarded at the beginning of the production cycle. If, instead, the priming rate could be adjusted together with recirculation rate, a constant output concentration, $c_{dtarget}$, may be obtained, while allowing the output to flow uncontrolled. This method would be unable to generate dialysate on demand, but would instead require useful output to be stored briefly. The optimisation of a controller for this purpose is discussed in chapter 3.

2.6.2.2. High quality membrane

The analysis above was based on modelling of an available, low-quality membrane element. From the analysis in section 2.3.2.3, it would appear that the system's efficiency may be greatly improved simply by improving the quality¹⁸ of the membrane element. This would allow a lower overprime factor, longer effective production time, less-frequent backwashing and a corresponding reduction in the set flow rate and trans-membrane flux, which would reduce the impact of ECP and ICP. The experiments in the following chapters (3, 4 and 5) include testing the system using a higher-quality membrane in the hope of reaping its many associated improvements in production efficiency.

2.6.2.3. Osmotic backwashing

The analysis shows that the system backwashing and recovery time, t_{bf} , is critical to apparent production-volume optimisation. It may be possible to end the backwash phase sooner than in the time suggested in the analysis above, trading an improvement in downtime for a loss of useful productive time. The optimisation of this relationship, together with an analysis of backwashing is the subject of chapter 5.

¹⁸“Quality” in this context refers to the ratio of B/A , where B is the membrane solute permeability and A is the membrane water permeability. The dependency of dialysate production time on membrane quality is shown in figure 2.3.3(b).

3. Dialysate production control

This chapter includes work on Fuzzy Logic Control contributed by a Masters student, Mr Hamid Kooshanfar, who worked on the project from July 2013 to July 2014. The theory and implementation of Fuzzy Logic Control in MATLAB™ and LabVIEW™ described in section 3.1.3 were largely contributed by the Masters student

The design and calibration of the conductivity sensor, tuning of the Fuzzy Logic Controller and subsequent experiments (section 3.2) were carried out collaboratively by both the author (Mr Smith) and Mr Kooshanfar. All other hardware and software development, implementation and analysis were the work of the author.

3.1. Introduction and background

The previously discussed aim of on-line FO dialysate production depends on the ability to control the draw-side dialysate output concentration at a constant value (see theoretical analysis in chapter 2). Furthermore, by injecting dialysate concentrate at a fixed rate, a constant trans-membrane concentration difference may also be maintained, stabilising the dialysate output flow-rate at its target value.

The pilot experiment and analysis showed that this simple approach to production was feasible yet inefficient. The prototype's production cycle was relatively short and was delayed by a long wind-up time before the output conductivity reached its setpoint (see section 2.4.4). During this initial priming stage, the output flow-rate was relatively high, but the dialysate produced at the output was excessively dilute. By the time production had stabilised, most of the available osmotic potential energy of the cycle appeared to have been wasted, limiting the effective volume to half that of the total fluid volume produced.

It is much simpler to implement linear controllers of single rather than multiple variables (Tan et al., 1999, pg 189). Both single- and multi-variable control is difficult when systems behave non-linearly (Kovacic and Bogdan, 2005; Wang, 1997), as was the case for the prototype, given its severe ECP and ICP (see section 5.4.1.2 in chapter 5). Rather than attempt to develop and tune a PI-based multi-input/multi-output (MIMO) controller, a Masters student working within the project team suggested using a Fuzzy Logic Controller (FLC) (see Kooshanfar (2014)). The student used

a rationale based on the ability of an FLC to easily handle non-linear processes by incorporating expert knowledge as linguistic variables, as described in Passino et al. (1998); Kovacic and Bogdan (2005); Wang (1997); Ebner et al. (2010). This is typical of linguistic approaches, such as those of Mamdani and Assilian (1975), rather than of numerical approaches, such as that of Takagi and Sugeno (1983). The student proceeded to develop the necessary theory and to implement various FLC controllers in both MATLAB™ and LabVIEW™.

3.1.1. Ideal production profile

The theoretical analysis suggested that an ideal dialysate production profile would be one with maximum effective production time and minimum time spent in priming and recovery (see section 2.6.2.1). It can be described in terms of four production stages, each with their own characteristics (see figure 3.1.1):

1. Priming stage: injection and recirculation at the maximum possible rate to reduce output conductivity rise-time and production delay.
2. Effective production: output flow-rate greater or equal to its target value, with conductivity regulated at its target value by a gradual reduction in the recirculation rate to compensate for salt accumulation on both the draw- and feed-sides.
3. Tail-end production: zero recirculation with a gradual reduction in the injection rate to maintain the conductivity at the target value.
4. Backwash/recovery: removal of accumulated salt from both sides of the element so that production can continue (see discussion and modelling of backwashing in chapter 5).
- 5.

The *priming* stage would ideally be used to introduce draw-solution into the membrane in a way that would bring the draw-side output conductivity up to the target level as quickly as possible. The rapid injection of concentrate needed to achieve this would be likely to result in a brief peak in output flow-rate due to a brief but large trans-membrane salt-difference.

With the system primed with salt, an ideal *effective production* stage would be one with constant-valued conductivity and flow-rate, both at target levels. It would be most desirable for this stage to continue for much longer than the 20 min or so shown.

It is expected that a *tail-end production* stage would be a relatively short period of decreasing production during which a small amount of excess dialysate fluid might be recovered. This would be done simply in the interest of maximising effective production volume and minimising waste. The method of backwashing and *recovery* is described in-detail in chapter 5.

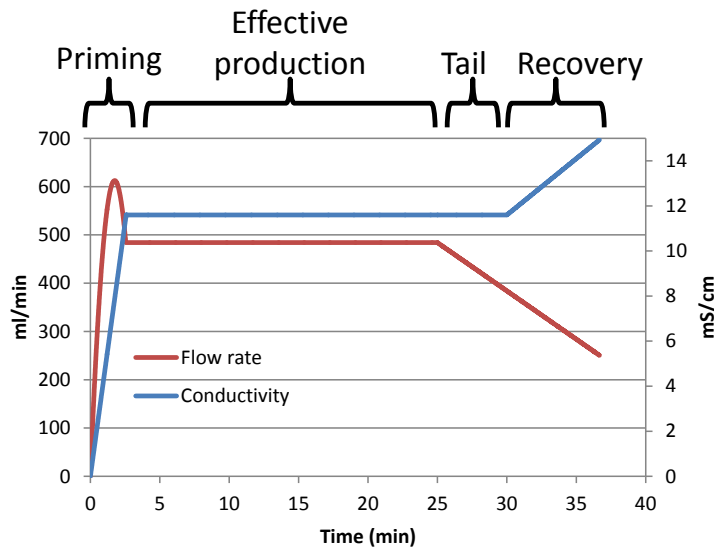


Figure 3.1.1.: Idealised output response

This idealised protocol would depend on the ability to vary both the concentrate injection rate together with the recirculation rate in response to the performance of the membrane process. To develop a controller to meet this aim, various alternative control strategies were implemented, including proportional-integral (PI) control of the output conductivity by varying the draw-side recirculation rate, the use of fixed and stepped injection rates, fuzzy-logic control of both recirculation and injection rates, and batch-control of the dialysate output stream. Examples and discussion of the experimental data from each control strategy are presented below.

3.1.2. Single-variable controller principles

The theoretical analysis highlighted the significance of conductivity control. For this reason, the initial focus was on controlling *conductivity* as a main process variable. By using a fixed concentrate injection rate, the other significant process variable, output *flow-rate*, was expected to be self-regulating, and to therefore stabilise near to its target.

A simple controller was developed, with the aim of driving the process variable for output conductivity, σ_{out} , to match its setpoint, σ_{target} . Among the simplest single-input/single-output (SISO) approaches are PI controllers (see Tan et al., 1999).

3.1.2.1. Recirculation rate

A classical parallel PI controller was implemented using tuned constants for K_p and K_i to calculate a recirculation factor, r_f , which could then be applied to regulate the

draw-side pump. The controller design was specified here in terms of discrete time samples, t_k :

$$\begin{aligned} e(t_k) &= \sigma_{target} - \sigma(t_k) \\ i(t_k) &= i(t_{k-1}) + e(t_k) \\ r_f(t_k) &= K_p \times e(t_k) + K_i \times i(t_k) \end{aligned} \quad (3.1.1)$$

The error term, $e(t_k)$, was calculated directly from the difference between the process variable and its setpoint, while the integral term, $i(t_k)$, was calculated from the previous integral value, $i(t_{k-1})$.

3.1.2.2. Injection rate

The ideal injection rate for these experiments, Q_{win0} , was calculated from the target flow-rate, $Q_{wtarget}$, according to the theoretical analysis. This was then adjusted by using an *overprime* factor, $F_{OP} = \frac{Q_{win}}{Q_{win0}}$, according to the membrane and feed-water quality, then combined with a prime-rate factor, p_f , to calculate the base injection rate, Q_{win} , as needed:

$$Q_{win} = p_f \times F_{OP} \times Q_{win0} \quad (3.1.2)$$

For the simplest cases, the prime-rate factor was set at $p_f = 1.0$, but could be stepped through other values as required, limited to $p_f = 4.0$ by the maximum injection rate of the pump hardware.

3.1.3. Multi-variable and fuzzy control

As discussed above (see section 3.1), a fuzzy controller was developed in an attempt to better match the target production profile shown in figure3.1.1.

3.1.3.1. Basic principles

Prime-rate and recirculation factors were calculated using fuzzy-logic methods as follows:

1. Membership functions were applied to the measured process variables for output conductivity, σ , and flow-rate, Q_{wout} .
2. A set of linguistic rules were applied.
3. The significance of each rule was “defuzzified” to determine p_f and r_f for the system at any given time.

3.1.3.2. Linguistic rules

The FLC's linguistic rules were developed from a basic description of the production needs, based on the idealised output response shown above (see figure 3.1.1). The following textual summary of the design needs was given to the FLC designer by the author:

The system starts in a neutral state, with equal salt concentrations on each side of the membrane and no net output flow. Useful output can only be obtained when sufficient salt has accumulated on the draw-side to allow the output-end to reach the target concentration, so the initial phase should involve a rapid injection of concentrate and high recirculation. This should raise the concentration to a useful level as quickly as possible. Once this state is attained, injection may be reduced to the normal level and recirculation may be gradually reduced in order to maintain a fixed output concentration while the total salt in the membrane element accumulates. As the recirculation rate approaches zero, the total salt may approach its maximum level. At this point, the injection rate may be reduced to prolong the production time, while reducing the output flow rate and maintaining a fixed output concentration. Eventually this will no longer be sustainable, the element will be saturated with salt and production will be unable to continue without backwashing the element.

This paragraph of design concepts was then translated into linguistic rules, combining four input states for conductivity and two for flow rate with four possible output levels for both the prime-rate and recirculation factors (see table 3.1.1).

The linguistic qualities for the prime-rate and recirculation factors were also set to specific values in vectors, \mathbf{p} and \mathbf{r} :

$$\mathbf{p} = \begin{bmatrix} p_{max} \\ p_{max} \\ p_{max} \\ p_{high} \\ p_{high} \\ p_{normal} \\ p_{low} \\ p_{normal} \end{bmatrix} \quad \mathbf{r} = \begin{bmatrix} r_{max} \\ r_{max} \\ r_{high} \\ r_{high} \\ r_{normal} \\ r_{normal} \\ r_{zero} \\ r_{zero} \end{bmatrix} \quad (3.1.3)$$

3.1.3.3. Membership functions

The linguistic qualities for conductivity and flow were translated into logical membership functions, according to the target values, σ_{target} and $Q_{wtarget}$. The membership functions for conductivity were numbered from 0 \rightarrow 3 and took forms similar to those

1. If the conductivity is in the *startup* state and the flow is *low*, the recirculation rate and prime factor should both be at *maximum*.
2. If the conductivity is in the *startup* state and the flow is *OK*, the recirculation rate should be at *maximum*, while the prime factor should be at *maximum*.
3. If the conductivity is in the *low* state and the flow is *low*, the recirculation rate should be *high* and prime factor should be at *maximum*.
4. If the conductivity is in the *low* state and the flow is *OK*, the recirculation rate should be *high* and prime factor should be *high*.
5. If the conductivity is in the *OK* state and the flow is *low*, the recirculation rate should be *normal* and the prime factor should be *high*.
6. If the conductivity is in the *OK* state and the flow is *OK*, the recirculation rate should be *normal* and the prime factor should be *normal*.
7. If the conductivity is in the *high* state and the flow is *low*, the recirculation rate should be *zero* and the prime factor should be *low*.
8. If the conductivity is in the *high* state and the flow is *OK*, the recirculation rate should be *zero* and the prime factor should be *normal*.

Table 3.1.1.: FLC linguistic rules

3.1 Introduction and background

shown in figure 3.1.2 (a). Each function was defined piecewise based on a Gaussian distribution¹, centred at σ_i , with spread determined by a tuned factor, a_i :

$$m_{\sigma i} = \begin{cases} 1 & \text{if } (i \leq 1) \text{ and } (\sigma < \sigma_i) \\ 1 & \text{if } (i = 3) \text{ and } (\sigma > \sigma_i) \\ e^{-\frac{1}{2} \left(\frac{\sigma - \sigma_i}{a_i} \right)^2} & \text{otherwise} \end{cases} \quad (3.1.4)$$

The membership functions for flow-rate were numbered from 1 \rightarrow 2 and took forms similar to those shown in figure 3.1.2 (b). Each was based on a simple, first-order, linear relation between lower and upper limits, Q_L and Q_R .

The *low* flow-rate membership function, m_{Q1} , was defined:

$$m_{Q1} = \begin{cases} 1 & \text{if } Q_{wout} < Q_L \\ \frac{Q_{R1} - Q_{wout}}{Q_{R1} - Q_{L1}} & \text{if } (Q_{wout} \geq Q_L) \text{ and } (Q_{wout} \leq Q_R) \\ 0 & \text{if } Q_{wout} > Q_R \end{cases} \quad (3.1.5)$$

Similarly, the *OK* flow-rate membership function, m_{Q2} , was defined:

$$m_{Q2} = \begin{cases} 0 & \text{if } Q_{wout} < Q_{L2} \\ \frac{Q_{wout} - Q_{L2}}{Q_{R2} - Q_{L2}} & \text{if } (Q_{wout} \geq Q_{L2}) \text{ and } (Q_{wout} \leq Q_{R2}) \\ 1 & \text{if } Q_{wout} > Q_{R2} \end{cases} \quad (3.1.6)$$

Each of these allowed a membership vector to be assembled according to the linguistic rules above. The first membership-value was concerned with conductivity in the *start-up* state, with both conductivity and flow being *low*. This allowed a weighting for the first rule to be written as $u_1 = m_{\sigma 0} \times m_{Q1}$. The remaining rules were added to a rule vector, \mathbf{u} , as follows:

$$\mathbf{u} = \begin{bmatrix} m_{\sigma 0} \times m_{Q1} \\ m_{\sigma 0} \times m_{Q2} \\ m_{\sigma 1} \times m_{Q1} \\ m_{\sigma 1} \times m_{Q2} \\ m_{\sigma 2} \times m_{Q1} \\ m_{\sigma 2} \times m_{Q2} \\ m_{\sigma 3} \times m_{Q1} \\ m_{\sigma 3} \times m_{Q2} \end{bmatrix} \quad (3.1.7)$$

¹The use of the symbol, σ_i , was chosen to be consistent with the symbol for conductivity used elsewhere in this document. This was considered to be a higher priority than the traditional use of σ as a term to denote measures of spread such as *standard deviation* where probability distributions such as Gaussian curves are used.

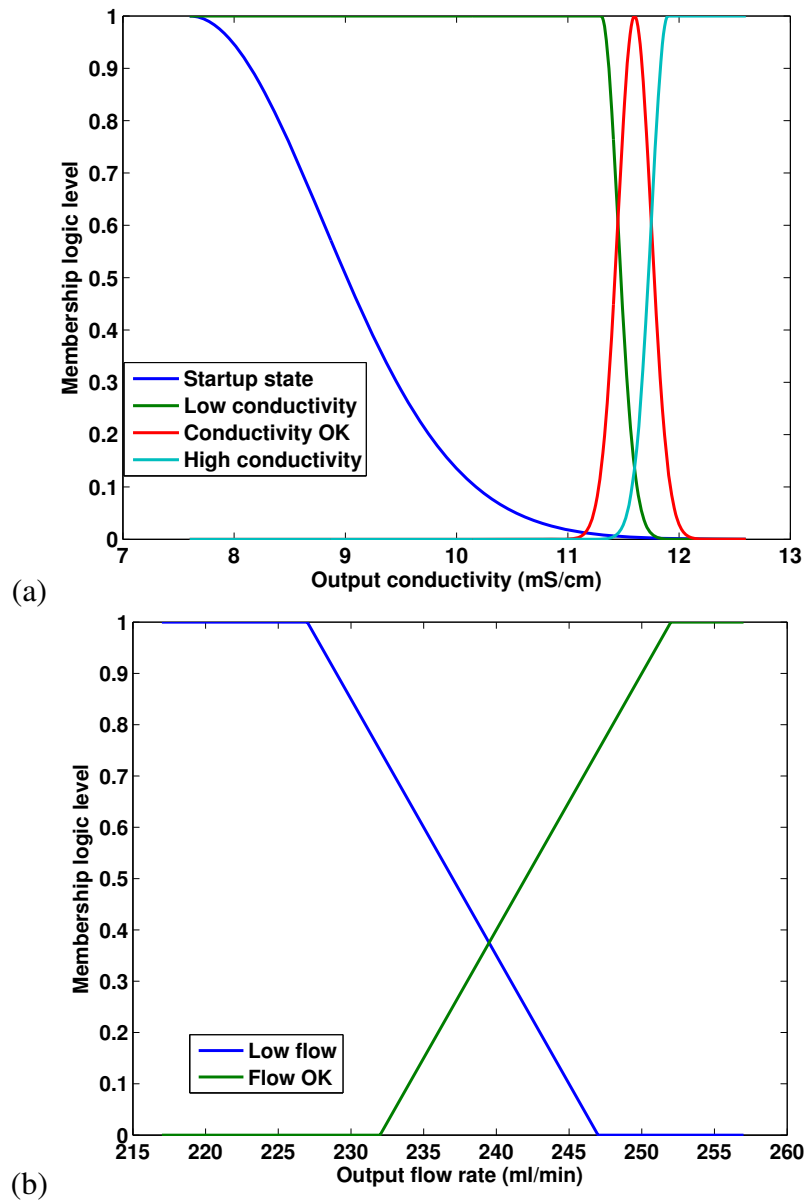


Figure 3.1.2.: FLC conductivity (a) and flow (b) membership functions for set-targets of $\sigma_{target} = 11.6$ mS/cm and $Q_{wtarget} = 242$ ml/min.

In practical systems, this rule-vector corresponds to a set of weights that may be used for determining which process variables and actuator responses are to be given the highest priority.

3.1.3.4. Defuzzification

The rule vector, \mathbf{u} , and the output vectors, \mathbf{p} and \mathbf{r} , were combined (using vector dot-products) to determine values for p_f and r_f which were then able to be passed to the hardware controller to adjust the physical actuators:

$$\begin{aligned} p_f &= \frac{\mathbf{u} \cdot \mathbf{p}}{\Sigma \mathbf{u}} \\ r_f &= \frac{\mathbf{u} \cdot \mathbf{r}}{\Sigma \mathbf{u}} \end{aligned} \quad (3.1.8)$$

3.2. Materials and Methods

A series of experiments were carried out, with the protocols for each experimental method selected according to the needs identified in preceding experiments (see section 3.2.6). Each experimental protocol is described first in detail here.

3.2.1. Apparatus

3.2.1.1. Membrane assembly

A polyamide TFC RO membrane element (ESPA2-4040, Hydranautics, Nitto Denko), with an active area of 8.9 m², was selected and placed within a suitable pressure vessel (300-E41, Wave Cyber Ltd., Shanghai). The vessel was constructed with end-cap fluid connections for both the high-pressure (RO feed/brine) side of the membrane spiral and the central (RO permeate) tube. The assembly was mounted vertically to facilitate the removal of entrapped air. The RO brine/feed-side of the membrane was used as the draw-side in the experimental FO process. Similarly, the RO permeate side was used as the FO feed-side.

3.2.1.2. Fluid handling

A process diagram showing the experimental fluid connections is shown in figure 3.2.1. The uppermost draw-side connector was fitted with a T-piece to allow recirculation of the draw-side fluid through two branches, and the injection of draw solution via the third branch. A piston-diaphragm displacement pump (Model 671353, Fresenius

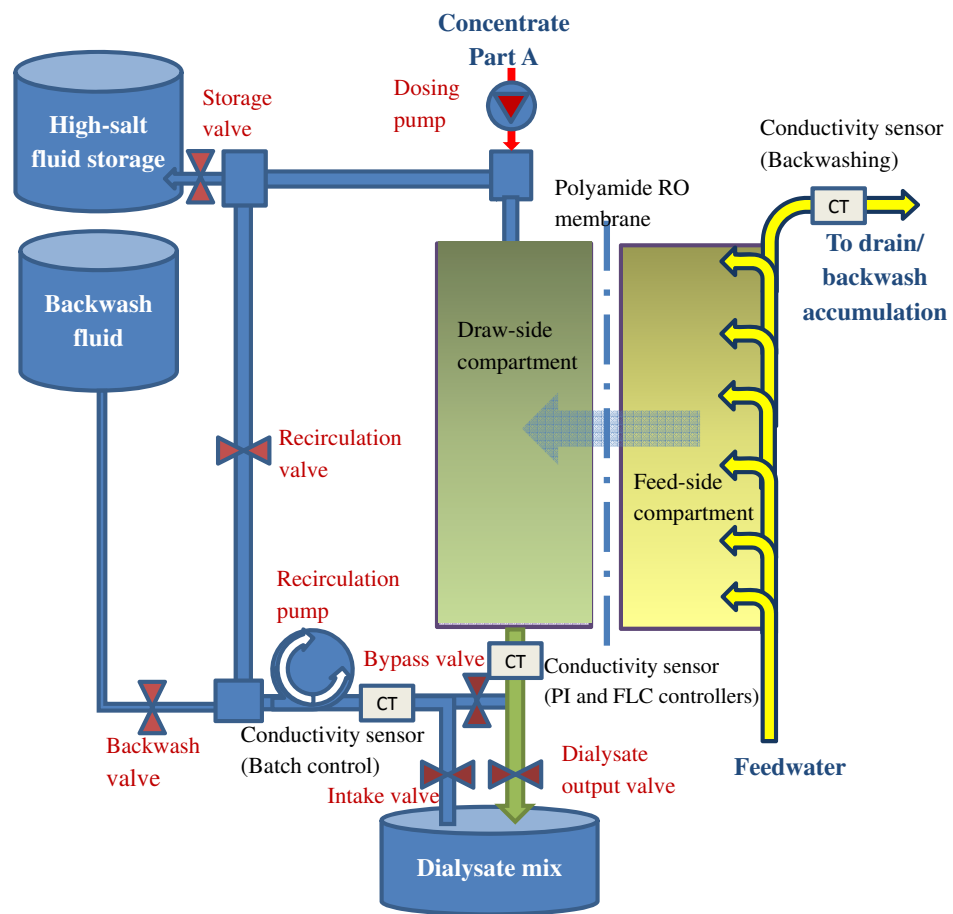


Figure 3.2.1.: Hardware arrangement for dialysate production

3.2 Materials and Methods

Medical Care) was recovered from a disused Fresenius dialysis machine and connected so as to draw concentrate from a container and inject it into the system's draw-side compartment via the third branch of the upper T-piece. The pump's dosing chamber had a fixed volume of ~ 1.1 ml and its stepper-motor was driven by a 24 V circuit that, when triggered, delivered its chamber volume in ~ 0.6 s. Triggering was set so that one pulse was delivered in a fixed period, called a "switching cycle". This was a rate derived from the Fresenius™ dialysis machine's hardware, which is normally configured so as to deliver the set dialysate flow rate in a series of discrete 30 ml volume pulses: one per switching cycle.

The fluid path immediately above the injection point was fitted with a small, PVC air-trap chamber of about 50 mL volume, that was able to be vented to atmosphere to release trapped air. The draw-side fluid path was connected from this point to a recovered 24 VDC gear pump (Model KW34/06, Fresenius Medical Care) that was arranged to recirculate fluid between the upper and lower membrane draw-side fluid connections. The pump motor was driven by a chopped 24 VDC excitation wave that was able to be varied to control the motor speed. The motor direction was also able to be reversed as needed. The pump's maximum flow rate under-load was ~ 1400 ml/min. At a 12% duty speed setting, its flow rate was measured at ~ 50 ml/min.

24 VDC solenoid valves (Model R092004, RAPA Valves) were used to manage the system's fluid paths during different production phases (see figure 3.2.1). During the production phase, the *Dialysate output valve*, *Intake valve* and *Recirculation valve* were open, while all other valves were closed. During backwashing, the *Backflush and makeup fluid* container was filled with a low-osmolarity fluid, then the *Backflush valve*, *Bypass valve* and *Storage valve* were opened, while all other valves were closed. This enabled backwash fluid to be pumped upwards from its container, through the draw-side of the element and discarded into the *High-salt storage* container.

3.2.1.3. Solutions

Dialysate concentrate *Part A* (Concentrated Haemodialysis Solution AC-F 2135LG-Part-A, Fresenius Medical Care, Australia) was used as a draw-solution. The feed-side was supplied with tap-water that was pre-treated by passing it through carbon and micron filters to remove chlorine, chloramines and particulate. The pre-treated supply was similar to that which would normally be used to supply an RO machine. The feedwater supply was connected to the lower feed-side connector on the pressure vessel end-cap. The upper feed-side connector was connected to drain. A desktop RO unit (WRO 95, Gambro Inc.) was used to fill the *Backflush and makeup fluid* container with RO water when required for backwashing.

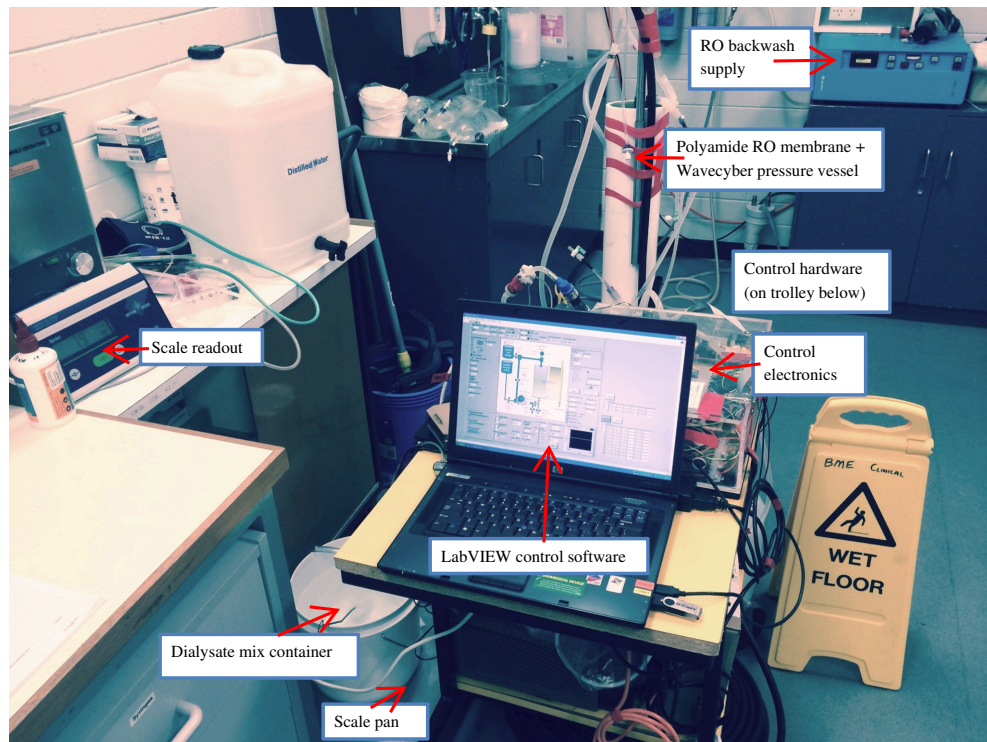


Figure 3.2.2.: Hardware arrangement for dialysate production

3.2.1.4. Instrumentation

A conductivity sensor was recovered from a disused Fresenius 4008 series dialysis machine. It was driven by a 5.0 VAC, 1.0 kHz excitation. The resulting voltage signal amplitude was temperature-compensated and calibrated against a reference instrument (UMED D0094, Fresenius Medical Care). The sensor was connected near the dialysate intake tube to measure the conductivity of the dialysate output mix. Dialysate output was directed into a large, stirred collection container that was placed on a set of scales (Spider 1, Metler-Toledo International Inc.) to record output volumes.

3.2.1.5. Control

All measurement and control was automated using an A/D interface (NI-DAQmx 6008, National Instruments Inc.) and LabVIEW software (ver 8.2, National Instruments Inc.) running on a Windows/Intel PC laptop (Compaq nc8230, HP Inc.). The program was custom-made and arranged to enable the automation of various production phases. The software interface allowed the input of various parameters, such as desired target conductivity levels, flow rates and overprime factors.

3.2 Materials and Methods

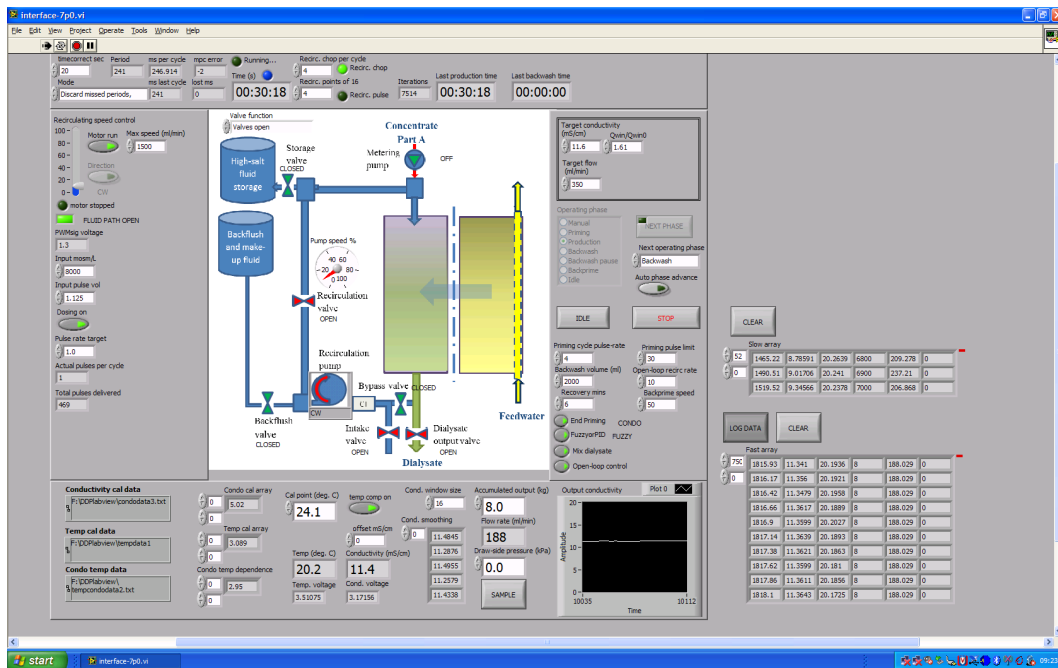


Figure 3.2.3.: Hardware arrangement for dialysate production

3.2.2. Osmotic backwashing

The element was backwashed before and after each experiment for at least 10 minutes. This was achieved by running the recirculation pump at maximum speed in a counter-clockwise direction to continuously push low-osmolarity fluid through the element's draw-side compartment, displacing any draw-solution. During this stage, the backwashing fluid was allowed to permeate through the membrane and flush saltier feed-side fluid to drain via the feed-side tube until the trans-membrane concentration difference was negligible. A full analysis of the mechanism of osmotic backwashing is described in chapter 5.

3.2.3. Injection protocols

3.2.3.1. Simple injection

For the initial experiments, the prime factor was fixed at $p_f = 1.0$, with the expectation that the output flow-rate would stabilise close to its target value once the conductivity had been stabilised by the controller.

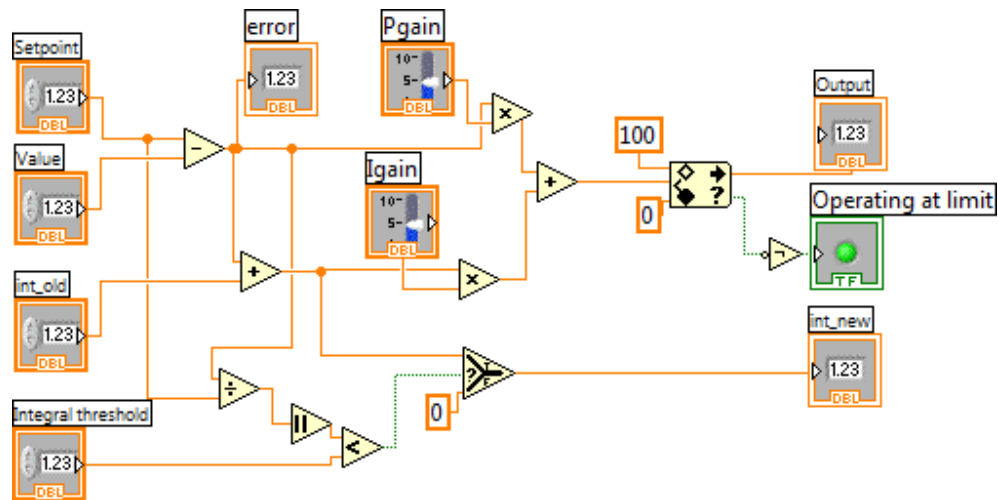


Figure 3.2.4.: PI controller implementation in LabVIEW™

3.2.3.2. Two-stage injection

In order to shorten the priming stage without resorting to multi-variable control, the injection rate was increased during this stage so that the bulk, draw-side concentration needed for effective production would be obtained sooner. A range of prime-rate factors were tested to facilitate this. As soon as the output conductivity reached its target value, the prime-rate was reduced back to its normal rate of $p_f = 1.0$.

3.2.4. Control protocols

3.2.4.1. PI control of recirculation

A parallel-type PI controller was developed and implemented using LabVIEW. To avoid wind-up problems or saturation, the *integral* contribution was disabled ($K_i = 0$) until a specified threshold was reached (see method in Parr, 1998). The output was limited to the operating range of the pump ($0 \rightarrow 100\%$).

The PI controller was tuned as required by trial-and-error (see Tan et al., 1999).

3.2.4.2. Fuzzy logic control

An FLC was implemented in LabVIEW™ according to the principles described above (see section 3.1.3). The same setpoints were used for the FLC as for the PI controllers. The tuning of the FLC controller was relatively complicated and proceeded as follows:

1. Conductivity membership function centres, σ_i , and spread factors, a_i , were chosen and adjusted according to the desired system response.

3.2 Materials and Methods

2. Flow-rate membership function limits were fixed using limits at $Q_{L1,2}$ and $Q_{R1,2}$.
3. Through several iterations, optimal p and r values were chosen by trial-and-error.
4. Steps 1-3 were repeated to until an optimal output response with fast rise-time and minimal ripple was able to be obtained.

For experiments using this protocol, the *priming* conductivity membership function was found to be unhelpful and was therefore disabled by setting the relevant p and r values to zero. The flow-rate membership function parameters were chosen in relation to the flow-rate target, $Q_{wtarget}$:

$$\begin{aligned}
 Q_{L1} &= Q_{wtarget} - 15 \\
 Q_{R1} &= Q_{wtarget} + 5 \\
 Q_{L2} &= Q_{wtarget} - 10 \\
 Q_{R2} &= Q_{wtarget} + 5
 \end{aligned} \tag{3.2.1}$$

Similarly, conductivity membership function centres were chosen in relation to the conductivity target, σ_{target} :

$$\begin{aligned}
 \sigma_0 &= \text{(unused)} \\
 \sigma_1 &= \sigma_{target} - 0.4 \\
 \sigma_2 &= \sigma_{target} \\
 \sigma_3 &= \sigma_{target} + 0.3
 \end{aligned} \tag{3.2.2}$$

The conductivity membership spread factors, a_i , were chosen manually over several iterations:

$$\begin{aligned}
 a_0 &= \text{(unused)} \\
 a_1 &= 0.07 \\
 a_2 &= 0.2 \\
 a_3 &= 0.1
 \end{aligned} \tag{3.2.3}$$

Lastly, the actuator vectors were chosen to optimise the rise time and minimise ripple:

$$\mathbf{p} = \begin{bmatrix} 0 \\ 0 \\ 4.0 \\ 4.0 \\ 1.6 \\ 1.6 \\ 1.2 \\ 1.2 \end{bmatrix} \quad \mathbf{r} = \begin{bmatrix} 0 \\ 0 \\ 100 \\ 100 \\ 100 \\ 100 \\ -50 \\ -50 \end{bmatrix} \tag{3.2.4}$$

In particular, the actuator vectors were constructed to render the membership of either *flow* state irrelevant: the output was set to be the same whether the flow rate was *low*

or *OK* for each rule. Furthermore, the *high* conductivity recirculation rates were set to negative values, even though any negative signal sent to the recirculation pump would be rounded to zero. This was done to artificially lower output in the region where the *OK* and *high* conductivity membership functions were both partially *true*. The effect of this adjustment should be interpreted as a re-shaping of the right-hand-side of the *OK* conductivity function, rather than the imputation of any negative recirculation factor.

3.2.5. Output management protocols

3.2.5.1. Recirculation chopping

For experiments with this protocol, the output valve was left open throughout the production cycle, while opening and closing (“chopping”) the recirculation valve once per switching cycle. This was done to average the output concentration between the system’s natural output value and the effect of forced dilution caused by high values of recirculation (see discussion on paradoxical flow in section 3.3.7). Furthermore, the output recirculation was set such that high recirculation rates were only used during the *priming* stage, at which time the forced dilution of the output was not so critical. The *production* stage recirculation rates were set to low values to minimise this sensitivity to non-ideal paradoxical behaviour:

$$\mathbf{p} = \begin{bmatrix} 2.0 \\ 2.0 \\ 2.0 \\ 2.0 \\ 1.0 \\ 1.0 \\ 0.8 \\ 0.8 \end{bmatrix} \quad \mathbf{r} = \begin{bmatrix} 80 \\ 80 \\ 20 \\ 20 \\ 0 \\ 0 \\ 0 \\ 0 \end{bmatrix} \quad (3.2.5)$$

$$\begin{aligned} \sigma_0 &= \sigma_{target} - 4.0 \\ \sigma_1 &= \sigma_{target} - 0.3 \end{aligned} \quad (3.2.6)$$

$$\begin{aligned} a_0 &= 1.2 \\ a_1 &= 0.15 \\ a_2 &= 0.15 \\ a_3 &= 0.15 \end{aligned} \quad (3.2.7)$$

3.2.5.2. Alternating output

For experiments with this protocol, flow was alternately diverted between output and recirculation fluid paths once in each switching cycle. This was done to allow dialysate output to flow freely without the membrane performance being disturbed by simultaneous recirculation effects:

1. The bypass valve was opened to allow the free recirculation of fluid from the output to the injection end of the membrane element.
2. The output valve and recirculation valve were then alternated between being open and closed, ensuring that at no time would both be open simultaneously.
3. The valves were arranged to maximise output flow, by setting the timing so that the output valve was open $3/4$ of the time, while the recirculation valve was open only $1/4$ of the time.
4. The recirculation pump was fitted with a bypass valve that allowed it to cycle a small fluid quantity around a closed loop whenever the recirculation valve was closed, to save frequently turning the pump on and off. This was done at a sacrifice of recirculation efficiency (down to $1/4$ of the maximum equivalent rate).

3.2.5.3. Free-flow output

To increase the sensitivity of the recirculation pump for some experiments, the valve management was adjusted so that both the dialysate output and recirculation valves were open throughout the *production* stage. During transitions from low to high recirculation rates, negative pressures were observed at the system output. These were counteracted by adding a check valve to the output tube to eliminate any backflow into the system.

3.2.5.4. Batch output

For these experiments, the conductivity sensor was moved to its secondary position where it was used to monitor the conductivity of the accumulating dialysate output fluid. The FLC was used as above, although careful FLC tuning was unnecessary due to the slow response time of this configuration. The controller was used mainly to manage the transition from *high* to *low* recirculation rates during the *production* stage, in order to maximise the effective production time.

3.2.6. Experimental methods

3.2.6.1. Experiment one: Fixed injection, PI recirculation, alternating output

The method for experiment *one* was most similar to the original intended method as proposed in the theoretical analysis (see chapter 2). The following tuning and other parameters were selected:

$$\begin{aligned}
 p_f &= 1.0 \\
 Q_{wtarget} &= 242 \text{ ml/min} \\
 \sigma_{target} &= 11.6 \text{ mS/cm} \\
 F_{OP} &= 1.61 \\
 K_p &= 80 \\
 K_i &= 0.2
 \end{aligned} \tag{3.2.8}$$

The recirculation rate, r_f was determined by the PI controller. Dialysate was alternately diverted through the output and recirculation fluid paths.

3.2.6.2. Experiment two: Two-stage injection, PI recirculation, alternating output

The same parameters and approach were used for experiment *two* as for experiment *one*, with the exception of the value of p_f . This experiment was repeated using various initial levels of $p_f = 2.0, 3.0, \text{ and } 4.0$. In each case, the prime-rate factor was immediately reduced to its typical value of $p_f = 1.0$, as soon as the conductivity target was reached.

3.2.6.3. Experiment three: Fuzzy-logic control, alternating output

Similar parameters were used for experiment *three* as for experiments *one* and *two*, with the exception of both p_f and r_f : for this experiment, both were managed by the FLC instead of the PI controller.

3.2.6.4. Experiment four: Fuzzy-logic control, free-flow output

Experiment *four* was similar to experiment *three*, except that for this experiment there was no alternation between recirculation and output fluid paths. The two fluid paths were both allowed to be open simultaneously. Backflow was limited by a check-valve at the dialysate output.

3.2.6.5. Experiment five: Fuzzy-logic control, recirculation chopping

This experiment was similar to experiment *four*, except that in this experiment the recirculation fluid path was chopped to average the output conductivity and to reduce the problem of paradoxical dilution (see discussion in section 3.3.7).

3.2.6.6. Experiment six: Fuzzy-logic control, free-flow output, batch output

Experiment *six* was also similar to experiment *four*, except that for this experiment the output fluid was collected in a stirred container throughout the whole production stage.

3.3. Results and discussion

The results presented here were each selected from a series of repeated experiments carried out during a process of iterative design. As such, each experiment was repeated three to five times, depending on whether or not it appeared to be producing desirable performance. When the performance was poor, parameters were altered with the aim of optimising the behaviour. As such, each general design protocol or experiment was repeated dozens of times, with variations in parameters added when the system did not appear to be performing. The best examples in each protocol are presented here.

3.3.1. Experiment one: Fixed injection, PI recirculation, alternating output

Given that the aim of this experiment was to produce stable output conductivity as a first priority, and stable output flow as a second, the most significant findings of these results is shown in the conductivity data (rather than the flow data) graphed in figure 3.3.1.

The figure shows that in the 30 min production cycle, the peak output flow-rate occurred long before the output conductivity had reached its target value. The output conductivity appeared to stabilise at 17 min and continue for about 13 min. There was a brief period of oscillation at 26 min. This represents a relatively brief effective-production time, compared with the significantly longer priming stage. This highlighted the need for a more efficient controller design, as discussed in section 3.1.

There was no evidence of the expected stabilisation of the output flow-rate at its target, as predicted by the theoretical analysis (see section 2.5.3.3), although the flow-rate remained greater than its target for most of the production phase. This lack of stability in the output flow-rate was somewhat perplexing, considering that the theoretical analysis

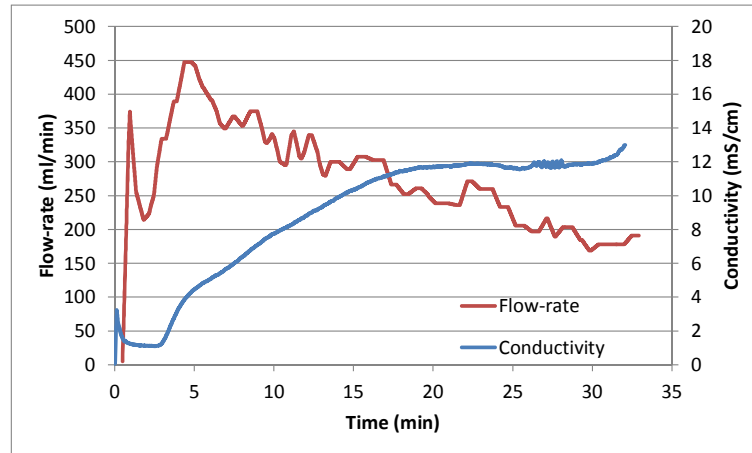


Figure 3.3.1.: Experiment one: Target flow at 242 ml/min; target conductivity at 11.6 mS/cm; PI control of conductivity; fixed injection rate; alternating output and recirculation valves throughout.

predicts simultaneous stability of both conductivity and flow-rate. However, the theory also depends on calculating F_{OP} based on fixed approximations to ECP and ICP. Given that concentration polarisation effects are more severe at high flux-rates (which occur early in the production stage) and at high concentrations (later in production), the rates of salt-leak and fluid flux may have been incorrectly estimated for these stages.

3.3.2. Experiment two: Two-stage injection, PI recirculation, alternating output

This experiment was designed in order to improve upon the production profile of experiment *one* towards the ideal by shortening the priming phase and startup time. The improved response can be seen in the rise-time and stability of the conductivity response curve in the example shown in figure 3.3.2.

This technique of increasing the injection rate during the priming phase had the advantage of rapidly advancing the time from which effective output was able to be obtained. In this example, effective output was obtained from 5 min, but production only lasted half as long as in the previous experiment and conductivity was out of range by about 10 min. Meanwhile the peak output flow-rate occurred well before the target conductivity was reached and was more than twice as high as that of experiment *one*. There was also a noticeable drift away from the target conductivity value during the production stage, following the return of the prime-rate factor to its normal level at $p_f = 1.0$. This drift was likely to have been caused by the need for the system to restabilise following the drop in the salt injection rate and corresponding loss of trans-membrane fluid flux.

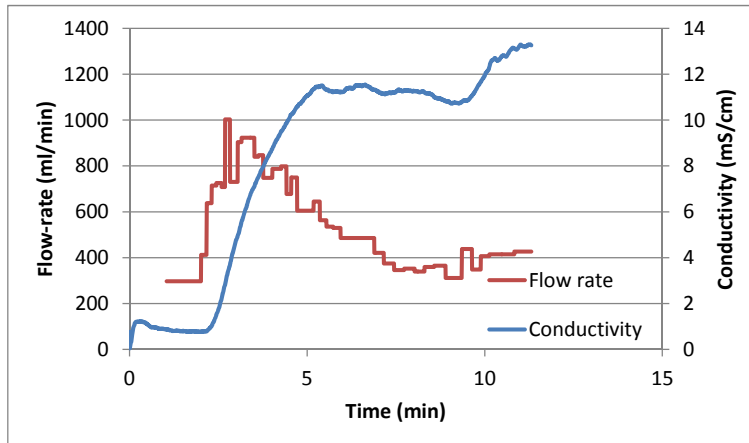


Figure 3.3.2.: Experiment two: Target flow at 242 ml/min; target conductivity at 11.6 mS/cm; PI control of conductivity; injection at $p_f = 4.0$ until the conductivity target was reached and at $p_f = 1.0$ thereafter; alternating output and recirculation valves throughout.

3.3.3. Experiment three: Fuzzy-logic control, alternating output

To address the loss of conductivity stability during the transition from a high to a low injection rate, an FLC was used to gradually reduce the input injection rate rather than reducing it suddenly. An example of the response typical of this experiment is presented in figure 3.3.3.

In this experiment, the priming stage was shorter than that of previous experiments, but neither the output conductivity nor flow-rate stabilised during the production stage. The controller performance appeared to be better for conductivity control than its PI equivalent, yet caused occasional and sudden drops in conductivity (see artifacts in the conductivity graph shown in figure 3.3.3 at 6 min, 9.0 min, 11 min and 13 min). Despite this, the average output conductivity was relatively stable over the production stage.

While it can be shown that for an ideal element, the net trans-membrane flow is independent of the internal salt-distribution along the membrane channel (see theoretical analysis in section 2.2.2.2), for practical elements the effects of ECP and ICP vary whenever the internal salt distribution of a membrane process is changed (see theoretical analysis in chapter 2). This implies that for this experiment, the trans-membrane flux and corresponding output flow-rate were likely to have varied together with ECP and ICP effects, whenever the recirculation rate, r_f , was changed. This was suspected to have been further exacerbated by the paradoxical behaviour discussed below in section 3.3.7.

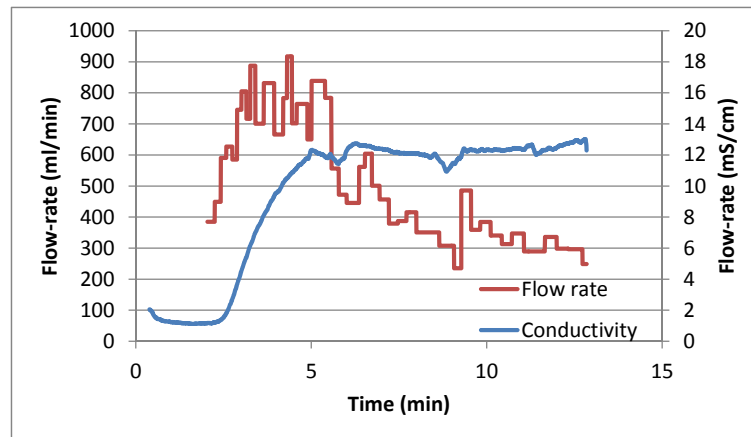


Figure 3.3.3.: Experiment three: Target flow at 242 ml/min; target conductivity at 11.6 mS/cm; FLC control of conductivity and injection; alternating output and recirculation valves throughout.

3.3.4. Experiment four: Fuzzy-logic control, free-flow output

By allowing unrestricted output flow with simultaneous recirculation, it was expected that the sensitivity of the FLC would be improved by enabling faster response to changes in conductivity around the target setpoint. The other intended advantage of this protocol was that it would allow for much higher output flow-rates compared with other methods (see flow-rate graph in figure 3.3.4).

The output production peak occurred at a time when the target conductivity had already

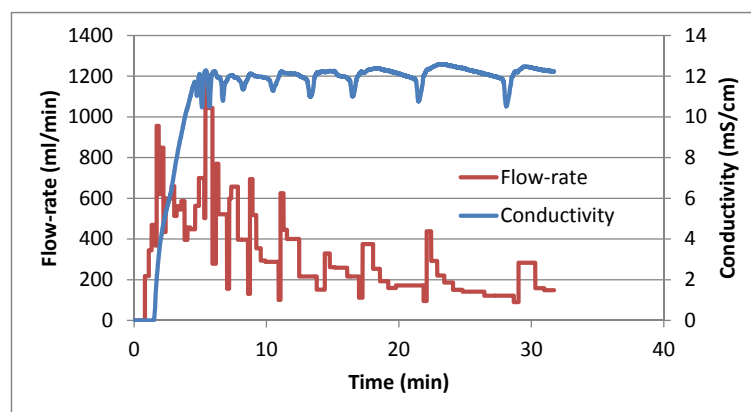


Figure 3.3.4.: Experiment four: Target flow at 242 ml/min; target conductivity at 11.6 mS/cm; FLC control of conductivity and injection; open recirculation and output valves throughout.

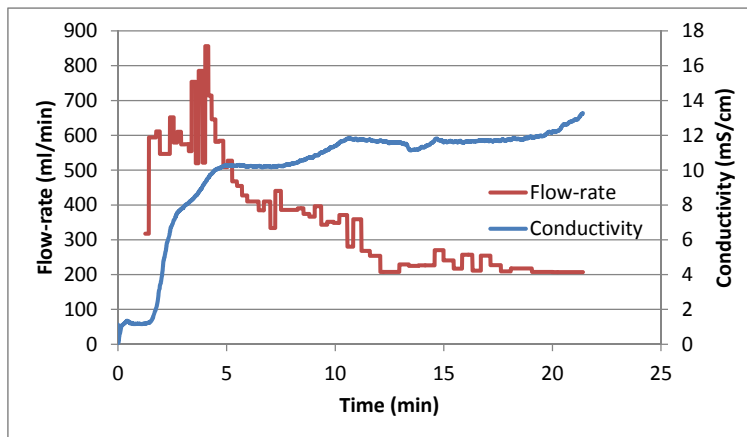


Figure 3.3.5.: Experiment five: Target flow at 242 ml/min; target conductivity at 11.6 mS/cm; FLC control of conductivity and injection; chopped recirculation valves; open flow at output.

been reached (6 min). This was likely to be due to the inherent compliance in the system, such that whenever the recirculation rate was at maximum, the distribution of draw-side fluid was shifted towards the injection-end of the element. This lasted until any time when the pump speed was reduced, at which point, the stored compliance pressure was seen to be transferred to the output end, causing a brief peak in output flow. Frequent oscillation in recirculation therefore resulted in corresponding oscillations in output flow-rate – a behaviour less visible in previous experiments where an *alternating* output protocol was used.

This arrangement resulted in a high volume of useful dialysate output, at $V_{cycle} = 5.6$ L, as the peak output flow occurred during the effective production time, after the concentration target had already been reached. The disadvantage in this method was the inherent instability visible in both the conductivity and flow-rate responses. Nevertheless, this was one of the more successful experimental methods in terms of having a production profile most similar to the ideal profile described above (see figure 3.1.1).

3.3.5. Experiment five: Fuzzy-logic control, recirculation chopping

In an attempt to mitigate the instability shown in the data from experiment *four*, a chopped recirculation protocol was applied to the system. This had the unwanted side effect of reducing the effectiveness of the recirculation pump by half, but was intended to reduce the unwanted paradoxical dilution effect by averaging the output between dilute and non-dilute (see section 3.3.7), thus improving the output quality and the performance of the FLC (see figure 3.3.5).

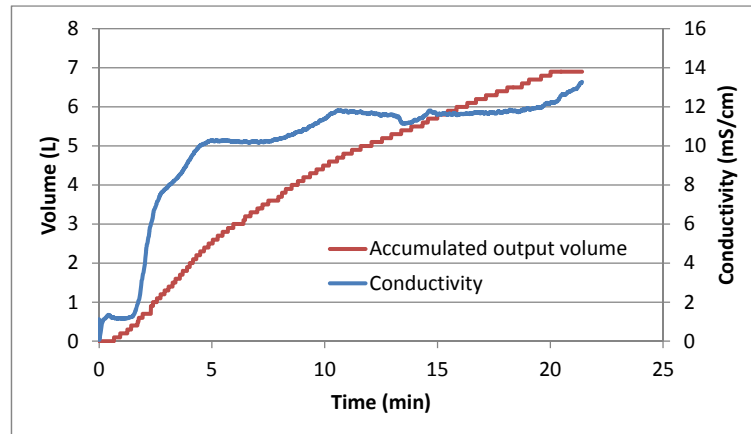


Figure 3.3.6.: Experiment five accumulated volume response: Target flow at 242 ml/min; target conductivity at 11.6 mS/cm; FLC control of conductivity and injection; chopped recirculation valves; open flow at output.

This method had the desired effect of reducing the instability in the controlled variable seen in experiment *four*, but at the cost of eliminating the convenient fluid storage-effect of having open recirculation and output flow. Response curves for this experiment were similar to that of experiments *three* and earlier, where the peak output flow occurred before the conductivity had reached its target.

This indicated that the available design options seemed to be restricted to either having good production time and volume but an unstable output conductivity, or having stable output conductivity but only over a limited effective production time. By examining a graph of accumulated output volume for the same experiment, the level of dialysate production waste was highlighted (see figure 3.3.6).

The data showed that by the time the output conductivity was in range (at around 10 min), about 4.6 L of dilute dialysate had been delivered, leaving only 2.1 L of useful dialysate to be delivered before the feed-side was saturated with salt. This seemed an unfortunate waste of production capacity despite the controller being reasonably well-tuned. If this method were used for medical environment, most of the generated output fluid would not be suitable for treatment.

3.3.6. Experiment six: Fuzzy-logic control, free-flow output, batch output

To attempt to mitigate the wastage shown in experiment *five*, a similar experiment was carried out, but with the entire fluid output over *all* stages collected in a mixed, stirred container. Thus, the early-stage, dilute output could be retained and mixed with the salt-rich tail-end output fluid, wasting as little fluid as possible and maximising pro-

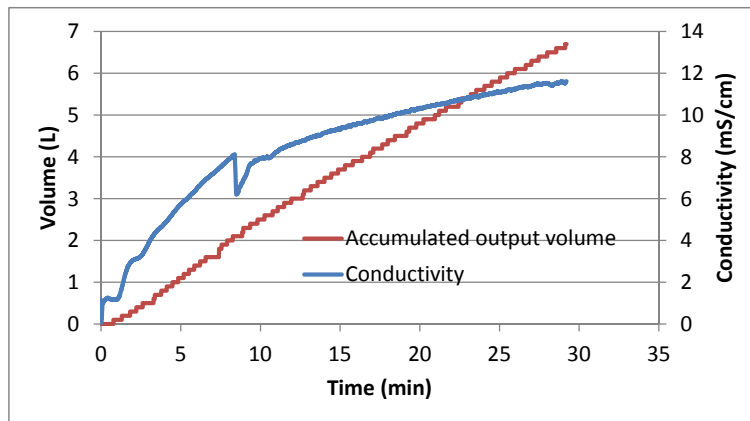


Figure 3.3.7.: Experiment six: Target flow at 242 ml/min; target conductivity at 11.6 mS/cm; FLC control of conductivity and injection; open flow at output; batch-produced dialysate stored and mixed.

duction volume. By measuring conductivity of the fluid batch, and by comparing it against accumulated output *volume* instead of against output *flow-rate*, the production profiles generated by such experiments (see example in figure 3.3.7²) had little in common with those of preceding experiments or with the ideal profile suggested above (see figure 3.1.1).

This approach to both output control and storage was found to be the simplest and most reliable way to produce a maximum output volume of dialysate with the minimum wastage of fluid.

3.3.7. Paradoxical conductivity response

For experiment *three* and, most notably in experiment *four*, severe oscillation of conductivity and flow-rate were observed whenever the conductivity measurement crossed its setpoint. This was most severe at any moment when the conductivity decreased below its setpoint, causing the FLC to respond by setting a rapid increase in r_f , which was designed to redistribute more salt towards the output-end of the element in order to counteract the falling output conductivity. Instead, what was observed was a rapid *decrease* in output conductivity, resulting in negative feedback, further decrease in conductivity and a corresponding increase in recirculation rate. Instead of acting to reduce the conductivity error as intended, the controller was found instead to run-away to its maximum speed, until the system as a whole had re-adjusted at its natural rate.

²The artifact visible at ~ 9 min was due to the transfer of the accumulated fluid from a small, overflowing mixing container (~ 250 ml) to the larger stirred vessel (~ 10 L). This was necessary to avoid entrainment of air in the uptake line during the initial production phase before sufficient volume was accumulated in the larger vessel.

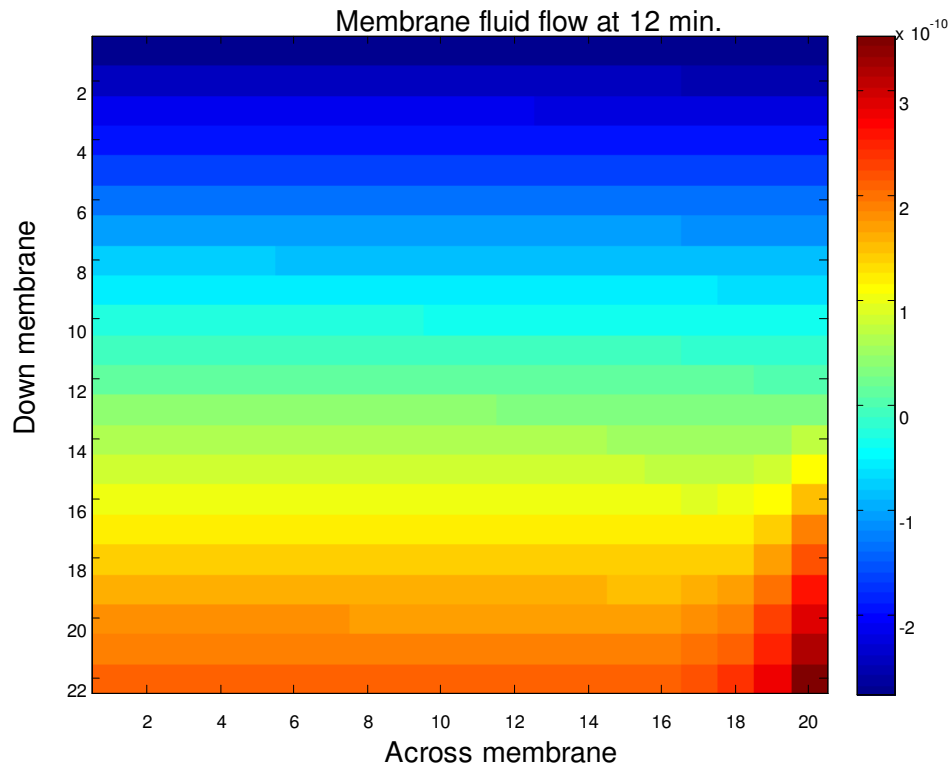


Figure 3.3.8.: Peak trans-membrane flux distribution simulation (in arbitrary units) as seen from the draw-side of a single membrane sheet, during simulated conditions similar to those in experiment *four*. The injection-end of the element is uppermost, while output is collected from the lowest row. Positive flux through the sheet, causing excessive local dilution is shown in red, while negative flow is shown in blue.

Similarly, whenever the conductivity would then drift back towards the setpoint, the resultant reduction in r_f would cause this reduction in error to accelerate and overshoot, quickly reducing the recirculation to $r_f = 0$. The system would then slowly recover towards the setpoint at its natural rate. This oscillation is most noticeable in the data generated by experiment *four*, where the conductivity can be seen to oscillate around the setpoint, while the flow-rate can be seen to vary with each corresponding change in the draw-side salt-distribution. The likely cause of this was able to be demonstrated by mathematical modelling of flow within the membrane's draw-side compartment³ (see figures 3.3.8 and 3.3.9).

From the sheet simulation image shown in figure 3.3.8, there is a clearly visible net flow from the draw-side to the feed-side at the injection-end of the element; meanwhile,

³A full development and discussion of the modelling method is described in chapter 5.

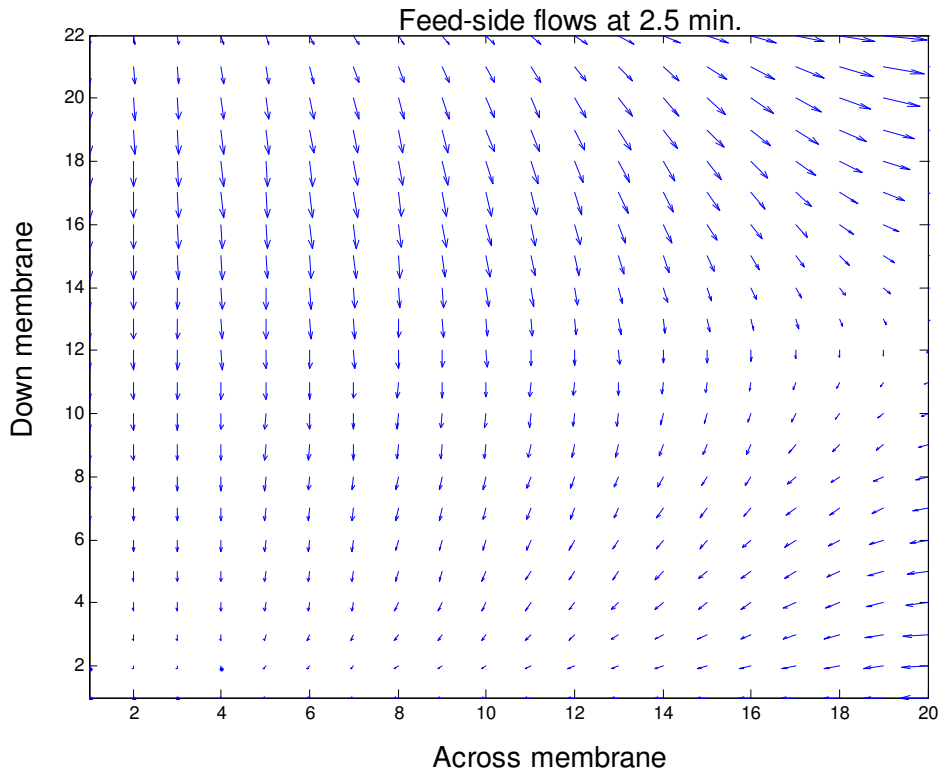


Figure 3.3.9.: Simulated feed-side fluid flow direction under similar peak recirculation conditions as those modelled in figure 3.3.8.

there is a net flow from the feed- to draw-side in the lower half of the sheet, causing an undesirable dilution of the dialysate output (obtained from the lowest row in the sheet). The mechanism of this dilution is visible in the surface flows within the feed-side envelope (see figure 3.3.9): there is the expected flow from top-to-bottom generated by the recirculation pump, and an extra push towards the low-pressure feedwater tube on the top-right-hand-side due to increased local injection-end pressure caused by the longitudinal flow-resistance of the membrane element. There is a similar suction away from the feedwater tube by the applied negative pressure on the output-end of the draw-side⁴.

These unwanted flows generated in the feed-side and corresponding changes in trans-membrane flux were responsible for the apparent output-end dilution observed at high recirculation rates. Since the aim of increasing the recirculation rate was to *increase* the output concentration, rather than dilute it, the unwanted membrane flux was likely to

⁴Draw-side flows are not shown; at this point they are driven by the flow-pump at maximum output. The draw-side flow vectors are therefore uniform, parallel, vertical and all pointing from top-to-bottom due to the direction of flow of the recirculation pump

have caused the observed paradoxical response in the output conductivity. This effect was clearly reduced by the protocol of 50% recirculation-chopping used in experiment *five*, with its associated increase in conductivity rise-time and overproduction of dilute dialysate during the priming stage. This highlights the dependency of this system on low recirculation rates for controller stability, yet high rates for efficient dialysate production.

3.4. Conclusions

One aim of this experimental design process was to produce dialysate on-line – that is, to have it produced at a rate similar to that which would typically be needed for medical treatment. If the idealised production profile were attainable, both the priming and recovery stages would be relatively short in comparison with the total effective production time, t_{eff} . The experimental method whose output came closest to this ideal was that of experiment *five*, which was governed by a tuned FLC, high recirculation rates and freely flowing output. Despite its long effective production time, its conductivity was unstable due to paradoxical effects at the membrane surface. A glance at the data suggests that this may be managed by simply averaging the output conductivity in a small mixed vessel - the equivalent of a moving-average-filter for a saline fluid stream.

The logical extension of the need to mix and average a small quantity of fluid output would be the mixing of the *entire* output so as to maximise the total production volume while minimising wastage. This would also dispense with the need for crisp control of the output conductivity, which, as the data shows, is relatively difficult to achieve. This is shown in experiment *six* to be a relatively simple and reliable method. This method of batch-mode dialysate production is explored further in the chapter 4.

4. Dialysate production limitations

*This chapter was adapted from a paper published as Smith, M. C., & Reynolds, K. J. (2015). Forward osmosis dialysate production using spiral-wound reverse-osmosis membrane elements: Practical limitations. *Journal of Membrane Science*, 484, 18-26.*

4.1. Introduction and background

In the preceding chapters the medical function of dialysate fluid, its general composition and usual RO-based method of production have been discussed. The potential benefits of an alternative, FO-based dialysate production system, together with the advantages of using inexpensive spiral-wound RO membrane elements in FO applications have also been discussed (see chapter 1). A description of an analytical theory for the FO production of dialysate using a standard RO membrane element has been presented (chapter 2) and various control strategies for maintaining a medical targets of dialysate concentration and production flow-rates have been tested (chapter 3). Of the various strategies, batch-mode production showed the most promise in terms of simplicity, practicality and overall production volume. This chapter explores this control method further, in order to ascertain the practical production limitations of this approach.

4.1.1. Considerations when using an RO membrane in FO mode

As highlighted by others, RO membrane elements are difficult to use in FO mode (Xiao et al., 2011; Cath et al., 2006). The difficulties stem from the fact that the permeate side of an RO membrane element is formed in envelopes that are sealed on three-sides, having been designed for fluid to exit that side, rather than enter it. In the proposed design, feedwater must be supplied to the element via its permeate tube, causing salt to accumulate within the feed-side envelopes and a corresponding loss of osmotic drive. It is suggested here that this accumulation be compensated for by injecting excess concentrate until the element reaches its saturated capacity, at which point the membrane may be recovered by osmotic backwashing.

4.1.1.1. Feed-side salt accumulation

In an ideal process, draw-solution injectate of concentration, c_{din} , would be added at a rate, Q_{win0} , to match the loss of salt via the production output flow and concentration targets, $Q_{wtarget}$ and $c_{dtarget}$:

$$Q_{win0} = \frac{Q_{wtarget} \cdot c_{dtarget}}{c_{din}} \quad (4.1.1)$$

The theoretical analysis (see chapter 2) discusses two sources of salt accumulation in an FO dialysate production process: reverse-solute flux from the draw-solution, and rejection of feedwater solutes. Both of these rates are closely related to membrane characteristics, osmotic potential difference and feedwater quality. As discussed, for a practical membrane excess concentrate must be injected into the process' draw-side at a factor of F_{OP} , to compensate for these two sources of accumulation and to maintain sufficient osmotic potential to drive the process.

$$F_{OP} = \frac{\frac{\lambda}{V_f} \left(\frac{k_s}{k_w} + c_{feed0} \right) + \frac{\mu}{V_d} \left(\frac{k_s}{k_w} + c_{dtarget} \right)}{\frac{\lambda}{V_f} \left(\frac{k_s}{k_w} + c_{feed0} \right) + \frac{\mu}{V_d} \cdot \left(\frac{k_s}{k_w} + c_{din} \right)} \cdot \frac{c_{din}}{c_{dtarget}} \quad (4.1.2)$$

This *overprime* factor is independent of the target flow rate ($Q_{wtarget}$), provided that appropriate approximations for ECP and ICP are made via μ and λ ¹. By injecting excess draw-side salt, the total salt mass on both sides of the membrane can be expected to gradually increase, until high draw-side concentration causes the system's output concentration to increase above its target level, at which point the output will no longer be useful. This point is designated here as *saturation*, and it is the point at which the element can produce no further useful output and must be backwashed.

4.1.1.2. Osmotic backwashing

The proposed system could be recovered from its saturation state by displacing its salt-rich draw-side fluid with a lower-osmolarity one, and allowing that fluid to diffuse across the membrane to flush salt from the feed-side. The use of osmotic principles to backwash a membrane has been described by others (Sagiv and Semiat, 2010; Ramon et al., 2010; Werner et al., 2013) but has not yet been explored in this particular application.

There is a particular complication associated with the introduction of fluid into the draw-side of a *medical* FO process: the displacing fluid must also be of medical grade. The use of this approach in any practical application would require an additional, high-quality water source, such as that supplied by a separate RO unit. This implies that FO

¹A discussion of the approximation of these constants can be seen in the theoretical analysis in chapter 2

4.1 Introduction and background

dialysate production using an RO element cannot be effective without also using an additional RO supply.

4.1.1.3. Production limits

The theoretical analysis shows that the total useful volume produced by the proposed system is limited by the salt-storage capacity of the membrane element's feed-side. If the initial and saturated feed-side salt concentrations, c_{ft0} and c_{fts} , can be estimated, an upper limit for V_{cycle} can be calculated (see equation A.8.10):

$$V_{cycle} \leq \frac{(c_{fts} - c_{ft0}) V_f}{\frac{k_s}{k_w} + c_{feed0}} \quad (4.1.3)$$

4.1.1.4. Apparent flow rate

The rate at which this volume, V_{cycle} , is produced is designated as the *net* flow rate: $Q_{wout} = \frac{V_{cycle}}{t_{eff}}$, where t_{eff} is the effective production time. However, for a practical system, production must also be paused to backwash the element, and extra dialysate product fluid must be stored briefly to compensate for this down-time. When the backwashing time, t_{bf} , is taken into consideration, an *apparent* production rate, $Q_{wtarget}^*$, can be estimated.

$$Q_{wtarget}^* = \frac{V_{cycle}}{t_{eff} + t_{bf}} \quad (4.1.4)$$

A glance at equation 4.1.3 shows that the cycle production volume, V_{cycle} , is independent of the target flow rate, $Q_{wtarget}$. Furthermore, a preliminary analysis of osmotic backwashing in this context suggests that the time taken to backwash a saturated element, t_{bf} , is independent of the rate at which the element became saturated (see section 5.4.2.1). If extremely rapid *net* production rates are allowed, the *apparent* production rate will be limited to Q_{wmax} by the backwashing time:

$$Q_{wmax} = \frac{V_{cycle}}{t_{bf}} \quad (4.1.5)$$

The experimental analysis that follows describes the measurement of the practical volume, time and rate limits of FO dialysate production using a single 4040-size RO membrane element.

4.2. Materials and Methods

4.2.1. Apparatus

A full description of the hardware and its operation can be found in section 3.2.1 in chapter 3.

4.2.2. Dialysate production

4.2.2.1. Preparation by osmotic backwashing

Before each production cycle, the membrane element was osmotically backwashed. The backwash fluid container was filled with a low-osmolarity fluid, then the backwash, bypass and storage valves were opened, while all other valves were held closed. The recirculation pump was run in a counter-clockwise direction at maximum speed to pump backwash fluid through the draw-side of the element and into the storage vessel. The backwash fluid was allowed to permeate through the membrane and flush the feed-side fluid to drain via the feed-side central tube.

4.2.2.2. Target settings

The dialysate output concentration target, $c_{dtarget}$, was converted to an equivalent conductivity target of $\sigma_{target} = 11.6 \text{ mS/cm}$ for all experiments². The set flow rate target for each experiment was selected from the range $Q_{wtarget} = 121 \rightarrow 900 \text{ ml/min}$. The overprime factor was fixed at the rate used for the previous experiments at a mid-range target production value of 242 ml/min, and fixed at $F_{OP} = 1.61$. The injection rate prime factor, Q_{win} , was calculated by the software. The typical values used for the various experimental parameters are shown in table 4.2.1³.

²As discussed in section 2.3.1.1, a typical treatment demands dialysate fluid with a conductivity of 14.0 mS/cm, at $\sim 500 \text{ ml/min}$. As out dialysate precursor is unbuffered, its equivalent targets would be $\sigma_{target} = 11.6 \text{ mS/cm}$ with a production rate of $Q_{wtarget} \approx 484 \text{ ml/min}$. Production at half speed would be at a rate of $\sim 242 \text{ ml/min}$; One-quarter speed would be $\sim 121 \text{ ml/min}$ etc. The target conductivity would remain the same regardless of the target rate.

³Notes on the values given in table 4.2.1: The value given for *Hydrostatic pressure at output* was defined as atmospheric pressure ($\sim 0 \text{ kPa}$) relative to the pressures given elsewhere in the system. The value given for *Feed rate* was an estimate only: feed solution was supplied at low-pressure and was allowed to be drawn into the system at a rate determined by the trans-membrane osmotic gradient.

4.2 Materials and Methods

Parameter	Symbol	Typical value	Units
Draw-side			
Injectate concentration	c_{din}	8000	mosm/L
Ideal injection rate	Q_{win0}	1.45×10^{-4} (8.70)	L/s (ml/min)
Practical injection rate	Q_{win}	2.33×10^{-4} (14.0)	L/s (ml/min)
Salt-mass injection rate	Q_{sin}	1.87×10^{-3} (112)	osm/s (mosm/min)
Bulk draw-side concentration	c_d	297 \rightarrow 8000	mosm/L
Equivalent osmotic pressure	Π_d	0.736 \rightarrow 19.8	MPa
Hydrostatic pressure at output	—	~ 0	kPa
Hydrostatic pressure at input	—	39.4	kPa
Recirculation flow-rate	—	8.33×10^{-4} (50.0)	L/s (ml/min)
Average membrane fluid flux	J_{wm}	5.10×10^{-4} (30.6)	L/s/m ² (ml/min/m ²)
Average reverse-salt flux	J_{sm}	5.28×10^{-4} (31.7)	osm/s/m ² (mosm/min/m ²)
Operating temperature	T	298	K
Dialysate output concentration	c_{dout}	297	mosm/L
Equivalent osmotic pressure	—	736	kPa
Equivalent conductivity	σ_{out}	11.6	mS/cm
Dialysate output flow-rate	Q_{wout}	4.03×10^{-3} (242)	L/s (ml/min)
Dialysate output salt-mass rate	Q_{sout}	1.20×10^{-3} (71.9)	osm/s (mosm/min)
Feed-side			
Feedwater concentration	c_{feed0}	11	mosm/L
Feed rate	—	~ 283	ml/min
Feed-side bulk concentration	c_f	0 \rightarrow 1000	mosm/L
Equivalent osmotic pressure	Π_f	0 \rightarrow 2.48	MPa
Supply hydrostatic pressure	—	1.0	kPa
Operating temperature	T	298	K
Process parameters			
Draw-side volume	V_d	2.38	L
Feed-side volume	V_f	0.67	L
Membrane area	A_{mem}	7.90	m ²
Hydraulic permeability	A	1.56×10^{-8}	m/kPa/s
Reverse solute flux constant	B	4.00×10^{-8}	m/s
Solute permeability	k_s	4.00×10^{-8}	m/s
Water permeability	k_w	3.87×10^{-8}	m · L/s/mosm
Mass-transfer for ECP	K_{ECP}	2.29×10^{-5}	s · m ² /L
Mass-transfer for ICP	K_{ICP}	2.29×10^{-6}	s · m ² /L
Flow-rate target	$Q_{wtarget}$	4.03×10^{-3} (242)	L/s (ml/min)
Concentration target	$c_{dtarget}$	297	mosm/L
Equivalent conductivity	σ_{target}	11.6	mS/cm
Overprime factor	F_{OP}	1.61	(unitless)
Production cycle volume	V_{cycle}	8.9	L
Effective production time	t_{eff}	33.9	min
Backwashing time	t_{bf}	8.0	min
Apparent production rate	$Q_{wtarget}^*$	3.33×10^{-3} (200)	L/s (ml/min)
Approximation for ECP effect	λ	1.25	(unitless)
Approximation for ICP effect	μ	1.01	(unitless)

Table 4.2.1.: Process parameter settings

4.2.2.3. Output, sampling and recirculation

Dialysate output product was continuously collected in a large stirred vessel. A fraction of the output was continuously sampled and passed through the draw-side compartment of the element. Recirculation was set to the lowest possible setting above the stalling speed ($r_f \approx 12\%$). To avoid the entrainment of air into the element's draw-side compartment, the output and intake tubes were initially placed in a small, 200 ml mixing vessel that was primed with backwash fluid and placed within the larger collecting vessel. Once approximately 2 L of total output volume had overflowed from the small vessel into the larger container, the intake and output tubes were both moved into that container.

4.2.2.4. Measurement

The mass of the net, accumulated product fluid was recorded each time an additional 100 mL⁴ was delivered. The conductivity of the fluid drawn into the intake tube was recorded every ~ 0.1 s and monitored. The conductivity values were converted to equivalent concentration values, which were then combined with values for accumulated volume to produce data for accumulated solute and solution quantities. These accumulated values were then filtered using a moving-average, rectangular-window of size 4.0 minutes, then differentiated and combined to infer values for instantaneous conductivity and flow-rates at the system's output. As soon as the target conductivity was reached, production was ceased and the membrane was backwashed before beginning the next cycle.

4.3. Results and discussion

4.3.1. Dialysate production

4.3.1.1. System response

Two types of response profiles were generated for each experiment. The first type is concerned with the accumulating output fluid which was collected in a stirred vessel whose volume and conductivity were constantly monitored. For this profile, the critical point was when the accumulated dialysate volume was found to be at the target conductivity, at which point production was ended. Conductivity and volume data for the accumulating output fluid were plotted against time (see example in figure 4.3.1(a)⁵).

⁴Volume measurements were inferred from mass measurements made by a set of scales. The approximation $1.0 \text{ kg} = 1.0 \text{ L}$ was used.

⁵The artifact visible in the conductivity plot at ~ 8 min was due to the removal of the output and intake tubes from the 200 ml vessel to the large output collection container.

4.3 Results and discussion

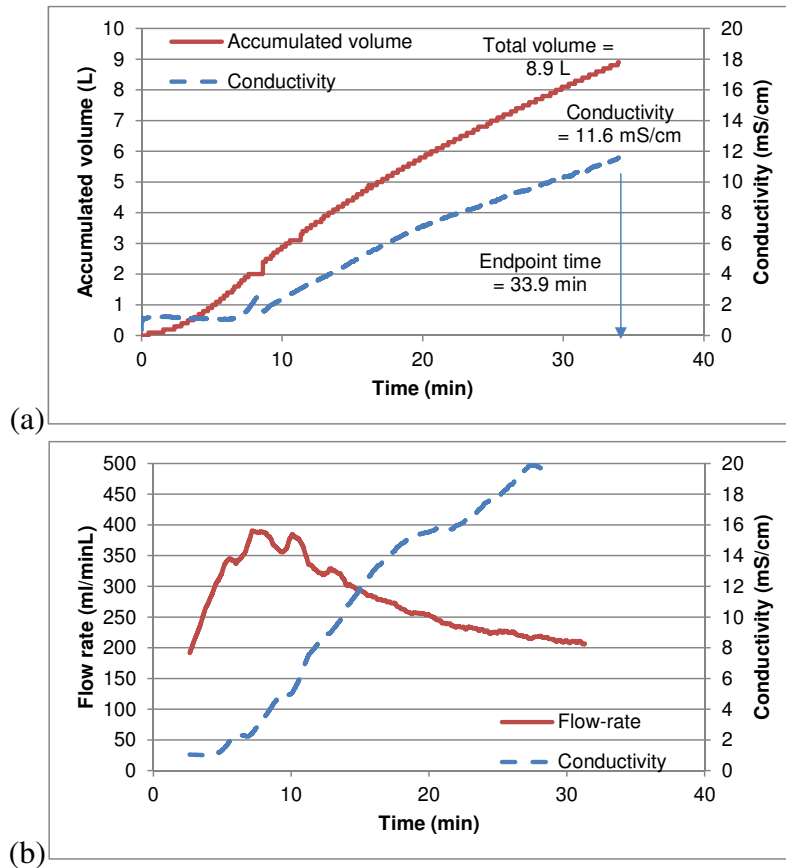


Figure 4.3.1.: Production response curves for dialysate production with target flow rate set at 242 ml/min and target conductivity at 11.6 mS/cm.

The second type of profile was recorded by measuring the conductivity and flow-rate of the dialysate output at the point just before it is added to the stirred vessel. Values for the output fluid's instantaneous flow-rate and conductivity are graphed in figure 4.3.1(b). As such, the first profile is essentially an integration-over-time of the second profile. The curves show reasonably steady output flow rates and gradually rising output concentration. The graph endpoint shown in the accumulated conductivity curve indicates the time, $t_{eff} = 33.9$ min, at which the output conductivity was considered to have reached its target, $\sigma_{target} = 11.6$ mS/cm. The corresponding value of the accumulated output volume was recorded as $V_{cycle} = 8.9$ L for that production cycle.

4.3.1.2. Production time

Production cycle time data is presented in figure 4.3.2. The severe decline in production cycle time with increasing target flow-rates was to be expected, as the theoretical

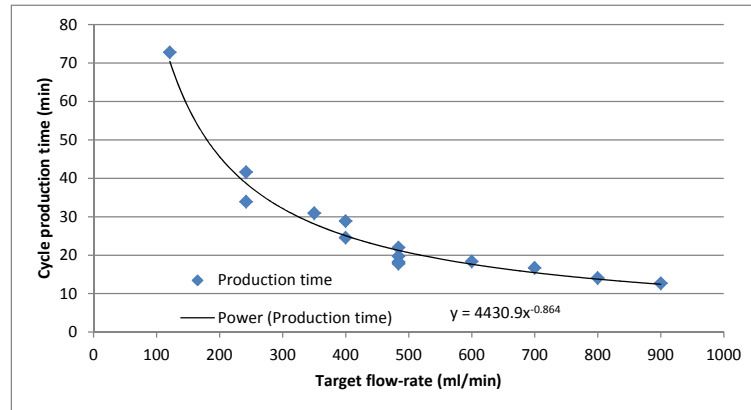


Figure 4.3.2.: Production times for a range of target flow rates

analysis predicts that effective production time is dominated by a factor of $1/Q_{wtarget}$ ⁶. These results suggest a great advantage in operating the system at lower target flow-rates in order to obtain longer cycle production times.

4.3.1.3. Production volume

The accumulated production volumes measured at each target flow-rate setting are shown in figure 4.3.3. While the maximum production-cycle volume limit is independent of the target flow-rate setting, (see equation 4.1.3), the figure shows a clearly decreasing production volume with increasing target flow-rate. This is predicted by the theoretical analysis (see chapter 2) and is likely to be due to the effects of ECP and ICP at higher target flow-rates with their corresponding higher trans-membrane fluxes⁷. Similar to the results for production time, these results also suggest an advantage in operating the system at lower target flow-rates in order to obtain increased production volumes.

⁶It can be shown that when the output conductivity is tightly controlled, the effective production time of a production cycle, t_{eff} , has a form similar to $t_{eff} \approx \frac{k_1+k_2}{Q_{wtarget}}$, with the parameter k_2 vanishing at high values of $Q_{wtarget}$. For these reasons, a trend-line based on $1/x$ was fitted to the data in figure 4.3.2. Further detail is shown in the analysis in chapter 2.

⁷It can be shown that production cycle volume is dependent on ICP due to the bulk trans-membrane fluid flux. While difficult to calculate analytically, an appropriate estimate of the flux can be used to create a simple relation between production cycle volume and target flow-rate, $V_{cycle} \approx k_1 + k_2 e^{-k_3 Q_{wtarget}}$. For these reasons, a trend-line based on e^{-kx} was fitted to the data in figure 4.3.3. Further detail is shown in the theoretical analysis in chapter 2.

4.3 Results and discussion

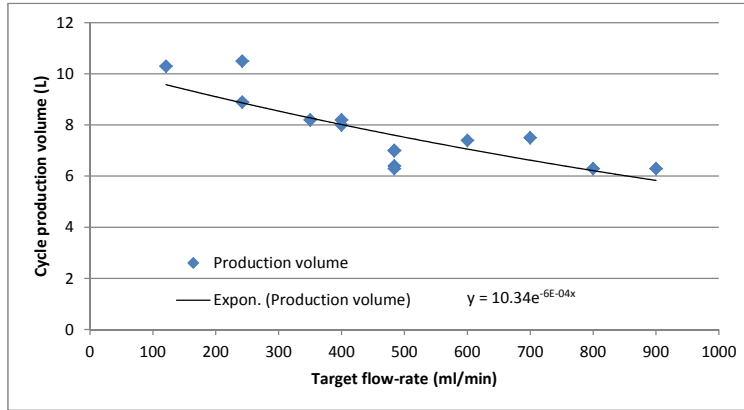


Figure 4.3.3.: Production volumes for a range of target flow rates

4.3.1.4. Production flow rates

The production volume, V_{cycle} , and production time data, t_{eff} , from each experiment were combined to estimate values for *net* production flow-rate:

$$Q_{wnet} = \frac{V_{cycle}}{t_{eff}} \quad (4.3.1)$$

These are graphed as a function of set target flow-rate in figure 4.3.4. There is a significant discrepancy between the set target and net flow-rate values shown in the graph - a discrepancy that was found to be more severe at higher target flow-rates. The theoretical analysis suggests that this was also likely to be due to the severity of ECP and ICP at higher target flow-rates. In order to compensate for the effects of ECP and ICP, the overprime factor, F_{OP} , must be re-calculated to increase the draw-solution injection rate, Q_{win} . As shown in the theoretical analysis, the calculation of this factor is quite complicated and depends on fore-knowledge of estimates of average ECP and ICP (see chapter 2). As these values were unknown, experiments were instead carried out with a fixed value for F_{OP} , so that the effects of ECP and ICP might be revealed. The impact of these two effects is clearly visible in the graph in figure 4.3.4⁸. Similar effects are shown in work by (You et al., 2012; Lay et al., 2012) and in the theoretical predictions (see chapter 2).

Apparent flow-rates, $Q_{wtarget}^*$, were calculated from the experimental values for production volume, V_{cycle} and production time, t_{eff} , by adding a fixed estimate of back-

⁸It can be shown that net flow-rates can be approximated using a rational polynomial form such as $Q_{wnet} \approx \frac{k_1 e^{k_5 Q_{wtarget}} + k_2}{k_3 e^{k_5 Q_{wtarget}} + k_4} \cdot Q_{wtarget}$. At low values, $Q_{wnet} \rightarrow Q_{wtarget}$, while at higher values, Q_{wnet} is asymptotic to a linear function of the form, $Q_{wnet} \rightarrow k_6 Q_{wtarget}$.

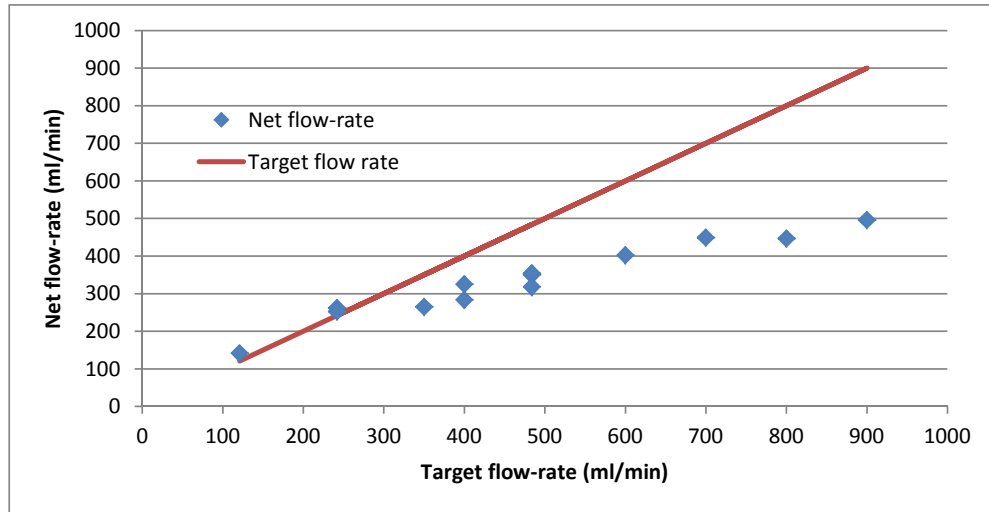


Figure 4.3.4.: Comparison of target flow rates and net flow rates over single production cycles

washing time at $t_{bf} = 8.0 \text{ min}$ ⁹ to each recorded value of production time:

$$Q_{wtarget}^* = \frac{V_{cycle}}{t_{eff} + t_{bf}}$$

These re-calculated apparent flow-rate values represent the dialysate production rate as it would appear to an outside observer such as a medical patient or dialysis machine. The values are shown graphed as a function of the set target flow-rate in figure 4.3.5. The inclusion of backwashing time further exacerbates the discrepancy between target and apparent flow rates.

4.3.2. Production limits

4.3.2.1. Maximum production

The net production rate appears to decrease with increasing target flow rate past the highest set rate of 900 ml/min. If the accumulated output volume were to stabilise at the lowest measured value of 6.3 L at higher flow rates, a best-case analysis may be completed. With a very high *net* flow rate, the *apparent* flow rate would approach the limit dependent on the backwashing time of $t_{bf} = 8.0 \text{ min}$:

⁹Backwashing experiments (see chapter 5) suggest that an optimised backwash time of $t_{bf} = 8.0 \text{ min}$, with a backwashing volume of $\sim 2.3 \text{ L}$ might be adequate to recover an RO membrane of this type.

4.3 Results and discussion

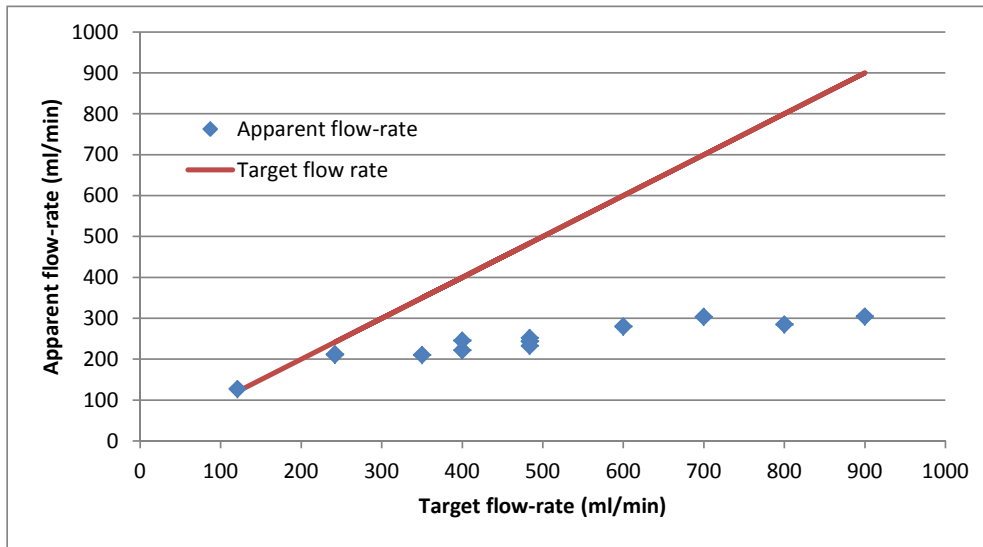


Figure 4.3.5.: Comparison of target flow rates and apparent flow rates adjusted for backwashing time

$$\begin{aligned}
 Q_{wmax} &= \frac{V_{cycle}}{t_{bf}} \\
 &= 788 \text{ ml/min}
 \end{aligned}$$

This high apparent flow rate would be more than adequate to perform dialysis treatment, if only such a high net production rate were attainable. Even if dialysate concentrate could be injected into the draw-side compartment of a system at infinite speed, the effects of ECP and ICP would slow the permeation of fluid through the membrane down to realistic rates.

The prototype was mechanically limited to operating at or below a target rate of ~ 900 ml/min. At this rate, the system produced a maximum net output rate of ~ 500 ml/min. It was difficult to estimate the maximum possible net production rate for the system, although an estimate of an upper limit was made as follows: By making a linear approximation to the last four data points shown in figure 4.3.4, it was possible to extrapolate to *maximum possible* net flow rates at higher target flow rates. For example, a doubling of the maximum injection rate to meet a target of $Q_{wtarget} = 1800$ mL/min would produce a net flow rate of no more than $Q_{wout} = 741$ ml/min. At this rate, if there were no loss in total production volume below 6.3 L, this would correspond to an effective production time of $t_{eff} = 8.49$ min. With a backwash time of $t_{bf} = 8.0$ min, the optimistic apparent production rate would be $Q_{wtarget}^* = 382$ ml/min. Some confidence can be had that the actual production rate would be less than this value as both the V_{cycle} and net production curves appear to be monotonically decreasing, consistent

with the expected effects of ECP and ICP. This is consistent with the predictions of both the theoretical analysis (2.6.1) and experimental data, of which the highest output values were close to $Q_{wtarget}^* = 300$ ml/min (see figure 4.3.5).

4.3.2.2. Typical production

The data showed that there were clear advantages in operating the system at lower target flow-rates. Achieving a practical flow-rate of $Q_{wtarget}^* = 484$ ml/min as needed for dialysis treatment from a single 4040-size element would be difficult and wasteful. A better strategy might be to duplicate the system, with two 4040-size elements arranged to each operate at half the necessary practical rate. For example, to produce dialysate at an apparent rate of 484 ml/min, a pair of elements would have to generate un-buffered dialysate at an apparent rate of $Q_{wtarget}^* = 242$ ml/min each. According to the *apparent* flow-rate data (see figure 4.3.5), this would require each element to be set at a target rate of at least $Q_{wtarget} = 400$ ml/min, which would then enable production of about 8.0 L over a 25 min production cycle. Duplicating the system in this way would allow each element to operate more efficiently by shifting their operating points closer to the middle of their effective production ranges.

4.3.2.3. Minimum production

If a scenario was such that equipment size were no obstacle, the target per-element production rate could be halved again, and dialysate production could be spread between arrays of four elements per machine. The data shows that at a set rate of $Q_{wtarget} = 121$ ml/min, the apparent flow rate would be *greater* than the target rate, at $Q_{wtarget}^* = 127$ ml/min¹⁰. At this lower rate, a long production period of 70 min for a volume of ~ 10 L was observed. This result shows the efficiency gains that are to be had by operating the FO process at a low flow rate.

4.3.3. Practical considerations

4.3.3.1. Consumption of concentrate

The data shows that high flow-rates can be achieved by increasing the target flow rate. However, the modest gains in output rate may be offset by impractically high concentrate injection rates. Even at the highest target flow rate of 900 ml/min, the experiments showed a maximum net output of only 500 ml/min. With an overprime factor

¹⁰This paradoxical increase in both net and apparent production rates is to be expected when using an overprime factor based on a fixed approximation for ECP and ICP from a higher target rate (see section 4.2.2.2).

of $F_{OP} = 1.61$, this would mean that dialysate concentrate would be being consumed at nearly three times the rate at which it would normally be if a traditional RO-based system were used. While dialysate concentrate is not expensive, a typical treatment might consume five litres of *Part A*; and a three-fold increase in the purchase, handling and storage of concentrate might not be desirable to any dialysis service.

4.3.3.2. Consumption of water

As suggested in the introduction (section 1.3), one advantage of FO technology over RO is its potential for water conservation. The prototype system was designed to compensate for accumulating salt by adding excess salt on the draw-side, instead of continually flushing the membrane feed-side in the manner of an RO process. By this method, water is only lost from the system during the backwash phase. The prototype backwash method was estimated to consume RO water at ~ 286 ml/min over 8.0 min for a total of 2.3 L (see figure 5.4.2). The benchtop RO system had its recovery rate measured at 65 %. An RO backwash of the system would therefore consume about 3.5 L of feedwater, and the whole system would consume $9.8 \rightarrow 14.0$ L of feedwater to produce $6.3 \rightarrow 10.5$ L of dialysate: a “recovery” rate of $65 \rightarrow 75$ %.

4.3.3.3. Consumption of energy

Another major advantage of FO over RO is its low energy consumption. The prototype produces dialysate without the need for a high-pressure pump, which is a major source of energy loss in an RO system. The major energy losses in the prototype were due to the valves and the recirculation pump, which drew a combined 20 W during production experiments. During backwashing, the recirculation pump was operated at maximum speed, doubling the prototype’s total consumption to 40 W. Thus, for a production cycle with flow target set at 242 ml/min, a net production time of 34 min, a backwash time of 8.0 min consuming about 2.3 L of RO water (produced over 2.6 min at 325 W), the typical energy consumed by the prototype within a production cycle was estimated:

$$\begin{aligned} & 20 \text{ W} \times 34 \text{ min} \\ + & 40 \text{ W} \times 8 \text{ min} \\ + & 325 \text{ W} \times 2.6 \text{ min} \\ = & 1845 \text{ W} \cdot \text{min} \end{aligned}$$

For a production cycle volume of 8.0 L, this gives:

$$\frac{1845 \times \text{W} \cdot \text{min}}{8.0 \times \text{L}} = 230 \text{ W} \cdot \text{min/L}$$

By comparison, the bench RO system was rated at 325 W and was able to be used to mix dialysate at a maximum rate of 927 ml/min, for a net efficiency of 350 W·min/L.

From these estimates, the backwashed FO-based prototype appeared to consume power at 66% of the rate of an equivalent RO-based dialysate system - an energy saving equivalent to about 0.35 kWh, or about 10 cents¹¹ per treatment. If backwashing were possible without an RO supply, the energy consumption of the system would be halved to $\sim 112 \text{ W}\cdot\text{min/L}$.

4.4. Conclusions

The prototype showed water efficiency comparable to that of existing RO-based systems, while its overall energy consumption was significantly less than an RO equivalent. Whether this energy saving alone would warrant the change to new technology seems unlikely: the economic benefit seems to be relatively small.

The Achilles heel of this method is its need for backwashing with a medical-grade, low-osmolarity fluid. Backwashing with RO-water produced by a separate unit is a design choice that is demanding of energy, water and time, and greatly diminishes the benefits of the FO-based process. Unfortunately, for the practical production rates explored in the experiments shown here, much of the apparent production time was taken up by backwashing time. If the backwashing time could be drastically reduced, or the net production time made much greater, the ratio of the backwashing time to the net production time could be reduced to a much more practical size, allowing for lower target production flow-rates and more efficient dialysate production.

The data shows no immediate answer to the problem of reducing the backwashing time without resorting to the use of a specialty FO membrane element, although this problem is explored and modelled in chapter 5. The use of a continuous FO process, using a specialty FO membrane element (with accessible feed-side compartment), might avoid the accumulation of salt and therefore reduce the demand for backwashing to a negligible level.

The data *does* show that by drastically decreasing the target flow-rate, the production efficiency can be greatly increased, resulting in large production volumes and long production times. This comes at the cost of having to produce and store dialysate in advance of any treatment, or to use multiple parallel membrane elements - a design choice that would require the purchase of many pieces of membrane process hardware at a loss of system compactness and cost-efficiency.

The data suggests that there would be little to be gained by increasing the quality of the membrane. Improvements in the membrane's hydraulic water permeability would be dwarfed by the effects of ICP, unless improvement could also be made to the thickness or tortuosity of the membrane's support-layer. Similarly, a reduction in reverse-salt flux would not decrease the main source of feed-side salt accumulation, which is largely due

¹¹Current Northern Territory electricity tariffs are about AUD\$0.30 per kWh (Jacana, 2014)

4.4 Conclusions

to the feedwater salinity. The experimental production times were relatively short, such that the need for backwashing was likely to have been largely determined by the accumulation of feed-side salt, rather than any membrane fouling effects. A longer-term analysis would need to be carried out to explore the relationship between backwash frequency and membrane fouling.

There is one other significant advantage of the proposed system: it is quiet¹². For large dialysis sites, the RO room's high-pressure pumps and equipment could be replaced by an array of silent elements driven by quiet flow-pumps, each slowly producing a small quantity of dialysate over many hours. The data shows that the proposed FO system is most efficient at low production targets: an array of elements could silently and efficiently produce dialysate for several hours between backwash cycles.

The benefits of the proposed method appear to show little economic or environmental benefit, relative to the existing RO-based technology. If the need for backwashing could be reduced or resolved, then the method's inherent water and energy efficiency may become more useful. Until then, the method may show utility in niche applications where the noise and maintenance of high-pressure RO pumps is undesirable.

¹²The significance of dialysis workplace noise appears during the contextual analysis - see results in section 7.4.1

5. Osmotic backwashing: a computational model

This chapter was adapted from a paper submitted to the Journal of Membrane Science in February, 2015: Smith, M. C., & Reynolds, K. J. (2015). Osmotic backwash recovery of a reverse osmosis element used for forward osmosis: a computational model.

5.1. Introduction and background

The preceding theoretical analysis and experiments have shown that it should be possible to produce dialysate from groundwater and dialysate concentrate by using an RO membrane element in FO mode. Since the RO membrane's brine-side is being used here as the draw-side for FO purposes, with the permeate tube being used to supply feedwater, the feed-side compartment will tend to accumulate salt (see chapter 2). However, the apparent production rate depends on a quick and efficient method of membrane backwashing (see chapter 4). The implementation of this backwashing process is one of the major challenges to the use of this method (see chapter 1). Due to the physical construction of spiral-wound RO membrane elements, their internal behaviour is unobservable during operation¹. Since the design of the system required optimisation of the backwashing process, computational analysis was necessary.

5.1.1. Osmotic backwashing

The use of osmotic backwashing in RO membrane elements has primarily been concerned with the management of membrane fouling (see Ramon et al., 2010; Sagiv et al., 2008; Sagiv and Semiat, 2005, 2010; Qin et al., 2009, and others). Osmotic backwashing typically involves the execution of a temporary and local reversal of membrane

¹It is unobservable by any simple, practical, affordable means. There may be some elaborate method involving X-rays, laser, gamma emission or similar that may enable the mapping of flows within the sealed membrane element, but the exploration of these methods was clearly beyond the scope of this thesis. Or to put it another way, the simplest way to examine the flow of salt and water within the membrane during operation was to create a computational model.

flux, after which production is expected to immediately return to its normal state. In the various applied methods, backwashing is usually brief: 20 → 50 s (Qin et al., 2009; Sagiv and Semiat, 2005), with flow directed *towards* the high-pressure side of the element.

5.1.1.1. Application to RO

The approach that is most relevant to this application is that of Qin et al. (2009) who suggest the injection of a high-salinity bolus into an RO feed stream to provide a localised FO² effect, temporarily reversing the direction of flow across the working membrane, without the need for its production settings to be adjusted. As this application is concerned with the localised reversal of an FO rather than an RO effect, the injection of a *low* osmolarity bolus into the system's draw-side compartment may achieve the required aim. The bolus and dwell time are also likely to be much greater in this application compared with others: rather than simply de-fouling a membrane, the aim here is to flush accumulated salt from the entire feed-side compartment.

5.1.1.2. Optimising backwashing time

As found by Sagiv and Semiat (2005) and Qin et al. (2009), backwashing has diminishing effectiveness with increasing time. For the prototype discussed here, there may be a point during a backwashing stage beyond which no further gains are able to be had, but it is expected that an earlier optimal moment will be found, beyond which the benefits of further backwashing are outweighed by the gains from a swift return to production. The lost production time must then be compensated for by increasing the net production rate so that the apparent rate over an entire production/backwash cycle is sufficient to cover the medical needs of dialysis treatment. This can be quantified by considering effective output volume, V_{cycle} , over any production period, t_{eff} , to establish a net production rate, Q_{wout} :

$$Q_{wout} = \frac{V_{cycle}}{t_{eff}} \quad (5.1.1)$$

This can then be modified to give an *apparent* output rate, $Q_{wtarget}^*$, which includes the backwash downtime, t_{bf} :

$$Q_{wtarget}^* = \frac{V_{cycle}}{t_{eff} + t_{bf}} \quad (5.1.2)$$

²Qin et al. (2009) refer to this as “direct-osmosis” rather than FO. The terms are used here interchangeably.

It is clear that $Q_{wtarget}^*$ can be maximised by either minimising the backwashing time, t_{bf} , or maximising Q_{wout} . However, short backwash times will end each cycle leaving salt in the feed-side compartment, reducing V_{cycle} in the subsequent production stage. To estimate the optimal time at which to end each backwashing stage, a computational model was developed to simulate the production of dialysate, the accumulation of feed-side salt and its removal by osmotic backwashing.

5.1.2. Computational modelling

The theoretical analysis (see chapter 2) used a one-dimensional analytical model to predict bulk membrane process performance. For estimates of steady-state dialysate production this has been adequate. To examine osmotic backwashing, however, more attention must be paid to two-dimensional flows across both sides of the membrane sheet during transient backwashing periods. It was found that the development of a two-dimensional analytical model was prohibitively difficult, as others have also found (Gu et al., 2011; Gruber et al., 2011). Instead, this type of problem is well-suited to computational modelling (Karlberg et al., 2013).

5.1.2.1. Membrane considerations

Osmotically driven membrane processes have been modelled both analytically and computationally. Researchers concerned with localised membrane performance have tended to use finite-element analysis (FEA) software such as COMSOL^{TM3} to solve Navier-Stokes equations for mass-flow, and convection-diffusion equations for dissolved solutes, over two dimensions—typically channel length and height above the membrane surface (Ramon et al., 2010; Sagiv and Semiat, 2011; Park et al., 2011). Others who have been more concerned with bulk membrane processes have used various iterative numerical tools to solve analytical models similar to that first expressed by Loeb et al. (1997) (see equation 5.1.3). Of these, some authors have examined simple membrane flux (Tan and Ng, 2008; McCutcheon and Elimelech, 2007; Phuntsho et al., 2012; You et al., 2012; Xiao et al., 2011); some have looked at modelling long channels with a finite height (Gruber et al., 2011); some have attempted to model the two-dimensional layout of a membrane sheet (Jung et al., 2011); and some have modelled the performance spiral wound sheets in three-dimensions (Gu et al., 2011).

This study was concerned with examining the *bulk* properties of a spiral-wound membrane sheet, rather than with mass-flows immediately adjacent to the membrane sheet. For these reasons, a numerical approach to the solution of a modified version of the standard model of Loeb et al. (1997) was used, rather than FEA methods. To reduce

³This software package is often mentioned in literature without citation. The version used is not stated, however, the software can be sourced from COMSOL Inc., Burlington, MA, USA.

the model's complexity, the three-dimensional spiral-wound geometry of the element was not modelled, accepting that this decision would probably lead to some inaccuracy in the modelling of salt concentration distributions.

5.1.2.2. General model

When using a membrane with the active layer adjacent to the draw-solution (AL-DS mode), the most widely accepted analytical model for trans-membrane fluid flux (including ICP) can be rewritten from a version shown in Gruber et al. (2011):

$$J_{wm} = A \left(\left(\frac{B}{A} + \Pi_d \right) - \left(\frac{B}{A} + \Pi_f \right) e^{J_{wm} \cdot K} \right) \quad (5.1.3)$$

The simplest interpretation of equation 5.1.3 is that fluid flux, J_{wm} , is proportional to the difference of the osmotic pressures of the draw- and feed-solutions, Π_d and Π_f , according to the membrane's pure water permeability constant, A . If the membrane has significant reverse-salt leak, a salt permeability constant, B can be used to modify the osmotic pressures. If the membrane feed-side includes a thick support layer, concentration polarisation may be significant, causing the feed-side solution to appear to be much higher at the membrane surface than in the bulk solution by a factor of $e^{J_{wm} \cdot K}$.

There are many corrections and approximations to this form, such as correcting K for feed-side concentration (Tan and Ng, 2008), and the simplification of $\frac{B}{A} \rightarrow 0$ for high-rejection membranes (Gruber et al., 2011). A similar formulation is often used for active-layer feed-solution (AL-FS) mode, to describe *dilutive* ICP, but it can be shown that this form simplifies to an equivalent equation when Π_d and Π_f are transposed, and the sign of J_{wm} is changed in the exponent to indicate reverse flow. ECP can be modelled in a similar way, although the effect is usually greatly reduced (perhaps to one-tenth that of ICP (You et al., 2012)).

A general analytical model can be written that includes not only ECP and ICP, but also allows for continual variation in the direction of flux. For the process described here, the normal production state is AL-DS mode, and so, positive *fluid* flux, J_{wm} , was defined as being *towards* the draw-side, active layer, while positive *salt* flux, J_{sm} , was defined as being towards the feed-side, porous support layer. This analytical model is consistent with those described by Gruber et al. (2011), even though there may be times when the "feed" side osmotic pressure is locally higher than the "draw" side concentration, causing a net reversal of fluxes and a useful osmotic backwashing effect. It is presented here in terms of draw- and feed-side concentrations (c_d and c_f) with terms added for both draw- and feed-side hydrostatic pressures (P_d and P_f), and the membrane's intrinsic resistance, μ_{Ri} .

$$J_{wm} = k_w \left(c_d \cdot e^{-\frac{J_{wm}}{K_{ECP}}} - c_f \cdot e^{\frac{J_{wm}}{K_{ICP}}} \right) - \frac{P_d - P_f}{\mu_{Ri}} \quad (5.1.4)$$

As discussed above, models like this cannot be solved without resorting to numerical methods, as J_{wm} appears as both the subject of the formula and in the exponent terms for ECP and ICP.

5.2. Model development

Given that modelling of the membrane process called for numerical methods, it was thought sensible to choose a procedural programming language with built-in mathematical functions for root-finding or one at least where such root-finding algorithms could be easily implemented. Due to the author's familiarity with the MATLAB™ programming language, it was used to develop the numerical implementation of the mathematical models described above, and a simulation engine to execute various implementations of membrane systems.

The use of numerical simulation to both design and verify practical prototypes is now commonplace (Karlberg et al., 2013). Design efforts were helped by the simultaneous development of a working prototype, the structure of which was analogous to the simulated hardware components within the computational model (see section 5.3.1).

5.2.1. Membrane modelling

In order to develop a realistic simulation, a specific membrane element was modelled. Membrane parameters were based on the selected high-rejection membrane element (ESPA2-4040, Hydranautics, Nitto Denko) used in the experiments (see previous chapters), consisting of a spiral-wrapped membrane package of five membrane-sheet pairs wrapped around a central supply tube. Each sheet-pair consisted of two sheets placed with their membrane support-layers adjacent and separated by thin spacer material. The sheet-pairs were glued around the border on three sides, leaving the fourth side connected to the central tube. By treating each membrane sheet as separate and parallel, the element was modelled as ten identical membrane sheets operating in parallel.

5.2.1.1. Fluid flux estimation

Equation 5.1.3 was first converted to a function f of J_{wm} so that various numerical root-finding methods could be applied. This was then differentiated to provide a derivative function $f'(J_{wm})$:

$$f'(J_{wm}) = k_w \cdot \left(-\frac{1}{K_{ECP}} \cdot c_d \cdot e^{-\frac{J_{wm}}{K_{ECP}}} - \frac{1}{K_{ICP}} c_f \cdot e^{\frac{J_{wm}}{K_{ICP}}} \right) - 1 \quad (5.2.1)$$

Algorithm 5.1 Applying Newton's method over a matrix was a fast way to calculate ECP and ICP affected fluxes

```

1  i = 0;                                % Iteration counter
2  xi = x0;                              % Initialise the output variable
3  inrange = 0;                          % Initialise a stopping-case flag
4
5  while (i <= nlimit)&&(~inrange)
6      xi = x0 - f(x0)./df(x0);
7          % Newton's method for the next approximation
8      inrange = (max(max(abs((xi - x0)./xi))) < tol);
9          % Test for in-tolerance
10     x0 = xi;
11     i = i + 1;
12 end

```

The *bisection* and *secant* root-finding methods (see examples in Epperson, 2002, pg 81 ff.) were compared with Newton's method and also with the use of the MATLAB™ `fzero` function (Mathworks Inc., Natick, Massachusetts, ver. 7.12.0 (R2011a)). Each method was applied element-wise over matrices containing the concentrations and pressures of a sample state of the membrane to determine which method would be sufficiently fast for the purposes of this simulation (see discussion of the comparison in appendix B.4). An algorithm for Newton's method was written in MATLAB™ (see algorithm 5.1) based on a similar algorithm for the secant method (Epperson, 2002, pg 115 ff.).

The algorithm was applied over a range of typical trans-membrane flux and concentration values to gather data on combined ECP and ICP effects.

5.2.1.2. Conservation of fluid mass

Equations for the conservation of fluid mass were developed, first for the draw-side of each membrane cell. The cell pressure is P , while the pressure in adjacent cells are marked by subscripts (left, right, top and bottom: subscripts L , R , T and B). The net surface flow for any cell is labelled Q , with similar subscripts indicating the direction of flow, such that flows in four directions were modelled as summing to zero. The surface resistance to flow between adjacent cells was labelled R_d :

$$Q_L + Q_R + Q_T + Q_B = 0$$

$$\frac{(P - P_L)}{R_d} + \frac{(P - P_R)}{R_d} + \frac{(P - P_T)}{R_d} + \frac{(P - P_B)}{R_d} = 0 \quad (5.2.2)$$

Trans-membrane flow, Q_{wm} , and membrane compliance flow, Q_{wc} , were modelled. As such, a positive membrane flow was defined as one that was crossing the membrane

5.2 Model development

into the cell, which could then push fluid *out* of the cell or into the cell's compliant volume. This was modelled as a simple, linear compliance, C_{cell} , where positive flow into the compliance was considered to cause a positive increase in local cell pressure:

$$Q_{wc} = C_{cell} \cdot \frac{dP}{dt} \quad (5.2.3)$$

The time-dependent nature of compliance modelling was managed by calculating compliant flows in terms of the simulation's iterative sample period, τ_s . To manage the derivative term, the definition $dP = P - P_0$ was used, where P_0 is the cell pressure at any previous iteration, and $dt = \tau_s$. The mass-flow equation in 5.2.2 was re-written to include time-dependent compliance flows. The time-dependent term, P_0 , was left as an input on the right-hand-side (RHS), while the independent term was added on the left-hand-side (LHS) to the coefficient for the local cell pressure, P :

$$\begin{aligned} \left(\frac{4}{R_d} + \frac{C_{cell}}{\tau_s} \right) P + \left(\frac{-1}{R_d} \right) P_L + \left(\frac{-1}{R_d} \right) P_R + \left(\frac{-1}{R_d} \right) P_T + \left(\frac{-1}{R_d} \right) P_B \\ = Q_{wm} + \left(\frac{C_{cell}}{\tau_s} \right) P_0 \end{aligned} \quad (5.2.4)$$

In this way, each draw-side cell was able to be described by a linear combination of cell pressures, using coefficients independent of time on the LHS. The RHS contained variables that were likely to be calculated separately as inputs at each iteration of the model. Equations for cells on the boundary of the modelled membrane sheet were written without the terms for flow in the direction of any closed, neighbouring boundaries. The general equation for each cell (5.2.4) was rewritten for each numbered cell, referencing specific neighbouring cells. For example, the cell equation for cell P_{57} was written as follows:

$$\begin{aligned} \left(\frac{4}{R_d} + \frac{C_{cell}}{\tau_s} \right) P_{57} + \left(\frac{-1}{R_d} \right) P_{56} + \left(\frac{-1}{R_d} \right) P_{58} + \left(\frac{-1}{R_d} \right) P_{47} + \left(\frac{-1}{R_d} \right) P_{67} \\ = Q_{wm} + \left(\frac{C_{cell}}{\tau_s} \right) P_{57,0} \end{aligned} \quad (5.2.5)$$

By adjusting the equations according to cell position on the membrane sheet, a similar cell equation was written for every cell on the membrane sheet. To handle this matrix of membrane cells, each was given a row and column number, beginning with indices at 1, 1 at the top-left, and ending with m, n at the bottom right. This was represented by an $m \times n$ array of pressures, that was then reshaped into a pressure vector, \mathbf{P}_d , by ordering cells from left-to-right then top to bottom:

$$\begin{array}{ccccccc}
& & & & & P_{11} & \\
& & & & & P_{12} & \\
& & & & & \vdots & \\
& & & & & P_{1n} & \\
P_{11} & P_{12} & \cdots & P_{1n} & \leftrightarrow \mathbf{P}_d = & P_{21} & \\
P_{21} & P_{22} & \cdots & P_{2n} & & P_{22} & \\
\vdots & \ddots & & \vdots & & \vdots & \\
\vdots & & \ddots & \vdots & & P_{2n} & \\
P_{m1} & P_{m2} & \cdots & P_{mn} & & \vdots & \\
& & & & & P_{m1} & \\
& & & & & P_{m2} & \\
& & & & & \vdots & \\
& & & & & P_{mn} &
\end{array} \quad (5.2.6)$$

Similar vectors were created for cell inputs, so that the system of draw-side membrane cells could be described by a coefficient matrix, \mathbf{A}_d , a state vector \mathbf{P}_d , its value at the previous sample, \mathbf{P}_{d0} and the sum of any inputs, \mathbf{Q}_{winput} , so that by inverting the system matrix, the pressure everywhere on the membrane draw-side, \mathbf{P}_d , was able to be calculated. A similar approach was used to calculate feed-side pressure, \mathbf{P}_f , using a system matrix for the feed-side, \mathbf{A}_f , although in this case, the only modelled input was the trans-membrane loss of fluid to the draw-side, $(-\mathbf{Q}_{wm})$, as there was no significant feed-side compliance or need for any other forced input to be modelled:

$$\begin{aligned}
\mathbf{Q}_{winput} &= \mathbf{Q}_{wm} + \frac{C_{cell}}{\tau_s} \mathbf{P}_{d0} + \cdots \\
\mathbf{A}_d \mathbf{P}_d &= \mathbf{Q}_{winput} \\
\mathbf{P}_d &= \mathbf{A}_d^{-1} \mathbf{Q}_{winput} \\
\mathbf{P}_f &= \mathbf{A}_f^{-1} (-\mathbf{Q}_{wm})
\end{aligned} \quad (5.2.7)$$

By modelling the membrane in this way, the two system matrices, \mathbf{A}_d and \mathbf{A}_f , were able to be inverted just once at the initialisation of each simulation, with their inverted forms then used to update values at each iteration.

5.2.1.3. Membrane fluid flow

The most relevant input into the equations for each draw- and feed-side cell was the vector containing trans-membrane flows, \mathbf{Q}_{wm} . These flows were related to the trans-membrane flux, which is driven by osmotic potential in the general analytical model (see equation 5.1.4 in section 5.1.2.2). A vector was created for each variable in the general model, so that it could be applied to the entire membrane sheet at once:

5.2 Model development

$$\mathbf{J}_{wm} = k_w \left(\mathbf{c}_d \cdot e^{-\frac{\mathbf{J}_{wm}}{k_{ECP}}} - \mathbf{c}_f \cdot e^{\frac{\mathbf{J}_{wm}}{k_{ICP}}} \right) - \frac{\mathbf{P}_d - \mathbf{P}_f}{\mu_{Ri}} \quad (5.2.8)$$

The flow from each feed-side to draw-side cell was then able to be calculated using the cell segment area, A_{cell} :

$$\mathbf{Q}_{wm} = \mathbf{J}_{wm} \cdot A_{cell} \quad (5.2.9)$$

5.2.1.4. Compliance

The flow into the draw-side membrane compliance was used to calculate changes in the stored fluid volume in each cell from past and present draw-side pressure vectors. The time-dependent equivalent was written as the modified \mathbf{Q}_{wc}^* :

$$\mathbf{Q}_{wc} = \frac{C_{cell} (\mathbf{P}_d - \mathbf{P}_{d0})}{\tau_s} \quad (5.2.10)$$

$$\mathbf{Q}_{wc}^* = \frac{C_{cell} \cdot \mathbf{P}_{d0}}{\tau_s} \quad (5.2.11)$$

The volume of each draw-side cell was then able to be adjusted according to any additional flow stored within its compliance:

$$\mathbf{V}_d = \mathbf{V}_{d0} + \mathbf{Q}_{wc} \cdot \tau_s \quad (5.2.12)$$

5.2.1.5. Concentrate injection

In the experimental prototype, dialysate concentrate was added by a fixed-displacement diaphragm dosing pump. The injection flow-rate of this fluid was modelled as a vector of independent flow-rate inputs, \mathbf{Q}_{wi} . The physical distribution of injection was first modelled as a matrix \mathbf{I}_{struct} of flow fractions into the top-most row of n draw-side cells in the membrane-sheet model:

$$\mathbf{I}_{struct} = \begin{matrix} & \frac{1}{n} & \frac{1}{n} & \frac{1}{n} & \dots & \frac{1}{n} \\ & 0 & 0 & 0 & & 0 \\ & 0 & 0 & 0 & & 0 \\ & & \vdots & & \ddots & \vdots \\ & 0 & 0 & 0 & \dots & 0 \end{matrix} \quad (5.2.13)$$

In a similar manner to the reshaping of \mathbf{P} into \mathbf{P}_d , the matrix \mathbf{I}_{struct} was reshaped into a vector, \mathbf{I}_{struct} , and used to model the injected flow by using the fixed flow-rate of the dosing pump, Q_{win0} :

$$\mathbf{Q}_{wi} = \mathbf{I}_{struct} \cdot Q_{win0} \quad (5.2.14)$$

5.2.1.6. Draw-side recirculation

In the experimental prototype, a recirculation pump was used to move the draw-side salt distribution in order to vary the output the draw-side concentration (see figure 3.2.1). To model this, equal flows were added and subtracted from the top- and bottom-most rows of the membrane sheet model, according to the structure, \mathbf{R}_{struct} , at the recirculation rate, r_0 :

$$\mathbf{R}_{struct} = \begin{matrix} & \frac{1}{n} & \frac{1}{n} & \frac{1}{n} & \dots & \frac{1}{n} \\ & 0 & 0 & 0 & & 0 \\ & 0 & 0 & 0 & & 0 \\ & & \vdots & & \ddots & \vdots \\ \frac{1}{n} & \frac{1}{n} & \frac{1}{n} & \dots & \frac{1}{n} \end{matrix} \quad (5.2.15)$$

By reshaping \mathbf{R}_{struct} into the vector, \mathbf{R}_{struct} , a recirculation flow vector was able to be calculated from the recirculation pump rate, Q_{wr} :

$$\mathbf{Q}_{wr} = \mathbf{R}_{struct} \cdot Q_{wr} \quad (5.2.16)$$

Combining equations 5.2.9, 5.2.10, 5.2.14 and 5.2.16 allowed the calculation of the total effect of all forced fluid inputs into the membrane system:

$$\mathbf{Q}_{winput} = \mathbf{Q}_{wm} + \mathbf{Q}_{wc}^* + \mathbf{Q}_{wi} + \mathbf{Q}_{wr} \quad (5.2.17)$$

5.2.2. Surface mass-flow

5.2.2.1. Fluid flow between cells

Fluid flows between cells were calculated from values for pressure and the local estimate of surface flow resistance. For any draw-side cell, the flow in direction Z , was calculated and stored in a matrix, \mathbf{Q}_{dZ} , using the original $m \times n$ pressure matrix for the draw-side, \mathbf{P}_d , and a similar matrix, \mathbf{P}_{dZ} , which was offset by one cell in the direction from which the flow was directed. Pressures at sheet boundaries were determined by modelling cells as having no flow in that direction, therefore the values on that edge of the \mathbf{P}_{dZ} matrix were copied from that of the \mathbf{P}_d matrix, forcing the values for flow at those locations to zero. For example, the pressure matrix \mathbf{P}_{dL} was formed by shifting all the values by one cell to the *right*, so that the pressure value for the relevant cell

5.2 Model development

would be that which would normally be found in the cell to the *left*, hence the subscript *L*. The left and right sides of the draw-side compartment are closed, so the pressures on the left-most edge of the shifted matrix P_{dL} were copied from the original pressure matrix P_d :

$$P_d = \begin{matrix} P_{1,1} & P_{1,2} & P_{1,3} & \cdots & P_{1,n} \\ P_{2,1} & P_{2,2} & P_{2,3} & \cdots & P_{2,n} \\ \vdots & \vdots & \vdots & \ddots & \vdots \\ P_{m,1} & P_{m,2} & P_{m,3} & \cdots & P_{m,n} \end{matrix} \quad (5.2.18)$$

$$P_{dL} = \begin{matrix} P_{1,1} & P_{1,1} & P_{1,2} & \cdots & P_{1,n-1} \\ P_{2,1} & P_{2,1} & P_{2,2} & \cdots & P_{2,n-1} \\ \vdots & \vdots & \vdots & \ddots & \vdots \\ P_{m,1} & P_{m,1} & P_{m,2} & \cdots & P_{m,n-1} \end{matrix} \quad (5.2.19)$$

Similar offset matrices were developed for pressures to the right, P_{dR} , top, P_{dT} , and bottom, P_{dB} . These were able to be combined with the estimated value for surface flow resistance, R_d , to form a matrix of flows for the draw-side of the membrane sheet:

$$Q_{dZ} = \frac{(P_d - P_{dz})}{R_d} \quad (5.2.20)$$

A similar approach was used to model flows on the membrane's feed-side, which is closed on three sides and open on the right-most side where the permeate tube meets the edge of the sheet envelope.

5.2.2.2. Salt flow between cells

With matrices for fluid flows established, the transfer of salt mass around both sides of the sheet was able to be estimated from values for concentration as used in the general model (see section 5.1.2.2). Any fluid volume flowing out of a cell was modelled as an incremental fluid mass containing salt at that same concentration. The total salt-mass lost from each draw-side cell, m_d^+ , was calculated for all four directions:

$$\begin{aligned} m_d^+ &= c_d (Q_{dL}^+ + Q_{dR}^+ + Q_{dT}^+ + Q_{dB}^+) \cdot \tau_s \\ &= c_d \sum_Z Q_{dZ}^+ \cdot \tau_s \end{aligned} \quad (5.2.21)$$

Here, the + superscript in Q_{dZ}^+ indicates positive flows *out* of any cell. Flows *into* each cell carry the fluid concentration of their *source*, not their destination. The corresponding mass-flows, m_d^- , were dealt with slightly differently and calculated separately:

$$m_d^- = \sum_Z c_{dZ} \cdot Q_{dZ}^- \cdot \tau_s \quad (5.2.22)$$

In this case, the concentration matrix, c_d , was not used; instead, using a method similar to that used to develop offset pressure matrices, a matrix for the concentration *adjacent* to each cell in each direction Z was calculated as c_{dZ} and corresponding to the flow *from* that direction, Q_{dZ}^- . A new concentration matrix was then able to be calculated using the matrix for cell volumes⁴:

$$c_d = c_{d0} + \frac{(m_d^- - m_d^+)}{V_d} \quad (5.2.23)$$

5.2.3. Model parameter estimates

5.2.3.1. Membrane geometry

Total membrane width, W_{mem} , was derived from published values for membrane area, A_{mem} , and length, L_{mem} (Hydranautics, 2011). By autopsying a similar membrane element, membrane sheet spacer widths, w_d and w_f , were measured for both the draw- and feed-side compartments, and then used to calculate the cross-sectional areas, A_{dcross} and A_{fcross} , through which fluid flows on the sheet surfaces. Instead of modelling each spacer as separating two parallel sheets, this arrangement was modelled as having each sheet separate two half-spacer volume compartments.

$$\begin{aligned} A_{dcross} &= 0.5 \times W_{mem} \times w_d \\ A_{fcross} &= 0.5 \times W_{mem} \times w_f \end{aligned} \quad (5.2.24)$$

5.2.3.2. Resistance

By combining an average of published RO feedwater and brine flows, Q_{avRO} , with a published value for typical applied RO pressure, P_{maxRO} , a value was estimated for longitudinal resistance, R_{equiv} , which was then generalised to estimate resistivity, ρ_{equiv} :

$$\begin{aligned} R_{equiv} &= \frac{P_{maxRO}}{Q_{avRO}} \\ \rho_{equiv} &= R_{equiv} \cdot \frac{A_{dcross}}{L_{mem}} \end{aligned} \quad (5.2.25)$$

⁴The usual convention for summing *positive* fluid flows *out* of a cell was followed. Unfortunately this leads to cognitive dissonance when associated positive mass flows are calculated as a *loss* of mass from any cell, while gains in mass are marked by negative flows. This is evident in equation 5.2.23, where salt gains are marked by a negative superscript, m_d^- , while losses are marked positive, m_d^+ .

5.2 Model development

By dividing the total membrane area, A_{mem} , into 10 separate sheet areas, A_{sheet} (to imitate the spiral-wound packaging of the ESPA-series 4040 membrane elements), and then dividing these into $m \times n$ cell areas, A_{cell} , flow-resistances, R_d and R_f for each cell were able to be calculated:

$$\begin{aligned} R_d &= \rho_{equiv} \cdot \frac{n}{m} \cdot \frac{L_{sheet}}{W_{sheet} \times 0.5 \times w_d} \\ R_f &= \rho_{equiv} \cdot \frac{n}{m} \cdot \frac{L_{sheet}}{W_{sheet} \times 0.5 \times w_f} \end{aligned} \quad (5.2.26)$$

5.2.3.3. Compliance

The approximate draw-side compliance of membrane element cells was estimated using the following method:

1. A known quantity of salt solution was injected into the sealed draw-side compartment of an element.
2. Feedwater was allowed to flow into the permeate tube and be drawn across the membrane to dilute salt in the draw-side compartment.
3. The bulk, draw-side pressure, P_{dmem} , and the feed-side flow, Q_{fmem} were recorded over time so that an estimate of the element's bulk compliance, C_{mem} , could be made.
4. The compliance of the whole membrane was then approximated to the compliance of individual cell segments, using the assumption that membrane compliance is proportional to membrane area⁵:

$$\begin{aligned} Q_{fmem} &= C_{mem} \cdot \frac{d}{dt} P_{dmem} \\ \frac{d}{dt} V_{dmem} &= Q_{fmem} \\ C_{mem} &\cong \frac{dV_{dmem}}{dP_{dmem}} \end{aligned} \quad (5.2.27)$$

$$C_{cell} = C_{mem} \cdot \frac{A_{cell}}{A_{mem}} \quad (5.2.28)$$

⁵By this method, the entire draw-side compliance was modelled as if it was distributed across only the membrane, even though compliance was also present in the fluid couplings and other draw-side components.

5.2.3.4. Membrane permeability

Values for water and salt permeabilities, A and B (see table 2.3.1), were converted into various useful quantities, such as intrinsic membrane resistance, μ_{Ri} , resistance per cell, R_{cell} , and membrane flux constants for water and salt, k_w and k_s :

$$\mu_{Ri} = \frac{1}{A} \quad (5.2.29)$$

$$R_{cell} = \frac{\mu_{Ri}}{A_{cell}} \quad (5.2.30)$$

$$k_w = \frac{i \cdot R \cdot T}{\mu_{Ri}} \quad (5.2.31)$$

$$k_s = B \quad (5.2.32)$$

5.2.4. Program structure

The simulation and model were developed to be analogous to the behaviour of the experimental hardware setup (see section 5.3.1). The core of the model was tasked with generating iterative solutions of differential fluid and salt flow equations, while discrete hardware changes were managed by a higher-level state machine. This approach was essentially an implementation of *discrete and continuous simulation* (see Karlberg et al., 2013), using MATLAB™ procedures.

5.2.4.1. Initialisation

The simulation was first initialised by setting scenario-specific parameters, such as target flow-rate and total simulated time, through the procedure `flatsheetinitialise` (see figure 5.2.1). Fixed values for the modelled membrane and other variables were initialised, then used to derive specific production parameters. At this stage, the major system matrices, A_d and A_f , were assembled and inverted. Timing variables, such as `tsincestart=0` and the two loop counters, `i=1`, and sample counter, `outsamp=1`, were also initialised.

5.2.4.2. Main loop

The main loop was constructed to manage iterations over several evaluation and variable-update procedures (see figure 5.2.1). After checking for the end of the simulation, the program would update any hardware state variables through the procedure `fsehardware` (see section 5.2.4.3). Any parameters specific to the production stage were set through the procedure `fsestagemanager` (see section 5.2.4.4). Solutions to the differential

equations for fluid and salt flows through and across the membrane were then calculated in the procedure `fsesystem`. Select values were periodically recorded at a low sample-period using the procedure `fseoutputsampl`. The main loop was set to iterate once every $\tau_s = 10$ ms. Once the end of the simulation was reached, the program closed any open files and printed a report using the procedure `makereports` before exiting.

5.2.4.3. Hardware update during production

Hardware emulation during production was arranged around a periodic switching cycle, to imitate the input characteristics of a typical dialysis machine (see figure 5.2.2). Fresenius 4008 and 5008 series dialysis machines regulate fluid balance via a calibrated balance chamber that allows ~ 30 ml dialysate fluid to be consumed in each switch cycle. The net dialysate consumption rate is therefore regulated by controlling the switch time. To simulate this, whenever the `fsehardware` procedure was called, a timer for each switch cycle, `switcht`, was compared against a calculated switch rate, `switchtime`, which was derived from the target flow-rate, $Q_{wtarget}$, during initialisation. At the end of each switch cycle, the accumulated output volume for that cycle was used to calculate an average output flow-rate. A similar timing variable, `stroket`, was also initialised at the beginning of each switch cycle and compared against the stroke delivery time, `stroketime`, which was also initialised at startup. In this way, each simulated switch cycle corresponded to one stroke of the injection pump and one accumulation of output fluid.

5.2.4.4. Production and backwashing stages

The two main production stages used for this simulated experiment were *Production* and *Backwashing* (see figure 5.2.3). During the *Production* stage, the `fsehardware` procedure was enabled, and concentrate injection and output accumulation were simulated at each iteration. Once the dialysate output conductivity, `Cdialysate`, had risen to within tolerance, `tol`, of its target value, `ctarget`, the state counter was set to the *Backwashing* stage and the corresponding timer, `cycllet=0`, was set.

During *Backwashing*, the main hardware update procedure was disabled, and values for the recirculation pump speed and direction were set to emulate the prototype hardware performance. After a fixed backwashing time had elapsed, `cycllet>backwashtime`, the cycle time was again reset and the state counter returned to *Production*.

5.2.4.5. System update

It was in the procedure `fsesystem` that the main numerical evaluations of the general analytical model (see section 5.2) were implemented (see figure 5.2.4). The ordering of

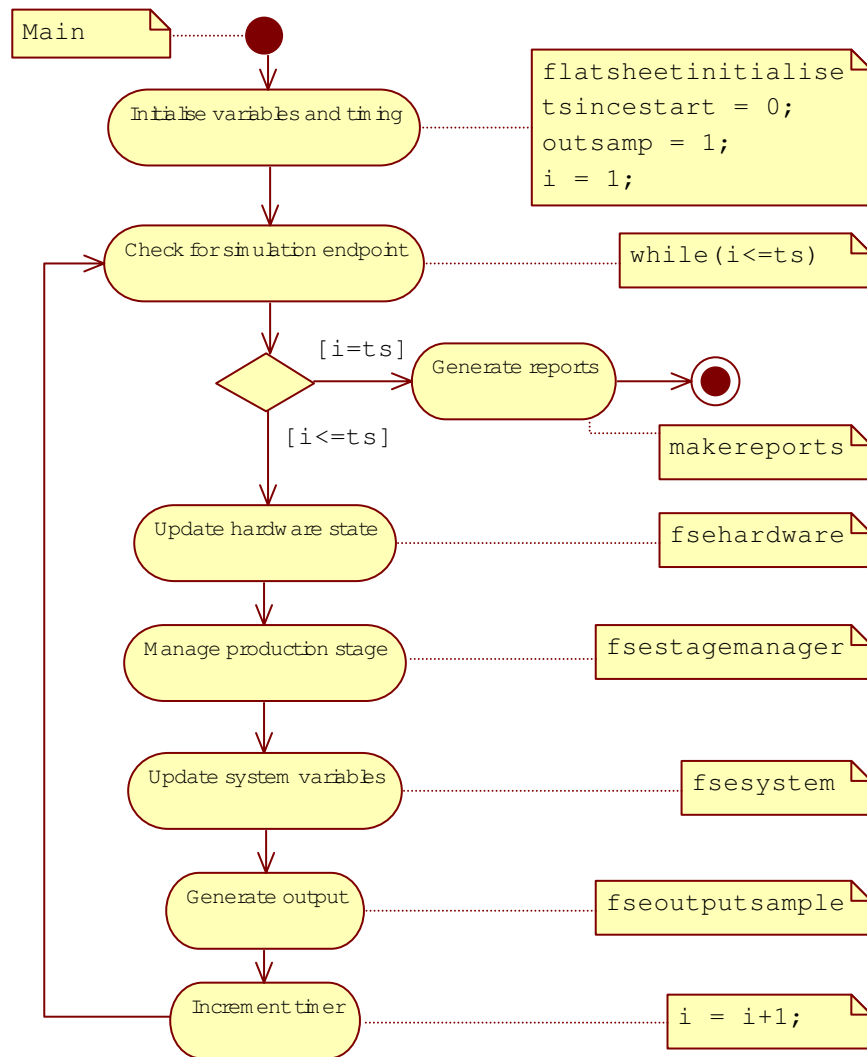


Figure 5.2.1.: Main process

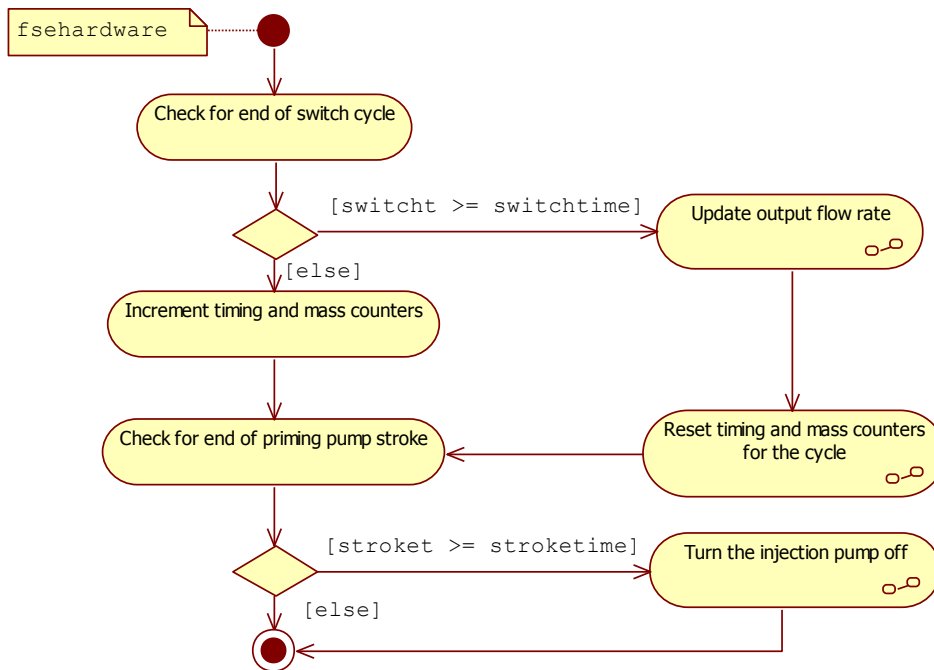


Figure 5.2.2.: Process for updating hardware variables

calculation sub-procedures was chosen for convenient debugging rather than according to an intuitive ordering. In particular, cell concentrations were updated by two separate sub-procedures: the first following trans-membrane flow calculations and the second following calculations of surface-flows. While it would have been possible to combine the two sub-procedures, they were kept separate to enable the easy checking of mass-balances during development and debugging.

5.2.4.6. Output generation

Infrequent data-sampling at $\tau_{sout} = 6000$ ms was performed by the procedure `fseoutputsample` to minimise the size of the output data files. It was necessary to maintain a high iterative sample rate for numerical evaluations (see discussion in appendix B.1), yet changes in the fluid system's bulk performance were able to be resolved at a much lower sample rate.

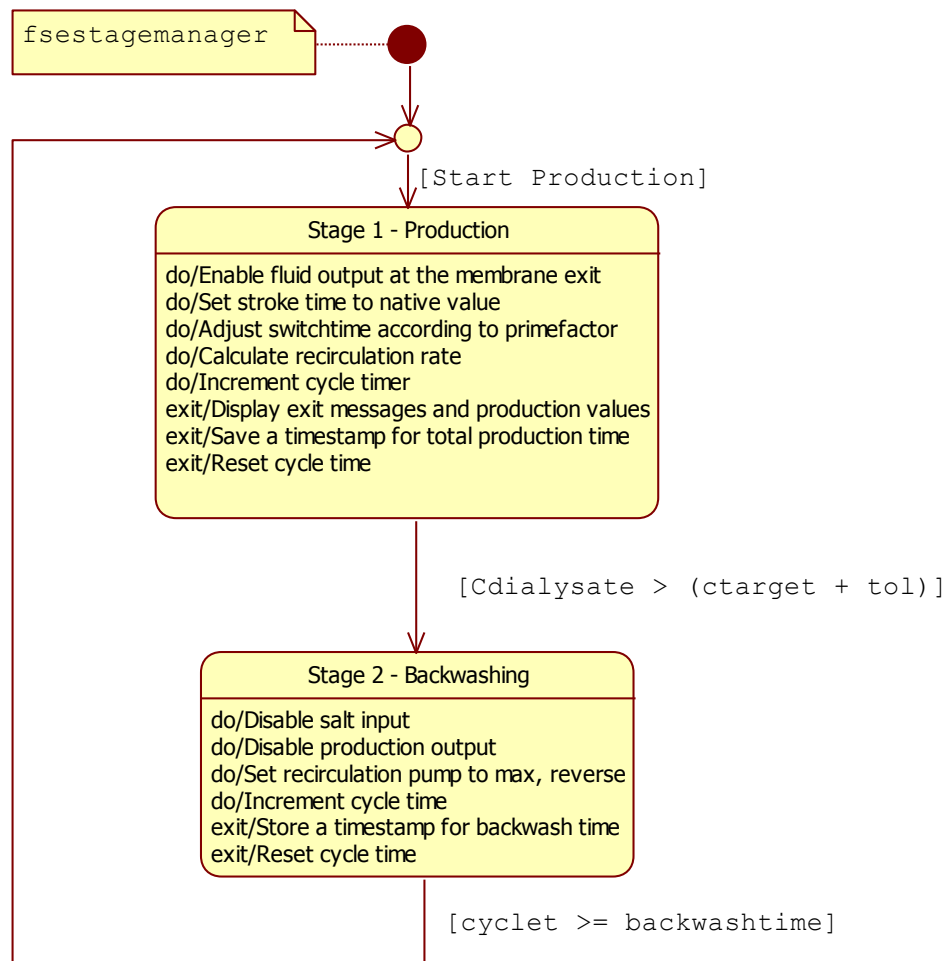


Figure 5.2.3.: Production stage management

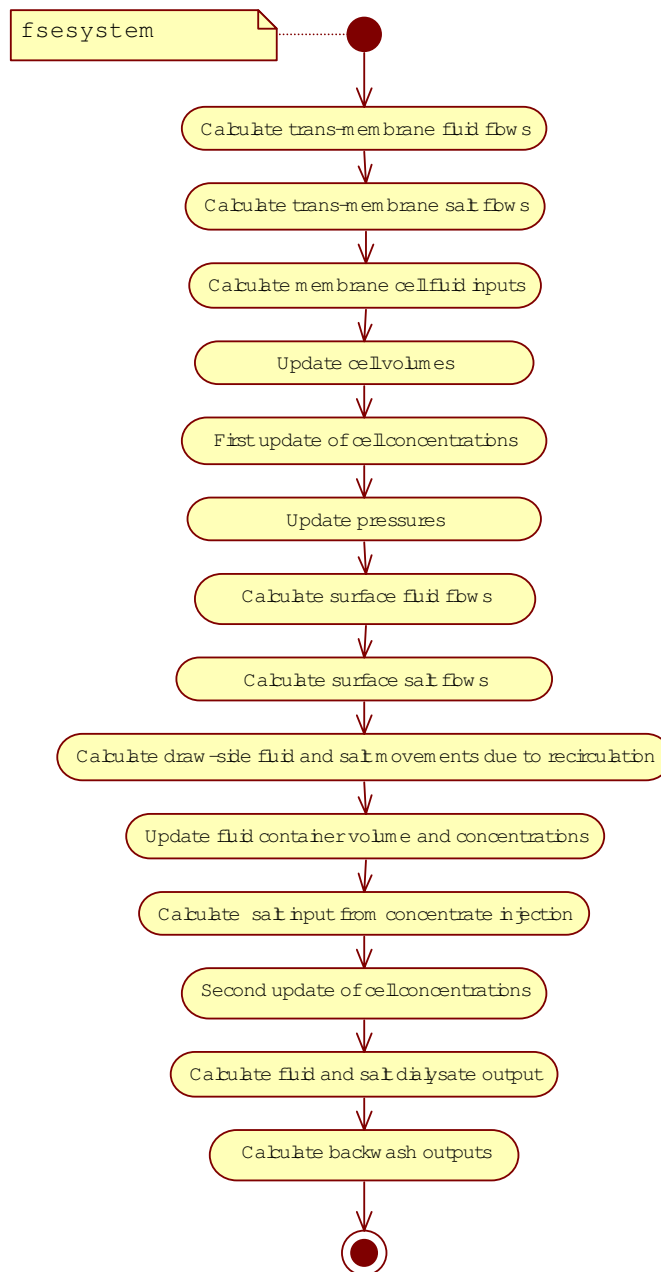


Figure 5.2.4.: Core system update procedure

5.3. Materials and method

5.3.1. Experimental setup

The experimental setup that was used is similar to that described in chapter 3. For backwashing experiments, an additional reference conductivity sensor (UMED D0094, Fresenius Medical Care) and scales (Spider 1, Metler-Toledo International Inc.) were placed at the drain-outlet of the feed-side tube so that flushed fluid characteristics could be collected and measured. The same spiral-wound RO membrane element (ESPA2-4040, Hydranautics Nitto-Denko) was used for all experimental work.

5.3.2. Production stage

Each production stage was carried out at a specified target flow-rate, $Q_{wtarget}$, which was then interpreted by the operating program and converted to a corresponding rate of dialysate concentrate injection. The same overprime factor was used as before, $F_{OP} = 1.61$. The draw-side compartment valves were set to allow simultaneous collection and recirculation of any dialysate output. The recirculation pump was set operate in a clockwise direction at its lowest practical speed, which was 12 % of its maximum value of ~ 1400 ml/min. Feedwater was supplied at neutral pressure, with a solute concentration estimated to be ~ 11 mosm/L. Production proceeded in each case from the backwashed state of the membrane until saturation point, when the accumulated dialysate output mixture had reached its target conductivity of $\sigma_{target} = 11.6$ mS/cm, as measured at the intake conductivity sensor. Timed samples of conductivity were recorded by the operating program every ~ 100 ms, while accumulated dialysate output volume was recorded manually by a trained operator⁶. When the conductivity target was reached, the final mass was recorded and discarded, and the system proceeded to its backwashing stage.

5.3.3. Backwashing stage

Each backwashing stage was carried out by setting the valves and recirculation pump such that low-osmolarity water⁷ was drawn from the backwash fluid container, pumped upwards through the draw-side membrane compartment displacing the draw-solution and allowed to permeate through the membrane towards the feed-side. To achieve this, the recirculating pump was set to 100% speed in a counter-clockwise direction. The permeating fluid was allowed to be both drawn by the higher-salinity feedwater it was

⁶Accumulated output was measured using scales reading in kg. This was converted and recorded as an equivalent volume in L using the approximation $1.0 \text{ L} = 1.0 \text{ kg}$.

⁷This water was typically drawn from an RO source.

intended to displace, and to be forced across the membrane by the draw-side pressure developed across the longitudinal resistance of the element's draw-side structure.

During this stage, the drain fluid was diverted to the emptied dialysate output container so that its accumulating mass could be recorded by a trained operator. Drain-fluid conductivity was measured by the secondary conductivity sensor and recorded manually by the same operator. The backwashing time, t_{bf} , was varied according to the needs of each experiment. Following each backwashing stage, the system was returned to its production stage.

5.3.4. ECP and ICP model tuning

The computational model was used to simulate various practical experiments. In order to reproduce them with accuracy, the model's parameters for ECP and ICP were first tuned by comparing simulated with experimental output. This was done by operating the simulation at the mid-rate target flow-rate of $Q_{wtarget} = 242$ ml/min, and varying only the value of K_{ICP} (together with $K_{ECP} = 10 \times K_{ICP}$ — see equation 2.3.2) until the response curve of the simulated output was as close as possible to the experimental response (see comparison of output responses in figure 5.4.2). Once established, the new values for K_{ECP} and K_{ICP} were used for all other simulations.

Data was collected from the simulated model to estimate a typical range of values for draw- and feed-side concentrations, c_d and c_f . These were combined into a set of trans-membrane concentration differences $\Delta c = c_d - c_f$, then used to calculate a corresponding set of ECP and ICP inclusive trans-membrane fluid fluxes, J_{wm} , using the numerical method described above (see algorithm 5.1).

5.3.5. Backwashing and production analysis

5.3.5.1. Backwash nature

The nature of the backwashing mechanism was analysed by examining the system's conductivity and accumulated volume responses over time. Experimental and computational model data were collected at a setting of $Q_{wtarget} = 242$ ml/min. This was then simulated using the computational model at a range of rates from $Q_{wtarget} = 121 \rightarrow 800$ ml/min to establish any dependence of the backwashing profile on the production target of the previous cycle.

5.3.5.2. Backwash location

To observe the location of the backwashing mechanism within the membrane, data was collected from a simulated dialysate production experiment at $Q_{wtarget} = 242$ ml/min,

followed by a simulated backwash stage. This was done to enable the visualisation of simulated two-dimensional salt concentrations over both sides of the membrane sheet.

5.3.5.3. Production time optimisation

A series of experimental backwash/production cycles were carried out, using a fixed target production rate close to a practical medical value of $Q_{wtarget} = 484$ ml/min. Dialysate production volume, V_{cycle} , was recorded against the backwashing time of the previous cycle, t_{bf} , to indicate backwashing effectiveness. Backwash time was reduced incrementally between production cycles until no further useful output was produced in the subsequent production stage. The apparent production rate, $Q_{wtarget}^*$, was then calculated for each cycle using equation 5.1.2.

5.4. Results and discussion

5.4.1. ECP and ICP estimates

5.4.1.1. Model tuning

The adjusted values for K_{ECP} and K_{ICP} were found to be much lower than their initial estimates, with $K_{ICP} = 0.18 \times K_{ICP0}$. As discussed by Tan and Ng (2013), the analytical model used here tends to overestimate solute diffusivity, D , and therefore $K_{ICP} = \frac{D}{S_{me}}$ at higher concentrations⁸. Furthermore, as the initial estimate for K_{ICP} was derived from a structural parameter, S_{me} , for a similar RO membrane (see Tiraferri et al., 2013), the estimate may have been more appropriate for RO applications, where cross-flow and turbulence are more significant. This bias in the estimation of S_{me} has been explored in depth by Park et al. (2011). Knowledge of the membrane structural parameter is crucial to the evaluation of membrane performance and is difficult to estimate without employing numerical or experimental methods (see Tiraferri et al., 2013). An empirical approach to the bulk estimation of K_{ECP} and K_{ICP} was found to be effective enough to produce reasonable agreement between experimental and computational data.

5.4.1.2. ECP and ICP severity

The simulated effects of ECP and ICP in the system were quite severe over the sampled range of concentration gradients (see figure 5.4.1). Similarly severe results have been

⁸As in section 5.1.2.2, the convention in Lay et al. (2012) has been followed where the mass transfer coefficient is written as $K_{ICP} = \frac{D}{S_{me}}$, rather than as its inverse, the resistance to solute diffusion ($K = \frac{S_{me}}{D}$).

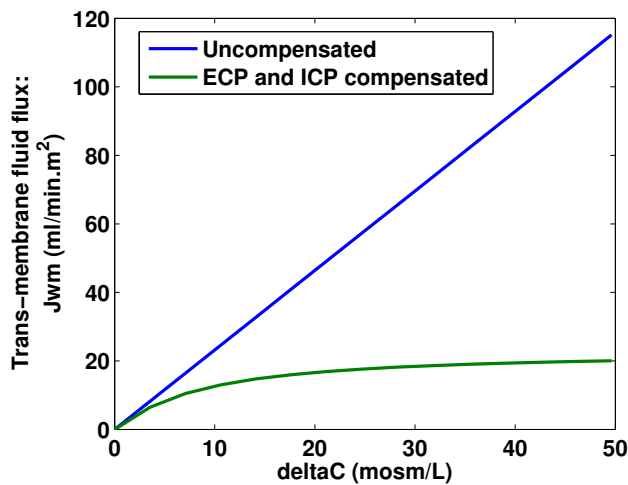


Figure 5.4.1.: Severity of ECP and ICP in simulated trans-membrane fluid flux

recorded and predicted by others (Zhao et al., 2012), by the theoretical analysis (figure 2.3.5) and in the experimental work (see section 4.3.1.4). This severity implies that to obtain the maximum possible fluid flux, the system should be operated at the highest possible target flow-rate, even though at higher rates the flux would not be greatly increased.

5.4.2. Backwashing mechanism

5.4.2.1. Nature of effect

Experimental and simulation data revealed that the system's backwash flow was largely driven by hydrostatic pressure, with a small osmotic component (see figure 5.4.2). The osmotic effect was most clearly visible in the gradient of the accumulated volume curve, which was slightly increased in the early stage of production. The conductivity response showed that the rate of salt removal from the feed-side appeared to diminish after about four minutes of backwashing. Backwashing had diminishing usefulness after about 10 min. After about 20 min, the total feed-side salt had been reduced to a negligible level, and backwashing was seen to have no further useful effect.

The rate at which salt was flushed from the feed-side during backwashing appeared to be independent of the original target flow-rate setting, with the simulated conductivity response curves converging before any were reduced to a negligible level (see figure 5.4.3). The theoretical analysis shows that in this method, draw and feed-side salt accumulation are closely determined by $Q_{wtarget}$ (see section 2.3.3.2). This was evident in the peaks of the conductivity response curves: higher peaks were indicative of greater accumulated feed-side salt due to lower flow-rate targets. The backwash rate

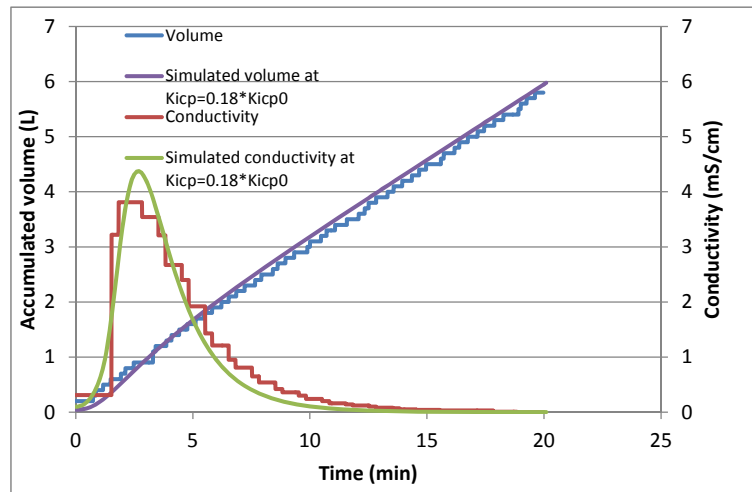


Figure 5.4.2.: Model response at $Q_{wtarget} = 242$ ml/min with K_{ICP} tuned to match experimental output.

was likely to have instead been limited by membrane element geometry: in particular, the width of the membrane sheet.

5.4.2.2. Location of effect

As discussed in previous chapters, the accumulation of salt in the feed-side compartment is a critical problem with this method of FO dialysate production. At the point of saturation (figure 5.4.4b), the simulated feed-side had accumulated salt in the region of the membrane sheet furthest from the drain tube. During backwashing (figure 5.4.5a), the osmotic component of backwashing was strongest in regions of high salinity, yet its effect was rapidly diminished as the bulk of the feed-side salt was spread to cover most of the sheet. The hydrostatic component appeared to be distributed over the sheet, causing further flushing of fluid from regions of the sheet where the salinity was already reduced⁹.

The dominance of the hydrostatic backwashing component was advantageous in that it continued to flush diluted salt after the osmotic effect had diminished. Having an osmotic component was also useful as it caused increased fluid flux where it was needed most: the high-salinity regions of the membrane sheet. An ideal scenario would be one where both hydrostatic and osmotic backwashing effects could be focused on the region of the sheet furthest from the drain tube. Unfortunately, due to the single draw-side input at each end of the pressure vessel, it would be difficult to arrange backwashing in this way without major modification to the vessel and/or its enclosed element.

⁹A video of the simulation described here is embedded in digital version of this document. It can be viewed by clicking on figure 5.4.4 (a).

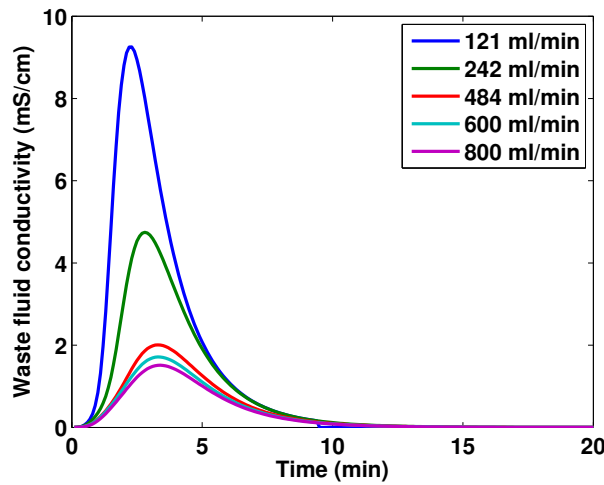


Figure 5.4.3.: Simulated backwash conductivity response comparison over a range of target flow-rate settings

5.4.3. Production optimisation

5.4.3.1. Output volume

The experimental data showed that there was little improvement in production volume following backwashing stages longer than 11 min (see figure 5.4.6¹⁰). Decreasing backwashing times below 11 min caused decreased production efficiency. The production volume following a backwash time of 2.0 min was negligible. This was consistent with the predictions of the computational model: that a backwash time $t_{bf} \lesssim 4.0$ min would result in most of the feed-side salt being retained, and cause the following production stage to be unlikely to produce any useful output. This result suggests that the optimal backwash time lies somewhere between $t_{bf} = 4.0 \rightarrow 11$ min. As discussed above (see section 5.1.1.2), the determination of this optimal time depends on the competing values of backwash time and subsequent production volume.

5.4.3.2. Apparent production rate

Apparent production rates were able to be estimated from experimental data (see figure 5.4.7). The data showed a local maximum of $Q_{wtarget}^* \approx 240$ ml/min. Approximation

¹⁰In this experimental sample, there was a small apparent improvement in production volume following a backwash time of 11 min. It is not clear exactly why this occurred, although it is suspected that it was simply due to experimental noise. Further repetition of the experiment at that data point showed that a variation of $\sim \pm 5\%$ was typical of these volume measurements.

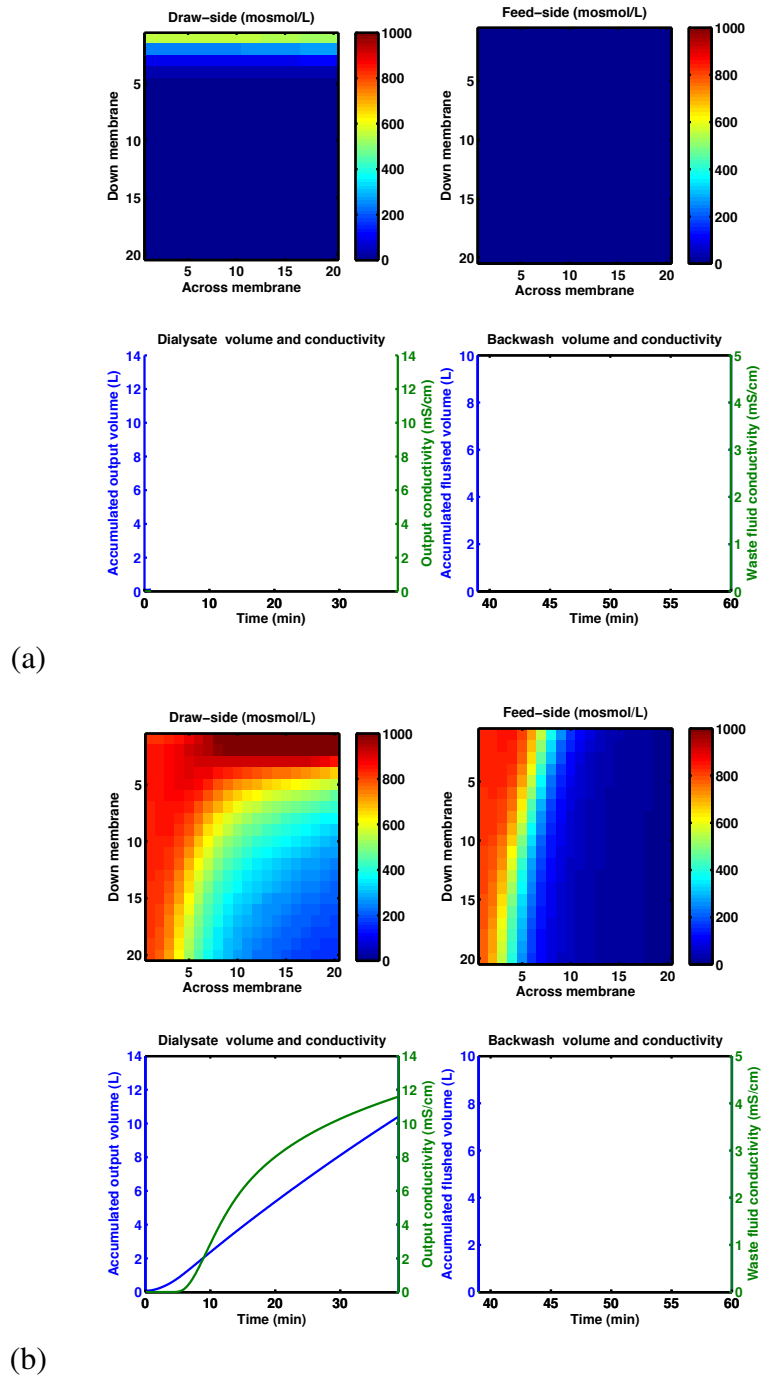


Figure 5.4.4.: Production and backwash progression at 242 ml/min: start (a), saturation (b)

5.4 Results and discussion

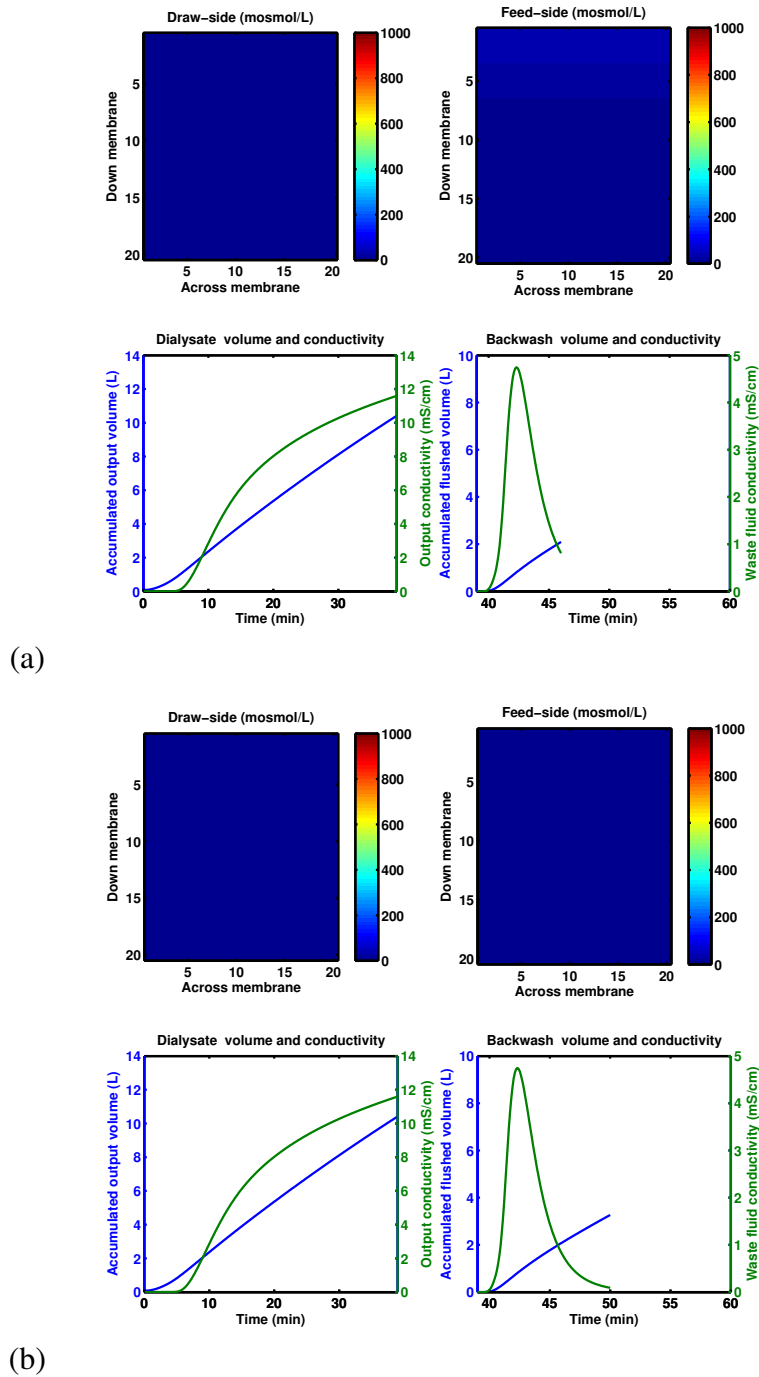


Figure 5.4.5.: Production and backwash progression at 242 ml/min: minimum recovery (a) and complete recovery (b).

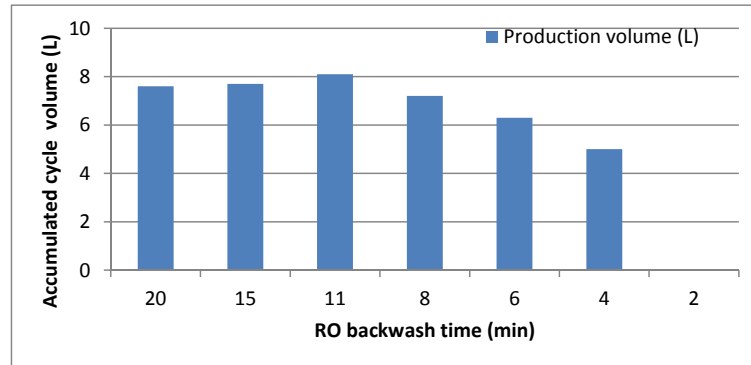


Figure 5.4.6.: RO backwash efficiency indicated by accumulated volume at the point of saturation, following production at $Q_{wtarget} = 484$ ml/min

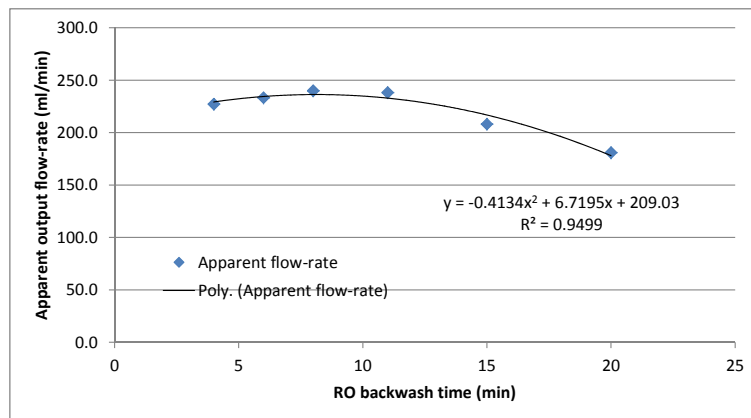


Figure 5.4.7.: Apparent output flow-rate dependency on backwash time

by a quadratic curve shows that this maximum corresponds to $t_{bf} \approx 8$ min¹¹. This need for a relatively long backwashing time poses a major practical limit on this method of FO dialysate production.

5.5. Conclusions

5.5.1. Significant findings

The experimental and simulation data suggest the following for the described system and method:

¹¹A quadratic approximation conveniently highlights the suggested conclusion: that there exists an optimal backwashing rate. However, this curve fit was chosen for its simplicity and is not intended to suggest that the response is generally quadratic in nature.

5.5 Conclusions

1. High production flow rates were likely to have been limited by severe ECP and ICP
2. Backwashing time was independent of any previous production flow-rate
3. Backwashing occurred over the entire sheet and was constrained by the structure of the spiral-wound element
4. The primary mechanism of backwashing was hydrostatic rather than osmotic pressure
5. Backwashing for $t_{bf} < 4.0$ min was inadequate
6. Backwashing for $t_{bf} > 11$ min showed little further benefit
7. When combined with measures of production efficiency, the optimal backwashing time appeared to be close to ~ 8 min
8. Within the chosen test parameters, the best-case apparent production rate was about $Q_{wtarget}^* \approx 240$ ml/min, which was about 50 % of the set flow-rate target

5.5.2. Summary

The described approach to backwashing was similar to the bolus method described by Qin et al. (2009), except that the size of bolus needed in this application was larger than the total volume of the draw-side compartment¹². It is unfortunate that the necessary backwashing time was significantly large at ~ 8 min – much larger than the time others have needed to briefly reverse the flow local to the membrane surface (see section 5.1.1.1). The data shows no easy way to avoid this long backwash time, as it appeared to be constrained by the element geometry. This limitation may be improved upon by perhaps using a pair of smaller-diameter elements, or a single element with more and narrower membrane sheet-pairs allowing feed-side salt to be more quickly driven across the sheet towards the drain-tube.

Lastly, the *significance* of the backwashing time might be decreased by instead increasing t_{eff} . The experimental work (chapter 3) shows that this may be done by operating the system at a lower target production rate. While the simulation data shows that this is unlikely to affect the backwash time, it should at least allow more efficient production over a longer period. The required apparent flow-rate could then be achieved by sharing the production workload between two or more elements, each of which would be less affected by ECP and ICP, and therefore be able to produce dialysate at a more efficient rate. This would likely be necessary anyway, as the single element examined here struggled to achieve an apparent output that was more than half of its target flow-rate.

¹²Pilot experiments were attempted to assess whether smaller boluses could likely be used, but it was found difficult to keep the solutions from mixing, and no useful data was generated. Nevertheless, it was felt that this approach is worth pursuing in future work.

In general, it would appear that this approach to dialysate production in particular and to the use of RO elements for FO in general is possible and may yet prove to be practical. For applications where the output product is needed only at a relatively low rate, or where there is plenty of space for multiple elements, or where energy and noise consumption of a full-time RO system is unwanted, this approach to backwashing may make inexpensive FO viable without the need for specialised FO membrane elements.

6. Design for remote Aboriginal health: a methodology

6.1. Introduction and background

This chapter is significantly different to those preceding it in that it is largely concerned with engineering design methodology. As such, it refers less to *what* is designed, and is instead concerned with *how* it is designed. It also pays attention to peoples' values, preferences and cultures, and the many ways in which people, context and dialysis technology interact. Addressing issues around *how* things are designed is fundamentally important to the success of those designs for their intended users, especially when it comes to healthcare for vulnerable people (see rationale in section 1.3.4).

The discussion so far has focused on the technical nature of an FO-based dialysate production method. In particular, it was found that an FO-based implementation was likely to have greater energy efficiency than its RO-based equivalent, at the cost of increased size due to its need to incorporate extra membrane surface area (see chapter 4.4). However, as highlighted in the introduction (chapter 1), it is necessary to consider the impact of any design variations on the social context in which the technology is used. Furthermore, such consideration is critical to the successful design of medical devices (Wilcox, 2012; Rajkomar and Blandford, 2012).

Proposed here is an engineering design methodology that has been developed specifically to address this need, particularly for use in the context of remote Australian Aboriginal desert communities. The methodology includes practical methods for exploring a remote health context in a purposive, efficient way, and for systematically recording and translating collected data so that outcomes due to design variations can be predicted and verified against the needs and preferences of the user community.

6.1.1. The need for a context-sensitive design methodology

When considering medical device design for remote Aboriginal health, a suitable methodology must be one that enables the social context within which remote Aboriginal community dialysis operates into design parameters. This need for the incorporation of social context into the process of engineering design has been emphasised by many,

often while simultaneously decrying the failure of designers to adopt suitable methods. Ovaska and Stapleton (2009) describe the high failure-rate of Information Systems (IS) designs, and suggest that ambiguous requirements and a lack of user involvement are part of the trouble. Love (1998) suggests that the trouble stems from engineers having a particularly mechanistic and positivistic perspective. Hughes et al. (1994) suggest that a periodic ethnography should be incorporated into the design process, while Oates et al. (2004) find that under-usage of such empirical methods has been a source of criticism. In general, it is suggested that a design process should proceed by combining a qualitative or interpretivistic approach to social context research with a positivistic approach to technology development (Love, 1998; Oates et al., 2004; Leys, 2003; Dawson et al., 2003).

With such a well-emphasised need being identified by many, it seems unfortunate that such methodologies are rarely used. Some authors point to the lack of suitable design methodologies. For example, while referring to such a lack within the healthcare industry, Hempe et al. (2010) writes:

Currently no structured design process for these complex health and care services exists.

(Hempe et al., 2010, pg 125)

Other authors suggest that the problem is not a lack of suitable methodologies, but a failure of design teams to make use of them. For instance, Ehn (1998) suggests:

What we don't need is another design methodology. Bookshelves around the world are already full of them. What we need is an understanding of why they are not being effectively used.

(Ehn 1998, quoted in Wotherspoon, 2001, pg 7)

Before adding yet another design methodology to the corpus, it is worth exploring further the obstacles to the use of such design methodologies.

6.1.2. The challenges of social research in engineering design for remote communities

Engineers traditionally use a *positivistic* approach to knowledge, where truths are revealed through experiment and analysis. Sociology, by contrast, is less concerned with absolute truths and instead uses *interpretivism*, where the meaning of concepts is more important, and depends on the lens through which they are viewed. It is this fundamental conflict between converging positivism and diverging interpretivism that makes incorporating social context into engineering design difficult.

6.1.2.1. Interpretivism

In a dynamic and political social context, the symbols and meanings of events can be more important than their factual nature – qualities that call for a more *interpretivistic* approach to analysis (Liker et al., 1999). As Kaplan and Duchon (1988) describe it:

Because the study of social systems involves so many uncontrolled – and unidentified – variables, methods for studying closed systems don't work so well in natural settings. . . Field experimentation should always include qualitative research to describe and illuminate the context and conditions under which research is conducted.

(Kaplan and Duchon, 1988, pg 572)

The most significant aspects of interpretivism are also its downfall: that it is inherently open-ended; that its exploration diverges; that its process is inductive. It generates *sets* of truths and may answer questions different to those posed or expected. This can be trouble for engineers who are seeking a certain, stable, positivist-type answer to design questions. However, interpretivist approaches are good for dealing with open-ended questions and incomplete data – a situation that describes most social and political contexts. Several authors agree that both an interpretivist approach to context and a positivist approach to content are needed for a complete design (see for example, Adolph et al., 2008; Dawson et al., 2003; Oates et al., 2004).

6.1.2.2. Positivism

The positivistic nature of both engineering and health science conflict with the interpretivism required for social inquiry (Leys, 2003). Engineers tend to proceed as if design requirements were *truths* rather than interpretations, gathered once at the beginning of each design iteration (Loney, 2000). This discourages contextual information from being incorporated into the design process as it emerges (Koro-Ljungberg and Douglas, 2008), and instead limits translation of context to the definition of the design problem (Wotherspoon, 2001). This cannot work easily when applied to systems that are part of complex social contexts (Kaplan and Duchon, 1988; Love, 1998).

6.1.2.3. Determinism

Another tendency is for designers to think of social problems and solutions as being deterministically related. In business, technology is often thought of as being responsible for the shaping of organisations and for causing social change (Orlikowski and Barley, 2001) – a form of *technological determinism* that has often appeared in design history (Liker et al., 1999; Loney, 2000). In healthcare, this problem has plagued telemedicine (Martínez et al., 2005), and various “appropriate” technologies that have

been developed for low-resource communities, such as charcoal-burning stoves, solar water stills and mud-construction techniques (Wisner, 1988).

6.1.2.4. Limited resources

Exploring social context is resource-intensive. By the time qualitative research is complete and coded and specifications and prototypes have been developed, design requirements may have changed or be incomplete (Ovaska and Stapleton, 2009). Even if they are complete, it seems that such attention to requirements may be less useful than actually trialling prototypes with users (Tyldesley, 1988). This kind of social analysis can generate a lot of information, causing some designers to complain of information overload (Carayon, 2006), while others feel the pressure of their industry, where they are expected to get the design right the first time (Green et al., 2002). As Wotherspoon (2001) put it, the problems come down to:

...shifting technology, inadequate resources, social structures, and low organizational commitment.
(Wotherspoon, 2001, pg 60)

The resource-intensive nature of social research is exacerbated by its application in remote sites, especially Aboriginal communities. Most communities require permits for entry, with extra permission required to carry out research. Remote communities are typically accessed by unsealed road, requiring extra time, vehicles, fuel, accommodation and the management of the various risks associated with remote work and travel.

6.1.2.5. The need for cultural safety

Remote Aboriginal desert communities typically have a large indigenous population and a minority white¹ population. The white population dominates the remote health-care industry, which means that any in-community dialysis patient is likely to be an Aboriginal person, while their nursing care is likely to be provided by a white person. This arrangement tends to reinforce the Eurocentric nature of modern healthcare and can in some instances lead to institutional racism (Gray and McPherson, 2005) and a tendency to demean, diminish or dis-empower patients (Ogilvie et al., 2008; Papps and Ramsden, 1996). This tendency is not limited to healthcare services; it is also problematic in research on human subjects (Ogilvie et al., 2008); a problem that has not been overlooked in the development of ethnographic methods for this methodology (see section 7.2.2).

¹The usage of the term *white* in this context is discussed in section 1.2.1

6.1 Introduction and background

A *culturally safe* design methodology is one where the design team takes care not to cause cultural injury to the people it seeks to serve, primarily through an awareness of its *own* culture, rather than by attempting to thoroughly understand another culture:

- A culturally safe methodology must include a process whereby the design team can reflect on its own cultural identity, norms and values (Papps and Ramsden, 1996; Ogilvie et al., 2008; Anderson et al., 2003).
- A culturally safe designer should also be aware of the power imbalance associated with their role in healthcare (Gray and McPherson, 2005).
- Cultural safety has a focus on the priorities of those who receive healthcare, rather than those who provide it (Johnstone and Kanitsaki, 2007; Gray and McPherson, 2005).
- Some evidence suggests that attempting to operate from a position of limited or stereotypical cultural awareness or sensitivity can be counterproductive and may impair both patient health and healthcare delivery (Papps and Ramsden, 1996).

Technical safety and cultural safety are both aspects of good working practice for nurses, for which much of cultural safety theory was originally developed (Papps and Ramsden, 1996). While an engineering designer may have influence over only a few technical variables, the consequences of changes to them may be far-reaching. The responsibility for cultural safety should therefore be extended to include medical device design teams.

6.1.2.6. Ethical obligations

One part of the protection of Aboriginal people from cultural injury is provided by the Northern Territory's permit system, which prevents people from entering or remaining on Aboriginal land without a permit. Specific permits are required to carry out research, and these must be reviewed by relevant traditional landowners before any research can commence (Council, 2013). Part of a research permit application must include an ethics approval document, research methodology and other details of the research organisation, the purpose of the project and any benefits that may flow to the traditional owners.

Ethics approval has its own barriers: Aboriginal people are considered "vulnerable" by the Flinders University Social and Behavioural Research Ethics Committee, and as such, any Flinders University application for human research involving Aboriginal people must also be reviewed by Yunggoendi First Nations Centre at Flinders University. The level of scrutiny provided by these groups is designed to prevent careless or injurious research, but comes at the cost of a significant amount of time and effort on the part of researchers. These constitute yet another set of challenges to the use of social research in remote medical device design.

6.1.3. Methodology requirements

6.1.3.1. Necessary criteria

A collection of challenges has been identified: the need for less-familiar interpretivistic methods for dealing with context; engineering's natural tendency towards positivism; its false-confidence in determinism; the resource-intensive nature of remote social research and the need to carefully manage the cultural safety and ethical implications of research. An effective, culturally safe engineering design methodology for remote health Aboriginal health must therefore include:

1. A process whereby the design team can reflect on its own cultural identity
2. A focus on the perspective of the user community
3. A simple method for gathering qualitative social context data, that can operate during short visits to remote communities
4. A systematic method of interpreting that data and encoding it into technical constraints or parameters
5. A method for assessing the relevance of design variations for community members

6.1.3.2. Application-specific criteria

The above criteria are necessary but not sufficient for an engineering design methodology to be useful in practice. Through the development of a similar design methodology, *socio-technical systems engineering* (STSE), Baxter and Sommerville (2011) suggest a set of more application-specific evaluation criteria:

1. There needs to be agreement about which social and technical elements of the system need to be optimised
2. There is a need for system boundaries to be drawn in places agreed to by relevant stakeholders
3. There is a need to address conflicts between the value systems of different stakeholders
4. There is a need for stakeholders to agree on success criteria
5. There is a need for any analysis to be coupled to synthesis
6. There is a need for stakeholders to understand different disciplines
7. There is a need for researchers to be up-to-date with developments in organisational methods and technology
8. There is a need for fieldwork to include the selection of appropriate participants

The following methodology was designed with the aim of meeting all of the first set of requirements, while attempting to meet as many of the second set of requirements as possible.

6.2. Methodology

The main aspects of the proposed methodology are presented here, including the meaning of the concept of the *user*, how the social context should be explored and encoded, and how predicted outcomes due to design variations should be assessed against the values and preferences of interested stakeholders.

6.2.1. Identifying the *user*

Design methodologies are often concerned with the relationship between objects and users (Redström, 2006). For medical dialysis systems, neither the *user* nor the *object* are well-defined concepts. The difficulty in identifying the user is partly due to dialysis systems having several interfaces: one for the nursing operators, one for patients and a hidden one for service technicians. In remote locations, a nurse may take the role of technician, or a patient may act in the role of nurse and execute their own “self-care” treatment, with or without assistance from family members. Similarly, identifying the designed *object* can be difficult, as a dialysis system is distributed into at least three subsystems (a blood circuit, a dialysate circuit and a water treatment path - see 1.2.4.5), which may need to be dealt with separately or together, depending on the user.

If, instead, a dialysis *clinic* is thought of as the designed object, then the entire community may be thought of as the user. In this context, a dialysis clinic facilitates public health rather than patient healthcare. If a dialysis clinic is built into a truck body as a mobile clinic, then any changes in the installed dialysis system will cause changes to the truck layout, ergonomics and use: one cannot be redesigned without directly affecting the other. Similarly, a dialysis clinic can't be changed without affecting the public health of any community that it serves. These complex systems of entities and people suggest the need for a methodology that can handle a large inter-related set of abstract socio-technical subsystems. Similar methodologies have been developed with this need in mind, such as STSE (Baxter and Sommerville, 2011) or *whole-system design* (Charnley et al., 2011). Whole-system approaches also have the advantage of being able to incorporate sociological principles such as sustainability (Blizzard and Klotz, 2012) or, in this case, cultural safety. To develop a socio-technical model of the context, it was decided that a simple qualitative research method was needed to gather data about the relevant entities and identify relations between them, while keeping a focus on their perspectives rather than those of the designer.

6.2.2. Exploring context

Exploring context through qualitative methods is becoming increasingly popular as a design methodology (Neuenschwander, 2013). Any qualitative method that relies heavily on the perspectives of stakeholders is similar to *participatory design* (PD) - a widely used design methodology, often applied to healthcare contexts (Pilemalm and Timpka, 2008) that is becoming increasingly preferred over user-centred approaches (Dell’Era and Landoni, 2014). PD typically involves having users participate in the design team, whereas other ethnographic methodologies such as *empathic design* (Genco et al., 2011) and *contextual design* (Beyer and Holtzblatt, 1999) instead involve placing technical developers into the users’ world. An assumption behind PD is that participants are actually interested in the design, rather than simply affected by its outcomes. Importantly, such methods improve design and help avoid unintended consequences (Cady, 2012). When considering cultural safety, attempting to recruit Aboriginal people to participate in yet another discussion forum to facilitate PD might be problematic, and might sensibly be saved for later design stages. For these and other reasons, the preferred approach was to have a member of the technical design team participate in the remote context as part of an ethnographic process².

6.2.2.1. Ethnography

Traditional ethnography has been used extensively in the study of engineers and design processes (Hughes et al., 1994; Patel and Kushniruk, 1998; Martin et al., 2006; Adolph et al., 2008, 2011; Coleman and O’Connor, 2007; Kotabe et al., 2007) but seems to have been a frequently recommended but underused tool for informing engineering design. There are many reasons why designers have avoided the use of ethnography:

- Ethnographic methods are notoriously resource-intensive: by the time ethnographic research is complete, coded and implemented, design requirements may have changed (Ovaska and Stapleton, 2009).
- Such attention to requirements may be less useful than actually trialling prototypes with users (Tyldesley, 1988).
- Ethnographic analysis can generate an overload of information (Carayon, 2006)
- Industry pressure to get designs right-first-time further discourages its use (Green et al., 2002).

In a similar vein, the authors Ball and Ormerod (2000a) highlight three major reasons why ethnographic techniques are avoided:

²Ethnographic study of indigenous peoples is not without its own problems. To carry out yet another ethnographic study of Aboriginal people does nothing to reduce the problem of Aboriginal people being “...the most researched people in the world...” (Fredericks, 2008, pg 25.). The methodology attempts to compromise thoroughness for simplicity, partly with this in mind.

1. Ethnographic data acquisition is *resource-intensive*, may span several years and may not be cost effective or possible for most projects.
2. The difficulty of *verifying* storytelling and cultural data is a problem for design teams whose funding bodies crave certainty about their design decisions.
3. Ethnography generates *divergent* understandings of various themes. It is not so useful for hypothesis testing.

In the context of Aboriginal health, the risk of culturally unsafe ethnography must be added to this list, wherein a researcher might inadvertently cause harm to participants by intruding or appearing to trivialise their culture.

6.2.2.2. Cognitive ethnography

In order to address some of these shortcomings, *Cognitive Ethnography* (CE) was developed (see details in Ball and Ormerod, 2000a). CE borrows from traditional ethnography but leaves behind those parts that make ethnography impractical for some researchers. Cognitive ethnography has three key features (Ball and Ormerod, 2000b):

1. Small-scale data collection based on representative time slices of situated activity.
2. Purposive data collection with ultimate goal of some kind of intervention
3. Verifiability across observers, datasets and methodologies.

Cognitive ethnography typically uses observation and interviews to learn about the meanings that participants attach to their context (Cady and Finkelstein, 2013). While traditional ethnography continues until saturation (i.e. little new data is generated by continued research efforts), cognitive ethnography limits research efforts to short periods of study. It has been used to study technology in healthcare contexts such as telehealth (Cady and Finkelstein, 2013), healthcare team workflows and communication (Parush et al., 2014; Popovici et al., 2015), infusion pumps in intensive care departments (Rajkomar and Blandford, 2012), and other situations where medical devices, healthcare workers and other socio-technical systems interact (Baskerville and Myers, 2015).

An ethnography based around the features listed above should be more useful to engineering design teams than purer forms of ethnography. For instance, time-slices of situated activity might mesh neatly with design iterations; purposive data collection might mesh with specific design frameworks, such as that of *Questions, Options and Criteria (QOC)* (see MacLean et al., 1991); verifiability might please funding bodies who want to know that their money is being well-spent.

6.2.2.3. Engineering ethnography

Unlike traditional or cognitive ethnography, engineering's primary purpose is not to uncover social reality or truths: engineering is much more pragmatic. Without a social-research element to an engineering design project, design can proceed quite happily using only the intuition of the design team. It is suggested here that the inclusion of even a small amount of sociological data should result in better, more equitable and more useful designs. To demand the use of high-quality ethnography in an engineering design process may be counter-productive, as ethnography's resource-intensive nature is likely to prevent it from being carried out at all. Given that the priority in engineering is technical pragmatism rather than methodological or sociological purity, this methodology proposes some further modifications to cognitive ethnography to produce a specialised, *engineering* ethnography that includes:

1. Data sourced from anywhere, including published material, interviews, observations and surveys
2. Pre-determined codes such as those of QOC to make interfacing with design requirements easier
3. A Review of existing ethnographic studies to provide a lot of information at low cost
4. A program of data collection that is purposive, quick and adaptable
5. Ethnography and design iteration carried out concurrently to manage adaptability and emergence

Such an iteratively executed engineering ethnography would generate an intermittent stream of qualitative data, that would then need to be synthesised into a form from which design constraints could be developed. The general nature of this framework should allow cultural perspectives to be included in the same dataset as any design requirements. This should also enable the inclusion and prioritisation of Aboriginal user community perspectives and facilitate culturally safe design. An iteratively executed engineering ethnography based on cognitive ethnography was thought likely to be suitable for this project, provided that its interventionist principle would not be injurious to Aboriginal participants.

6.2.2.4. Seed data

While traditional ethnography may be carried out with very little initial information using *grounded theory* (Corbin and Strauss, 1990), any cognitive ethnography-based methodology requires a purposive, goal-directed approach, and must be seeded with at least an approximation of the desired data. While engineering intuition is not a recommended substitute for ethnography (Samaras and Horst, 2005; Marshall et al., 2010), it can provide a convenient source of seed data:

Good system designers are usually good at estimation – they can efficiently determine the relative sizes of physical parameters and identify those that can be safely neglected.

(Dym et al., 2005, pg 106)

An intuitive approximation may later be updated and refined through future iterations.

6.2.3. Encoding context

The translation of ethnographic context data into a form useful to engineers is difficult to do well (Hughes et al., 1994). However, it is a problem familiar in the field of architecture, where liveable building qualities must translate into structural specifications. The qualitative reasoning and design techniques used by architects (Richter et al., 2010; Schultz et al., 2009) may be adapted for engineering design, at least at an early conceptual design phase (Cao et al., 2013).

6.2.3.1. Causal relations, truth and value statements

Qualitative data of the type produced by ethnographic methods can easily be encoded into qualitative codes or data-types such as *causal relations*, *truth statements* and *value statements*. Causal relations may then be assembled into causal maps using signed, directed graphs, with truth statements as their initial conditions and value statements as the criteria against which any changes in outcomes may be compared. Conceptual design with causal maps is typical of *qualitative reasoning and modelling* (Li et al., 2013b) – an approach that was considered suitable for this methodology.

6.2.3.2. Qualitative Reasoning and Modelling

Qualitative Reasoning and Modelling (QRM) is a formal process for using causal logic to record the effects of design decisions in terms of resultant changes in the qualitative values attached to relevant entities. That knowledge may then be used as feedback to users to inform design. Its working principle is that dynamic systems can be represented as sets of interacting entities, where each interaction is described by a differential equation. While various artificial intelligence software tools have been developed, few include a visual representation of the interactions, while those that do tend to present static visualisations without modelling trends over time Yao et al. 2015. One exception is the QRM software package *Garp3* (see 7.2.3) which was developed to model and visualise dynamic systems over time to help people to understand how such systems work (Bredeweg et al., 2009). Similar software packages have been used to model social, biological and other abstract systems as diverse as river floodplain management (Wriggers et al., 2014), high-speed train technology design support (Wiltgen and Goel,

2015), complex ecosystem theory (Yao et al., 2015) and macroevolution's effect on the carbon-cycle (Kansou et al., 2013). There are, of course, many others. Few authors have attempted to achieve what is attempted here; that is, to use qualitative modelling of a socio-technical system to translate ethnographic data into design parameters as part of a complete design methodology.

QRM is an established method (see Bobrow, 1984) and was considered suitable for this project's study of the desert dialysis context. In a QRM analysis of such contexts, each stakeholder is seen as being primarily concerned with their own domain (Hempe et al., 2010), while the context's modelled structure is usually determined by ethnographic research (Leys, 2003). The design methodology proposed here suggests the use of QRM in this way, by taking value statements from stakeholders and constructing a model of the context based on ethnographic data, then choosing values for qualitative variables as they change through design iterations and socio-political variation. The effects of design variations should then be visible throughout the contextual model. The relative benefit or loss for different stakeholders may then be assessed against their preferences and/or presented to those stakeholders to generate further ethnographic data.

QRM may be used to manage engineering design processes in complex social contexts, such as in the development of healthcare technology for remote Australian Aboriginal communities. In such a context, social structure and values change relatively slowly, and each stakeholder is concerned primarily with the small parts of the context with which they are involved.

6.2.4. Assessing outcomes

Design outcomes are traditionally verified by comparing them with data from a needs-analysis (Li et al., 2013b; Pilemalm et al., 2007). In place of needs, the proposed methodology uses *value statements*, revealed by ethnography, which are to be compared against simulated outcomes from the QRM model. The input of participants in subsequent iterations (or the intuition of the design team in the first iteration) may be used to prioritise competing outcomes. Visualisation of the context in a map of signed, directed graphs (SDGs) may help facilitate this (Bouwer and Bredeweg, 2010), especially considering that individual outcomes may affect many stakeholders and that the causes of outcome variations may be dominated by technical rather than social considerations.

6.2.5. Methodological summary

- The methodology is designed to be applied to the design of elements of a socio-technical system situated within a large, remote user-community.

6.2 Methodology

- Data collection is to involve having a few members of the design team visit remote community sites as a participant-observer, in the style of participatory design.
- Researchers should undertake training in cultural safety or similar process of reflection on their own norms and values before making contact with remote community members.
- Researchers should be primed with background data and iteratively execute an *engineering ethnography*, based on a program of data collection that is purposive, quick and adaptable.
- Collected data should be encoded using simple concepts and processed using a formal system such as QRM to keep track of interactions between the socio-technical system's multiple entities, variables and outcomes.
- Outcomes should be compared against the stated preferences and priorities of the participants from the user-community.

As such, the proposed methodology frames the subject similarly to *socio-technical systems engineering*, while borrowing research methods from *participatory design* and *cognitive ethnography* to form an *engineering ethnography*. The difficulty in converting interpretivistic qualitative data to positivistic design criteria is addressed by borrowing *qualitative reasoning and modelling* from the fields of architecture and ecological development, while *cultural safety* principles are incorporated into the methodology by having researchers prepare and reflect before collecting data and by evaluating outcome data through the perspectives of the user community. These structural elements were chosen to meet the *necessary* criteria expressed above (section 6.1.3.1). By applying them in context, it should be possible to evaluate the methodology against the application-specific criteria above (section 6.1.3.2). The following chapter describes an application of the methodology, where variations to dialysis system size and energy efficiency are considered as variations within a larger socio-technical system in the context of non-profit dialysis service provision in Australia's remote Western Desert Aboriginal communities.

7. Design for remote Aboriginal health: application

7.1. Introduction

The preceding chapter (6) introduces a methodology that is specifically designed to incorporate social-context data into the medical device development process. Earlier chapters (2 to 5) present the work of the technical design team¹, which suggests that forward-osmosis dialysate production may benefit from design variations such as improved energy efficiency, with an associated increase in the membrane area and corresponding size of the system. In this chapter, socio-technical outcomes due to these variations are examined in the context of remote Aboriginal community dialysis, by using the proposed methodology. The aim of this analysis was to explore the significance of the proposed design variations in order to gain some perspective on whether they have value in their social context. Having tested the proposed methodology in the field, it was then evaluated against application-specific criteria.

7.2. Method

The proposed methodology was applied to the dialysis context of an Aboriginal community in Australia's Western Desert region, where a non-profit dialysis service provider was operating, both in that community and at a central location in Alice Springs². The service provider employed nurses and organised the visit of a mobile dialysis truck to the remote site.

¹The design team for this project consisted of the author of this thesis and a Masters student (see chapter 3) under the supervision of Prof. Karen Reynolds and with the input of other interested stakeholders (see acknowledgements in the frontmatter).

²The township of Alice Springs (pop. ~30,000) is located in the Northern Territory of Australia. It is a major regional centre for the sparse surrounding of central Australian towns and communities, including those of the Western Desert region and the specific community studied in this analysis. Alice Springs is often referred to as "town" by those whose home is normally in a remote area.

7.2.1. Research preparation

7.2.1.1. Identification of design variations

The original focus of this project was on the development of a dialysis system prototype, with the aim of improving its suitability to use in remote Aboriginal desert communities. The potential dialysis system design changes, such as improvements to energy and water efficiency, are demonstrated in chapters 2 to 5. In particular, the technical analysis in chapter 4 points to some important design implications for the designed FO dialysate production system:

1. The apparent “recovery” rate of the cyclically backwashed FO system is about 65 → 75 %. This is comparable to existing RO-based systems (see section 4.3.3.2). This implies that the design has no significant water efficiency advantage over the existing RO-based system.
2. The overall apparent energy consumption of the cyclically backwashed FO-based system is about 66 % of that of its RO-based equivalent. This would appear to be a significant gain in energy efficiency.
3. The FO-based system would need at least two 4040-sized elements to produce dialysate at a rate sufficient for a medical treatment, compared with the single 4.6” × 11” element required for the existing RO-based system.

With the recent introduction of mobile dialysis trucks, the value of working space and dialysis equipment robustness within mobile treatment areas has increased, as has the significance of associated issues such as water and electricity consumption. The compact nature of mobile treatment means that the optimisation of *any* part of its installed dialysis system will have immediate effects on the nurses and patients who spend time within the confines of a dialysis truck.

7.2.1.2. Cultural safety training, ethics and reflection

The lead researcher³ was encouraged to attend a tertiary level course with a cultural-safety focus. The lead researcher audited the course, *PHCA8504: Social determinants of Indigenous Health* at Flinders University. This course discussed Australian indigenous health, history decolonisation, culture, place and environment as social determinants, together with models of cross-cultural healthcare work, including cultural safety. An ethics application was submitted to the Flinders University’s Social and Behavioural Research Ethics Committee (SBREC) and the Northern Territory’s Central Australian Human Research Ethics Committee (CAHREC) via the National Ethics Application Form (NEAF). The Yunggoendi First Nations Centre reviewed the application and recommended that the lead researcher gather a small support-team of

³The “lead researcher” was also the author of this thesis.

experts in indigenous health research to supervise the social-research stage of the project. These processes of study, reflection and discussion with relevant experts from Flinders University were done to improve the lead-researcher's awareness of both the general nature of Aboriginal cultures, his own culture and colonial and post-colonial interactions between them.

7.2.1.3. Seed data

Background information such as anecdotes and web-based material were explored by the lead researcher. Major stakeholders and entities were identified within the target dialysis context, including:

1. Local community members
2. Dialysis service providers, administrators and support workers
3. Nursing staff
4. Patients

A map of these and other relevant entities and their expected preferences and relationships was developed intuitively by the lead researcher in order to seed the ethnographic process.

7.2.2. Engineering ethnography

An engineering ethnography (see section 6.2.2.3) was carried out by the author of this thesis, beginning with the seed data and progressing with semi-structured interviews, a focus-group discussion and participant-observation at each site, during a single research period from 07/05/2013 to 26/05/2013.

7.2.2.1. Site selection and participant categories

Two sites were selected: the first was the Alice Springs head-office of the non-profit Aboriginal corporation, *Western Desert Nganampa Walytja Palyantjaku Tjutaku* (WD-NWPT), which was also operating as a dialysis clinic. Nurses and administrators at this site were invited to participate. The second site was the remote community⁴ where the service's dialysis truck was scheduled to visit at the time of the research period. At the remote site, participants were recruited from among community members, dialysis nurses, support workers, remote clinic staff and patients.

⁴To protect the privacy of the community, its name has been withheld throughout this thesis, at the recommendation of the Yunggoendi First Nations Centre at Flinders University.

7.2.2.2. Participant observation

The lead researcher was also a trained dialysis technician and was able to participate in the operation of the service, in the spirit of reciprocity, by providing technical support while making observations. Due to the limited time available at the Alice Springs site, observations were made only at the remote site. Posters were temporarily placed at the remote dialysis clinic to notify staff and patients of the observation and research process. To limit the risk of invasion of privacy and to avoid the difficulties associated with gaining patient consent for observation, observations were made only of technology use and of the work-practices of nursing staff at the remote site.

7.2.2.3. Patients

Five *patients* were recruited to participate in this study. All participants from this category were Aboriginal Australians, and necessarily indigenous to the region in which their community was located, where they were receiving regular dialysis treatments. Few lived in-community full-time during the period of their illness. No patients were recruited from the local general clinic; it was the perspective of dialysis patients that was sought for this study, rather than the perspective of a general, remote patient, although such patients were not excluded from participating in the *community members* participant group.

7.2.2.4. Community members

Five *community members* were recruited to participate by the lead researcher, usually after first being introduced by a member of the dialysis service. The lead researcher made it known verbally to various community members that he was interested in speaking to people about the dialysis service. Community-member participants included local Aboriginal people and long-term resident non-Aboriginal people such as local healthcare workers.

7.2.2.5. Nurses

Four *nurses* were recruited from among both visiting and permanent staff at both sites. Most were highly experienced, both in renal nursing and Aboriginal health.

7.2.2.6. Support workers and administrators

There were very few dialysis *support workers and administrators* at the remote site, with only one available to participate in the study. Data from this group was also

collected from one other *administrator* at the Alice Springs head-office of the dialysis service.

7.2.2.7. Interviews and focus groups

Participants from each group were approached and consented according to a protocol approved by two ethics committees⁵. The research project was explained to the participants, while documentation detailing the project, the lead researcher, any rights and obligations, the use of any data and the right for patients to withdraw consent at any time was offered (see documents in appendix F). Patients with language difficulties were offered the use of interpreters. All participants were consented verbally and were willing to sign consent forms. Individual participants were approached and asked to participate in recorded interviews, each of which was less than one hour long. Thirteen interviews were carried out in-total. Due to time constraints, only one focus-group discussion was able to be organised: three nursing staff and one support worker were approached and asked to participate in a focus-group discussion at the end of the remote site visit.

The interviews and the focus-group discussion were designed to be general in their scope, encouraging participants to elaborate on their own perspectives on the technology, the service, their own health, the general health of the community and the local environment. Interview sheets were semi-structured with about 20 questions, adjusted for each participant group (see examples in appendix F). The interview questions were used as a guide for the lead researcher. The understanding of participants was tested by the use of “check-questions” following most responses, or by rephrasing questions and comparing the responses. The following example dialogue was typical of that recorded in the interviews:

M: OK, I had a question about the water - you know, the machines use a lot of water - this machine, and the truck use a lot of water. But yeah, we are in the desert, right? So it's OK for dialysis to use a lot of water in the desert?

Yeah it's OK to use a lot of water.

M: Is it a problem in your community do you think? Do you think it's wasteful?

No, it's alright to help people- dialysis patients.

M: It's alright to help people?

Yeah.

(Fieldnotes, 13/05/2013)

⁵Research was approved by the Social and Behavioural Research Ethics Committee (SBREC) at Flinders University (no. 5979), and by the Central Australian Human Research Ethics Committee (CAHREC no. 13-131).

Interviews, observations and the focus-group discussion were carried out at the remote site over a two-week period. Alice Springs interviews and observations were carried out over two days, before and after the remote site visit. Interviews and focus groups interviews were carried out and recorded digitally and on hand-written notes. Recordings were transcribed to create text for analysis.

7.2.3. Data encoding and modelling

The text was first coded according to the revealed concerns of the major stakeholders, using *NVivo* software (ver. 10.0.573.0, QSR International). The data was then coded again, according to the major entities in the context, as revealed by the first pass of coding. The set of entities included physical and abstract objects, such as the equipment on the dialysis truck, the truck itself, the mobile dialysis service, nurses and others. A total of eleven major entities were identified. *Truth* statements, *value* statements and *causal relations* were extracted from the text. Truth statements were typically encoded as constants, while qualitative variables were taken from the causes and effects extracted from the described causal relations⁶. The frequency of reference to particular *values* within the dataset was calculated for later comparison with the QRM output.

A QRM software package called *Garp3* (ver. 1.5.2, Human Computer Studies (HCS) laboratory, University of Amsterdam), was chosen to model the dialysis context. This software was chosen because of its use in similar studies and its graphical implementation of the qualitative reasoning process (see section 6.2.3.2). The core of a *Garp3* simulation is a set of *model fragments*, which are graphical representations of the relationships between *entities* and their associated qualitative *variables* and *constants*. These relations were encoded as a set of positive and negative causal relations called *proportionalities*. The main model ingredients⁷ are shown in table 7.2.1.

7.2.3.1. Scenarios

The *Garp3* reasoning engine proceeds from a set of initial conditions called a *scenario*, which is a set of constants indicating which variables are considered part of the design variation being simulated, and which are fixed for the simulation. The reasoning engine may then take these variations and test their effects through each of the model fragments, by propagating their changes through the causal relations encoded in each

⁶Some variable names, such as *efficiency*, are self-explanatory. Others, such as *Personal instability*, are labels that cover a range of meanings, such as the unpredictable and irrational behaviour that may arise as a result of the stress associated with remote work. For the sake of this analysis, the general nature of such variable labels was sufficient to identify the relevant causes and effects, despite the underlying complexity within such a concept.

⁷*Garp3* entities are labelled twice, as both an entity class and specific instance. In this application, only one instance was used for each class of entity.




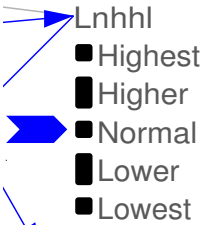
Object	Symbol
Major entities	 <i>Dialysis truck</i> Dialysis truck
Variables	 <i>Working space</i>
Causal relations	
Constants	

Table 7.2.1.: Model fragment symbols

model fragment. The resulting increase or decrease of any affected variables in the system can then be recorded as simulated outcomes that can then be compared against the preferences of the user community.

A scenario was constructed containing the dialysis system design variations, and initial conditions for each variable, which were extracted from the ethnographic data (see figure G.0.1). The two influences, *Efficiency improvement* and *Size increase* were set to *Plus* to cause an increase in the values of the variables, *Dialysis system efficiency* and *size* during simulation. These influences were characteristic of the likely design trajectory that emerged from the technical analysis, similar to that identified in section 7.2.1.1.

7.2.3.2. Model fragments

Garp3 Model fragments were constructed by representing each causal relation from the ethnographic data as a signed, directed graph (marked as $P+$ and $P-$ in the model fragments - see the example shown in figure 7.2.2) between relevant qualitative variables (marked as dial indicators). In *Garp3* these *proportionalities* indicate a transfer of the *derivative* of one variable to the next, regardless of the value of either. Constant-valued quantities were added as fixed variables (marked with blue flags on the the right-hand-side of each fragment). The dependent variables for each entity were aligned vertically on a string towards the right-hand-side of each fragment, while the left-hand strings showed relevant variables from other entities.

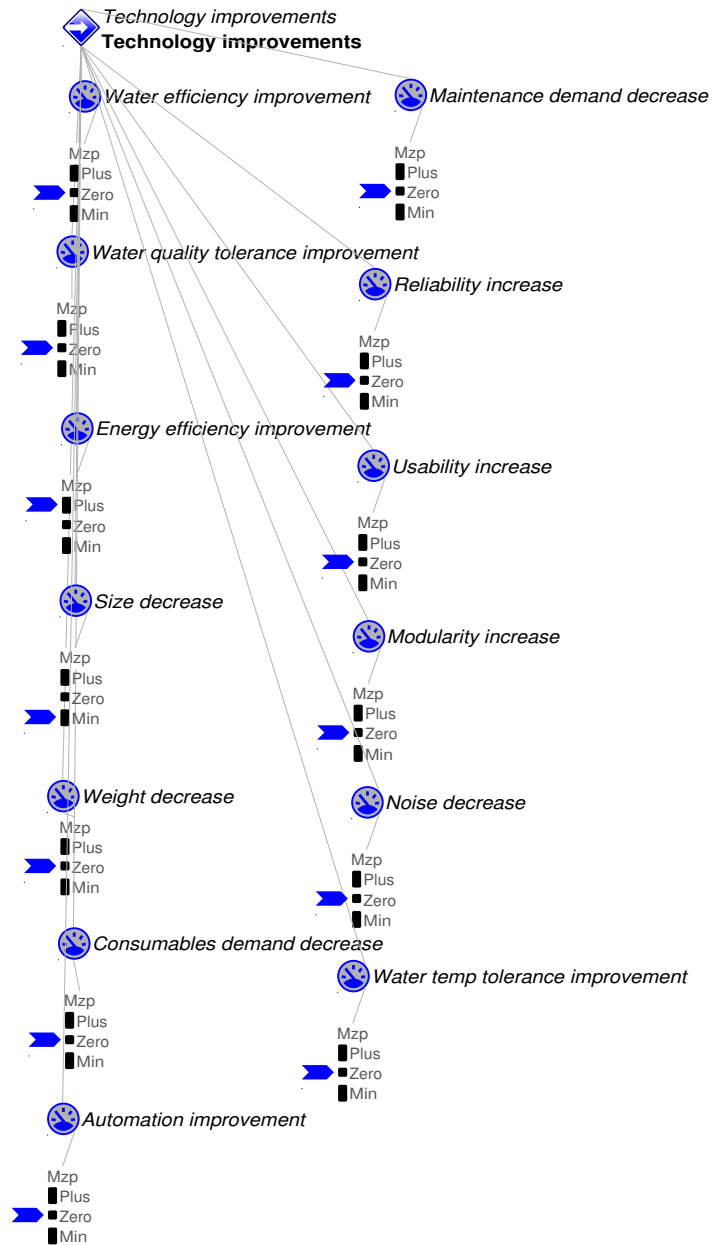


Figure 7.2.1.: Example *Garp3* scenario, “Technology improvements” showing variables, each marked as constant or with a fixed direction of change

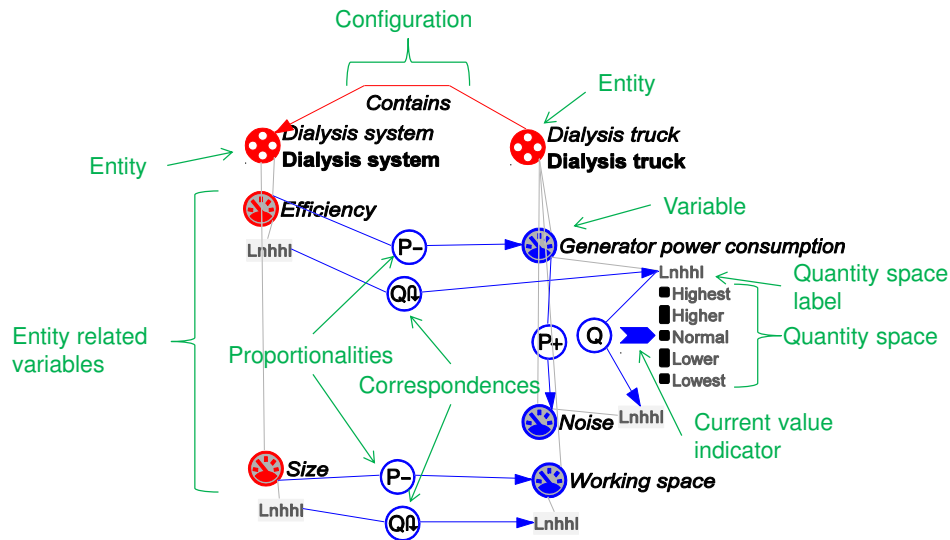


Figure 7.2.2.: Example *Garp3* model fragment showing entities, variables, causal proportionalities and correspondence constraints

One model fragment was developed for each of the eleven entities identified in the ethnographic data. The body of ethnographic data was encoded into model ingredients that, when assembled, resulted in fragments that were relatively large and complex (see the set of fragment graphs in appendix G). This was a problem for the reasoning engine, as an increasing number of variables means an exponential rise in computing time in *Garp3*.

7.2.4. Model simulation

7.2.4.1. Complexity

Garp3 usefulness is limited by its exponential growth in computational time with increasing variable count. For n variables⁸, *Garp3* will process 2^n possibilities. When all the model fragments for this study were constructed, 132 variable names were generated, some of which were applicable to more than one entity. To process outcomes for just 132 variables, at least $2^{132} \approx 5 \times 10^{39}$ outcome states would need to be generated: a calculation load that would take most current desktop computers trillions of years to evaluate.

Instead of attempting to consider multiple simultaneous design variations, simulation was limited to variations in just one or two closely related variables. In this way, the

⁸*Garp3* refers to qualitative variables as “quantities”. The term “variables” has been used instead for consistency.

complexity of the model was reduced to include only 19 affected variables (see figure 7.3.6), reducing the total computational load to only $2^{19} \approx 6 \times 10^5$ outcome states. While this may have been a more realistic computational load, it would have created an impossible amount of data to review.

To reduce the modelled complexity, logical constraints were added. In *Garp3*, these are represented by correspondences (marked Q , Q^\sim , dQ and dQ^\sim in the model fragments - see the example shown in figure 7.2.2), and were used to force the model to only accept states where corresponding variables had identical (or inverse) values or derivatives. To limit the output state-count further, three different types of constraints were added: simple constraints, implied constraints and competing constraints.

7.2.4.2. Simple constraints

Where a changing variable affected only one other variable in the model, a constraint was added so that the affecting variable's movement was always passed on. This was done with an associated loss of information as to the relative significance of the influence of each variable.

7.2.4.3. Competing constraints

Where two or more changing variables affected one other variable, their relative influences were constrained according to the intuition of the design team, allowing the most relevant to dominate the outcome for resultant variables.

If the variables were left unconstrained, ambiguous results may have been generated: the *Garp3* reasoning engine will add three outcome states for any affected variable, increasing the total number of output states to 3^n for n unconstrained, competing variables.

7.2.4.4. Implied constraints

Where unrelated variables were changing independently, constraints were added between these variables using intuition, according to the likely interdependence of these variables. With constraints added, the *Garp3* reasoning engine was able to be used to simulate the design scenario. The resulting outcome states were collected for analysis.

7.3. Results and discussion

Four useful types of data were generated: model fragment graphs, constraint details, simulation output and ethnographic preference frequencies. Of these, the preference

frequencies and model fragments were the most useful: the fragments showed which context variables were the most critical, while the preference frequencies showed which were at the forefront of concern for the various participants. The simulated output was less useful: most simulated outcomes could have been easily predicted or discovered by inspection. Constraint data was used as an indicator of the quality and applicability of the model.

7.3.1. Model analysis

The model fragments provided an immediate visual representation of the importance and influence of each entity within the context. The potential downstream effects of changes in any variable were immediately visible to any interested observer.

7.3.1.1. Community members

The fragment for *Community members* (see figure G.0.3) was representative of the system variables affecting the people of the studied remote community. The fragment highlighted how significant various disease states were within the studied community and how these were connected to the need for dialysis and other medical services. There were relatively few influences on the variables attached to the *Community members* entity, most of which had little to do with the dialysis service or its equipment. It was only the dialysis *service expansion rate* that was recorded as having any effect on the *members*, and at that, it was only mentioned as having positive effect on the *social capital* of the community.

7.3.1.2. Dialysis clinics

The *Dialysis clinics* fragment (see figure 7.3.1) was representative of the two dialysis clinics studied at the two sites during the research period, showing an even balance between dependent variables and constants. This suggested that the entity was neither a dominant source of influence on other variables within the model, nor was it heavily dependent on other entity variables for its state. In this fragment, the entity *Dialysis system* was recorded as having an effect on the *clinics*. Its variables, *water quality tolerance*, *maintenance burden* and *consumables demand* were all recorded as affecting the operation of the dialysis clinic. While these design aspects of the dialysis system were not examined in this project (as there was no evidence of any improvement in them in the technical analysis), they are worth noting for future dialysis system design.

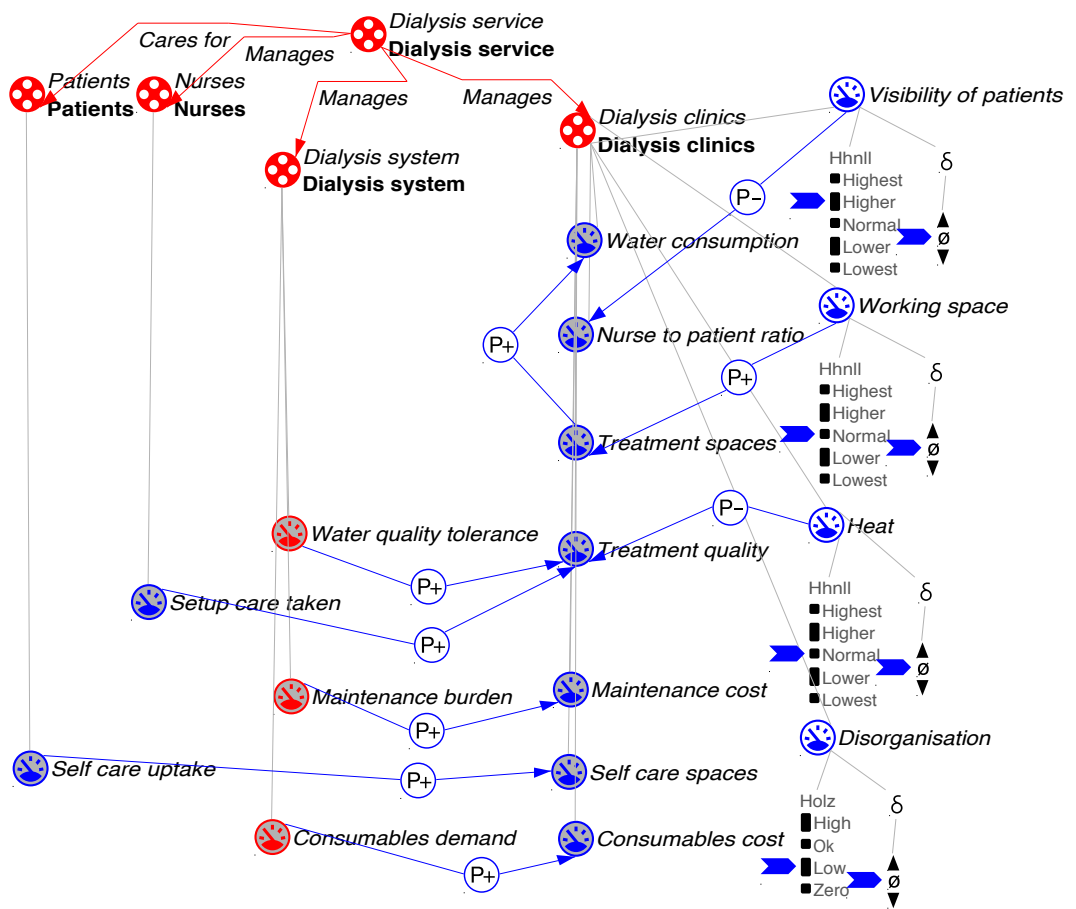


Figure 7.3.1.: Dialysis clinics model fragment

7.3.1.3. Dialysis service

This fragment was representative of the administrative or corporate entity that was the studied non-profit *Dialysis service*. The large number of constants in its model fragment (see figure G.0.5) indicate the relative stability of the service in general. The affected variables were largely concerned with the relationships between funding and service provision, and therefore the availability of treatment spaces. This stability translates to independence of the dialysis context, at least insofar as the operation of the dialysis service is concerned, and into a relatively predictable availability of treatment for patients, who can therefore organise their lives according to their own preferences, rather than according to the idiosyncrasies of funding fluctuations.

7.3.1.4. Dialysis system

The variables in the fragment for *Dialysis system* (see figure 7.3.2) were those that were immediately affected by the design variations specified in the *scenario*. A critical constraint was applied between the system's *energy efficiency* and *size*, which were tied together by a *correspondence* (Q), which is a *Garp3* ingredient used to force both variables to take the same value at the same time, so as to be consistent with the preceding technical analysis of FO-based dialysate production processes.

Otherwise, the *Dialysis system* entity was found to be relatively independent and non-influential, as indicated by the simplicity of its model fragment. One variable of note was that of the *heat* of the *Dialysis truck*, which was recorded as having a negative effect on the installed *RO system reliability*⁹. There is likely to be a similar effect on the performance of an FO-based process, although temperature dependency was not part of the technical analysis of this project: it should therefore be the subject of future work.

7.3.1.5. Dialysis truck

The model fragment for the entity, *Dialysis truck* (see figure G.0.7) suggests that the dialysis truck variables were moderately stable within the dialysis context. Most of the truck's practical functionality was built into its structure and was therefore unlikely to vary greatly until the end of the truck-module's lifespan. Some variables were found to

⁹*RO system reliability* in this context means the reliability of established systems, as perceived by the research participants. In particular, *reliability* was a discussion of the nuisance rate-of-failure with respect to the RO machine sensitivity to heat and salinity, rather than any catastrophic failure causing danger to patients or others. As such, opinions about *RO system reliability* were translated into design constraints rather than detailed design of any safety systems. The significance and technical limitations of the proposed system's performance and safety characteristics are discussed in section 1.3.1.

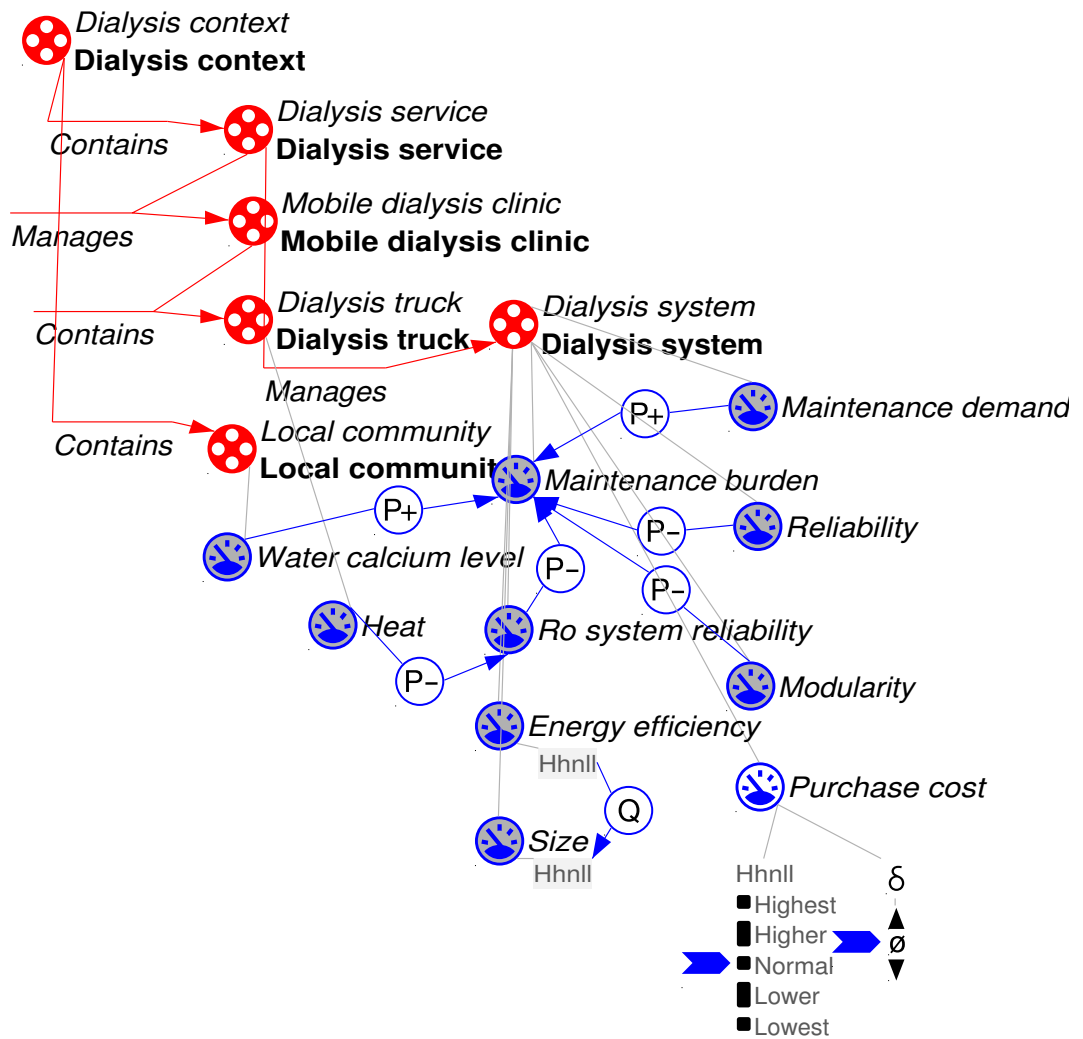


Figure 7.3.2.: Dialysis system model fragment

be dependent on the quality and availability of electrical power. This may be relevant to any future design improvements that are to be made to the dialysis technology. In the data, electrical power quality was closely linked to the use of generator power within the dialysis truck. The on-board diesel generator was associated with increased noise, vibration and diesel consumption, yet generator power was needed in response to high air-conditioning loads on high-temperature days, poor quality or unavailability of local plug-in power and the simultaneous use of multiple or inefficient appliances. The use and management of dialysis truck electrical systems is perhaps one of the more significant aspects, as it was shown to directly or indirectly affect many other aspects of the dialysis service, such as nursing comfort and stress, and ultimately patient safety.

7.3.1.6. Government and regulation

A fragment for *Government and regulation* (see *G.0.8*) was added to the model to map any effects of the dialysis service on the government of the state wherein the dialysis service was operating. The variables extracted from the data were largely concerned with the passing on of operational and other costs associated with service provision. One abstract cost was included: the public health costs due to any increased relocation of patients to town for dialysis treatment (see discussion on the problem of relocation in section 1.2.1). Quantifying or otherwise analysing this cost was beyond the scope of this project, although it appeared to have great significance. It is also worth noting that the political cost or value of dialysis service provision was not discussed or analysed, but must surely be of great importance to the provision and funding of dialysis services.

7.3.1.7. Local community

Some model fragments, such as *Local community* (see figure 7.3.3), were dominated by their constant-valued variables, rather than by dependent variables or external influences. This was due to the ethnographic data for these fragments being dominated by truth statements rather than by causal relations. The fragment for *Local Community* therefore showed relative stability in the dialysis context, with the only dependency discussed in the data being that of the need for dialysis treatment demand to be supported by making available a space where a dialysis truck may be parked. The remaining variables were all independent of other changes in the context. This suggests that the nature of the studied community was one that was generally slow to change in comparison to the in-community dialysis service.

7.3.1.8. Mobile clinic

The fragment for *Mobile clinic* is analogous to that of *Dialysis clinics* in that it represents the dialysis service in its mobile form. As such, the fragment contained variables

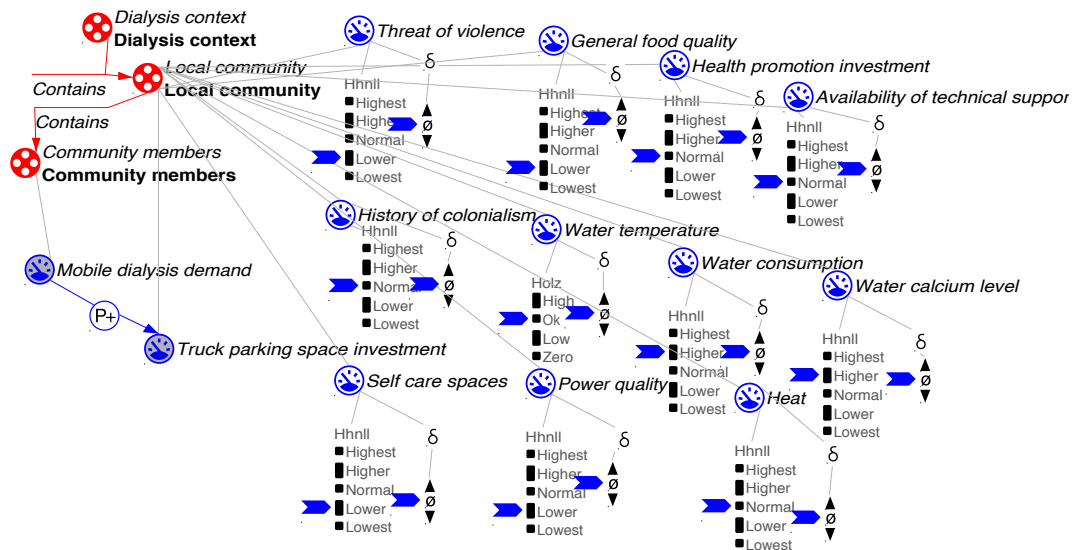


Figure 7.3.3.: Local community model fragment

such as *availability*, *treatment spaces* and *consumables cost* - variables that were part of the nature of medical services, as distinct from the physical hardware of the dialysis truck. In the *Mobile clinic* fragment, the effects of changes to the *truck* variables were seen to have an effect on the *Mobile clinic* entity. In the case of variations to the dialysis system design, an increase in *Dialysis system size* was found to cause a decrease in the *truck working space* (see the fragment diagram for *Dialysis truck* in figure G.0.7), which in turn affected the number of *treatment spaces* that were able to be offered to patients under the service.

7.3.1.9. Nurses

The fragment for *Nursing* staff (see figure 7.3.4) showed the relative volatility of nurses' situations and preferences. The model fragment showed relatively few stable aspects of nursing work, but highlighted the value of nurses being well connected with their patients, local community members, and local medical clinics. Nurses also liked to take care when setting up their workspace in order to minimise operational problems later; to have access to backup equipment in case of breakdowns and to generally avoid working alone - a situation that was found to be more likely while working on the dialysis truck. Meanwhile, a great many variables from other entities were identified as having positive and negative effects on nursing stress, comfort, the quality of their nursing practice and their general safety. This is important when considering technical variations to the dialysis context, particularly if those variations are to occur within the confines of the dialysis truck. For instance, *automation of equipment* was considered positively when it was able to lighten the nursing workload, and negatively if

during equipment breakdowns there was no backup available. In general, nurses were found to be well-served by improvements to levels of workplace noise, heat, vibration, disorganisation and equipment reliability. Since these and other variables were found to compete in their impact on nurses' wellbeing, care must be taken to minimise any negative impact during any dialysis truck design or innovation.

7.3.1.10. Patients

The fragment for *Patients* (see figure G.0.12) was relatively complex, having both a large number of affecting and affected variables. This was indicative of a state of dependency of patients on many different entities and stakeholders for their health and wellbeing. The effects on *Patients* due to the *Dialysis service* were largely related to the availability of treatment spaces and the rate of service expansion. The effects due to any nearby *Remote clinics* were related to the ability of the clinic to support the healthcare complexities associated with patient kidney failure: the availability of treatment spaces was limited to those patients whom the local clinic was willing to support in-between dialysis treatments.

The notable effects due to the studied dialysis system design variations were limited to that propagated through the *dialysis truck's* loss of *working space* associated with increasing *Dialysis system size*. This lack of space was recorded as corresponding to a loss of safety in patient care due to an increased likelihood of nursing staff making mistakes while working in a relatively confined space.

7.3.1.11. Remote clinic

The fragment for *Remote clinic* (see figure G.0.13) was representative of the general medical clinics found in most remote Aboriginal communities. The clinic at the remote site had little to do with the dialysis service except insofar as both institutions shared patients and community members. However, it was recorded that a good working *relationship between the dialysis service and the local clinic* was essential for an effective dialysis service.

The *Remote clinic* was recorded as bearing some of the operational costs of the *Dialysis truck*, whose function was dependent on the *clinic* providing a local water-supply connection and some degree of *plug-in power availability*. Data from the dialysis service administrators suggested that these were usually supplied free-of-charge as a courtesy (hence the need for a good working *relationship*) and that in any case the real cost was negligible compared with other operational costs such as staffing and insurance.

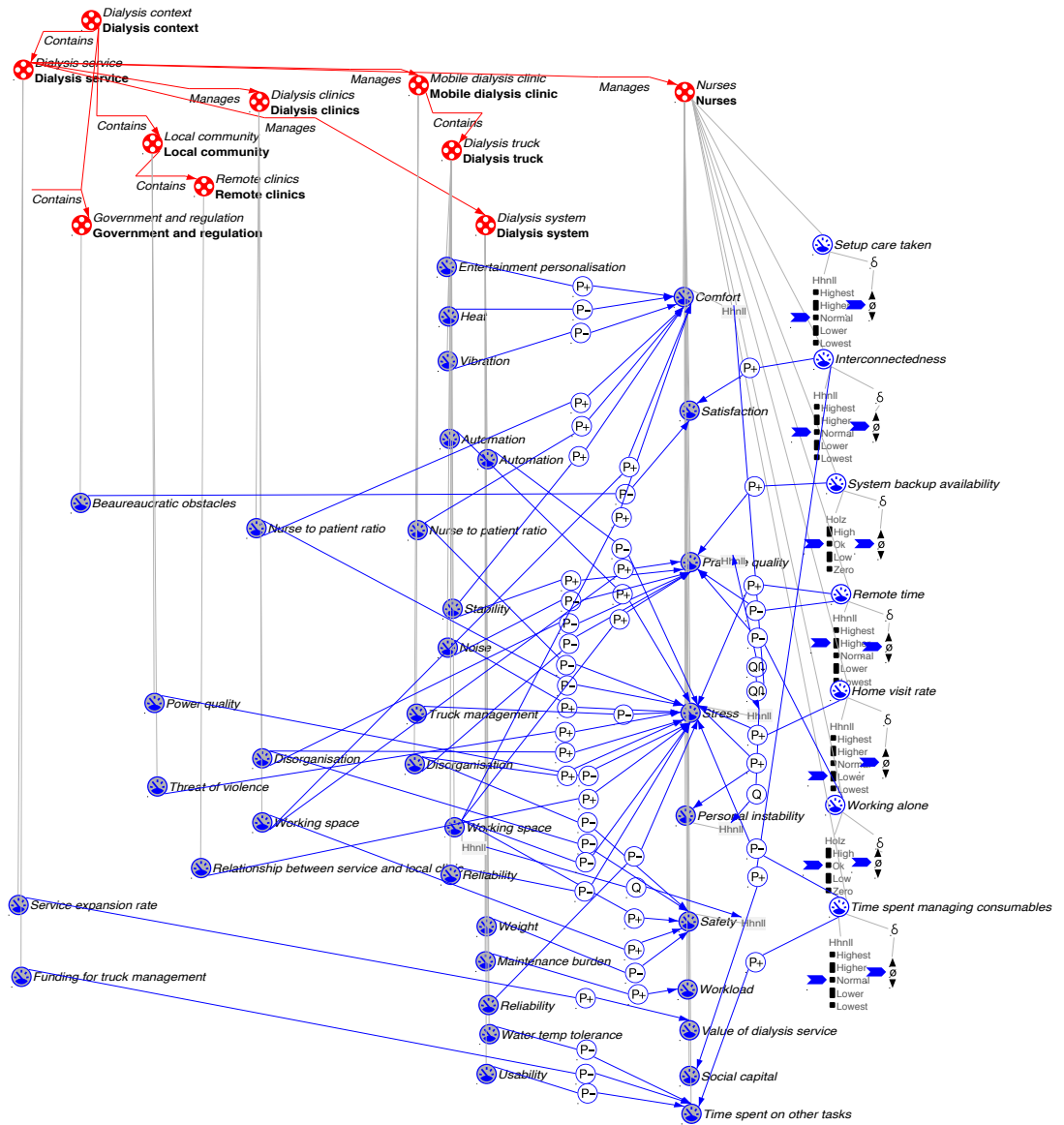


Figure 7.3.4.: Nursing model fragment

Simple and competing constraints	Reasoning
Dialysis truck noise $dQ >$ Dialysis truck working space [Competing]	The influence from any reduction in noise was thought likely to have a greater effect than any reduction in working space due to design changes.
Nursing personal instability $dQ <$ Dialysis truck working space [Competing]	It was thought likely that any risk due to <i>personal instability</i> would be mitigated by the service administration, while any loss of <i>working space</i> would increase the real, practical risk present during normal patient care.
Nursing stress $Q \sim$ Nursing practice quality [Implied]	It was thought that stress usually makes professional work more difficult to do well.
Nursing stress $Q \sim$ Nursing comfort [Implied]	It was thought that it is generally difficult to feel both comfortable and stressed simultaneously.

Table 7.3.1.: Competing and implied constraints

7.3.2. Constraints as data

There were relatively few constraints applied to the system. While a dozen *simple* constraints were used to ensure the propagation of change over singly-dependent variables, only a few *competing* and *implied* constraints were added (see table 7.3.1).

Of the four major dependent variables in the *Nursing* fragment, only three (*comfort*, *practice quality* and *stress*) were able to be constrained by intuition, probably because they were all qualities intrinsic to the person of the nurse, whereas the fourth variable, *safety*, was largely dependent on external, physical variables and influences. This left the variables *safety* and *stress* independent of each other.

The need for and reasoning behind the addition of the constraints was indicative of missing ethnographic information. A large number of constraints would have indicated either a significant loss of data integrity, or an impossible number of simulated output states were those constraints not applied. Very few constraints were necessary for the simulated model, suggesting both that its causal chains were relatively uncomplicated and that its associated ethnography had been sufficiently thorough.

This conclusion of thoroughness may, however, only be made for the oversimplified two-variable design trajectory. If more design parameters were to be varied, more constraints would be needed and the thoroughness of the ethnography would need to be reassessed. In any case, all constraints will need to be verified in future ethnographic iterations.

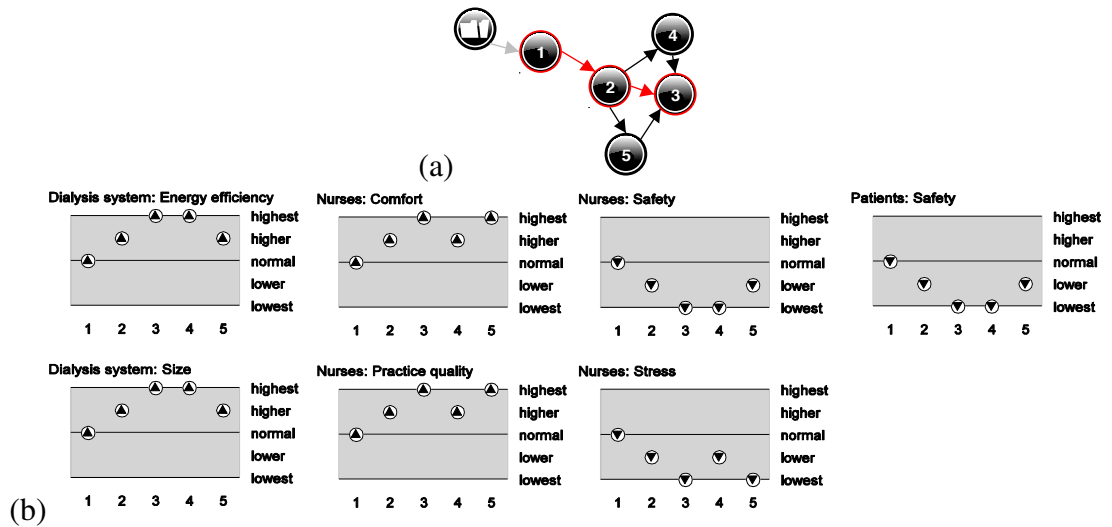


Figure 7.3.5.: Simulated state pathways (a) and outcomes (b) due to increases in both *dialysis system efficiency* and *dialysis system size*. At each state, the value of each variable is marked by a circle level with the corresponding value in the quantity space. Each circle contains an arrow indicating the direction of change of that variable.

7.3.3. Simulation output

The constrained model produced a set of five possible outcome states for the system. Starting with the chosen scenario, the reasoning engine progressed through three possible pathways before arriving at a final state (state no. 3 - see figure 7.3.5a). Values for all variables were collected and graphed for each state. The values for *Nurses* variables at each state are shown in figure 7.3.5b, together with the values for the two *Dialysis system* variables that were varied in this simulation.

The direction of change at the final state (no. 3) of each variable was marked on a graph of change propagation (see figure 7.3.6). This was done to facilitate the easy visualisation of outcomes due to the chosen design variations. The remaining variables were stationary throughout the simulation.

Simulation generated little new information that was not already apparent from inspection of the constrained model, for which only two major independent causal chains remained: the chain concerning *Nursing safety* and its associated variables, and the chain concerning *Nursing stress*, which, as has been mentioned, was dependent on many variables in the *Nursing* model fragment. These two competing chains were responsible for the three separate state-pathways generated by the reasoning engine (see figure 7.3.5a).

One perhaps unexpected outcome of the simulation was the apparent reduction in *Patient safety*, which was shown to decrease with the increase in *Dialysis system size* due

7.3 Results and discussion

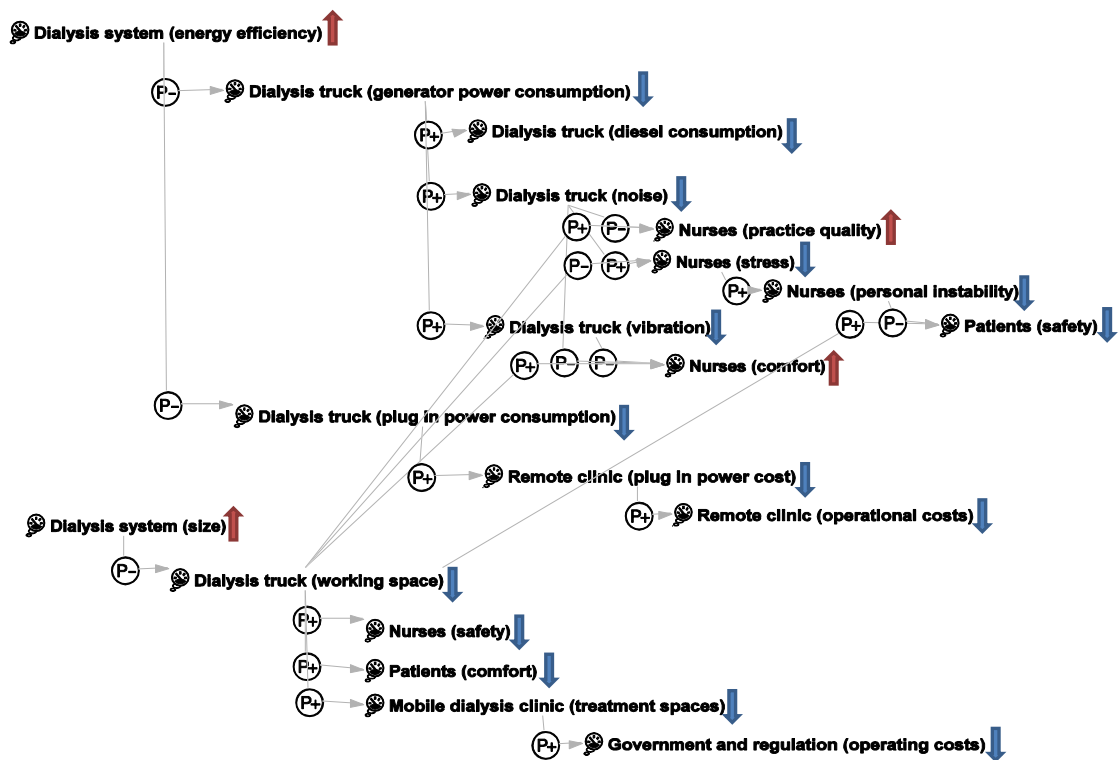


Figure 7.3.6.: Propagation of design variations through the social context of dialysis, modelled as a socio-technical system

to its encroachment on *Dialysis truck working space*. The simulation suggested that while a reduction in power consumption and noise would reduce *Nursing stress*, any loss in *working space* would be likely to result in more hazards. The associated ethnographic data suggested that this would be due to increased disorganisation, nurses bumping into things and other staff, and the inability for them to operate effectively in a confined space during medical emergencies. This outcome was not immediately obvious, neither from inspection of the causal map, model fragments or value listings. It is one of the few meaningful outcomes suggested only by the QRM simulation.

7.3.4. Ethnographic preference frequencies

7.3.4.1. Nursing preferences

The preferences of the various participants were derived from value statements such as the following:

N2: I found it really quite claustrophobic. I didn't enjoy dialysing people in there I have to say.

(Fieldnotes, 17/05/2013)

This comment from the *nurses* participant group was translated into the value statement: *Value of working space in truck HIGH*. In the raw data, nurses expressed value statements 227 times, concerning 48 separate values. Of these, 26 values were mentioned only once or twice and are not presented here as they were of minor significance compared with the remaining 22. The frequency at which nurses expressed certain values or preferences is shown in figure 7.3.7.

7.3.4.2. Patient preferences

The following anecdote from a dialysis service administrator summarises the significance of the value of *return-to-country* expressed by patients:

A: But after they finish dialysis they can go home and they can smile... and they do, God they smile- even the grumpiest ones smile. We put up a man out at [another community] who was with us for two weeks, and he asked, "Could I stay a couple of days longer?" We said "No- you can't because the truck's going..." I went to try and find him to go on the plane and I went I got up there I couldn't find him, and the plane was waiting... anyhow I got finally got back to the plane and he was there. Um, said I've been looking for you all over the place, said oh my family bought me down. And it was- this man of mid-fifties, tears rolling down his face you know...

(Fieldnotes, 16/05/2013)

7.3 Results and discussion

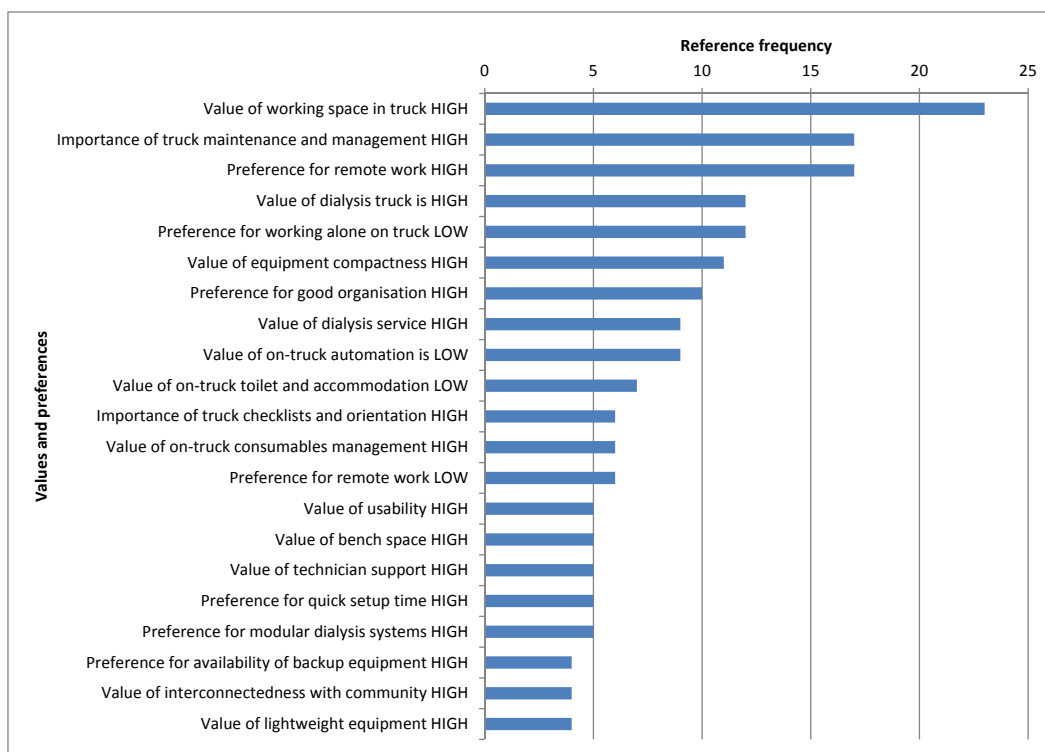


Figure 7.3.7.: Nursing values and preference frequencies from ethnographic data

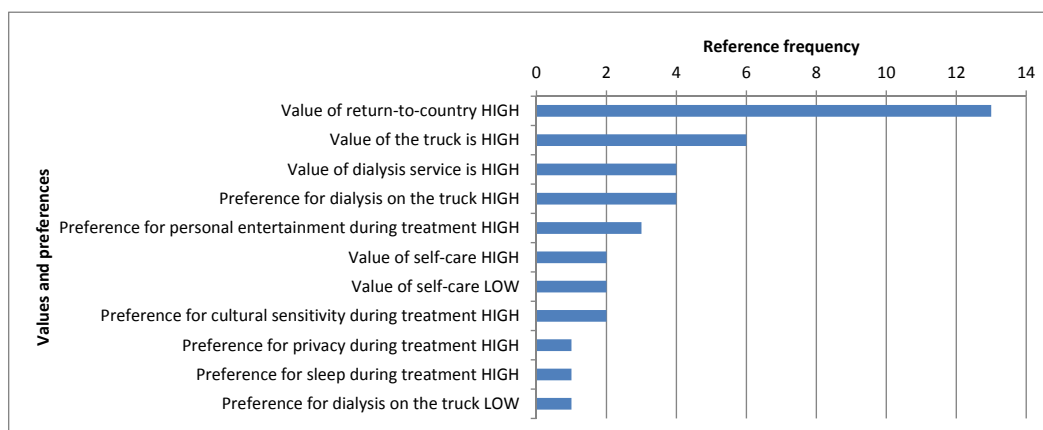


Figure 7.3.8.: *Patient* values and preference frequencies from ethnographic data

In the raw data, patient value statements were expressed 39 times, concerning 11 separate values. The frequency at which patients expressed certain values or preferences is shown in figure 7.3.8.

7.3.4.3. Community members preferences

Similar to the *Patient* participant group, *Community members* also valued *return-to-country* very highly.

When a truck like this when we go to a sports weekend, and, like for sorry too, like and for when we come to meeting, when we have a meeting like land council or meeting yeah - that's very good.

M: Yeah

Yeah, so we can have an extra people to come in and to have time. Yeah.

(Fieldnotes, 13/05/2013)

In the raw data, community members' value statements were expressed 66 times, concerning 10 separate values. The frequency at which community members expressed certain values or preferences is shown in figure 7.3.9.

7.3.4.4. A techno-centric perspective

A glance at the user preference tables (see figures 7.3.7 and 7.3.8) shows that increases in both dialysis system energy efficiency and size would be seen negatively by the nursing participants, and as irrelevant to both patients and community members.

The value most frequently expressed by the nursing community was that of *Dialysis truck working space*. The causal map (see figure 7.3.6) shows that increasing *Dialysis*

7.3 Results and discussion

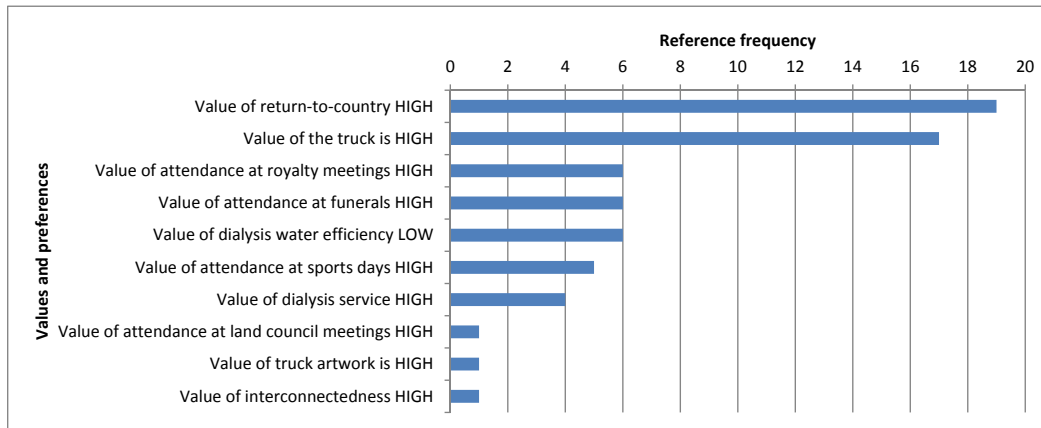


Figure 7.3.9.: *Community members* values and preference frequencies from ethnographic data

system size would cause a loss of working space. Even if the loss of space were negligible (or otherwise compensated for by a decrease in generator noise), nursing participants separately asserted the value of *Equipment compactness* (ranked sixth most-frequently mentioned in the table).

7.3.4.5. A user-centred perspective

If the design team were to use the preference frequency tables (see figures 7.3.7, 7.3.8 and 7.3.9) as part of a needs-analysis, they might proceed differently. For instance, the preference tables suggest that a dialysis system would be better suited to nurses if:

- It did not encroach on their working space
- It was compact, lightweight and modular, with backup subsystems
- It was easy to manage and maintain
- It was simple, and, if automated, hassle free
- It was easy to use and quick to set up

Most of these criteria may be the subject of later design phases, after the basic design concepts are finalised, and when technical decisions are likely to be more specific. Nevertheless, one criterion was applicable to and unfortunately contradicted by the proposed design variations: the preference against a loss of working space. Similarly, if the *Community members* and *Patients* were asked to participate in the design of a dialysis system, they might suggest:

- Anything that facilitates more patients returning-to-country would be better
- Anything that increases the availability of the truck would be useful

- Anything that doesn't interfere with patient privacy, entertainment or sleep would be better

These preferences are quite different to those of the nursing participants: none are specific to outcomes due to the design variations. This does not imply that the design variations are irrelevant: it instead suggests that at present the major concerns of patients and community lie elsewhere.

7.4. Conclusions

7.4.1. Significance of design variations

Of the studied design variations, neither equipment size, working space nor energy efficiency were mentioned by patients or community members as having any significant value. Furthermore, none of the listed preferences for these groups appeared on the causal chains for those design changes. This outcome has significance for the design team: it appears to give them permission to develop technology with little regard to the preferences of these two groups. However, this is not to say that these groups would not be affected by such changes, it only highlights that the effects of such variations were not among the stated preferences of these groups.

The reported preferences appeared to reflect the political needs of the user community, while the model fragments highlighted the real consequences of design variations. Another interpretation would be that the issues that were prioritised in discussion were those that were seen as problems, while things that were of little concern (yet high importance) appeared to receive little mention. One example of this was *Patient safety*, which is a fundamental principle of any healthcare system, yet was never mentioned as a preference (and only occasionally as a causal consequence). Meanwhile, items that might be perceived as optional extras or luxuries to a healthcare system designer, such as *Patient entertainment during treatment*, were seen by patients as significant enough to rate multiple mentions in the data.

This highlights a mistake that may be easily made by engineering designers: prioritising the needs emphasised by the user-community over those that go unmentioned. The above analysis suggests that the user community will tend to emphasise the needs that are seen as practical or political problems, while other needs that are important may go unmentioned if they are not seen as a problem at the time. To design using only user-preference data can therefore give designers a false-sense of freedom, with problems only appearing after designs are implemented as aspects of life that were previously stable and trouble-free become unsettled and cause complaint among the user-community.

With regard to the proposed design variations of increasing dialysis system energy-efficiency and size, the above analysis would suggest that these would be poor choices.

The analysis shows that these variations would lead to a decrease in both patient and nurse safety – compromises that most healthcare professionals would consider unacceptable. The associated loss of dialysis truck working space with increasing system size was the cause of most of the negative outcomes identified in this analysis. This suggests that any efforts to increase compactness would carry far greater value in-context than any small saving in energy consumption, despite the practical advantages in the reduction of generator noise and vibration.

7.4.2. Other design variations

One of this project's early expectations was that water would be considered a scarce and valuable resource in remote desert communities. A similar expectation was that energy efficiency would be a design principle that would be universally valued. Early aims of the project were oriented towards the development of a system that was energy and water efficient, robust and suitable for use in remote desert communities. While variations in these design parameters may have affected aspects valued by the participants, there were few mentions of them in the data. The data shows that, of these, water efficiency was the only aspect mentioned by the participants, yet it appeared to carry little importance for them. This was a remarkable observation given the project's assumptions about attitudes to water in the desert.

Of all the uses of water in the desert, the ethnography showed that dialysis water consumption was probably one of the more acceptable uses (see quoted example in section 7.2.2.7). This is not to suggest that there would be no benefit in improving system water efficiency, it is just that it was not considered a priority by community members. Another interpretation would be that community members would rather see more people returned-to-country at the cost of additional water consumption, than see water conservation at a loss of treatment availability.

7.4.3. Limitations of the method

7.4.3.1. Ethnographic limitations

Consistent with the proposed *engineering ethnography* (section 6.2.2.3), the fieldwork for this method was necessarily, “purposive, quick and adaptable.” In its application, this meant recruiting a small number of participants through briefly-formed relationships and allowing overlap between participant groups. All fieldwork was carried out by a single individual (in this case, the author), limiting the rigour of the research that is usually ensured in qualitative methods by having both fieldwork and analysis carried out by multiple individuals. As discussed in section 6.2.2.1, it would be impractical for an engineering design team to vastly increase the rigour of this method without also being overwhelmed by costs and data, yet this level of simplicity in research would

be inadequate for a formal ethnographic study. The proposed methodology attempts to mitigate this weakness by recommending that the dataset be continually revised and updated over multiple iterations, yet the scale of this project (an engineering PhD) limited the application of this methodology to only a single iteration. It should be noted, therefore, that the conclusions revealed by the data have only a limited scope, being intended only to inform and improve technical design.

7.4.3.2. Language and cultural difficulties

The methodology as it was applied here may appear to have been relatively harsh, despite its structure having been developed to include principles of cultural safety. In particular, the method depended on briefly-formed relationships; interviews with questions that may be confronting; discussion and analysis across cultural and language barriers; a tendency for the opinions of professional staff (such as nurses) rather than Aboriginal participants to dominate that data; and ultimately on having a dynamic social context translated into coded and modelled data with an associated loss of cultural integrity. The method also allowed for the use of interpreters for participants with limited English language skills, yet in practice participants declined the use of interpreters but still tended to use simple “Yes/No” answers during interviews. Lastly, there was no easy way for the researcher to determine the level of obligation experienced by participants, or the effect that such obligation may have had on the data.

At least having the researcher acknowledge an understanding of these weaknesses is consistent with the needs of cultural safety, insofar as it constitutes a reflection on the cultural norms of the research profession. The methodology was designed to mitigate this weakness, again by suggesting that research data be collected iteratively. Ideally, a design team would continue to develop respect and integrity in its relationships with remote Aboriginal community members over successive iterations, reducing the risk of cultural injury, yet the scale of this PhD project did not allow for more than one iteration to be completed during the study.

7.4.3.3. Dominance of simple preference analysis

It would appear that the most useful result from this applied methodology was the simple prioritisation of the preferences of the major stakeholders (see figures 7.3.7, 7.3.8 and 7.3.9), as derived directly from the ethnographic data. If this preference analysis were instead completed in the first case, design improvements may have progressed in the opposite direction: the development of a more compact but less energy efficient system would appear to have pleased more people. On the other hand, the graph of change propagation showed that a decrease in energy efficiency would increase noise, nursing stress and ultimately patient safety, despite *none* of these things being mentioned by nurses or patients as a priority.

In one sense, the method could have been improved by augmenting the set of value statements with values for variables that were connected by high numbers of graphs in the QRM model fragments. This would mean that variables such as *Nursing stress* would have been included with a LOW value, rather than only as a causal outcome. However, there is no need to homogenise all results into a list of value statements in order for them to be useful, as they may lose some of their meaning. For instance, nursing staff said nothing about how they feel about the level of *stress* in their jobs, but they did say a lot about the influences on and the impacts of that stress on other aspects of their environment.

7.4.3.4. Limited scope of QRM simulation

The modelling and simulation process highlighted the inherent complexity of even a simplified social context. The QRM model contained only eleven entities, yet resulted in large maps of causal relations that could not be simulated without first heavily constraining the interactions. If more than two design variations were to be used as inputs, the number of possible states could potentially grow to an unmanageable size. This is worth considering in the context of the limitations in scope of the engineering ethnography: improvements in rigour in the ethnographic process would generate even more data, which would then be decoded into a vast number of entities and causal relations, making QRM simulation unworkable. As discussed above (section 7.4.1), the QRM process has value in that it may be used to highlight major issues within the context that may not otherwise have been discussed by participants. To increase the length and depth of the ethnographic process would result in an unworkable QRM dataset, while reducing the ethnography would facilitate easy QRM analysis, yet any conclusions drawn from it would have questionable integrity. Care must therefore be taken when assembling a QRM model and simulation so as to maximise data integrity while minimising model complexity.

7.5. Methodology validation

7.5.1. External criteria

Presented here is an assessment of the application of the methodology against the application-specific evaluation criteria used to evaluate the similar *socio-technical systems engineering* methodology, borrowed from Baxter and Sommerville (2011) (see section 6.1.3.2).

7.5.1.1. Inconsistent terminology

The critical point is that there needs to be agreement about the social and technical elements of the system that need to be jointly optimised.
(Baxter and Sommerville, 2011)

Which elements should be optimised? The process has largely been driven by the data from semi-structured interviews, most of which was produced by nursing staff with an interest in their workplace dialysis service running smoothly. It was *their* preferences that dominated the data and thus optimisation by this method will tend to minimise their comfort and stress levels. This may not meet the preferences of other stakeholders in every case; the management of the service may have preferred that the resultant causal map emphasise financial considerations rather than work practices or patient care. Or perhaps they would have preferred something else, like the prioritisation of public health benefits rather than nursing or financial considerations.

The proposed methodology is strong on emphasising feelings. Things that participants were passionate about (such as working space in a dialysis truck) were mentioned many times, while other things that were working well may never have been mentioned at all, despite being necessary for the smooth functioning of the dialysis service. It is difficult, in this methodology, to assess whether appropriate attention has been given to social or technical ideas; the presumption is that if an issue becomes important, it will be mentioned more often, while once it is dealt with it will give way to other concerns. If this self-regulating tendency were applied to a machine, careful analysis would be performed to ensure the resulting system was stable over time. In this case, stability of the methodology may only be tested over multiple iterations and is unknown at present.
Assessment: Neutral.

7.5.1.2. Levels of abstraction

Rather than using different terms to describe the same thing, though, here we are talking about people describing the same system but using different levels of abstraction, often based on the fact that they draw the system boundaries in different places.
(Baxter and Sommerville, 2011)

There was some difficulty in identifying and delineating between different socio-technical subsystems. For example, the extent of a dialysis system is fairly easy to establish: you can put one in the back of a truck. However, some of the more abstract concepts were more difficult to define, and there was plenty of crossover. The simple question, “Who is a patient?” is revealing. Are they a patient while they are undergoing treatment? When they asleep? When they away from their home? When they are treated by another service? When they are deceased? Patient records are kept after a patient passes

away, and to some degree, the death of a patient may have more influence over health-care systems design than any other event.

Patients are also community members. They may be members of multiple communities, families, language groups etc. The concept of *Community Members* was used as an entity in the model, with characteristics such as disease prevalence and collective opinions. The concept of *Local Community* was treated separately, defined as the legal entity responsible for the management of water supplies and other local government priorities. It seemed sensible to separate these two entities based on how people spoke of them, yet clearly neither entity would not exist without the other.

The distinction between entities is fundamental to the modelling process. To change entities involves making changes everywhere in the SDG structure, as well as changing the coding of the ethnographic data. The entities were, in the first place, derived from the data with some interpretation from the design team. If a participant were to say, “What would the community think?”, that would be a very different use of the word “community” than in the question, “Where is the community located?”. Similar decisions were made throughout the modelling process according to natural grammar usage by the participants.

In this methodology, the focus is pushed firmly towards analysis of the context, which includes *everything* except changes to the designed device itself. There is no clear demarcation between user and context: as discussed above, the *user* is not a well-defined concept for medical devices (see section 6.2.1). By being both broad and simple in choosing entities, weighting between “user” and other contextual priorities is determined by the participants’ priorities, rather than the nature of the model structure.

Assessment: Neutral.

7.5.1.3. Conflicting value systems

There are, perhaps two sets of values that may conflict when describing context in terms of socio-technical systems:

The first set of values is a fundamental commitment to humanistic principles. In other words, the designer is aiming to improve the quality of working life and job satisfaction of the employee(s). ...The second set is often described as managerial values. In this view, socio-technical principles are regarded as a means of helping to achieve the company’s objectives (particularly economic ones).

(Baxter and Sommerville, 2011)

It has been suggested that both managers and device users might be discouraged from the use of socio-technical systems analysis due to the potential for the analysis to favour the conflicting priorities of one over the other (Baxter and Sommerville, 2011). A quick glance at the model fragments show that the comparison of competing priorities

is embedded in the nature of this methodology. This doesn't necessarily resolve the issue, as decisions still need to be made as to which should be prioritised when conflicts occur (see comments on constraints in section 7.2.4).

In one sense, there is no use in attempting to resolve these conflicts, nor should that be the role of any design methodology. Perhaps, any design process should be seen to be independent - aiming to avoid reinforcing anyone's particular priorities. To a degree, this can be done by making contextual information more accessible, to the benefit of all and the favour of none. However, as stated at the beginning of this article, there exists an ethical obligation to weight the preferences of community members (of whom patients are a subset) higher than those of dialysis service nurses or managers.

This weighting of preferences is not endemic to the modelling structure; it must be applied by the design team in the first instance, and by subsequent ethnographic analysis. The first is problematic, as the design team is too removed from the context to have the authority to set priorities: the design team does not appear as an entity in the SDGs - conceptual design is seen as a set of influences provided by an invisible and disinterested agent. Further ethnography is a better alternative but requires collaboration between the various gatekeepers.

This methodology is likely to work well where the key stakeholders are interested in making things better: if design improvements are seen to be helping everyone, the necessary co-operation will allow ethnography to proceed, providing insight into the context for everyone. If the process is seen to be favouring one group or another, or moving in an undesirable direction, managers may withhold funding for research; communities may deny permits for research; patients may decline to participate; nurses may move to protect patients from the invasion of privacy inherent in any social research. **Assessment: Neutral.**

7.5.1.4. Lack of agreed success criteria

Whilst benchmark tests can be used to determine whether the technical part of the system meets the appropriate criteria..., it is more difficult to determine if a system is a better fit to organisational needs... This evaluation is made harder by the fact that there are other, quite separate, influences on these factors and in many cases it may be impossible to link them directly to some new system... Each category of stakeholder is likely to have a different viewpoint on the system and different criteria for success.
(Baxter and Sommerville, 2011)

It is difficult to empirically assess a socio-technical methodology such as the one proposed here. A major problem is that the context may change faster than the technology. A typical medical device lifecycle lasts 10 years; a research project such as ours may take three or four years; election cycles have a similar timeframe. Meanwhile, patients

and nurses have spoken of recent riots in Aboriginal communities (*threat of violence* was a variable in the *Local Community* model fragment) – events that can quickly and dramatically change the socio-political landscape and its embedded socio-technical systems. Due to this external variability, apparently useful or damaging outcomes from design changes may be wrongly attributed to external effects. For this reason it will be difficult to evaluate the effectiveness of this design methodology based on apparent improvement in any outcome or indicator.

By repeating the ethnography through various iterations and feeding previously discovered data into subsequent iterations, this methodology includes at least some opportunity to continually accommodate major or minor context changes in the design cycle. Instead of comparing outcomes before-and-after each design implementation, the question changes: How would this methodology compare with the use of other methodologies in the same design situation?

This analysis includes this assessment of its features against criteria, which it is hoped would at least put us on the right path. This is close to the limit of possible evaluation, as no two contexts, designs or times are the same, making it difficult to establish a comparative control study. **Assessment: Disadvantage**

7.5.1.5. Analysis without synthesis

Socio-technical design methods have mostly been used to analyse existing systems, but these methods are limited in the support that they provide for the more constructive synthesis where the results of the analyses are systematically used in the software design process.

(Baxter and Sommerville, 2011)

Socio-technical systems have been used to assess existing designs and to inform the development of new designs, both of which have the problem of providing analytical data without being implemented. The methodology presented here at least is designed around *changes* to existing systems, incorporating synthesis directly into the modelling process. Furthermore, future iterations of device design will continue to add the generative effects of design change to produce further ethnographic data. **Assessment: Advantage**

7.5.1.6. Multidisciplinarity

The need for several disciplines to be involved is widely accepted, but the borders between the disciplines have been largely maintained, despite efforts at creating interdisciplinary teams by involving domain specialists in the design process.

(Baxter and Sommerville, 2011)

Ethnography is not within the traditional skill-set of engineers. It is, however, not difficult to learn although it requires social skills to approach, listen and respond to participants - strengths that are not necessarily typical of engineers. The methodology proposed here is relatively simple; interview questions are targeted and analysis is straight-forward. To address multidisciplinary problems, it is suggested that systems engineers carry out ethnography themselves to limit problems of cross-disciplinary communication. **Assessment: Advantage**

7.5.1.7. Perceived anachronism

The failure to reflect developments in organisational methods and technology can make STSD appear rather anachronistic and unfashionable.
(Baxter and Sommerville, 2011)

The original socio-technical systems principles were first presented in the 1970s; PD was developed at a similar time and as such, may be seen to be out of date. The proposed methodology borrows from STSD's humanist principles, but is otherwise relevant in the present era. The value of immersing designers in the context of their designed devices is reflected in current methods such as *empathic experience design* (Genco et al., 2011); analysis of a broad context is characteristic of *whole-system design* (Charnley et al., 2011), where the design includes many socio-technical sub-systems; the use of SDGs to analyse data is current (Li et al., 2013b). This proposed methodology should fit neatly into current design theory and practice. **Assessment: Advantage**

7.5.1.8. Fieldwork issues

More generally for fieldwork, there are problems with identifying the system stakeholders in the first place, before deciding which groups of stakeholders (and which individuals) should be involved.
(Baxter and Sommerville, 2011)

Ethnography and other qualitative methods are seen as time-consuming and unwieldy (see section 6.2.2.1). This has been addressed by borrowing from *cognitive ethnography*, to provide purposive, directed, short-term data collection phase. It seems that, at least in this case study, the relevant entities were revealed through the ethnographic process to generate a set larger than that contained in the seed dataset. Although it may not be clear to the design team at the outset exactly who the relevant stakeholders are, missing stakeholders will soon be revealed, whilst irrelevant ones will produce little data. The relevance of specific entities, variables and stakeholders is abundantly clear from a glance at the quantity of edges attached to them in the SDGs in the generated qualitative model fragments.

The question of “when to stop?” that has plagued other qualitative methodologies can be easy to determine for this methodology. Borrowing from the method of *grounded theory*, the ethnographic process should proceed until little new data is generated. It may be impractical for even a cognitive ethnography to proceed on this time-frame. Nevertheless, it may not be necessary to proceed to completeness in order to ascertain whether a particular design trajectory is truly preferred. In this study, a short ethnographic period was more than enough to answer basic design questions, as well as to generate large amounts of modelled contextual data. Further exploration would always be useful but would be unlikely to result in vastly different design decisions at this stage. **Assessment: Advantage**

7.5.2. Assessment summary

By comparing the proposed design methodology against the eight evaluation criteria of Baxter and Sommerville (2011), the methodology scored positively on four criteria, negatively on one and neutrally on three. The relevance of each criterion and a summary of the assessment of the methodology against each is presented below.

7.5.2.1. Neutral criteria

The proposed methodology scored neutrally on three criteria: *inconsistent terminology*; *levels of abstraction* and *conflicting value systems*, because it depends on iterative application. It is difficult to test objectively whether the right entities have been selected or the most relevant preferences weighted. Instead, iteration is recommended to test the relevance and significance of different stakeholders, objects and opinions. For the analysis presented here, only the first iteration has been completed, and further validation is needed to assess the iterative parts of the methodology.

7.5.2.2. Disadvantages

While iterative ethnography may help to measure the success of the proposed methodology, the relatively slow rate of iteration in medical device design would make it difficult to tell whether the methodology was actually helping, compared with intuitive design or any other design methodology. While a design team may feel confident that they are on the right track (as may other stakeholders), the *lack of agreed success criteria* may prevent adequate funding of this methodology’s required ethnography and analysis.

7.5.2.3. Advantages

The methodology's simplicity and present-day applicability reduces the problem of *perceived anachronism*. The problems of *multidisciplinarity* could be easily overcome by training designers in ethnography, and the methodology's focus on conceptual design should help keep its *analysis and synthesis* tightly coupled. Quick and simple fieldwork and subsequent graphing of results should benefit stakeholders and improve confidence in the choice of design trajectory at little additional cost, thus reducing any *fieldwork issues*.

7.6. General use of the methodology

It remains to be seen whether this methodology would be useful for effective dialysis system or other medical device design, although it has certainly been useful for *this* project, if only to show exactly how relevant or irrelevant the design efforts have been. Analysis of the ethnographic data alone may have been sufficient to carry out effective design intuitively, although outcomes from design changes would not have been able to be reliably or confidently predicted without the QRM model. The fact that increasing dialysis system energy efficiency and size were shown to have an *adverse* effect on patient safety while reducing nursing stress would not necessarily have been foreseen without the QRM model. This methodology has advantages over existing methodologies in that it incorporates cultural-safety principles, and provides both a visual representation, while prompting systematic interpretation of the social context, highlighting social and political preferences together with the real consequences of design variations.

8. Conclusion

8.1. Introduction

This project aimed to facilitate the return-to-country of Aboriginal dialysis patients through the development of more desert-suitable dialysis equipment. The aim of improved desert-suitability was originally interpreted to mean technical improvements in water and energy efficiency and in equipment robustness, implemented in a socially sensitive and culturally safe way (see 1.2.5). This in-turn leads to a particular innovation: using FO principles to produce dialysate from dialysate concentrate and groundwater, while retaining the benefits of the proven robustness of spiral-wound RO membrane elements (see section 1.3).

To test whether such an implementation of FO-based technology would be an improvement on the existing RO-based methods, several analyses were carried out. The first of these was done to establish the feasibility of the use of RO elements for FO, and whether dialysate could be produced practically at a rate sufficient for medical treatment (see chapter 2.2). This analysis identified further needs in-turn, such as the need for adequate control of the FO process' dialysate product, and the need for quick osmotic backwashing of the membrane element to remove accumulated salt from the feed-side.

The practical challenges of dialysate production and control were explored in chapters 3 and 4. The nature of and time needed for osmotic backwashing were explored in chapter 5, where the likely benefits and major design changes due to this FO dialysate production innovation were identified. These findings were then evaluated through an ethnographic methodology and QRM simulation to compare their impacts against the priorities of patients, nurses, community members and other stakeholders, and to identify any risk of cultural harm (see chapter 7). The major findings from each chapter are presented below.

8.2. Major findings

8.2.1. Theoretical analysis

The theoretical analysis (chapter 2) showed that the proposed innovation of dialysate production using a spiral-wound RO element in FO mode was feasible but conditional on having good production output control and quick osmotic backwashing of the element. The analysis also showed that the use of a higher quality membrane element would likely result in longer production times – a hypothesis that later turned out to be false (see section 8.2.4 below).

One important outcome from the theoretical analysis was the idea that production *volume* is more significant than production *time*. It was found that with an optimised controller for the production stage, about 5.0 L of dialysate was able to be generated in each cycle. This would be adequate for half-speed production, such that a pair of 4040-sized elements would be necessary in order to produce dialysate at a rate high enough for medical treatment. This estimate was also confirmed by experiment and computational models of production and backwashing cycles, as discussed in chapter 5.

Another significant prediction of the theory was that of the theoretical maximum of about 11.3 L of total dialysate output, based on estimates of the saturated feed-side salt concentration, and the membrane and feedwater quality. The difference between this value and that predicted for an optimised controller was one of the findings that prompted the further development of the batch-control approach explored in chapter 4.

8.2.2. Control optimisation

Attempts to develop a suitable controller for on-line dialysate production proved to be very difficult. The situation was not improved by using a high-quality ESPA2-4040 membrane element. By coupling a tuned FLC controller with high recirculation rates and freely flowing output, it was found that a production profile reasonably close to the ideal profile was able to be obtained (see 3.3.4). However, it was also found that instability in the output concentration due to paradoxical conductivity response could only be reduced at the expense of effective production time. In either case, the best net production volume able to be obtained was between 2.1 → 5.6 L, with most of the generated output being discarded as being too dilute for medical use. Compared with the theoretical maximum of 11.3 L estimated in the theoretical analysis, these best-case production volumes were thought to be relatively inadequate.

It was found that by simply accumulating and mixing the entire output volume, including that from the overly-dilute priming phase, through to the salt-rich fluid generated

past the saturation point of the membrane's feed-side, a batch of dialysate could be produced at precisely the desired output conductivity. By continually mixing and sampling the conductivity of the whole batch, the slower rate of variation in batch conductivity was able to be carefully monitored, so that the production stage could be stopped as soon as the desired conductivity was reached. It was found that a much higher net production volume was able to be obtained, at $V_{cycle} \approx 6.6$ L, with zero fluid discarded during the priming or production stages.

8.2.3. Production optimisation

Having found that on-line controller optimisation had limited success compared with simple batch-control dialysate production, it was decided to further explore the ways in which batch-production could be improved, with the aim of estimating the practical limitations of the proposed FO innovation (see chapter 4). The following major technical findings were made:

1. The FO-based prototype showed an equivalent water recovery rate of $65 \rightarrow 75$ %. This rate is comparable to that of existing RO-based systems.
2. The energy consumption of the FO prototype during the production stage was < 10 % of that used during dialysate production by a similar RO-based method.
3. The energy consumption over an *entire* FO production/backwash cycle was greatly affected by the energy demands of backwashing, including the need to operate a flow-pump at high speed, and the need to produce backwashing fluid from an RO unit. This reduced the equivalent energy efficiency to that of 66 % of an RO-based equivalent system.
4. There was little identifiable economic benefit in making this energy saving, at an equivalent cost saving of around \$0.10 per treatment.
5. The prototype FO-based system had other advantages over existing RO-based systems, such as relatively quiet operation.

8.2.4. Computational methods and Osmotic backwashing

Computational modelling and experimental validation of FO-based performance during production and backwashing enabled further understanding of the internal mechanisms of the prototype system. One particularly useful feature of the computational model was its ability to estimate membrane fluxes *including* the effects of ECP and ICP. This was a major limitation of the analytical method, which depended on constant approximations for ECP and ICP. By implementing numerical methods to solve a general analytical model of membrane fluid flux, the true nature of ECP and ICP and its effect on the performance of the FO-based process was able to be examined. The following implications were found:

1. The effects of ECP and ICP were severe.
2. ECP and ICP were likely to have dominated the theoretical estimates for production, rather than membrane quality.
3. ECP and ICP severity means that improvements in membrane quality would have little impact on output flow-rates. This was consistent with the finding that the use of a higher quality element had little effect on process performance.

The computational model also confirmed what was assumed in the theoretical analysis: that the rate at which a fixed quantity of salt was accumulated in the feed-side compartment had little effect on the time taken to remove that salt. This points to the major finding that backwashing time is independent of the production target flow-rate. This also means that backwashing time can be optimised separately to any production protocol.

Another major finding was that backwashing the element for more than 11 min was found to produce no significant improvement in net production volume, while backwashing for less than 4 min would result in most of the accumulated salt being retained within the membrane element. This highlighted the obvious conclusion that the optimal backwashing time for the system lay somewhere between those times, and that regardless of how production/backwashing was optimised, the system was still likely to need to be backwashed for at least the minimum time of 4 min.

Experimental validation showed that the optimal backwash time of ~ 8 min was the best compromise between retaining salt due to having shorter backwashing time, and delaying production, decreasing apparent output flow-rate and needing to increase trans-membrane flux due to having longer backwashing times. At this rate, the upper, apparent production-limit at $Q_{wtarget}^* = 240$ ml/min was about 50 % of the target rate, implying that two 4040-size RO membrane elements would be needed to produce dialysate at a rate comparable with the medical needs of dialysis treatment.

8.2.5. Technical summary

Conclusions from the various technical chapters can be summarised into a set of design features and limitations. In particular, this thesis suggests that:

1. Two 4040-size RO membrane elements would be needed to produce dialysate by FO at a rate necessary for medical dialysis treatment.
2. It would be difficult to increase the output significantly above this rate due to the ever-increasing severity of ECP and ICP at higher flux rates.
3. The need to backwash the element is associated with significant losses in energy, water and production efficiency.
4. At this rate, the apparent water efficiency of the backwashed prototype is comparable to that of existing RO-based technology.

5. The energy efficiency of the system is significantly improved compared with that of existing RO-based technology.

8.2.6. Technology in context

The technical analysis showed that the suggested technical innovation is likely to result in two competing primary outcomes:

- Increased energy efficiency, at the cost of
- Increased dialysis system size

Propagation of these variations over a causal map of the dialysis context showed that these variations would result in gains and losses to the stakeholders and processes (see chapter 7). Of particular note were the following:

- Increased energy efficiency would result in various gains for mobile dialysis, such as a reduction in generator load, fuel, vibration and noise, which in turn would reduce nursing stress, comfort and mental health.
- Increased dialysis system size would result in a loss of working space within the confines of a dialysis truck. This would in turn result in a loss of nurses safety, patient comfort and ultimately, a loss of patient safety due to the increased likelihood of mishaps during busy procedures or medical emergencies.
- *Increased system size would result in a loss of mobile dialysis treatment spaces!*

As stated in chapter 6, technical safety and cultural safety are both aspects of good working practice for nurses. (section 6.1.2.5). With a shift in dialysis design towards systems of increased size, the design will have failed on both counts due to a loss of both patient safety and a loss of return-to-country opportunities as a result of a loss of mobile treatment spaces.

This was confirmed by the comparison against the user preferences extracted from the ethnographic data (see section 7.3.4): Nursing staff valued *working space* highly and referred to it more often than any other preference. Patients valued *return-to-country* highly and referred to it more than twice as often as any other individual preference. Community members valued *return-to-country* highly, and the presence of the dialysis truck almost as highly.

The culturally-safe methodology was certainly useful in that it allowed unusual and competing social-context variables to be identified and visualised, while providing an opportunity for Aboriginal community members, patients and other stakeholders to participate in the planning of their own healthcare services. Were it not for their input, nursing staff may simply have asserted their preferences for a quieter workspace, and put up with a small loss of working space. The loss of a potential dialysis treatment space may never have been noticed, yet may have been a significant loss to the communities whose need for temporary and mobile dialysis services is increasing.

8.2.7. Comments on water consumption

As discussed above (see section 8.2.3), the technical innovations were shown to have little impact on the water efficiency of dialysate production when compared with that of existing RO-based technology. As such, water efficiency was not assessed as a potential or competing design variation in the application of the culturally-safe methodology. Nevertheless, the need for water efficiency was an original technical aim of this project, and as identified in the introduction, the use of water is subject to the values of various people and groups in the desert.

The ethnographic data showed that the value of water carried no significance among the dialysis nurses or patients that were surveyed. (Its economic cost was also dismissed as trivial by participants drawn from among dialysis service administrators). Community members who spoke about water consumption asserted that improving dialysis water efficiency was seen as a low priority. This was largely because medical uses of water were seen as valuable and acceptable. A glance at the preference data confirmed that dialysis services were highly valued, compared with the indifference expressed towards water conservation in medical applications.

The general attitude towards water conservation in remote communities is exemplified by the image of a lushly irrigated football field surrounded by red desert soil shown in figure 8.2.1. This use of water is likely to be one of the many high-consumption uses of water in remote communities that were identified in the published water-consumption data (see PowerWater, 2009c). Any potential savings in dialysis water consumption would pale in comparison to that spent annually on community irrigation demands such as this.

8.3. Future work

8.3.1. Ethnographic iteration

The culturally-safe methodology used in this project was designed to function over several iterations, only the first of which was able to be completed during the course of this project. As a consequence, the qualitative research presented here was limited in its scope, both in time, subject material and in the range of participants (see discussion in section 7.4.3). More importantly, the methodology itself was designed so that data and analysis from each cycle would be used to seed further investigation. It is recommended that as further technical work progresses, further ethnographic analysis also be carried out, as per the principles embedded in the described methodology.



Figure 8.2.1.: Football field irrigation in the desert (image supplied, 2013)

8.3.2. Membrane disinfection

Medical devices such as dialysis equipment are subject to strict disinfection protocols. For RO-based systems, both the RO unit and the main dialysis machine are chemically disinfected, with the RO system being disinfected daily and the dialysis system disinfected following each treatment. This is normally done by adding a liquid disinfectant to the heated RO permeate stream that is conveniently available for RO-based systems, but not so for the prototype FO-based system, which has no such permeate compartment. There may be several possible cleaning protocols that may suit such an FO-based system: a separate RO permeate stream may be used for cleaning cycles (similar to that needed for backwashing); membranes could be specified as single-use only; a membrane-safe disinfectant concentrate may be used as a draw-solution. For any FO-based technology to be used for medical treatment, a disinfection step must be proven, although this was beyond the scope of this project.

8.3.3. Membrane failure monitoring

As mentioned in section 1.3.1, the lack of a clean permeate stage means that it is difficult to monitor dialysate production quality. The small flow of ions across the

membrane from the feedwater in normal use needs to be monitored to detect dangerous flux of heavier ions such as boron; any gross leak due to membrane failure will also need to be detected immediately before feedwater gets anywhere near the patient. There is no simple method to monitor the FO-produced dialysate that is immediately obvious; the existing method's conductivity measurements would be swamped by the higher conductivity of the dialysate fluid. Perhaps some ion-selective probes would have to be placed on both sides of the membrane to measure a suitable indicator of trans-membrane salt-flux. Exploration of this safety control is critical but has been beyond the scope of this project.

8.3.4. Reverse salt-leak

As discussed in section 2.2.2.3, there is a non-zero quantity of salt that leaks in reverse across the membrane in any FO process. Where dialysate concentrate is used as a draw-solution, this reverse salt-leak represents a loss of some components of the finished dialysate solution. This change in the integrity of the medical product would need to be evaluated so as to prove that the resultant diluted dialysate fluid was still suitable for medical treatment. An alternative approach would be to compensate for the loss of specific ions by adding them to the draw-solution concentrate or the diluted dialysate product solution. The study of the rate of loss of ions due to reverse-salt leak and the consequent changes in composition of the dialysate output was beyond the scope of this project.

8.3.5. Excess use of dialysate concentrate

As discussed in section 2.2.2.3, the prototype depends on compensating for feed-side salt accumulation by injecting excess dialysate concentrate into the draw-side compartment. The rate of this excess is determined by an *overprime* factor, which was calculated for some experiments to be $F_{OP} = 1.61$. This factor also represents the rate of loss of salt mass into the membrane element – salt that is ultimately discarded during the backwashing stage. This excess salt is extra dialysate concentrate that must be purchased, transported and stored, and represents a cost to various stakeholders in the dialysis context. The minimisation of the economic burden of this salt wastage or its comparison against any economic benefit of water or energy conservation is worth exploring, but was beyond the scope of this project.

8.3.6. Use of FO membrane elements

The major difficulties associated with the use of RO membrane elements for FO included their propensity for severe ECP and ICP, and their need for cyclic backwashing.

While this project did manage to explore the nature and limitations of backwashing, the need for such backwashing eliminated most gains in water or energy efficiency. By using a specialised FO membrane, the benefits of FO-based processes may potentially be had without the need for frequent or prolonged backwashing. These benefits would be had at a loss of the necessary compactness and robustness required for use in the desert context. Nevertheless, future experimentation may discover benefits in the use of such specialised FO elements that outweigh these losses.

8.3.7. Large dialysis centres

The proposed FO-based technology may have usefulness in large dialysis centres elsewhere. The technology may potentially be used to prepare large quantities of dialysate in advance for later delivery in treatment, although this practice is uncommon in Australia. This could be achieved by operating an FO process at low-speed overnight, allowing for low trans-membrane flux-rates and therefore maximum production efficiency. If specialised FO membrane elements could be used, large quantities of dialysate may be able to be generated with very little energy input, and with the potential for significant gains in water efficiency. This may become advantageous in large centres with dozens of simultaneous daily treatments, and where water and energy bills are significantly large.

8.3.8. Summary

The technical innovations in this project were shown to have limited relevance to the remote desert context when compared against the ethnographic data, despite the good intentions of the design team. There were several reasons for this: firstly, the design's impact on water conservation was negligible, and in any case, water conservation in healthcare did not appear to be valued by patients, nurses or community members. Secondly, the innovation's impact on energy efficiency *was* a significant improvement, yet was shown to carry little economic benefit compared with other healthcare operating costs. Improvements in energy efficiency *did* appear to have some practical benefit in reducing the generator load for mobile dialysis, with associated benefits in noise and vibration reduction and therefore improvements in nursing quality and safety. This indicates that there may be further value in improvement in dialysis system energy efficiency, or perhaps in efficiency gains elsewhere within a dialysis truck. However, if the priorities of nurses, patients and community members are to be considered, these improvements should not be made at a loss of dialysis truck working space, due to the associated losses in nurse and patient safety, and in the number of available treatment spaces. While the technical benefits of the proposed FO-based dialysate production system may be limited in the context of remote Aboriginal desert community health, it may have applications in other dialysis contexts.

This project has been instructive in that it highlights the difference between the assumptions of engineering designers and the priorities of those for whom they are designing. In particular, there was a stark contrast between the importance of water conservation as seen by the project team and the priorities of the user-community (see discussion at 7.4.2 and 8.2.7). This serves to emphasise the importance of examining the technical development of medical devices within their social context, particularly when that context is remote Aboriginal health. It is hoped that the methodologies used here, both technical and ethnographic, may provide a useful guide for similar medical device development projects both in remote health contexts and elsewhere.

Appendices

A. Derivations for chapter 2

A.1. General principles

It is convenient to divide the element up into differential strips of length dx and area dA_{mem} , separating draw-and-feed-side differential volumes, dV_d and dV_f that have corresponding thicknesses, w_d and w_f :

$$\begin{aligned}dV_d &= w_d \cdot dA_{mem} \\dV_f &= w_f \cdot dA_{mem}\end{aligned}\tag{A.1.1}$$

By defining local draw- and feed-side concentrations, $c_d(x)$ and $c_f(x)$, in terms of differential quantities of solute mass, dm_d and dm_f , contained in their corresponding differential fluid volumes, dV_d and dV_f , osmotic effects can be estimated:

$$\begin{aligned}c_d(x) &= \frac{dm_d}{dV_d} \\c_f(x) &= \frac{dm_f}{dV_f}\end{aligned}\tag{A.1.2}$$

The local *absolute* trans-membrane concentration difference, $\Delta c(x)$, can be written based on these values, from which the Morse law for osmotic pressure, $\Pi(x)$, can be used to generate an equation for trans-membrane fluid flux:

$$\begin{aligned}\Delta c(x) &= c_d(x) - c_f(x) \\ \Pi(x) &= iRT\Delta c(x)\end{aligned}\tag{A.1.3}$$

If a local trans-membrane pressure, $\Delta P(x)$, is applied across the membrane, opposing the osmotic pressure, then an equation for the trans-membrane fluid flux, $J_{wm}(x)$ can be developed:

$$J_{wm}(x) = A (\Pi(x) - \Delta P(x))\tag{A.1.4}$$

The flux, J_{wm} , is related to the trans-membrane pressures by the membrane hydraulic permeability, A . A general model of ideal trans-membrane water flux can be written:

$$J_{wm}(x) = A (iRT\Delta c(x) - \Delta P(x))\tag{A.1.5}$$

A.2. Non-ideal properties

The form shown above only applies to ideal membranes that are not affected by ECP or ICP. When non-zero flow exists, the osmotic effect of the concentration difference is reduced. By describing an *apparent* trans-membrane concentration difference, Δc^* , a more applicable model may be developed:

$$\Delta c^*(x) = (c_d \cdot f)(x) - (c_f \cdot g)(x) \quad (\text{A.2.1})$$

Here, both f and g are functions of membrane water flux, J_{wm} , and take the form:

$$\begin{aligned} f(J_{wm}) &= e^{-\frac{J_{wm}}{k_{ECP}}} \\ g(J_{wm}) &= e^{\frac{J_{wm}}{k_{ICP}}} \end{aligned} \quad (\text{A.2.2})$$

These can be combined to form a general model for trans-membrane water flux:

$$J_{wm}(x) = A \left(iRT \left(c_d(x) \cdot e^{-\frac{J_{wm}(x)}{k_{ECP}}} - c_f(x) \cdot e^{\frac{J_{wm}(x)}{k_{ICP}}} \right) - \Delta P(x) \right) \quad (\text{A.2.3})$$

This formulation of the membrane flux model was originally proposed by Loeb et al. (1997). Since the concern here is largely with modelling at neutral pressure processes, the effect of hydrostatic trans-membrane pressure (ΔP) is omitted from this point forward. Despite its appearance, the model is complicated by the presence of $J_{wm}(x)$ as both an output and a variable and cannot be reduced algebraically. To complete the following analysis, a constant approximation must be used for f and g , the product of A and iRT can be simplified, and a substitute label, k_s , is used in place of the traditional label for the membrane reverse solute flux constant, B :

$$\begin{aligned} \Delta P &= 0 \\ f(J_{wm}) &= \mu \\ g(J_{wm}) &= \lambda \\ k_w &= A \cdot iRT \\ k_s &= B \end{aligned} \quad (\text{A.2.4})$$

A simplified model for trans-membrane fluid flow that includes ECP and ICP effects can then be written:

$$\begin{aligned} J_{wm}(x) &= k_w \Delta c^*(x) \\ &= k_w (c_d(x) \mu - c_f(x) \lambda) \end{aligned} \quad (\text{A.2.5})$$

A.3 Approximating bulk values from local values

A similar formula can be written for trans-membrane salt-flux, using k_s as membrane salt-flux-constant:

$$\begin{aligned} J_{sm}(x) &= k_s \Delta c^*(x) \\ &= k_s (c_d(x)\mu - c_f(x)\lambda) \end{aligned} \quad (\text{A.2.6})$$

A.3. Approximating bulk values from local values¹

The local flow through a differential element of the membrane of area, dA_{mem} can be calculated as follows:

$$dQ_{wm} = J_{wm}(x) \cdot dA_{mem} \quad (\text{A.3.1})$$

This can be combined with the equations above to derive a form for the differential flow in terms of draw- and feed-side differential salt-masses, dm_d and dm_f :

$$\begin{aligned} dQ_{wm} &= k_w (c_d(x)\mu - c_f(x)\lambda) dA_{mem} \\ &= k_w \left(\frac{\mu \cdot dm_d}{w_d \cdot dA_{mem}} - \frac{\lambda \cdot dm_f}{w_f \cdot dA_{mem}} \right) dA_{mem} \\ &= \frac{\mu k_w}{w_d} dm_d - \frac{\lambda k_w}{w_f} dm_f \end{aligned} \quad (\text{A.3.2})$$

When simple approximations for μ and λ are used, it is possible to estimate *bulk* properties from *local* properties by integrating A.3.2 over the whole element:

$$\begin{aligned} \int dQ_{wm} &= \frac{\mu k_w}{w_d} \int dm_d - \frac{\lambda k_w}{w_f} \int dm_f \\ Q_{wm} &= \frac{\mu k_w}{w_d} m_d - \frac{\lambda k_w}{w_f} m_f \\ &= k_w A_m \left(\frac{m_d}{V_d} \mu - \frac{m_f}{V_f} \lambda \right) \\ &= k_w A_m (c_d \mu - c_f \lambda) \\ &= k_w A_m \Delta c^* \\ J_{wm} &= k_w \Delta c^* \end{aligned} \quad (\text{A.3.3})$$

¹As mentioned in section 2.2.2.2, distributed quantities, such as trans-membrane flux $J_{wm}(x)$ or concentration difference $\Delta c^*(x)$ are written here as functions of their position in space (x). When integrated, J_{wm} , Δc^* and others become bulk quantities and variables in their own right, and are notated here without parentheses.

Here, the notation Δc^* refers to the *apparent* trans-membrane concentration difference that causes osmotic flows:

$$\Delta c^* = (c_d \mu - c_f \lambda) \quad (\text{A.3.4})$$

At low flux ranges, $\Delta c^* \rightarrow \Delta c$, where Δc is the *absolute* difference between the bulk solute concentrations c_d and c_f . A similar derivation can be used to show that J_{sm} is also related to this apparent concentration difference:

$$J_{sm} = k_s \Delta c^* \quad (\text{A.3.5})$$

A.4. Trans-membrane concentration difference and stability:

Balancing salt mass-flows on the draw-side, we have an input salt injection of Q_{sin} , a loss across the membrane of Q_{sm} , an output of Q_{sout} and a retained total draw-side salt mass m_d :

$$m_d = \int_{t=0}^t Q_{sin} \cdot dt - \int_{t=0}^t Q_{sout} \cdot dt - \int_{t=0}^t Q_{sm} \cdot dt \quad (\text{A.4.1})$$

Since salt is not lost once it passes through the membrane to the feed-side, the mass of salt there m_f grows with time. The salt contained in the supplied feedwater accumulates according to its concentration, c_{feed0} and the flow of water across the membrane from the feed- to the draw-side, Q_{wm} :

$$m_f = \int_{t=0}^t Q_{sm} \cdot dt + \int_{t=0}^t Q_{wm} \cdot c_{feed0} \cdot dt \quad (\text{A.4.2})$$

The input salt injection rate is constant, therefore:

$$\int_{t=0}^t Q_{sin} \cdot dt = Q_{sin} \cdot t \quad (\text{A.4.3})$$

The bulk trans-membrane salt and water flow rates, Q_{sm} and, Q_{wm} are proportional to the apparent concentration difference, Δc^* according to the membrane flux constants for salt and water, k_s and k_w . Other flow rates for fluid and salt exiting the system at its output, Q_{wout} and Q_{sout} , can be derived according to the output concentration, c_{dout} :

$$\begin{aligned} Q_{sm} &= k_s A_m \Delta c^* \\ Q_{wm} &= k_w A_m \Delta c^* \\ Q_{wout} &= Q_{wm} + Q_{win} \\ Q_{sout} &= Q_{wout} \cdot c_{dout} \end{aligned} \quad (\text{A.4.4})$$

A.4 Trans-membrane concentration difference and stability:

To simplify the derivation that follows, constants k_1 , k_2 , k_3 and k_4 are used to combine other fixed parameters for simplicity:

$$\begin{aligned}
 k_1 &= k_s A_m \\
 k_2 &= k_w A_m \\
 k_3 &= k_w A_m c_{dout} \\
 k_4 &= k_w A_m c_{feed0}
 \end{aligned} \tag{A.4.5}$$

The absolute concentration difference for the whole element can be estimated by combining equations A.4.1, A.4.2, A.4.3 and A.4.6:

$$\Delta c = \frac{m_d}{V_d} - \frac{m_f}{V_f} \tag{A.4.6}$$

The value of Δc can be expressed by substituting integrals for m_d and m_f :

$$\begin{aligned}
 \Delta c &= \frac{1}{V_d} \left(\int_{t=0}^t Q_{sin} \cdot dt - \int_{t=0}^t Q_{sout} \cdot dt - \int_{t=0}^t J_{sm} \cdot dt \right) - \frac{1}{V_f} \left(\int_{t=0}^t Q_{sm} \cdot dt + \int_{t=0}^t Q_{wm} c_{feed0} \cdot dt \right) \\
 &= \frac{1}{V_d} Q_{sin} \cdot t - \frac{1}{V_d} \int_{t=0}^t Q_{sout} \cdot dt - \left(\frac{1}{V_d} + \frac{1}{V_f} \right) \int_{t=0}^t Q_{sm} \cdot dt - \frac{c_{feed0}}{V_f} \int_{t=0}^t Q_{wm} \cdot dt \\
 &= \frac{1}{V_d} \left(Q_{sin} t - \int_{t=0}^t k_3 \Delta c^* \cdot dt - Q_{win} \cdot c_{dout} \cdot t \right) - \left(\frac{1}{V_d} + \frac{1}{V_f} \right) \int_{t=0}^t k_1 \Delta c^* \cdot dt - \frac{k_4}{V_f} \int_{t=0}^t \Delta c^* \cdot dt \\
 &= \frac{1}{V_d} (Q_{sin} - Q_{win} \cdot c_{dout}) t - \left(\frac{k_3}{V_d} + \frac{k_1}{V_d} + \frac{k_1 + k_4}{V_f} \right) \int_{t=0}^t \Delta c^* \cdot dt \\
 &= k_5 t - k_6 \int_{t=0}^t \Delta c^* \cdot dt
 \end{aligned} \tag{A.4.7}$$

Constants k_5 and k_6 are used here for simplicity and are defined below:

$$\begin{aligned}
 k_5 &= \frac{Q_{win} \cdot (c_{din} - c_{dout})}{V_d} \\
 k_6 &= \left(\frac{k_3}{V_d} + \frac{k_1}{V_d} + \frac{k_1 + k_4}{V_f} \right) \\
 &= \frac{(k_s + k_w c_{dout}) A_m}{V_d} + \frac{(k_s + k_w c_{feed0}) A_m}{V_f}
 \end{aligned} \tag{A.4.8}$$

Differentiating both sides of equation A.4.7 yields a differential equation :

$$\frac{d}{dt}\Delta c = k_5 - k_6\Delta c^* \quad (\text{A.4.9})$$

To solve this, we use the definition of the apparent concentration difference:

$$\begin{aligned} \Delta c^* &= c_d\mu - c_f\lambda \\ &= c_d - c_f + (\mu - 1)c_d - (\lambda - 1)c_f \\ &= \Delta c + (\mu - 1)c_d - (\lambda - 1)c_f \end{aligned} \quad (\text{A.4.10})$$

Rearranging equation A.4.10 and substituting for Δc using A.4.7:

$$\begin{aligned} \frac{d}{dt}\Delta c &= k_5 - k_6\Delta c^* \\ \frac{d}{dt}(\Delta c^* - (\mu - 1)c_d + (\lambda - 1)c_f) &= k_5 - k_6\Delta c^* \\ \frac{d}{dt}\Delta c^* - (\mu - 1)\frac{d}{dt}c_d + (\lambda - 1)\frac{d}{dt}c_f &= k_5 - k_6\Delta c^* \end{aligned} \quad (\text{A.4.11})$$

The rate of change of the bulk, feed-side solution, $\frac{d}{dt}c_f$, can be written in terms of instantaneous flow rates:

$$\begin{aligned} \frac{d}{dt}c_f &= \frac{Q_{wm} \cdot c_{feed0} + Q_{sm}}{V_f} \\ &= \frac{1}{V_f} (k_w A_m \Delta c^* \cdot c_{feed0} + k_s A_m \Delta c^*) \\ &= \frac{A_m}{V_f} (k_s + k_w c_{feed0}) \Delta c^* \\ &= \frac{(k_s + k_w c_{feed0}) A_m \Delta c^*}{V_f} \end{aligned} \quad (\text{A.4.12})$$

Similarly, the rate of change of the bulk, draw-side solution can be written:

$$\begin{aligned} \frac{d}{dt}c_d &= \frac{Q_{sin} - Q_{sm} - Q_{sout}}{V_d} \\ &= \frac{Q_{win} \cdot c_{din} - k_s A_m \Delta c^* - Q_{wout} \cdot c_{dout}}{V_d} \\ &= \frac{Q_{win} \cdot c_{din} - k_s A_m \Delta c^* - (k_w A_m \Delta c^* + Q_{win}) \cdot c_{dout}}{V_d} \\ &= \frac{Q_{win} \cdot (c_{din} - c_{dout}) - (k_s + k_w c_{dout}) A_m \Delta c^*}{V_d} \end{aligned} \quad (\text{A.4.13})$$

A.4 Trans-membrane concentration difference and stability:

Substituting this result into A.4.11:

$$\begin{aligned} \frac{d}{dt}\Delta c^* &= (\mu - 1) \left(\frac{Q_{win} \cdot (c_{din} - c_{dout}) - (k_s + k_w c_{dout}) A_m \Delta c^*}{V_d} \right) \dots \\ &\dots - (\lambda - 1) \left(\frac{(k_s + k_w c_{feed0}) A_m \Delta c^*}{V_f} \right) + k_5 - k_6 \Delta c^* \end{aligned} \quad (A.4.14)$$

$$\begin{aligned} &= \left(\frac{(\mu - 1) Q_{win} \cdot (c_{din} - c_{dout})}{V_d} + \frac{Q_{win} \cdot (c_{din} - c_{dout})}{V_d} \right) \dots \\ &\dots - \left(\frac{(\mu - 1) (k_s + k_w c_{dout}) A_m \Delta c^*}{V_d} + \frac{(k_s + k_w c_{dout}) A_m \Delta c^*}{V_d} \dots \right) \end{aligned} \quad (A.4.15)$$

$$\begin{aligned} &\dots + \frac{(\lambda - 1) (k_s + k_w c_{feed0}) A_m \Delta c^*}{V_f} + \frac{(k_s + k_w c_{feed0}) A_m \Delta c^*}{V_f} \end{aligned} \quad (A.4.16)$$

$$\begin{aligned} &= \left(\frac{\mu Q_{win} \cdot (c_{din} - c_{dout})}{V_d} \right) - \left(\frac{\mu (k_s + k_w c_{dout}) A_m}{V_d} + \frac{\lambda (k_s + k_w c_{feed0}) A_m}{V_f} \right) \Delta c^* \\ &= k_5^* - k_6^* \Delta c^* \end{aligned} \quad (A.4.17)$$

This is written using a modified form for k_5^* and k_6^* to indicate where these constants have been adjusted for ECP and ICP at high flux rates. As $J_{wm} \rightarrow 0$, both $\mu \rightarrow 1$ and $\lambda \rightarrow 1$, so that both $k_5^* \rightarrow k_5$ and $k_6^* \rightarrow k_6$:

$$\begin{aligned} k_5^* &= \mu k_5 \\ &= \frac{\mu Q_{win} \cdot (c_{din} - c_{dout})}{V_d} \end{aligned} \quad (A.4.18)$$

$$k_6^* = \frac{\mu (k_s + c_{dout} k_w) A_m}{V_d} + \frac{\lambda (k_s + c_{feed0} k_w) A_m}{V_f} \quad (A.4.19)$$

The values in k_6^* are time-invariant (provided that c_{dout} can be controlled), allowing the solution of:

$$\begin{aligned} \frac{d}{dt}\Delta c^* &= k_5^* - k_6^* \Delta c^* \\ \Delta c^* &= \frac{k_5^*}{k_6^*} \left(1 - e^{-k_6^* t} \right) \end{aligned} \quad (A.4.20)$$

The settling time determined by k_6^* is not so useful, as in practice, high-fluxes may appear during startup and significant process changes. However, the value at stabilisation is important for calculating other values:

$$\Delta c_{stable}^* = \frac{k_5^*}{k_6^*} \quad (A.4.21)$$

A.5. Input priming rate and *overprime* factor

Calculating the output water flow, Q_{wout} , as the sum of inputs to the draw-side and using the equations in A.4.4, taking substitutions from equations A.4.21, A.4.18, A.4.19 and rearranging:

$$\begin{aligned}
 Q_{wout} &= Q_{wm} + Q_{win} \\
 &= k_w A_m \Delta c_{stable}^* + Q_{win} \\
 &= k_w A_m \frac{k_5^*}{k_6^*} + Q_{win} \\
 &= k_w A_m \frac{\frac{\mu Q_{win} (c_{din} - c_{dout})}{V_d}}{\frac{\lambda (k_s + k_w c_{feed0}) A_m}{V_f} + \frac{\mu (k_s + k_w c_{dout}) A_m}{V_d}} + Q_{win} \\
 &= \frac{\frac{\mu}{V_d} \left(\frac{k_s}{k_w} + c_{din} \right) + \frac{\lambda}{V_f} \left(\frac{k_s}{k_w} + c_{feed0} \right)}{\frac{\lambda}{V_f} \left(\frac{k_s}{k_w} + c_{feed0} \right) + \frac{\mu}{V_d} \left(\frac{k_s}{k_w} + c_{dout} \right)} Q_{win} \tag{A.5.1}
 \end{aligned}$$

When an ideal system operates with zero salt leak ($k_s = 0$), the output salt flow, Q_{sout} , stabilises at the input salt injection rate, Q_{sin} . By defining the ideal flow rate, Q_{win0} , needed to carry this salt injection at a concentration of c_{din} to provide a stable output flow at target rate $Q_{wtarget}$ and concentration $c_{dtarget}$, the required non-ideal injection rate, Q_{win} , can be estimated by forcing the output to match the desired targets.

$$\begin{aligned}
 Q_{win0} \cdot c_{din} &= Q_{wtarget} \cdot c_{dtarget} \\
 Q_{win0} \cdot c_{din} &= \frac{\frac{\lambda}{V_f} (k_s + k_w c_{feed0}) + \frac{\mu}{V_d} (k_s + k_w c_{din})}{\frac{\lambda}{V_f} (k_s + k_w c_{feed0}) + \frac{\mu}{V_d} (k_s + k_w c_{dtarget})} Q_{win} \cdot c_{dtarget} \\
 \frac{Q_{win}}{Q_{win0}} &= \frac{\frac{\lambda}{V_f} (k_s + k_w c_{feed0}) + \frac{\mu}{V_d} (k_s + k_w c_{dtarget})}{\frac{\lambda}{V_f} (k_s + k_w c_{feed0}) + \frac{\mu}{V_d} (k_s + k_w c_{din})} \cdot \frac{c_{din}}{c_{dtarget}} \\
 FOP &= \frac{\frac{\lambda}{V_f} \left(\frac{k_s}{k_w} + c_{feed0} \right) + \frac{\mu}{V_d} \left(\frac{k_s}{k_w} + c_{dtarget} \right)}{\frac{\lambda}{V_f} \left(\frac{k_s}{k_w} + c_{feed0} \right) + \frac{\mu}{V_d} \left(\frac{k_s}{k_w} + c_{din} \right)} \cdot \frac{c_{din}}{c_{dtarget}} \tag{A.5.2}
 \end{aligned}$$

A.6. Effective production time

When the draw-side compartment is saturated with a mass of salt, m_{dts} , at time, t_s , the feed-side contains a salt mass m_{fts} , and the system's production output is no-longer useful. Similarly, during an initial priming phase, the system's output is not immediately useful until time t_0 , when output concentration has risen to the target value,

A.6 Effective production time

$c_{dtarget}$. At this time, the draw- and feed-side concentrations are m_{dt0} and m_{ft0} . The time during which the system is productive, $t_{eff} = t_s - t_0$, is useful to know. Combining A.4.1 with A.4.2 and 2.2.11 gives a derivation of t_{eff} :

$$\begin{aligned}
 m_{dts} + m_{fts} &= \int_{t=0}^{t_s} Q_{sin} \cdot dt - \int_{t=0}^{t_s} Q_{sout} \cdot dt + \int_{t=0}^{t_s} Q_{wm} \cdot c_{feed0} \cdot dt \\
 m_{dts} + m_{fts} &= m_{dt0} + m_{ft0} + \int_{t_0}^{t_s} Q_{sin} \cdot dt - \int_{t_0}^{t_s} Q_{sout} \cdot dt + \int_{t_0}^{t_s} Q_{wm} \cdot c_{feed0} \cdot dt \\
 &= m_{dt0} + m_{ft0} + [Q_{sin}t]_{t_0}^{t_s} - [Q_{sout}t]_{t_0}^{t_s} + c_{feed0} \cdot [Q_{wm}t]_{t_0}^{t_s} \\
 &= m_{dt0} + m_{ft0} + Q_{sin} \cdot (t_s - t_0) - Q_{sout} (t_s - t_0) + c_{feed0} \cdot Q_{wm} (t_s - t_0) \\
 &= m_{dt0} + m_{ft0} + Q_{sin} \cdot t_{eff} - Q_{sout} \cdot t_{eff} + c_{feed0} \cdot Q_{wm} \cdot t_{eff} \\
 &= m_{dt0} + m_{ft0} + (Q_{sin} - Q_{sout} + c_{feed0} \cdot Q_{wm}) \cdot t_{eff} \\
 t_{eff} &= \frac{(m_{dts} + m_{fts}) - (m_{dt0} + m_{ft0})}{Q_{sin} - Q_{sout} + c_{feed0} \cdot Q_{wm}} \tag{A.6.1}
 \end{aligned}$$

This applies whenever the system is at steady state, with Q_{sin} , Q_{sout} and Q_{wm} (and therefore, Δc^*) all stable. This form may be convenient, as some initial and final concentrations may be easily determined by modelling or measurement. It may only be necessary to determine some of these, as when production is steady, the relationship between c_d and c_f is fixed by the apparent salt difference Δc^* . If c_d is known at different times, c_f can be calculated:

$$\begin{aligned}
 \Delta c_{stable}^* &= c_d \mu - c_f \lambda \\
 c_f &= \frac{\mu c_d - \Delta c_{stable}^*}{\lambda} \tag{A.6.2}
 \end{aligned}$$

The effective production time can then be determined by using only the system parameters and the bulk draw-side concentration over time if known:

$$\begin{aligned}
 t_{eff} &= \frac{(m_{dts} + m_{fts}) - (m_{dt0} + m_{ft0})}{Q_{sin} - Q_{sout} + c_{feed0} \cdot Q_{wm}} \\
 &= \frac{(c_{dts} - c_{dt0}) V_d - (c_{fts} - c_{ft0}) V_f}{Q_{win} \cdot c_{din} - Q_{wtarget} \cdot c_{dtarget} + c_{feed0} \cdot (Q_{wtarget} - Q_{win})} \\
 &= \frac{(c_{dts} - c_{dt0}) V_d + \left(\frac{\mu c_{dts} - \Delta c_{stable}^*}{\lambda} - \frac{\mu c_{dt0} - \Delta c_{stable}^*}{\lambda} \right) V_f}{\left(\frac{Q_{win}}{Q_{win0}} - 1 \right) Q_{wtarget} \cdot c_{dtarget} + c_{feed0} \cdot Q_{wtarget} - \frac{Q_{win}}{Q_{win0}} \cdot \frac{Q_{wtarget} \cdot c_{dtarget} \cdot c_{feed0}}{c_{din}}} \\
 &= \frac{\mu (c_{dts} - c_{dt0}) \cdot \left(\frac{V_d}{\mu} + \frac{V_f}{\lambda} \right)}{\left(\frac{Q_{win}}{Q_{win0}} \left(1 - \frac{c_{feed0}}{c_{din}} \right) + \frac{c_{feed0}}{c_{dtarget}} - 1 \right) Q_{wtarget} \cdot c_{dtarget}} \tag{A.6.3}
 \end{aligned}$$

A.7. Backwashing and recovery compensation

Given a set flow rate, $Q_{wtarget}$, the useful volume delivered during a production cycle, V_{cycle} , can be estimated:

$$V_{cycle} = Q_{wtarget} \cdot t_{eff} \quad (A.7.1)$$

Combined with a backwashing delay of t_{bf} , the *apparent* output, $Q_{wtarget}^*$, can be estimated:

$$\begin{aligned} Q_{wtarget}^* &= \frac{V_{cycle}}{t_{eff} + t_{bf}} \\ &= \frac{V_{cycle}}{\frac{V_{cycle}}{Q_{wtarget}} + t_{bf}} \\ &= \frac{V_{cycle} Q_{wtarget}}{V_{cycle} + Q_{wtarget} \cdot t_{bf}} \end{aligned} \quad (A.7.2)$$

To force the system to produce the desired flow-rate, its *set* flow-rate must be artificially increased to compensate:

$$Q_{wtarget} = \frac{V_{cycle} Q_{wtarget}^*}{V_{cycle} - Q_{wtarget}^* \cdot t_{bf}} \quad (A.7.3)$$

Clearly, as $t_{bf} \rightarrow 0$, $Q_{wtarget}^* \rightarrow Q_{wtarget}$, as expected. Furthermore, there is a limit to the apparent flow rate, even if peak production can be infinitely large:

$$\begin{aligned} Q_{wtarget} &\rightarrow \infty \\ Q_{wtarget}^* &\rightarrow \frac{V_{cycle}}{t_{bf}} \end{aligned} \quad (A.7.4)$$

A.8. Production with non-constant flow

By examining the accumulated feed-side salt, m_{fts} , its mass is either salt from its initial state, m_{ft0} , or salt delivered by the feedwater, m_{feed} , or salt leaked across the membrane, m_{sm} :

$$m_{fts} = m_{ft0} + m_{feed} + m_{sm} \quad (A.8.1)$$

The mass of salt in the feed-and draw-side at initial and final times may be written in terms of concentrations:

$$\begin{aligned} m_{ft0} &= c_{ft0} \cdot V_f \\ m_{fts} &= c_{fts} \cdot V_f \end{aligned} \quad (A.8.2)$$

A.8 Production with non-constant flow

The salt delivered from the feedwater, m_{feed} , can be estimated for a given trans-membrane volume, V_{wm} , as follows:

$$m_{feed} = c_{feed0} \cdot V_{wm} \quad (A.8.3)$$

The salt lost through the membrane, m_{sm} , is lost at a rate, Q_{sm} , that is in proportion to the trans-membrane water flow, Q_{wm} :

$$\begin{aligned} Q_{wm} &= A_m k_w \Delta c^* \\ Q_{sm} &= A_m k_s \Delta c^* \end{aligned} \quad (A.8.4)$$

By dividing these functions together:

$$Q_{sm} = \frac{k_s}{k_w} Q_{wm} \quad (A.8.5)$$

The total delivered salt and water quantities, m_{sm} and V_{sm} , can be defined as the collected flows of salt and fluid over time:

$$\begin{aligned} V_{wm} &= \int Q_{wm} \cdot dt \\ m_{sm} &= \int Q_{sm} \cdot dt \end{aligned} \quad (A.8.6)$$

By integrating both sides over time, the total delivered trans-membrane salt and fluid quantities can be estimated:

$$\begin{aligned} \int Q_{sm} \cdot dt &= \frac{k_s}{k_w} \int Q_{wm} \cdot dt \\ m_{sm} &= \frac{k_s}{k_w} V_{wm} \end{aligned} \quad (A.8.7)$$

Thus, our original mass-balance equation (A.8.1) can be rewritten:

$$\begin{aligned} m_{fts} &= m_{ft0} + m_{feed} + m_{sm} \\ c_{fts} \cdot V_f &= c_{ft0} \cdot V_f + V_{wm} \cdot c_{feed0} + \frac{k_s}{k_w} V_{wm} \\ (c_{fts} - c_{ft0}) \cdot V_f &= \left(c_{feed0} + \frac{k_s}{k_w} \right) \cdot V_{wm} \\ V_{wm} &= \frac{(c_{fts} - c_{ft0}) \cdot V_f}{\frac{k_s}{k_w} + c_{feed0}} \end{aligned} \quad (A.8.8)$$

The total output volume also includes the fraction of injected concentrate volume, which is typically significantly smaller than the output flow:

$$\begin{aligned} V_{cycle} &= V_{wm} + V_{win} \\ &\approx V_{wm} \end{aligned} \tag{A.8.9}$$

If the input of the priming pump can be accounted for, then the remaining volume produced by the system cannot exceed this limit:

$$V_{cycle} \leq \frac{(c_{fts} - c_{ft0}) V_f}{\frac{k_s}{k_w} + c_{feed0}} \tag{A.8.10}$$

B. Notes for chapter 5

The following is a brief discussion of the computational decisions and limitations of the simulated dialysis system and membrane model.

B.1. Well-mixed membrane cell compartments

The approach to the calculation of salt mass-flows posed a challenge to the simulation's computational load. When considering each cell-segment as a well-mixed compartment (see section 5.2.2.2), salt mass-flows *into* each cell were calculated first at each iteration (see flow-chart in figure 5.2.4). When a cell's total accumulated salt was determined, a new value for its concentration was calculated then applied to the fluid flowing out of each cell. The total loss of fluid from any given cell could never be allowed to exceed the cell's volume. For a given surface flow-rate, Q_z , the time taken to empty a cell of fluid would be the maximum allowable sample period, τ_s :

$$\tau_s = \frac{V_{cell}}{Q_z} \quad (\text{B.1.1})$$

Cell volume, V_{cell} , was modelled in terms of the membrane sheet area, A_{sheet} , and spacer thickness, w_d , such that the volume was approximately inversely proportional to the square of the number of cells throughout the whole sheet, $m \times n \approx n^2$:

$$V_{cell} = w_d \cdot \frac{A_{sheet}}{n^2} \quad (\text{B.1.2})$$

By combining equations B.1.1 and B.1.2, the dependencies of τ_s can be shown:

$$\tau_s = \frac{w_d \cdot A_{sheet}}{n^2 \cdot Q_z} \quad (\text{B.1.3})$$

The total simulated time, t_{sim} , could be written in terms of the number of iterations, i_{total} , and the sample period, τ_s :

$$t_{sim} = i_{total} \cdot \tau_s \quad (\text{B.1.4})$$

Assuming that the number of floating-point calculations required to perform simple operations on a matrix or vector is in proportion to its size, then the total CPU time, t_{CPU} , required to carry out a simulation may be written by combining equations B.1.3 and B.1.4 as follows:

$$\begin{aligned}
 t_{CPU} &\propto i_{total} \cdot n^2 \\
 &= \frac{t_{sim}}{\tau_s} \cdot n^2 \\
 &= \frac{t_{sim} \cdot Q_z \cdot n^4}{w_d \cdot A_{sheet}}
 \end{aligned} \tag{B.1.5}$$

An increased spatial sampling frequency (increased n) would result in rapid and undesirable growth in CPU time with n^4 over the run-time of each simulation.

B.2. Diffusion considerations

To specify compartments of size similar to the diffusion length at a typical sample period, they would need to be very small and the size of n would have to be large:

$$\begin{aligned}
 L_{diff} &= \sqrt{4 \cdot D \cdot \tau_s} \\
 &\approx 7.34 \mu\text{m} \\
 n &= \frac{L_{mem}}{L_{diff}} \\
 &\approx 1.27 \times 10^5
 \end{aligned} \tag{B.2.1}$$

For a typical sampling time of $\tau_s = 10$ ms, an enormous value for n would be needed. It would be very difficult to model such a system in this way, were its compartments mixed by diffusion alone. Instead, the model has relied upon the flow of fluid across the cells to provide turbulent mixing. With the sampling time having been deliberately chosen to be similar to the time taken for a molecule to be carried across the cell compartment, this would seem to be a reasonable assumption.

B.3. Matrix inversion considerations

By segmenting the membrane into $n \times n$ cells, the resultant vectors of pressures, flows and all other variables were required to operate over $n^2 \approx 400$ cells on each side of the membrane sheet. In the initial case, the two matrices A_d and A_f , needed to be assembled and inverted. This was not trivial, as it required one row in A_d for every

element \mathbf{P}_d , each of which dealt with the mass-flow relationship between that one element and every other element on that side of the sheet. This took the size of A_d to $(n \times n) \times (n \times n) = n^4 = 160,000$ elements. A test sparse matrix of this size took about 191 ms to invert in MATLAB™. If the spatial sampling rate were doubled to $n = 40$ cells per linear meter of membrane, the size of A_d would increase by $2^4 = 16$ times to 2,560,000 entries. Examples tested took about 1500 ms for MATLAB™ to invert. To save computational time, the program was structured so that the inversion of each matrix of this type was carried out only once, before the beginning of the main program loop.

B.4. Numerical methods

Of the various numerical root-finding methods trialled to estimate solutions to the membrane flux equations, the built-in MATLAB™ function `fzero` was the slowest, taking typically 360 ms to optimise a set of flux calculations over a single membrane state. This function was written to be used element-wise over arrays of elements. Various implementations of classical root-finding methods were therefore written to take advantage of MATLAB™'s strength in operating on entire matrices rather than iterating over them element-wise. This was found to drastically reduce the computational time required to analyse a single membrane state down to < 3.0 ms, with Newton's method being the fastest at 1.10 ms per membrane state. Any of these numerical methods would have been fast enough for the purposes of this study. Newton's method was used for all simulations presented here.

C. Symbols and parameters

C.1. Symbols

Symbol	Definition	Units
A_{mem}	Total membrane area	m^2
dA_{mem}	Differential area of membrane	m^2
A	Membrane hydraulic permeability	$m \cdot Pa^{-1} \cdot s^{-1}$
B	Membrane reverse solute flux constant	m/s
$\frac{B}{A}$	Membrane quality indicator	Pa
$c_d(x)$	Distribution of draw-side concentration	mosm/L
c_d	Bulk draw-side concentration	mosm/L
c_{dt0}	Bulk draw-side concentration at time t_0 .	mosm/L
c_{dts}	Bulk draw-side concentration at time t_s .	mosm/L
$c_{dts}(x)$	Distribution of draw-side concentration at time t_s .	mosm/L
$c_f(x)$	Distribution of feed-side concentration	mosm/L
c_f	Bulk feed-side concentration	mosm/L
c_{feed0}	Feedwater concentration	mosm/L
c_{fts}	Bulk feed-side concentration at time t .	mosm/L
c_{ft0}	Bulk feed-side concentration at time t_0 .	mosm/L
c_{din}	Dialysate concentrate concentration	mosm/L
c_{dout}	Dialysate output concentration	mosm/L
$c_{dtarget}$	Target output concentration	mosm/L
$\Delta c(x)$	Distribution of concentration difference	mosm/L
Δc	Bulk trans-membrane concentration difference	mosm/L
$\Delta c^*(x)$	Apparent distribution of concentration difference	mosm/L
Δc^*	Apparent bulk concentration difference	mosm/L
D	Solute diffusivity	m^2/s
F_{OP}	Overprime factor for excess salt injection	(unitless)
f	Corrective function for ECP	(unitless)
g	Corrective function for ICP	(unitless)
i	van t' Hoff factor	(unitless)
$J_{sm}(x)$	Distribution of trans-membrane solute flux	$mosm \cdot s^{-1} \cdot m^{-2}$
J_{sm}	Bulk trans-membrane solute flux	$mosm \cdot s^{-1} \cdot m^{-2}$
$J_{wm}(x)$	Distribution of trans-membrane water flux	$L \cdot s^{-1} \cdot m^{-2}$
J_{wm}	Bulk trans-membrane water flux	$L \cdot s^{-1} \cdot m^{-2}$
J_{wmAVG}	Test value of water flux for evaluating μ and λ .	$L \cdot s^{-1} \cdot m^{-2}$
k_s	Membrane solute permeability	m/s
k_w	Membrane water permeability	$m \cdot L \cdot s^{-1} mosm^{-1}$
K_{ECP}	Mass-transfer coefficient for ECP	$s \cdot m^2 \cdot L^{-1}$
K_{ICP}	Mass-transfer coefficient for ICP	$s \cdot m^2 \cdot L^{-1}$

Table C.1.1.: List of symbols and units (1 of 2)

C.1 Symbols

Symbol	Definition	Units
L_{mem}	Membrane length	m
$\Delta P(x)$	Distribution of hydrostatic pressure difference	kPa
ΔP	Bulk trans-membrane hydrostatic pressure	kPa
$Q_s(x)$	Longitudinal solute flow	mosm/s
$Q_{sm}(x)$	Distribution of solute flow across membrane	mosm/s
$Q_w(x)$	Longitudinal water flow	L/s
$Q_{wm}(x)$	Distribution of water flow across membrane	L/s
Q_{sin}	Dialysate concentrate solute injection rate	mosm/s
Q_{win}	Dialysate concentrate volume injection rate	L/s
Q_{win0}	Ideal dialysate concentrate volume injection rate	L/s
$\frac{Q_{win}}{Q_{win0}}$	Overprime factor for excess salt injection	(unitless)
Q_{wnet}	Net production cycle flow-rate	L/s
Q_{sout}	Dialysate solute output rate	mosm/s
Q_{wout}	Dialysate volume output rate	L/s
$Q_{wtarget}$	Target dialysate flow-rate	L/s
$Q_{wtarget}^*$	Apparent production cycle flow-rate	L/s
R	Universal gas constant	$L \cdot kPa \cdot K^{-1} mmol^{-1}$
S_{me}	Membrane structural parameter	m
t_{eff}	Effective production time	s
t_{bf}	Backwashing time	s
T	Temperature	K
V_d	Total draw-side compartment volume	L
V_f	Total feed-side compartment volume	L
V_{cycle}	Production cycle dialysate volume	L
V_{max}	Maximum dialysate cycle volume	L
V_{total}	Total dialysate treatment volume	L
W_m	Total membrane width	m
w_d	Draw-side spacer thickness	m
w_f	Feed-side spacer thickness	m
ϵ_f	Feed-side spacer volume fraction	(unitless)
ϵ_d	Draw-side fluid volume fraction	(unitless)
μ	Constant for approximating ECP equations	(unitless)
λ	Constant for approximating ICP equations	(unitless)
σ_{target}	Target conductivity	mS/cm
x	Distance along membrane element	m
dx	Differential length of membrane element	m

Table C.1.2.: List of symbols and units (2 of 2)

C.2. Symbols for derivations

Symbol	Definition	Units
Δc_{stable}^*	Apparent concentration difference at stable production	mosm/L
$k_{1...6}$	Dummy constants for stability and production time	-
k_5^*, k_6^*	Dummy constants for including ECP and ICP effects	-
m_d	Bulk draw-side solute mass	mosm
dm_d	Differential quantity of draw-side solute mass	mosm
m_f	Bulk feed-side solute mass	mosm
dm_f	Differential quantity of feed-side solute mass	mosm
m_{ft0}	Total feed-side salt mass at the beginning of production	mosm
m_{fts}	Total feed-side salt mass at the point of saturation	mosm
m_{feed}	Total salt delivered by the feedwater	mosm
m_{sm}	Total salt diffused across the membrane	mosm
V_{wm}	Total fluid volume diffused across the membrane	L
$\Pi(x)$	Trans-membrane osmotic pressure	kPa

Table C.2.1.: List of symbols used for derivations

C.3. Symbols for modelling

Symbol	Definition	Units
A_{cell}	Membrane cell area	m^2
A_d	Draw-side pressure matrix	Pa
A_{dcross}	Draw-side compartment cross-sectional area	m^2
A_f	Feed-side pressure matrix	Pa
A_{fcross}	Feed-side compartment cross-sectional area	m^2
A_{sheet}	Membrane sheet area	m^2
C_{cell}	Cell compliance	L/Pa
\mathbf{c}_d	Draw-side cell concentration vector	mosm/L
\mathbf{c}_{d0}	Draw-side cell concentration vector at previous iteration	mosm/L
\mathbf{c}_{dZ}	Draw-side concentration matrix, offset in direction Z	mosm/L
c_f	Bulk feed-side concentration	mosm/L
\mathbf{c}_f	Feed-side cell concentration vector	mosm/L
\mathbf{c}_{f0}	Feed-side cell concentration vector at previous iteration	mosm/L
C_{mem}	Bulk draw-side membrane compliance	L/Pa
I_{struct}	Draw-solution injection structure matrix	(unitless)
i_{total}	Total simulation iterations	(unitless)
\mathbf{J}_{wm}	Trans-membrane water flux vector	$L \cdot s^{-1} \cdot m^{-2}$
K	Resistance to solute diffusion	s/m

Table C.3.2.: Additional symbols for computational modelling (1 of 3)

Symbol	Definition	Units
L_{diff}	Fick diffusion length	m
L_{sheet}	Membrane sheet length	m
m	Number of modelled membrane cell rows	(unitless)
m_d^+	Draw-side salt mass output quantity matrix	mosm
m_d^-	Draw-side salt mass input quantity matrix	mosm
n	Number of modelled membrane cell columns	(unitless)
P	Cell pressure	Pa
P_0	Cell pressure at previous iteration	Pa
\mathbf{P}_0	Cell pressure vector at previous iteration	Pa
P_d	Draw-side cell pressure	Pa
\mathbf{P}_d	Draw-side cell pressure vector	Pa
\mathbf{P}_{d0}	Draw-side cell pressure vector at previous iteration	Pa
P_{dL}	Draw-side cell pressure matrix, offset in direction L	Pa
P_{dmem}	Bulk draw-side pressure	Pa
P_{dZ}	Draw-side cell pressure matrix, offset in direction Z	Pa
P_f	Feed-side cell pressure	Pa
$P_{L...B}$	Neighbouring cell pressure in direction L, R, T, B	Pa
P_{maxRO}	Bulk hydrostatic pressure over membrane element	Pa
P_{mn}	Sheet pressure matrix value at cell index, m, n	Pa
P_Z	Neighbouring cell pressure in direction Z	Pa
Q_{avRO}	Typical RO element feedwater and brine flow-rate	L/s
Q_{dZ}	Draw-side cell flow matrix, offset in direction Z	L/s
Q_{dZ}^-	Draw-side flow out-of-cell matrix, offset in direction Z	L/s
Q_{dZ}^+	Draw-side flow in-to-cell matrix, offset in direction Z	L/s
Q_{fmem}	Bulk feed-side input flow-rate	L/s
$Q_{L...B}$	Neighbouring cell flow-rate in direction L, R, T, B	L/s
Q_{wc}	Membrane cell compliance flow	L/s
\mathbf{Q}_{wc}	Membrane compliance flow vector	L/s
\mathbf{Q}_{wi}	Membrane injectate flow vector	L/s
\mathbf{Q}_{winput}	Combined membrane model forced input flow vector	L/s
Q_{wm}	Trans-membrane cell fluid flow	L/s
\mathbf{Q}_{wm}	Trans-membrane fluid flow vector	L/s
\mathbf{Q}_{wr}	Membrane recirculation flow vector	L/s
Q_{wr}	Instantaneous recirculation rate	L/s
Q_Z	Cell flow in direction Z	L/s

Table C.3.3.: Additional symbols for computational modelling (2 of 3)

Symbol	Definition	Units
R_{cell}	Cell trans-membrane flow resistance	$\text{Pa} \cdot \text{s} \cdot \text{L}^{-1}$
R_d	Draw-side cell surface flow-resistance	$\text{Pa} \cdot \text{s} \cdot \text{L}^{-1}$
R_{equiv}	Bulk equivalent longitudinal resistance	$\text{Pa} \cdot \text{s} \cdot \text{L}^{-1}$
\mathbf{R}_{struct}	Recirculation structure matrix	$\text{Pa} \cdot \text{s} \cdot \text{L}^{-1}$
\mathbf{R}_{struct}	Recirculation structure vector	$\text{Pa} \cdot \text{s} \cdot \text{L}^{-1}$
t_{CPU}	Total simulation CPU time estimate	s
t_{sim}	Total simulated time	s
\mathbf{V}_d	Draw-side cell volume vector	L
\mathbf{V}_{d0}	Draw-side cell volume vector at previous iteration	L
W_{sheet}	Membrane sheet width	m
μ_{Ri}	Membrane intrinsic resistance	$\text{Pa} \cdot \text{s} \cdot \text{m} \cdot \text{L}^{-1}$
Π_d	Draw-side cell osmotic pressure	Pa
Π_f	Feed-side cell osmotic pressure	Pa
ρ_d	Draw-side surface flow resistivity	$\text{Pa} \cdot \text{s} \cdot \text{m} \cdot \text{L}^{-1}$
ρ_f	Feed-side surface flow resistivity	$\text{Pa} \cdot \text{s} \cdot \text{m} \cdot \text{L}^{-1}$
τ_s	Simulation sample period	s
τ_{sout}	Output sample period	s

Table C.3.4.: Additional symbols for computational modelling (3 of 3)

C.4. Model parameters

Parameter	Symbol	Value	Units
Membrane hydraulic permeability ^a	A	1.56×10^{-11}	m/Pa·s
Reverse solute flux constant ^a	B	4.00×10^{-8}	m/s
Membrane structural parameter ^b	S_{me}	5.89×10^{-4}	m
Solute diffusivity ^h	D	1.35×10^{-9}	m^2/s
Adjusted mass transfer coefficient ^b	K_{ICP}	$0.18 \times 2.29 \times 10^{-6}$	$kL \cdot m^{-2} \cdot s^{-1}$
Adjusted mass transfer coefficient ^b	K_{ECP}	$0.18 \times 2.29 \times 10^{-5}$	$kL \cdot m^{-2} \cdot s^{-1}$
Membrane area ^c	A_{mem}	7.9	m^2
Membrane length ^c	L_{mem}	0.93	m
Membrane total width ^c	W_{mem}	8.49	m
Draw-side spacer thickness ^d	$2 \cdot w_d$	0.66	mm
Draw-side fluid volume fraction ^d	ϵ_d	0.9	$\frac{m^3}{m^3}$
Feed-side spacer thickness ^d	$2 \cdot w_f$	0.25	mm
Feed-side volume fraction ^d	ϵ_f	0.68	$\frac{m^3}{m^3}$
Draw-side total volume ^d	V_d	2.35	L
Feed-side total volume ^d	V_f	0.67	L
Feedwater osmolarity ^e	c_{feed0}	11 (259)	mosm/L (mg/L)
Draw-side concentrate input ^f	c_{din}	8000	mosm/L
Target conductivity ^g	σ_{target}	11.6	mS/cm
Equivalent target concentration ^g	$c_{dtarget}$	247	mosm/L
Target flow-rate ^g	$Q_{wtarget}$	484	ml/min

Values derived from these sources: ^aArias et al. (2011); ^bTiraferri et al. (2013); ^cHydranautics (2011); ^dElement autopsy; ^eSA Water (2013); ^fFresenius (2014); ^gFresenius (2007); ^h(Lynch, 1974).

Table C.4.1.: The system, membrane element and environmental parameters used to evaluate the computational model.

D. Patent document



10 October 2013

A.P.T. Patent and Trade Mark Attorneys
PO Box 222
MITCHAM SA 5062
Australia



ABN 38 113 072 755

Discovery House, Phillip ACT 2606
PO Box 200, Woden ACT 2606
Australia

P 1300 651 010
Int +61 2 6283 2999
www.ipaustralia.gov.au

Provisional Application Filing Receipt

Application Number: 2013903865

Application Name(s): FBE Pty Ltd

Your Ref: 6197

Thank you for filing a provisional patent application with IP Australia on 8 October 2013. The documents filed have been allocated application number 2013903865. Please refer to this number in any future correspondence with IP Australia.

Documents Lodged: A specification comprising:

- Description
- Drawing(s)

If the filing fee for this application has not been fully paid, an Invitation to Pay will be issued to you. Please note that filing of this application does not entitle the applicant to claim that a patent has been granted at this stage.

You are reminded that in order to claim association with this application a complete application must be filed on or before 8 October 2014. IP Australia can provide further information explaining the requirements in filing a complete application.

If you need any further information please contact 1300 651 010. Alternatively, please visit us at www.ipaustralia.gov.au.

Yours faithfully

Patent and Plant Breeder's Rights Administration

RECEIVED

17 OCT 2013

A.P.T.



Robust intellectual property rights delivered efficiently

Figure D.0.1.: Provisional patent filing receipt, 2013903865 (pg 1 of 2)

Bibliographic Details at Filing

Details for Provisional Application

Application number: 2013903865

Your Reference: 6197

Applicant Name and Address *(as it will appear on certificate/s):*

FBE Pty Ltd
Flinders DR, BEDFORD PARK, SA, 5042, Australia

Title: Dilution of a concentrate by forward osmosis

Inventors: Smith, Michael Christopher

Agent Name: A.P.T. Patent and Trade Mark Attorneys

Address for Correspondence: PO Box 222
MITCHAM SA 5062
Australia

Address for Legal Service: PO Box 222
MITCHAM SA 5062
Australia

Lapsing Date: 8 October 2014

Figure D.0.2.: Provisional patent filing receipt, 2013903865 (pg 2 of 2)

E. Ethics documents

Fieldwork for this project was carried out with ethics approval from Central Australian Human Research Ethics Committee (CAHREC: 13-13) and Flinders University's Social and Behavioural Research Ethics Committee (SBREC: 5789) with input from Yunggoendi Mande First Nations Centre.

18/04/2013

5979 SBREC - Final approval

5979 SBREC - Final approval

Human Research Ethics [human.researchethics@flinders.edu.au]

Sent: Tuesday, March 26, 2013 10:23 AM**To:** Michael Smith (smit1089@flinders.edu.au); Karen Reynolds [karen.reynolds@flinders.edu.au]; Mark Shephard [mark.shephard@flinders.edu.au]**Importance:** High

Dear Michael,

The Chair of the [Social and Behavioural Research Ethics Committee \(SBREC\)](#) at Flinders University considered your response to conditional approval out of session and your project has now been granted final ethics approval. Your ethics final approval notice can be found below.

FINAL APPROVAL NOTICE

Project No.:	<input type="text" value="5979"/>
Project Title:	<input type="text" value="Context sensitive dialysis in Indigenous Australian desert communities"/>
Principal Researcher:	<input type="text" value="Mr Michael Smith"/>
Email:	<input type="text" value="smit1089@flinders.edu.au"/>
Address:	<input type="text" value="School of Computer Science, Engineering and Mathematics"/>
Approval Date:	<input type="text" value="25 March 2013"/>
Ethics Approval Expiry Date:	<input type="text" value="30 March 2016"/>

The above proposed project has been **approved** on the basis of the information contained in the application, its attachments and the information subsequently provided with the addition of the following comment:

Additional information required following commencement of research:

1. Provision of a copy of the final ethics approval notice from the Northern Territory's Central Australian Human Research Ethics Committee *on receipt*. Please note that data collection should not commence until the researcher has received the relevant ethics committee approvals (item G1 and Conditional approval response – number 5).

RESPONSIBILITIES OF RESEARCHERS AND SUPERVISORS

<https://hloprd0111.outlook.com/owa/?ae=Item&f=IPM.Note&id=RgAAAADxBrMXWpsBQLyUpapwQ4AeBwBzrV81oValLT64dhsJRFthAAAAx#iLAABZrV81...> 1/3

Figure E.0.1.: Ethics approval from Flinders University SBREC (5789) (pg 1 of 3)

18/04/2013

5979 SBREC - Final approval

1. Participant Documentation

Please note that it is the responsibility of researchers and supervisors, in the case of student projects, to ensure that:

- all participant documents are checked for spelling, grammatical, numbering and formatting errors. The Committee does not accept any responsibility for the above mentioned errors.
- the Flinders University logo is included on all participant documentation (e.g., letters of Introduction, information Sheets, consent forms, debriefing information and questionnaires – with the exception of purchased research tools) and the current Flinders University letterhead is included in the header of all letters of introduction. The Flinders University international logo/letterhead should be used and documentation should contain international dialling codes for all telephone and fax numbers listed for all research to be conducted overseas.
- the SBREC contact details, listed below, are included in the footer of all letters of introduction and information sheets.

This research project has been approved by the Flinders University Social and Behavioural Research Ethics Committee (Project Number 'INSERT PROJECT No. here following approval'). For more information regarding ethical approval of the project the Executive Officer of the Committee can be contacted by telephone on 8201 3116, by fax on 8201 2035 or by email human.researchethics@flinders.edu.au.

2. Annual Progress / Final Reports

In order to comply with the monitoring requirements of the *National Statement on Ethical Conduct in Human Research (March 2007)* an annual progress report must be submitted each year on the **25 March** (approval anniversary date) for the duration of the ethics approval using the [annual progress / final report pro forma](#). Please retain this notice for reference when completing annual progress or final reports.

If the project is completed *before* ethics approval has expired please ensure a final report is submitted immediately. If ethics approval for your project expires please submit either (1) a final report; or (2) an extension of time request and an annual report.

Your first report is due on **25 March 2014** or on completion of the project, whichever is the earliest.

3. Modifications to Project

Modifications to the project must not proceed until approval has been obtained from the Ethics Committee. Such matters include:

- proposed changes to the research protocol;
- proposed changes to participant recruitment methods;
- amendments to participant documentation and/or research tools;
- change of project title;
- extension of ethics approval expiry date; and
- changes to the research team (addition, removals, supervisor changes).

To notify the Committee of any proposed modifications to the project please submit a [Modification Request Form](#) to the [Executive Officer](#). Please note that extension of time requests should be submitted prior to the Ethics Approval Expiry Date listed on this notice.

<https://hikprd0111.outlook.com/owa/?ae=Item&f=IPM.Note&id=RgAAAADxBrMXWpsBQLyUpapwQ4AeBwBzrV81oValLT64dhsJRFthuAAAxiLAABZrV81...> 2/3

Figure E.0.2.: Ethics approval from Flinders University SBREC (5789) (pg 2 of 3)

18/04/2013

5979 SBREC - Final approval

Change of Contact Details

Please ensure that you notify the Committee if either your mailing or email address changes to ensure that correspondence relating to this project can be sent to you. A modification request is not required to change your contact details.

4. Adverse Events and/or Complaints

Researchers should advise the Executive Officer of the Ethics Committee on 08 8201-3116 or human.researchethics@flinders.edu.au immediately if:

- any complaints regarding the research are received;
- a serious or unexpected adverse event occurs that affects participants;
- an unforeseen event occurs that may affect the ethical acceptability of the project.

Andrea Fiegert
Executive Officer
Social and Behavioural Research Ethics Committee

c.c Prof Karen Reynolds
Mr Mark Shephard

Andrea Fiegert

Executive Officer, Social and Behavioural Research Ethics Committee

Research Services Office | Union Building Basement

Flinders University

Sturt Road, Bedford Park | South Australia | 5042

GPO Box 2100 | Adelaide SA 5001

P: +61 8 8201-3116 | F: +61 8 8201-2035 | Web: [Social and Behavioural Research Ethics Committee](#)

CRICOS Registered Provider: The Flinders University of South Australia | CRICOS Provider Number 00114A

This email and attachments may be confidential. If you are not the intended recipient,

please inform the sender by reply email and delete all copies of this message.

<https://hloprd01111.outlook.com/owa/?ae=Item&f=IPM.Note&id=RgAAAADxBrMXWpsBQLyUpapwQ4AeBwBZrV81oValLT64dhsJRFthAAAAx#iLAABZrV81...> 3/3

Figure E.0.3.: Ethics approval from Flinders University SBREC (5789) (pg 3 of 3)

CENTRAL AUSTRALIAN HUMAN RESEARCH ETHICS COMMITTEE
Centre for Remote Health
PO Box 4066 Alice Springs NT 0871
Ph: (08) 8951 4700 Fax: (08) 8951 4777
Email: cahrec@flinders.edu.au

Mr Michael Smith
Flinders University
Rm 3E-124 Flinders Medical Centre
Flinders Dr
Bedford Pk SA 5042

3rd April 2013

Our Ref: HREC-13-131

Dear Mr Smith

RE: Ethics Application – Approval

The Central Australian Human Research Ethics Committee (CAHREC) Chair has considered your response to the Committee's request for further information about your research project '**Context sensitive dialysis in Indigenous Australian desert communities**'.

The Chair agreed that this project now meets the requirements of the National Statement on Ethical Conduct in Human Research.

The Chair decided to **grant approval** for your project to proceed.

The period for which approval has been given is from the date of this letter until the **31st December 2015**. If you do not complete the research within the projected time please request an extension from CAHREC.

Ethics Approval is contingent upon the submission of an annual Progress Report and a Final Report upon completion of the project. It is your responsibility to ensure you provide these reports. Please make a note of the following dates as failure to submit reports in a timely manner will result in your Ethics Approval lapsing.

Your reports are due on:

3rd April 2014

3rd April 2015

31st December 2015

Copies of the report form can be downloaded from the CAHREC website.

All the best with your research project.

Yours sincerely

Chris Schwarz
Secretariat Support
Central Australian Human Research Ethics Committee

Figure E.0.4.: Ethics approval from CAHREC (13-13) (pg 1 of 1)

F. Fieldwork documents



**This is information about the
desert dialysis technology project**

Supervisor:
Professor Karen Reynolds

School of Computer Science, Engineering
and Mathematics
Faculty of Science and Engineering
Room 453 Engineering Building
Flinders University
Adelaide SA 5001
Tel: +61 8 8201 5190
Fax: +61 8 8201 2904
karen.reynolds@flinders.edu.au

To whom it may concern,

This letter is to introduce Mr Michael Smith who is a PhD student at the school of Computer Science, Engineering and Mathematics, in the Faculty of Science and Engineering at Flinders University. He will produce his student card, which carries a photograph, as proof of identity.

Michael is undertaking social research leading to the development of dialysis technology that is better suited for use in remote Aboriginal desert communities. His main focus is on how people use and think about dialysis technology and services in remote Aboriginal desert communities. He will be observing the use of existing dialysis technology and discussing its use and impacts with interested people. These observations and conversations will later be analysed and presented in a thesis or other publications.

Michael would be most grateful if you would agree to participate in an interview or focus group discussion, or allow your interactions with dialysis technology to be observed for a short time. Focus groups and interviews may take 30 mins of your time but may be shortened or extended if you prefer.

Participation is voluntary, and you may choose to withdraw your participation or comments at any time.

Any comments or opinions that you express will be kept confidential, however *you should be aware that others may be able to guess about who you are based on information that you share*. Conversations from any focus group or interview will be digitally recorded and transcribed. All identifying information will be removed from the transcript. The transcript will be available for you to check if you wish. Once the transcribed data is analysed, original recordings and transcripts will be destroyed. Consent forms will be kept securely for five years.

An information sheet and a consent form are available with further details. For the location of the next focus group discussion, or if you have any other questions or enquiries, you are welcome to contact Mr Smith or myself using the contact details above.

Regards,

.....
Professor Karen Reynolds
Supervisor for Phd candidate Michael Smith

This research project has been approved by the Flinders University Social and Behavioural Research Ethics Committee (Project Number 5979) and by the Central Australian Human Research Ethics Committee (HREC-13-131). For more information regarding ethical approval of the project the Executive Officer of the SBREC Committee can be contacted by telephone on 8201 3116, by fax on 08 8201 2035 or by email human_researchethics@flinders.edu.au. The Executive Officer of the CAHREC committee can be contacted by telephone on 08 8951 4700, by fax on 08 8951 4777 or by email at cahrec@flinders.edu.au

Figure F.0.1.: Qualitative research documents - *Letter of introduction* (pg 1 of 1.)



Ms Sarah Brown
CEO,
**Western Desert Nganampa
Walytja Palyantjaku Tjutaku
Aboriginal Corporation**
PO Box 5060
Alice Springs, NT, 0871
ph: 0448685610
Fax: 08 89536444
Email: sarah@wdnwpt.com.au

31/1/13

TO WHOM IT MAY CONCERN

This document represents a letter of support for the research project being formulated by Mr Michael Smith, PhD candidate at Flinders University. In consultation with us, Michael has developed a proposal to investigate dialysis technology in remote areas of Central Australia.

Western Desert Nganampa Walytja Palyantjaku Tjutaku Aboriginal Corporation (WDNWPT) is a community controlled health service.

The significance of Michael's project

As the only non government provider of dialysis services in the Northern Territory, WDNWPT has made ground breaking developments in the provision of culturally and clinically safe dialysis in remote areas. We now have been dialysing for eight years in a number of challenging settings. As the number of people suffering End Stage Renal Failure increases and survival rates improve, more communities and families are coming to us asking for assistance to set up their own units.

Poor water quality and quantity, intermittent power sources, limited community infrastructure, remote locations, road quality and extremes in environmental conditions all make dialysis in our region more challenging.

We would welcome the opportunity to work with Michael to reflect on the lessons learnt so far and to creatively come up with solutions which will have implications across remote Australia and indeed perhaps to home care settings.

We have known Michael for a number of years now. Our Directors are confident that we can work together to do this important work. Michael will be mentored and supported by our Directors who are elders and leaders in their communities. He will have access to communities through them and will of course be supported by our staff. As CEO of the organisation I will have the ultimate responsibility of ensuring that Michael is able to complete his project in a culturally respectful way and that his work is valued and used. Research tools involving clients will be developed with clients and directors. We expect that they will be approved by the Executive before they are used.

The WDNWPT Story

In the 1990's community members from Kiwirrkurra, Mt Liebig and Kintore were already talking about the difficulties for communities and families of an increasing number of *Yanangu* being forced to move to Alice Springs for renal dialysis treatment. They were concerned about these people missing country and family, not being able to do what they should be doing out in their communities and on country-teaching their children and grandchildren.

Figure F.0.2.: Qualitative research documents - *Letter of support* (pg 1 of 4)

Senior Kintore community leader Mr Zimran, had started dialysis and understood, through first hand experience, the challenges and sadness facing renal dialysis patients as a result of dislocation and the consequent loss of cultural engagement and connection to family and country. He understood the enormous implications of this phenomenon for cultural continuity and well-being. Although kidney disease is now expanding to affect younger community members, the largest proportion of those with end-stage renal failure tend to be in their late forties and beyond. This group possesses the richest understanding and knowledge of language and traditional culture and is responsible for transferring that knowledge to younger generations, those “coming up behind”. Their permanent removal from their communities fractures this process and creates significant stress for individuals who are unable to meet their cultural obligations and feel a tremendous sense of loneliness and despair.

Apart from the severe dislocation suffered by individuals who face homelessness, loneliness and the shame of living on other people’s traditional country, this group recognized the terrible loss to their own community’s pool of knowledge of family (*walytja*), country (*ngura*), stories (*tjukurrpa*) and ceremonies (*tulku*). These elements are the determinants of *Yaṅangu* well-being and the obligation to know (*kulintjaku*) and learn (*nintintjaku*) is the very basis of *Yaṅangu* Law.

Mr Zimran and other senior community members started talking to Papunya Tula and Sothebys about getting dialysis machines out in Kintore. In order to raise funds, a unique partnership was formed between *Yaṅangu*, sympathetic members of the Aboriginal Art industry and local politics, and community controlled health services. Papunya Tula Artists Pty Ltd. then commissioned four remarkable collaborative paintings by senior Pintupi men and women in Kintore and Kiwirrkurra. These were auctioned by Sothebys along with a range of donated works at the Art Gallery of NSW in Sydney, November 2000.

The auction raised over AUS\$1 million and was used to establish our organisation, The Western Desert Nganampa Walytja Palyantjaku Tjutaku Aboriginal Corp (WDNWPT). This name loosely translates as “*Making all our families well*”, in recognition of *Yaṅangu* desire to mitigate the extent to which kidney disease threatens the preservation of *Walytja* or extended familial relatedness at a fundamental level.

Figure F.0.3.: Qualitative research documents - *Letter of support* (pg 2 of 4)

WDNWPT Services for *Yanangu* Families

In April 2004, the organisation opened the first remote renal dialysis clinic in Central Australia at Kintore. Since then we have been returning people home for dialysis and providing alternative dialysis facilities and patient support in Alice Springs from a converted suburban house. Patient support includes advocacy, housing, linking clients with other services, case management for high needs clients, strong partnerships with organisations and agencies .

As the project has grown we have added more services. We currently have a GP clinic two mornings each week, podiatry, exercise physiology, chinese medicine, ngangkari. We are also proud of the opportunities we have created in Indigenous employment. Fifty percent of our current employees are indigenous. We have a social enterprise which incorporates the making of bush balms and remedies and a catering business.

The main goal of WDNWPT is hence to significantly improve the quality of life of *Yanangu* on dialysis by supporting them holistically in Alice Springs through our Social Support Program and by providing them with the opportunity to return home as frequently as possible, for short as well as extended stays. We also encourage people to learn self care dialysis to return home permanently.

A thorough and detailed evaluation of this program released in 2006, demonstrated its success and cost-effectiveness and has enabled WDNWPT to negotiate successfully for Government funding.

In 2010 WDNWPT opened a dialysis facility in Yuendumu and one in Ntaria. Both facilities are staffed with nurses and offer dialysis six days per week. , Our 'Purple Truck' was launched twelve months ago with financial support from Medicines Australia. It provides mobile dialysis to a number of remote communities. In February we will fit a second dialysis machine in this vehicle. In March our two chair unit will open in Lajamanu, 1300kms North West of Alice Springs. We are currently working on plans for permanent dialysis in Warburton and Kiwirrkurra in WA. WDNWPT now supports over 80 dialysis patients and their families.



Current service provision

Figure F.0.4.: Qualitative research documents - *Letter of support* (pg 3 of 4)

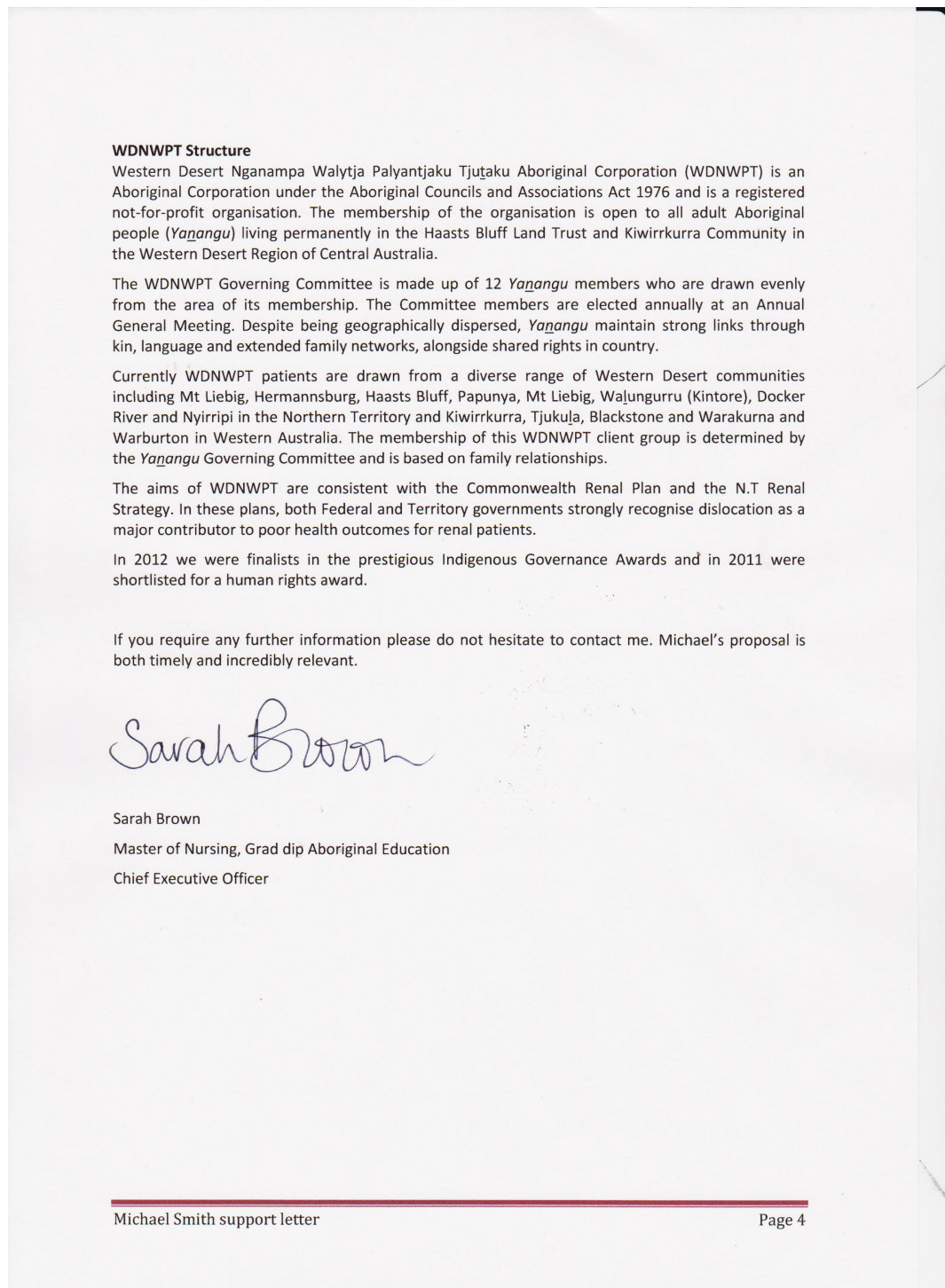


Figure F.0.5.: Qualitative research documents - *Letter of support* (pg 4 of 4)



Mr Michael C. Smith
School of Computer Science, Engineering
and Mathematics
Faculty of Science and Engineering
Room 1012, Physical Sciences building
Flinders University
Adelaide SA 5001
Tel: +61 8 8204 3194
Fax: +61 8 8204 5840
Smit1089@flinders.edu.au

**OBSERVATION OF ACTIVITY
COMING SOON TO THIS COMMUNITY**

A researcher will be visiting your community/workplace soon to talk about dialysis technology and services.

During the visit, the researcher will be observing interactions between people and dialysis equipment. There will also be an opportunity to discuss your own ideas about dialysis technology and services. You can join a focus-group discussion or have a private, one-on-one interview.

You are welcome to participate or withdraw at any time. Your responses will be kept confidential. If you do not wish to be observed, please let the researcher know and your activity will not be recorded.

For more information, or if you would like to participate, please contact:

Michael C. Smith
(08) 8204 3194
School of Computer Science, Engineering and Mathematics
Flinders University, South Australia

You can also contact:
Western Desert Nganampa Walytja Palyantjaku Tjutaku
Aboriginal Corporation (WDNWPT)
(08) 8953 6444

This research project has been approved by the Flinders University Social and Behavioural Research Ethics Committee (Project Number 5979) and by the Central Australian Human Research Ethics Committee (HREC-13-131). For more information regarding ethical approval of the project the Executive Officer of the SBREC Committee can be contacted by telephone on 8201 3116, by fax on 08 8201 2035 or by email human_researchethics@flinders.edu.au. The Executive Officer of the CAHREC committee can be contacted by telephone on 08 8951 4700, by fax on 08 8951 4777 or by email at cahrec@flinders.edu.au

inspiring
achievement

Figure F.0.6.: Qualitative research documents - *Observation Poster* (pg 1 of 1)



Mr Michael C. Smith
 School of Computer Science, Engineering
 and Mathematics
 Faculty of Science and Engineering
 Room 1012, Physical Sciences building
 Flinders University
 Adelaide SA 5001
 Tel: +61 8 8204 3194
 Fax: +61 8 8204 5940
 Smit1089@flinders.edu.au

This is for you to keep

INFORMATION SHEET for OBSERVATION of PARTICIPANTS

Title: 'Context sensitive dialysis in Indigenous Australian desert communities'

Investigator:

Mr Michael C. Smith
 School of Computer Science, Engineering and Mathematics
 Faculty of Science and Engineering
 Flinders University
 Tel: +61 8 8204 3194
Smit1089@flinders.edu.au

Description of the study:

This study is part of the project entitled, '*Context sensitive dialysis in Indigenous Australian desert communities*'. This project will investigate the use of dialysis technology and the needs of user communities in urban and remote settings. This project is supported by Flinders University's School of Computer Science, Engineering and Mathematics.

Purpose of the study:

This project aims to find out:

How people use and interact with existing dialysis technology

- How users and others feel about the dialysis technology in their communities
- How the technology can be made more suitable to use in remote Aboriginal communities.

This information will be used to inform the development of new, commercially available dialysis technology, optimised for desert community use. *This study does not aim to collect intellectual property or culturally sensitive information from community members.*

What will be happening?

A researcher will be spending some time observing the interactions between people and dialysis equipment. Activity that relates to use of and attitudes towards the equipment will be recorded. No personal details will be recorded and any data will be kept confidential. Participation in this research is voluntary.

inspiring
achievement

Figure F.0.7.: Qualitative research documents - *Observation information sheet*
 (pg 1 of 2)

What benefit will I gain from being involved in this study?

During the time of the study, the lead researcher (Mr Smith) will also be providing additional dialysis technical support to help the service run smoothly. This extra support will finish at the end of the study time. The observation of your activity will help improve the design and delivery of future dialysis services. We are very keen to help deliver a service that is as good as possible.

Will I be identifiable by being involved in this study?

We do not need your name and you will be anonymous. Once records have been typed-up and saved as a file, any notes will then be destroyed. Any identifying information will be removed and the typed-up file stored on a password protected computer that only the coordinator (Mr Michael Smith) will have access to. Your activity will not be linked directly to you.

Are there any risks or discomforts if I am involved?

The investigator anticipates few risks from your involvement in this study, however, *you should be aware that others may be able to guess about your participation based on observations of your interactions.* If you have any concerns regarding anticipated or actual risks or discomforts, please discuss them with the investigator.

How do I agree to participate?

Participation is voluntary. You may answer are free to withdraw from being observed at any time without effect or consequences. A consent form accompanies this information sheet. If you agree to participate please read and sign the form return it to the investigator (Mr Smith). These forms will be stored for five years, then destroyed. You may also declare that you do not wish to be observed if you prefer.

How will I receive feedback?

Outcomes from the project will be summarised and given to you by the investigator if you would like to see them. After notes on the observations have been analysed they will be destroyed.

Thank you for taking the time to read this information sheet and we hope that you will accept our invitation to be involved.

This research project has been approved by the Flinders University Social and Behavioural Research Ethics Committee (Project Number 5979) and by the Central Australian Human Research Ethics Committee (HREC-13-131). For more information regarding ethical approval of the project the Executive Officer of the SBREC Committee can be contacted by telephone on 8201 3116, by fax on 08 8201 2035 or by email human_researchethics@flinders.edu.au. The Executive Officer of the CAHREC committee can be contacted by telephone on 08 8951 4700, by fax on 08 8951 4777 or by email at cahrec@flinders.edu.au

Figure F.0.8.: Qualitative research documents - *Observation information sheet*
(pg 2 of 2)



Mr Michael C. Smith
 School of Computer Science, Engineering
 and Mathematics
 Faculty of Science and Engineering
 Room 1012, Physical Sciences building
 Flinders University
 Adelaide SA 5001
 Tel: +61 8 8204 3194
 Fax: +61 8 8204 5940
 Smit1089@flinders.edu.au

This is for you to keep

INFORMATION SHEET for INTERVIEW PARTICIPANTS

Title: 'Context sensitive dialysis in Indigenous Australian desert communities'

Investigator:

Mr Michael C. Smith
 School of Computer Science, Engineering and Mathematics
 Faculty of Science and Engineering
 Flinders University
 Tel: +61 8 8204 3194
Smit1089@flinders.edu.au

Description of the study:

This study is part of the project entitled, '*Context sensitive dialysis in Indigenous Australian desert communities*'. This project will investigate the use of dialysis technology and the needs of user communities in urban and remote settings. This project is supported by Flinders University's School of Computer Science, Engineering and Mathematics.

Purpose of the study:

This project aims to find out:

- How people use and interact with existing dialysis technology
- How users and others feel about the dialysis technology in their communities
- How the technology can be made more suitable to use in remote Aboriginal communities.

This information will be used to inform the development of new, commercially available dialysis technology, optimised for desert community use. *This study does not aim to collect intellectual property or culturally sensitive information from community members.*

What will I be asked to do?

You are invited to attend a one-on-one interview with a student researcher who will ask you a few questions about your views on dialysis technology. The interview will take about 30 minutes. The interview will be recorded using a digital voice recorder to help with handling the results. Once recorded, the interview will be transcribed (typed-up) and stored as a computer file, then destroyed once the results have been finalised. Participation in this research is voluntary.

inspiring
achievement

Figure F.0.9.: Qualitative research documents - *Interview information sheet*
 (pg 1 of 2)

Can I have an interpreter assist with this interview?

Yes. If you would prefer to use a language other than English, please contact the lead investigator (Mr Michael Smith) and specify what language and whether you would prefer a male or female interpreter to be present.

What benefit will I gain from being involved in this study?

During the time of the study, the lead researcher (Mr Smith) will also be providing additional dialysis technical support to help the service run smoothly. This extra support will finish at the end of the study time. We intend that the sharing of your experiences will also help improve the design and delivery of future dialysis services.

Will I be identifiable by being involved in this study?

We do not need your name and you will be anonymous. Once the interview has been typed-up and saved as a file, the voice file will then be destroyed. Any identifying information will be removed and the typed-up file stored on a password protected computer that only the coordinator (Mr Michael Smith) will have access to. Your comments will not be linked directly to you.

Are there any risks or discomforts if I am involved?

The investigator anticipates few risks from your involvement in this study; however, *you should be warned that others may become aware of your participation*. If you have any concerns regarding anticipated or actual risks or discomforts, please discuss them with the investigator.

How do I agree to participate?

Participation is voluntary. You may answer 'no comment' or refuse to answer any questions and you are free to withdraw from the discussion at any time without effect or consequences. A consent form accompanies this information sheet. If you agree to participate please read and sign the form return it to the investigator (Mr Smith). These forms will be stored for five years, then destroyed.

How will I receive feedback?

Outcomes from the project will be summarised and given to you by the investigator if you would like to see them. You may also see a copy of the transcript to see if you are still happy for your comments to be used. After the transcripts have been analysed, all text and recordings will be destroyed.

Thank you for taking the time to read this information sheet and we hope that you will accept our invitation to be involved.

This research project has been approved by the Flinders University Social and Behavioural Research Ethics Committee (Project Number 5979) and by the Central Australian Human Research Ethics Committee (HREC-13-131). For more information regarding ethical approval of the project the Executive Officer of the SBREC Committee can be contacted by telephone on 8201 3116, by fax on 08 8201 2035 or by email human_researchethics@flinders.edu.au. The Executive Officer of the CAHREC committee can be contacted by telephone on 08 8951 4700, by fax on 08 8951 4777 or by email at cahrec@flinders.edu.au

Figure F.0.10.: Qualitative research documents - *Interview information sheet*
(pg 2 of 2)



Lead Researcher:
Mr Michael C. Smith

Supervisor:
Professor Karen Reynolds

School of Computer Science, Engineering
and Mathematics
Faculty of Science and Engineering
Room 1012, Physical Sciences building

Flinders University
Adelaide SA 5001

Tel: +61 8 8204 3194
Fax: +61 8 8204 5840
Smit1089@flinders.edu.au

**Focus group and interviews – Group 1: Dialysis service
providers and administrators
HREC-13-131/SBREC 5979**

Discussion points

Basics

Tell us a little about this service. Are things going well? Why?
What is happening in this community at the moment?
What are the greatest challenges for Aboriginal dialysis in the bush?

Demand for resources

When there are competing demands for resources, what tends to be prioritised?
Who makes those decisions?
What proportion of resources are consumed by equipment, maintenance etc?

Water, energy, consumables

Do you pay for all of these or are they subsidised or provided by others?
Is there any pressure to prioritise one resource over another?
How do local communities feel about the extra demand for resources presented by having a dialysis service in-community?

Infrastructure and maintenance

How do you find the maintenance needs for dialysis equipment?

- Frequency of failures
- Downtime, repairs
- Maintenance cost
- Backups, parts, technical support

In what ways do you feel the technology could be improved to facilitate more and better dialysis services in the bush?

- Cheaper? Lower maintenance? Better tech. support?

Nursing and staff recruitment

How do you recruit and keep dialysis nurses and support staff?
What are the biggest staffing issues for dialysis services?

Community perception

How do communities feel about dialysis services?
Is there opposition from local clinics?
What about this particular community?

Patient perception

Has dialysis in-country been well received?
Is there squabbling over the privilege of using the few in-country dialysis chairs?

Figure F.0.11.: Qualitative research documents - *Interview question guide example*
(pg 1 of 2)



Mobile dialysis

I think mobile dialysis is very clever. When I talk to people about the dialysis truck, the first idea is that the patients stay in-country and the truck travels to visit them. This seems impractical – instead, the patients stay in-town and travel with the truck to visit communities. Is this model working?

What are the limitations of working in a truck as opposed to in a clinic?

What are the advantages of mobile dialysis?

How does it compare to clinic-services in terms of demand on resources? Quality of service?

The future of dialysis services for Aboriginal Australians

I understand that the rate of kidney disease is growing. This will mean more demand for your services in time. What do you see in the future of dialysis in the bush?

Figure F.0.12.: Qualitative research documents - *Interview question guide example*
(pg 2 of 2)

G. QRM scenario and model fragments

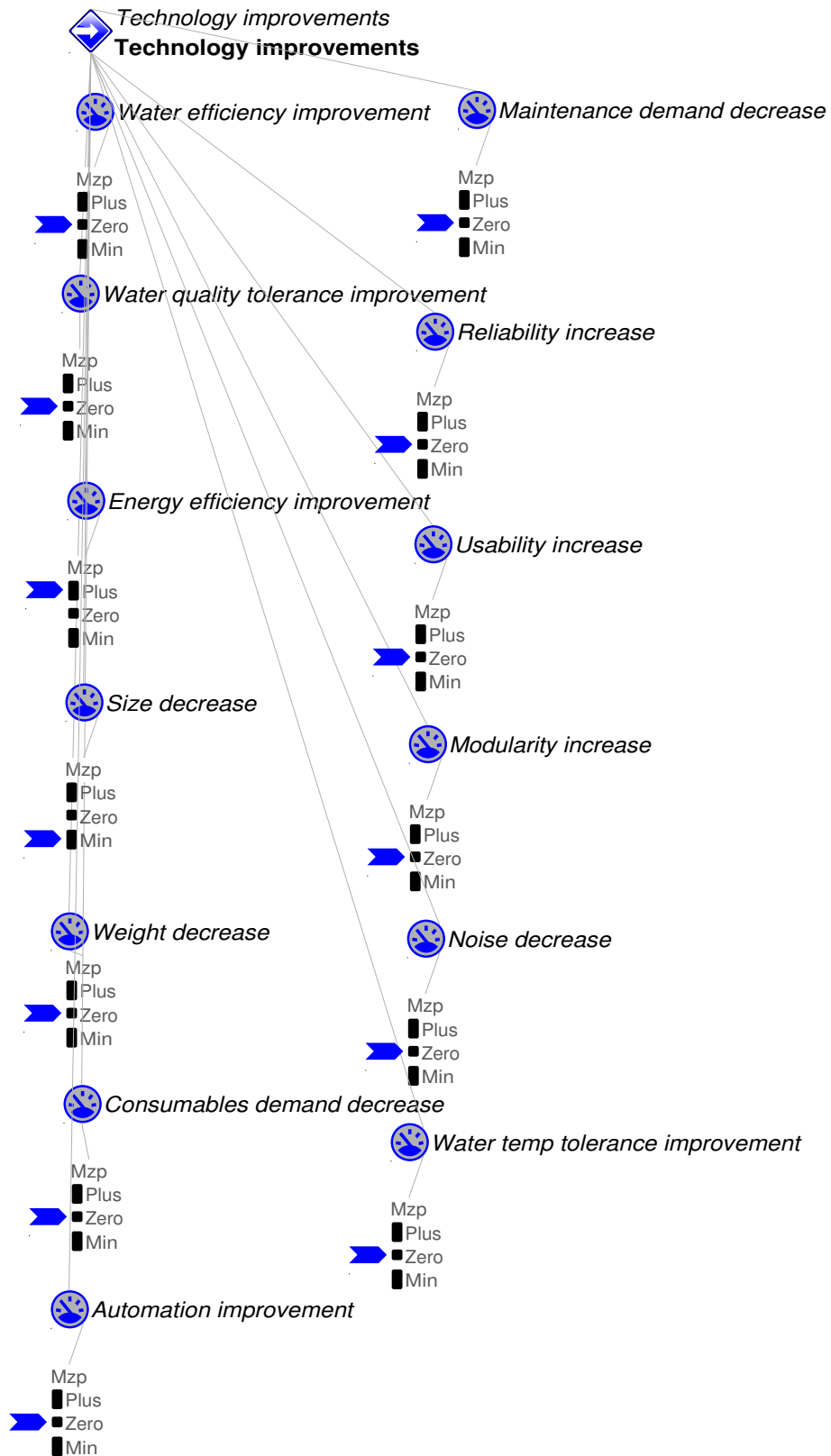


Figure G.0.1.: Desert dialysis *Garp3* scenario

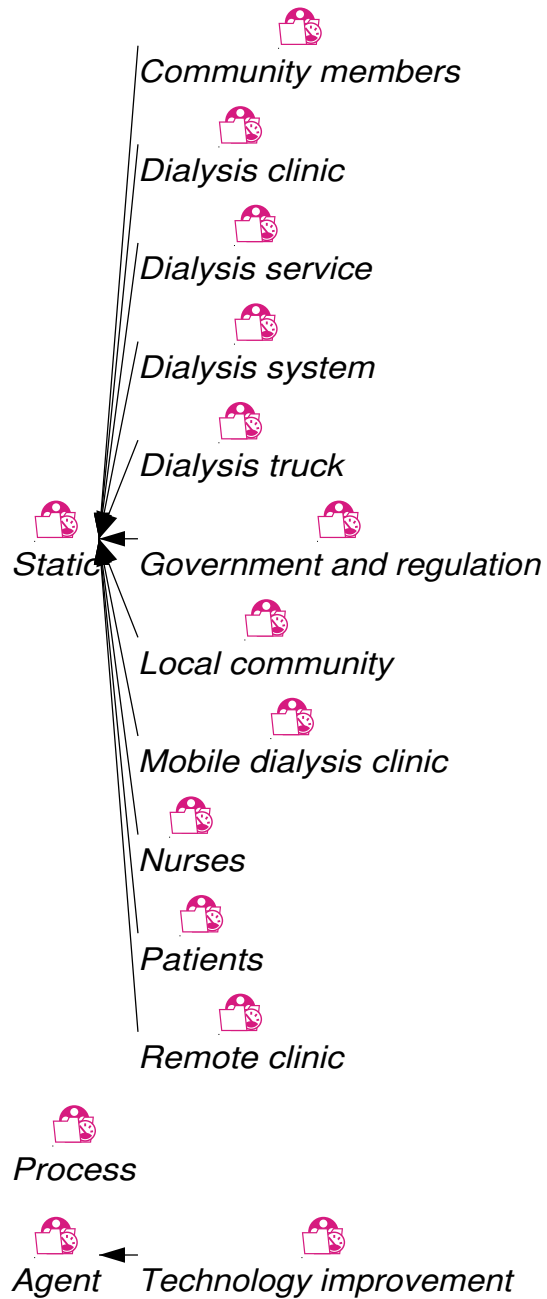


Figure G.0.2.: Desert dialysis *Garp3* model fragment hierarchy

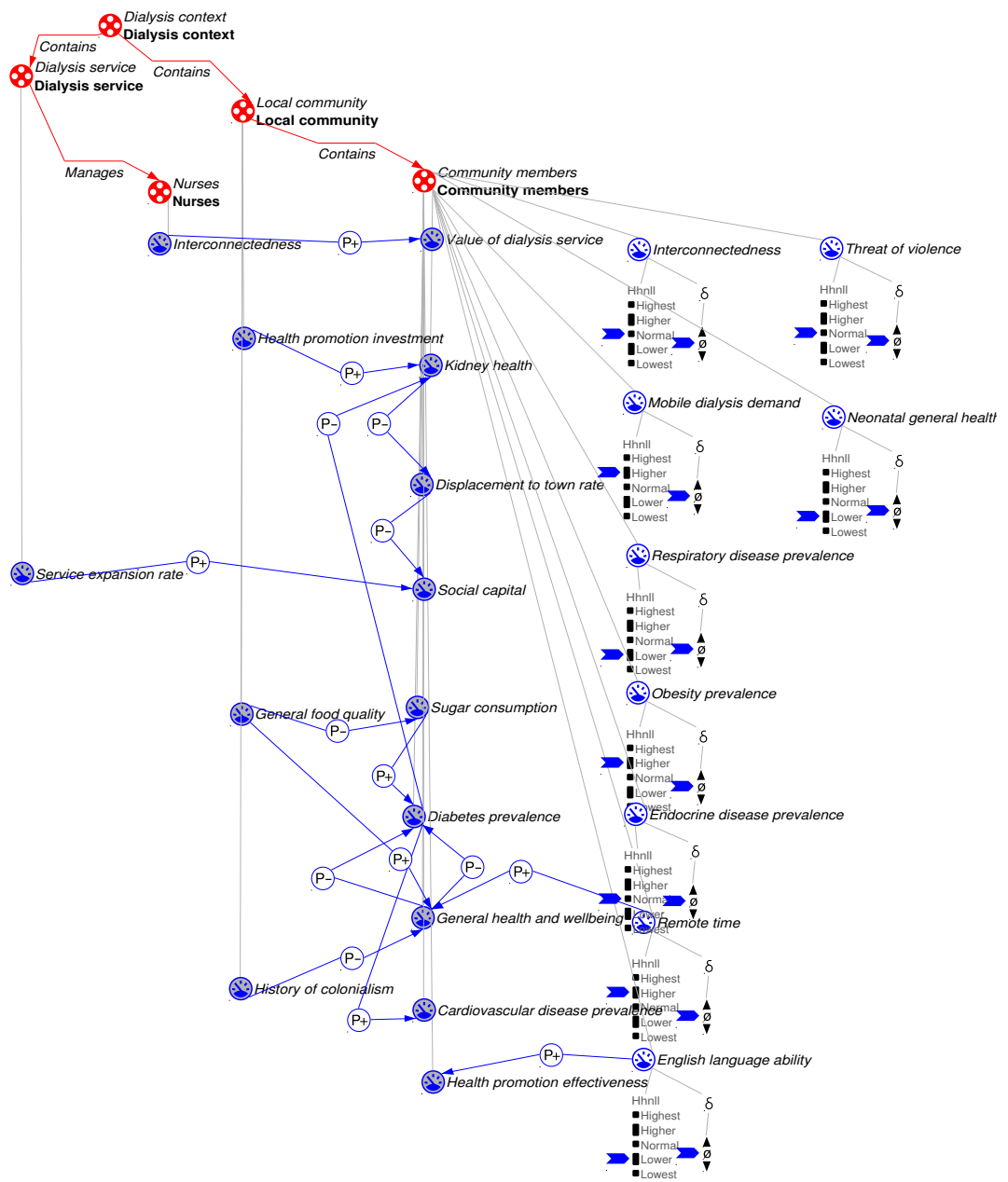


Figure G.0.3.: Community members *Garp3* model fragment

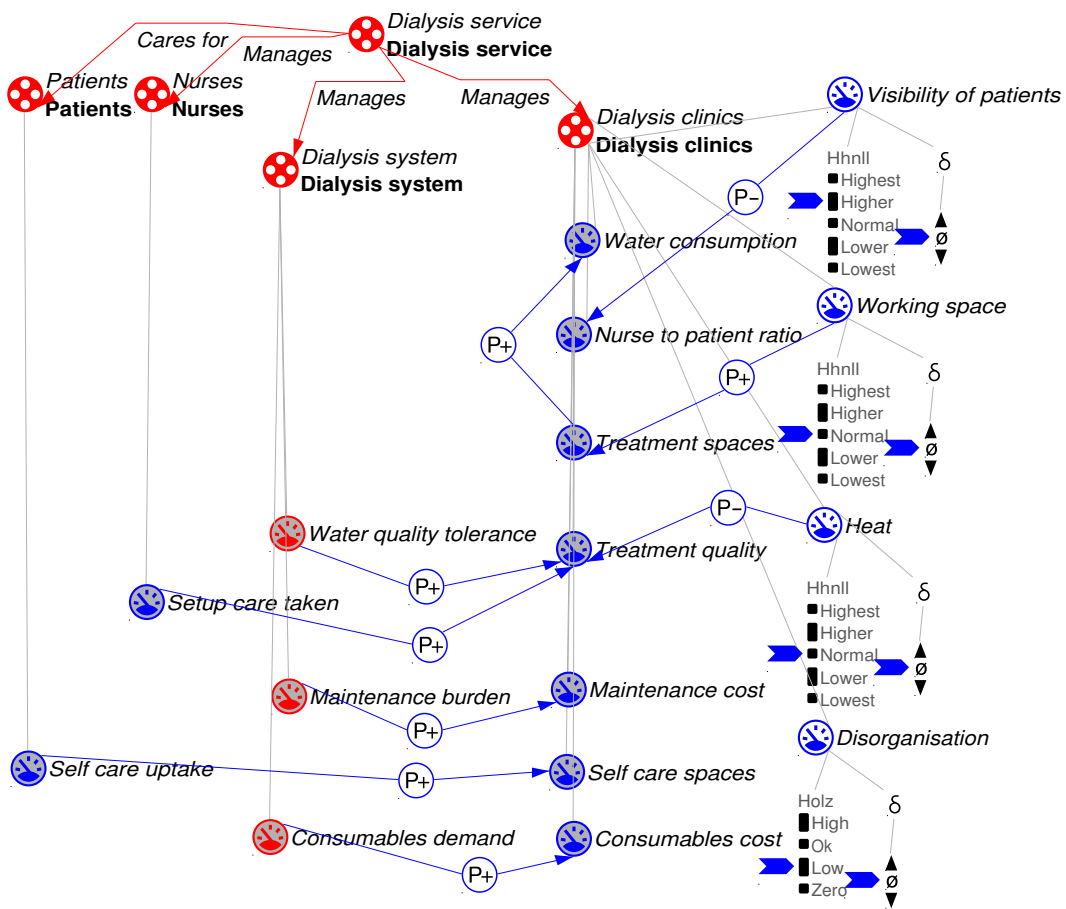


Figure G.0.4.: Dialysis clinics *Garp3* model fragment

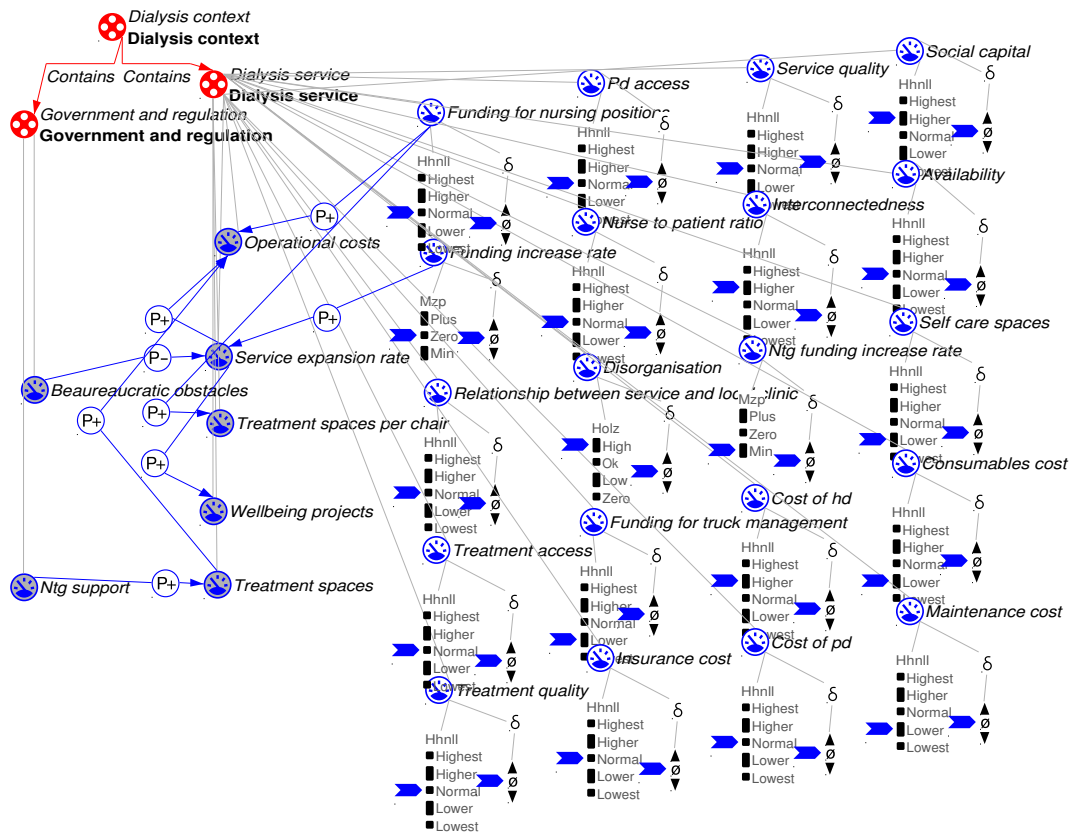


Figure G.0.5.: Dialysis service *Garp3* model fragment

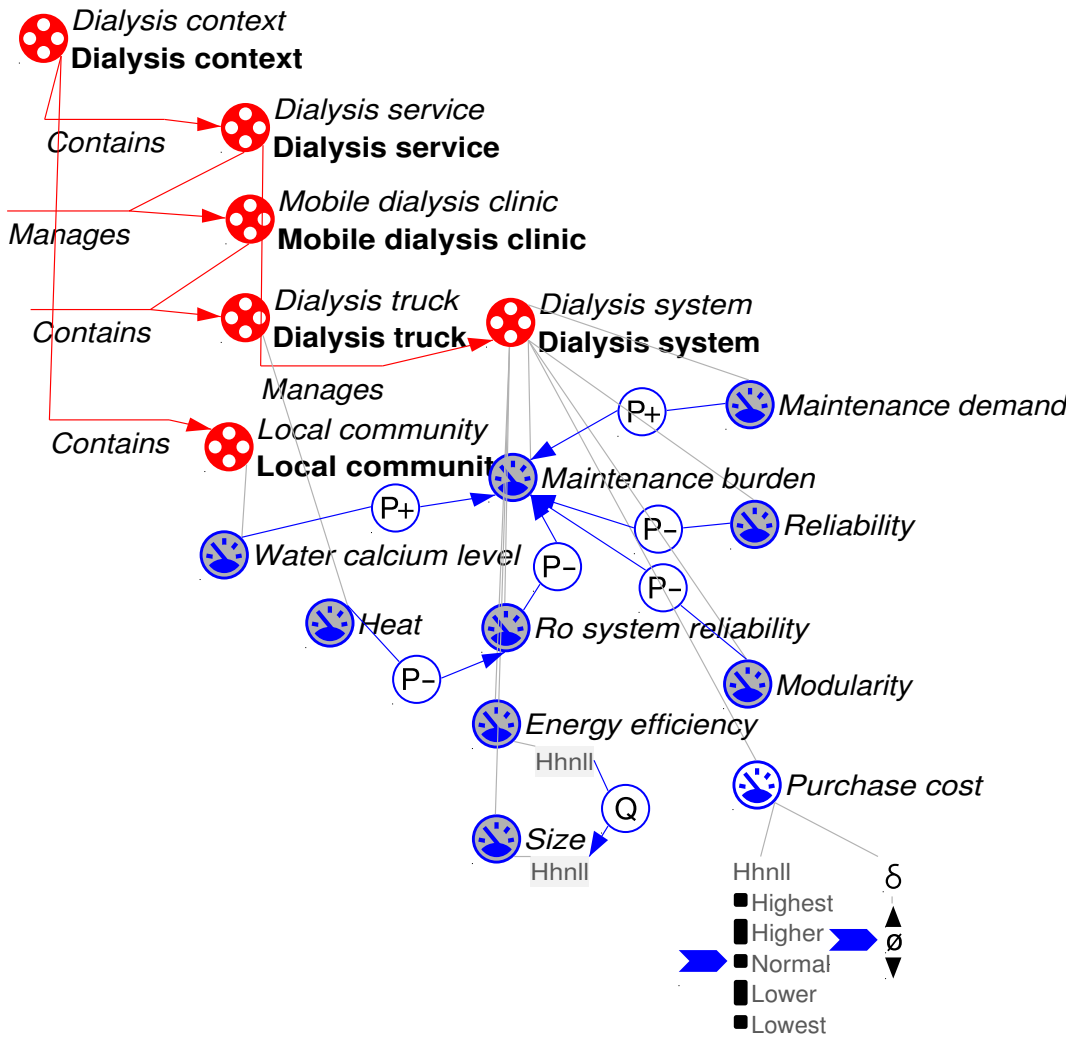


Figure G.0.6.: Dialysis system *Garp3* model fragment

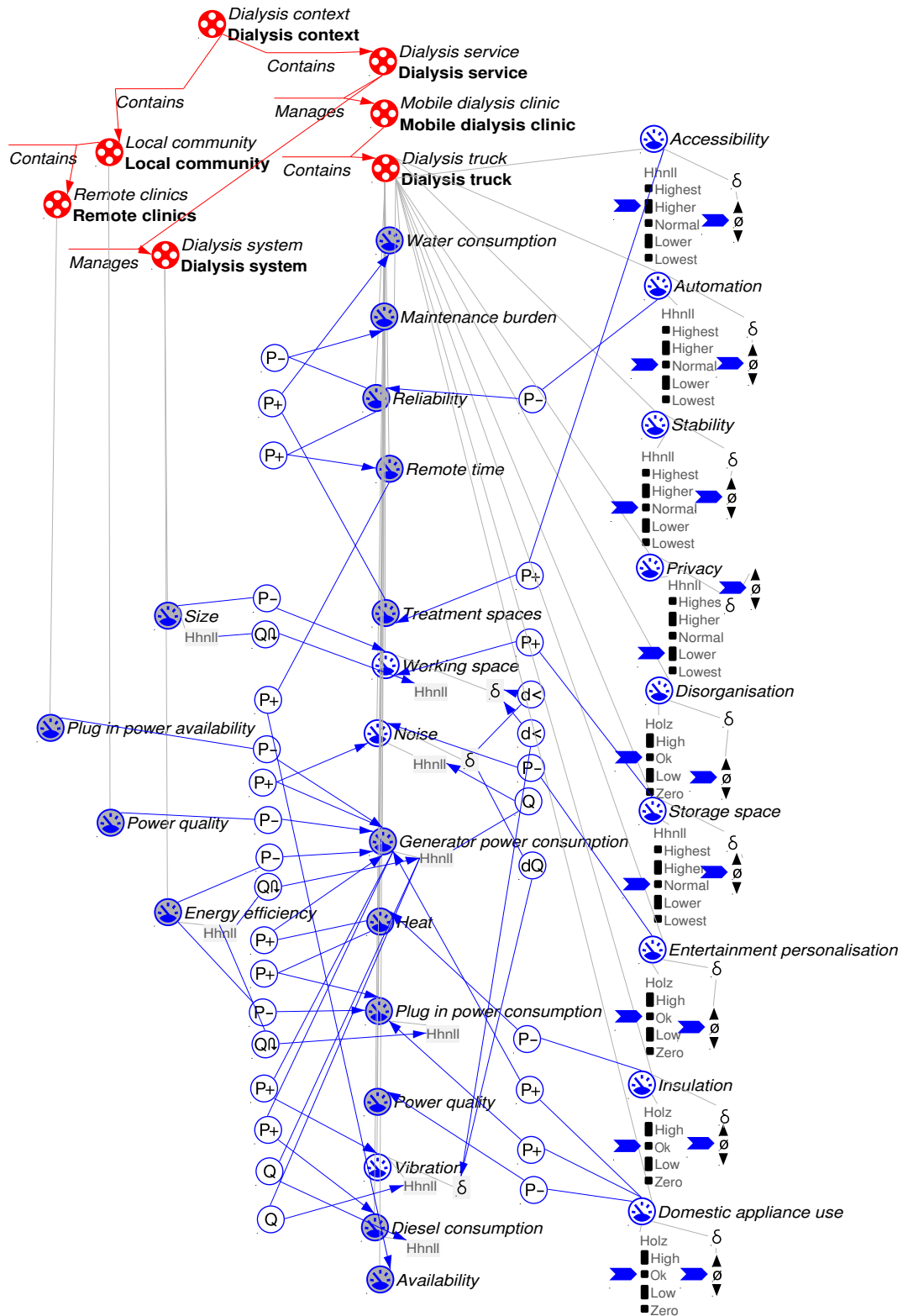


Figure G.0.7.: Dialysis truck *Garp3* model fragment

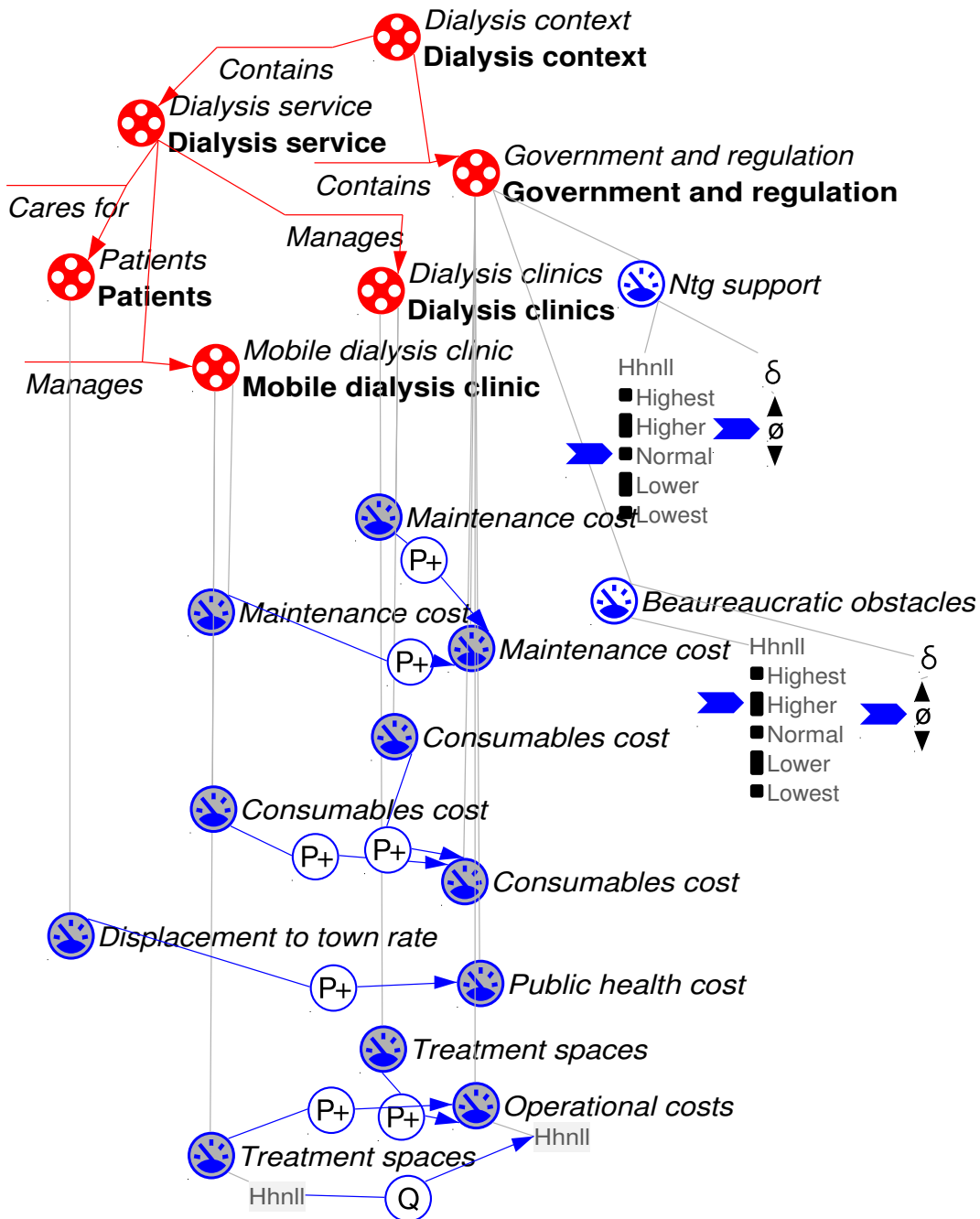


Figure G.0.8.: Government and regulation *Garp3* model fragment

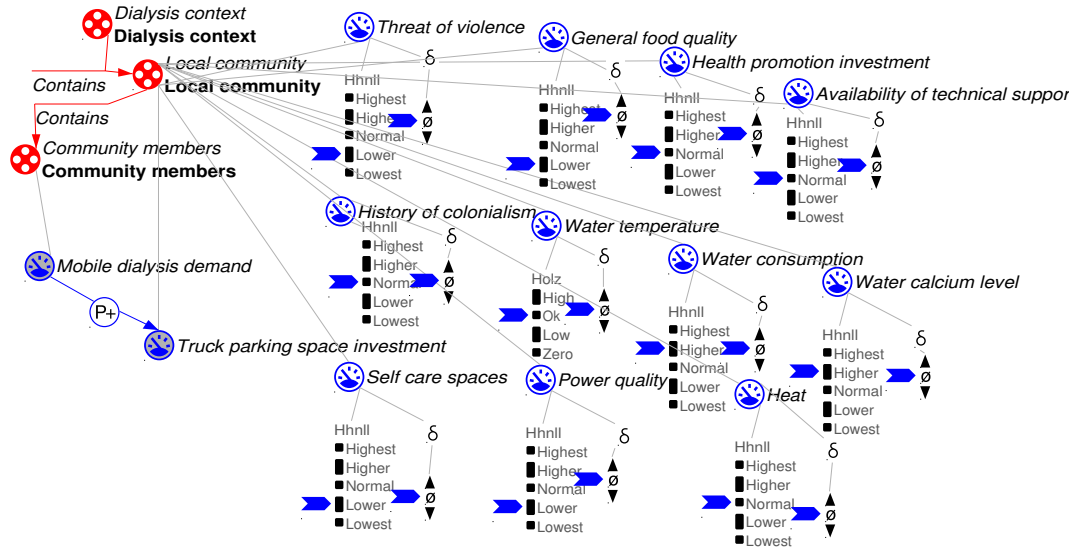


Figure G.0.9.: Local community *Garp3* model fragment

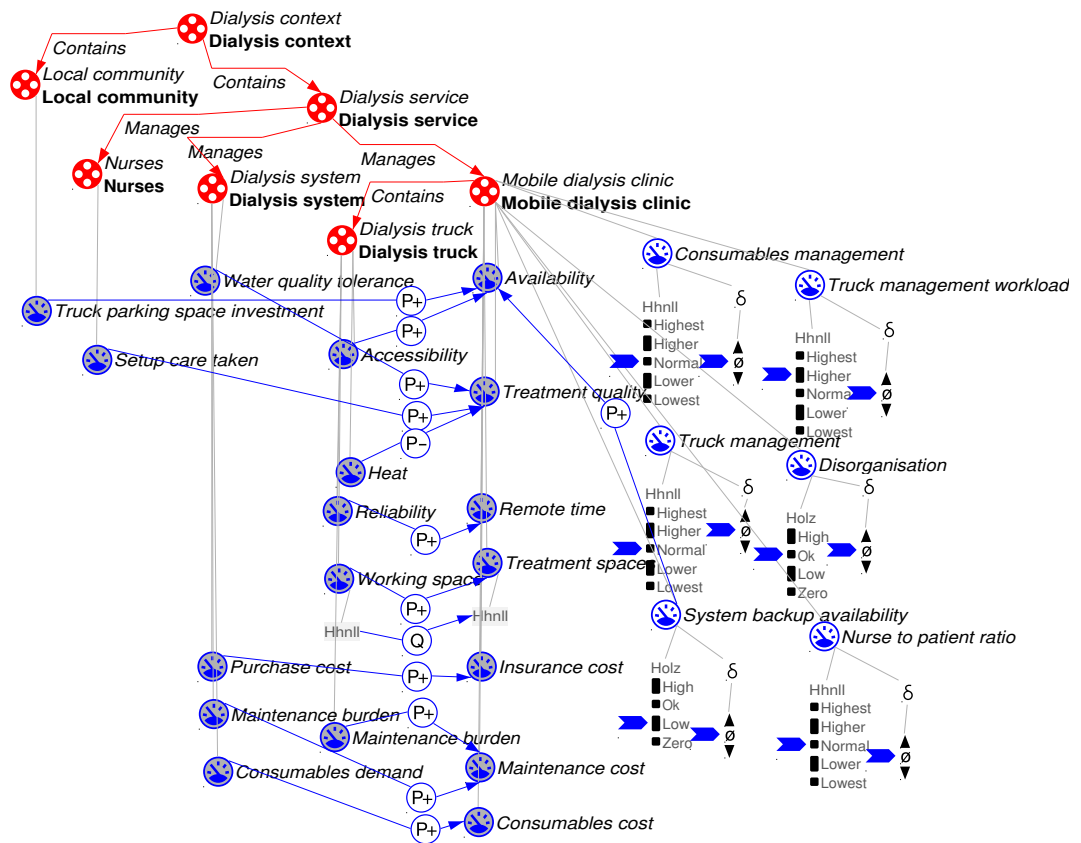


Figure G.0.10.: Mobile dialysis clinic *Garp3* model fragment

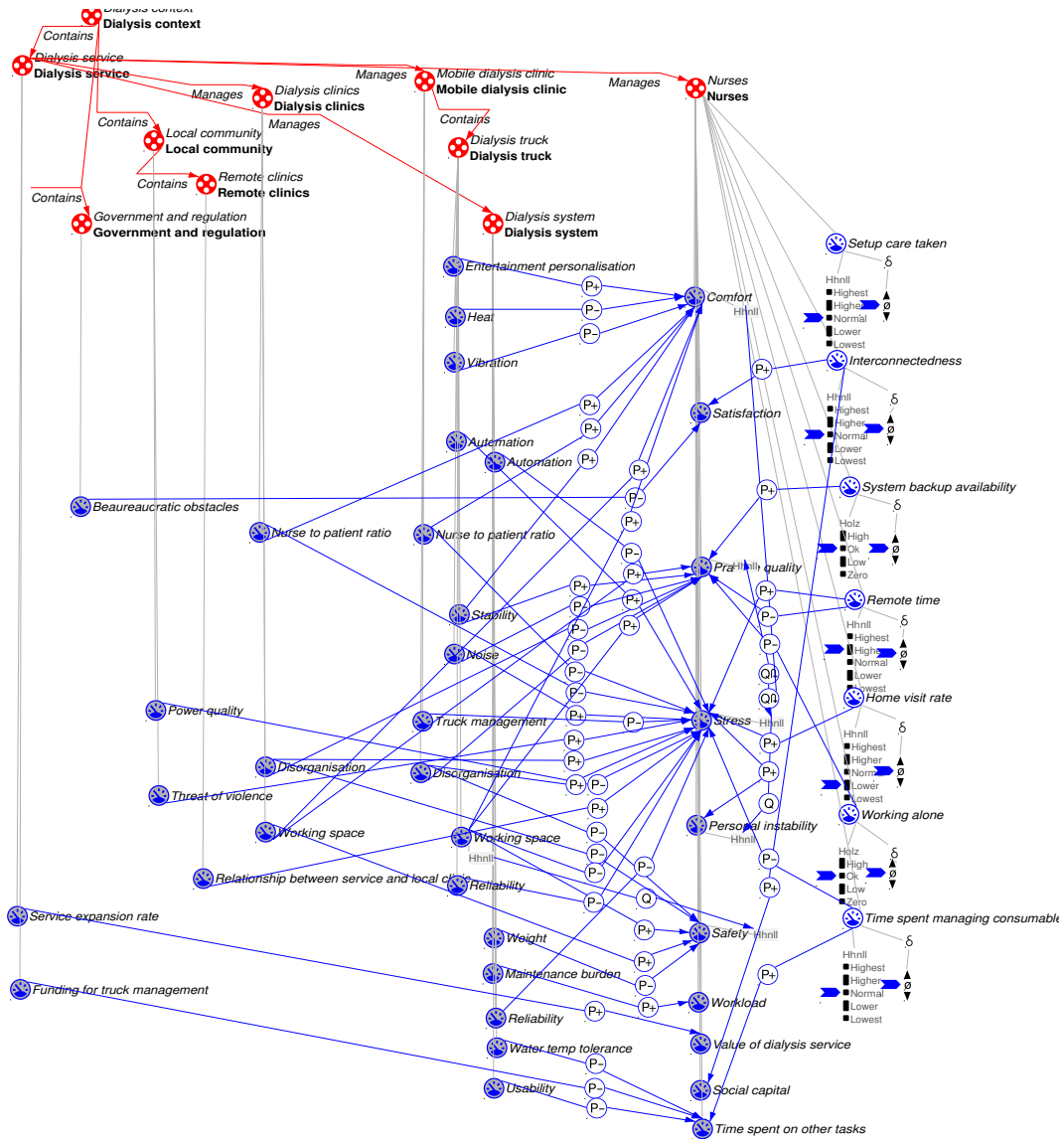


Figure G.0.11.: Nurses *Garp3* model fragment

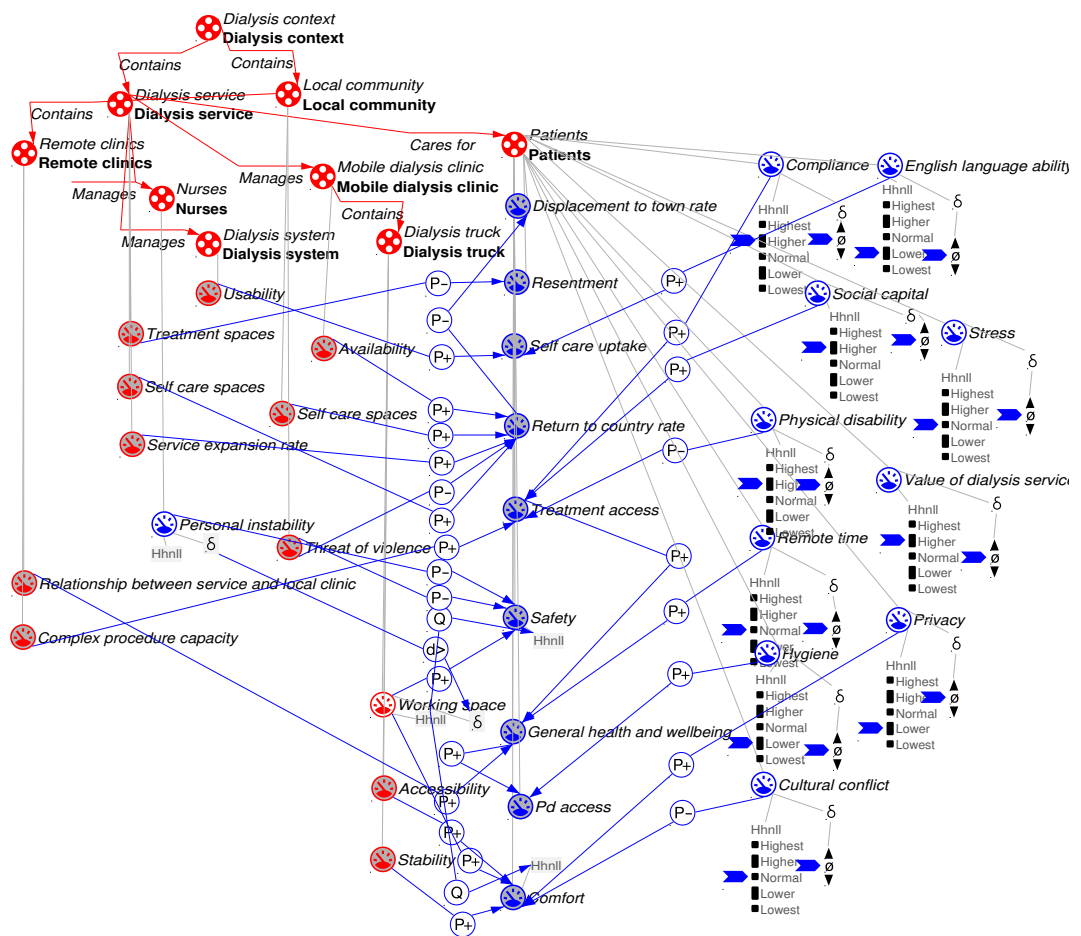


Figure G.0.12.: Patients Garp3 model fragment

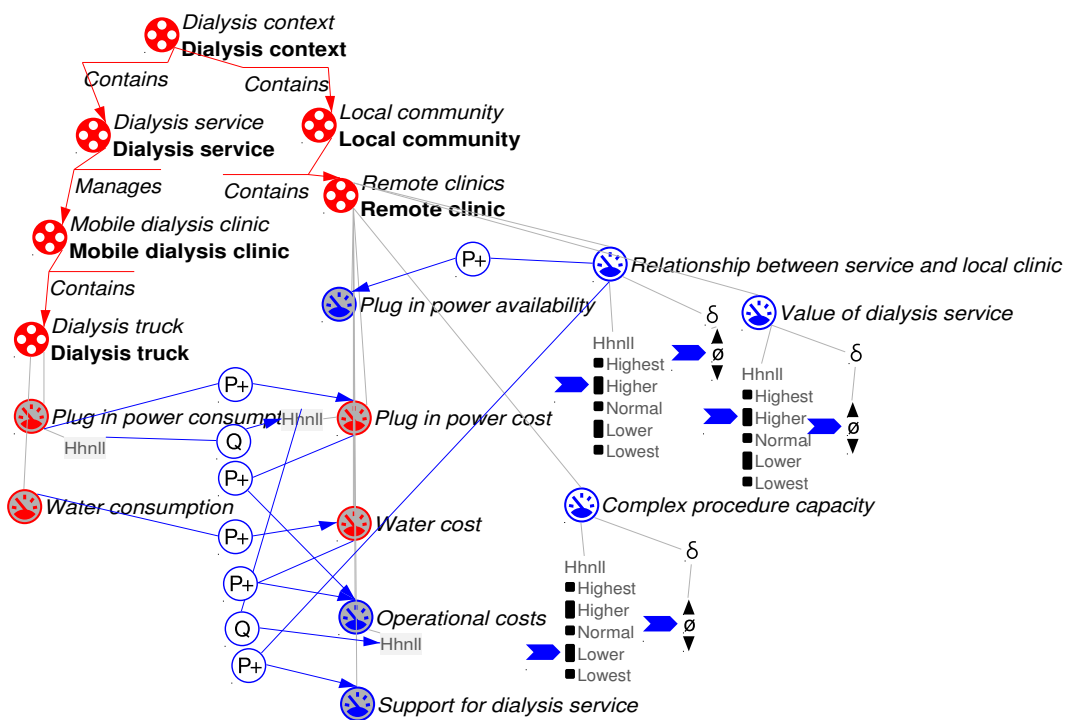


Figure G.0.13.: Remote clinic Garp3 model fragment

References

- Achilli, A., Cath, T., and Childress, A. (2009). Power generation with pressure retarded osmosis: An experimental and theoretical investigation. *Journal of Membrane Science*, 343(1):42–52.
- Adolph, S., Hall, W., and Kruchten, P. (2008). A methodological leg to stand on: lessons learned using grounded theory to study software development. In *Proceedings of the 2008 conference of the center for advanced studies on collaborative research: meeting of minds*, page 13. ACM.
- Adolph, S., Hall, W., and Kruchten, P. (2011). Using grounded theory to study the experience of software development. *Empirical Software Engineering*, 16(4):487–513.
- Anderson, J., Perry, J., Blue, C., Browne, A., Henderson, A., Khan, K. B., Kirkham, S. R., Lynam, J., Semeniuk, P., and Smye, V. (2003). "rewriting" cultural safety within the postcolonial and postnational feminist project: Toward new epistemologies of healing. *Advances in Nursing Science*, 26(3):196–214.
- Arias, M. F. C., Rico, D. P., Galvañ, P. V., et al. (2011). Kinetic behaviour of sodium and boron in brackish water membranes. *Journal of Membrane Science*, 368(1):86–94.
- Ball, L. and Ormerod, T. (2000a). Applying ethnography in the analysis and support of expertise in engineering design. *Design Studies*, 21(4):403–421.
- Ball, L. and Ormerod, T. (2000b). Putting ethnography to work: the case for a cognitive ethnography of design. *International Journal of Human-Computer Studies*, 53(1):147–168.
- Bartolomei, J. (2007). Qualitative knowledge construction for engineering systems: extending the design structure matrix methodology in scope and procedure. Technical report, DTIC Document.
- Baskerville, R. L. and Myers, M. D. (2015). Design ethnography in information systems. *Information Systems Journal*, 25(1):23–46.
- Baum, F. et al. (2008). *The new public health*. Number Ed. 3. Oxford University Press.
- Baxter, G. and Sommerville, I. (2011). Socio-technical systems: From design methods to systems engineering. *Interacting with Computers*, 23(1):4–17.

- Belkacem, M., Bekhti, S., and Bensadok, K. (2007). Groundwater treatment by reverse osmosis. *Desalination*, 206:100–106.
- Beyer, H. and Holtzblatt, K. (1999). Contextual design. *interactions*, 6(1):32–42.
- Blizzard, J. L. and Klotz, L. E. (2012). A framework for sustainable whole systems design. *Design Studies*, 33(5):456–479.
- Bobrow, D. (1984). Qualitative reasoning about physical systems: An introduction. *Artificial intelligence*, 24(1-3):1–5.
- Bouwer, A. and Bredeweg, B. (2010). Graphical means for inspecting qualitative models of system behaviour. *Instructional science*, 38(2):173–208.
- Bredeweg, B., Linnebank, F., Bouwer, A., and Liem, J. (2009). Garp3: Workbench for qualitative modelling and simulation. *Ecological informatics*, 4(5):263–281.
- Brown, K. (2001). Water use assessment for a remote indigenous community. Technical report, National Centre for Epidemiology and Population Health.
- Brown, S. (2011). History of the western desert dialysis project. Online. Accessed 19/20/2011.
- Cady, R. G. (2012). *Measuring the Impact of Technology on Nurse Workflow: A Mixed Methods Approach*. PhD thesis, UNIVERSITY OF MINNESOTA.
- Cady, R. G. and Finkelstein, S. M. (2013). Mixed-methods approach for measuring the impact of video telehealth on outpatient clinic triage nurse workflow. *Computers Informatics Nursing*, 31(9):439–449.
- Cao, D., Qin, S., and Liu, Y.-S. (2013). *Advances in Conceptual Design Theories, Methodologies, and Applications*. Hindawi Publishing Corporation, New York.
- Carayon, P. (2006). Human factors of complex sociotechnical systems. *Applied Ergonomics*, 37(4):525–535.
- Cath, T., Childress, A., and Elimelech, M. (2006). Forward osmosis: Principles, applications, and recent developments. *Journal of Membrane Science*, 281(1):70–87.
- Charnley, F., Lemon, M., and Evans, S. (2011). Exploring the process of whole system design. *Design Studies*, 32(2):156–179.
- Chung, T.-S., Li, X., Ong, R. C., Ge, Q., Wang, H., and Han, G. (2012a). Emerging forward osmosis (fo) technologies and challenges ahead for clean water and clean energy applications. *Current Opinion in Chemical Engineering*, 1(3):246–257.
- Chung, T.-S., Zhang, S., Wang, K. Y., Su, J., and Ling, M. M. (2012b). Forward osmosis processes: yesterday, today and tomorrow. *Desalination*, 287:78–81.
- Coleman, G. and O'Connor, R. (2007). Using grounded theory to understand software process improvement: A study of irish software product companies. *Information and Software Technology*, 49(6):654–667.

References

- Corbin, J. M. and Strauss, A. (1990). Grounded theory research: Procedures, canons, and evaluative criteria. *Qualitative sociology*, 13(1):3–21.
- Council, N. L. (2013). Northern land council research/survey permit application. <http://www.nlc.org.au/files/various/NLCMedia-Research-SurveyApplication.pdf>. Accessed 27/01/2015.
- Cresswell, R., Wischusen, J., Jacobson, G., and Fifield, K. (1999). Assessment of recharge to groundwater systems in the arid southwestern part of northern territory, australia, using chlorine-36. *Hydrogeology Journal*, 7(4):393–404.
- Dawoud, M. (2005). The role of desalination in augmentation of water supply in gcc countries. *Desalination*, 186(1):187–198.
- Dawson, R., Bones, P., Oates, B., Brereton, P., Azuma, M., and Jackson, M. (2003). Empirical methodologies in software engineering. In *Software Technology and Engineering Practice, 2003. Eleventh Annual International Workshop on*, pages 52–58. IEEE.
- Dell’Era, C. and Landoni, P. (2014). Living lab: A methodology between user-centred design and participatory design. *Creativity and Innovation Management*, 23(2):137–154.
- Devitt, J. and McMasters, A. (1998). *Living on Medicine: A Cultural Study of End-Stage Renal Disease Among Aboriginal People*. IAD Press.
- Dolnicar, S. and Schäfer, A. (2009). Desalinated versus recycled water: Public perceptions and profiles of the accepters. *Journal of Environmental Management*, 90(2):888–900.
- Dym, C., Agogino, A., Eris, O., Frey, D., and Leifer, L. (2005). Engineering design thinking, teaching, and learning.
- Ebner, M., Stalph, P., Michel, M., and Benz, R. (2010). Evolutionary parameter optimization of a fuzzy controller which is used to control a sewage treatment plant.
- Ehn, P. (1998). Manifesto for a digital bauhaus 1. *Digital Creativity*, 9(4):207–217.
- Eldridge, P. (2006). *Module 1 – Basics of Water*. Fresenius Medical Care, 17/61 Lavender Street Milsons Point NSW 2061 (02) 9466 8000.
- Epperson, J. (2002). *An Introduction to Numerical Methods and Analysis*. John Wiley & Sons, New York, first edition.
- Ettori, A., Gaudichet-Maurin, E., Schrotter, J.-C., Aimar, P., and Causserand, C. (2011). Permeability and chemical analysis of aromatic polyamide based membranes exposed to sodium hypochlorite. *Journal of Membrane Science*, 375(1):220–230.
- Farrington, K. and Greenwood, R. (2011). Home haemodialysis: trends in technology. *NDT plus*, 4(suppl 3):iii23–iii24.

- Fortnum, D., Mathew, T., and Johnson, K. (2012). A model for home dialysis - australia 2012. *Kidney Health Australia* www.homedialysis.org.au/publications.
- Fredericks, B. (2008). Making an impact researching with australian aboriginal and torres strait islander peoples. *Studies in Learning, Evaluation, Innovation and Development*, 5(1):24–35.
- Fresenius (2007). *4008 S Haemodialysis Machine Operating Instructions*. Fresenius Medical Care, AG.
- Fresenius (2014). Concentrated haemodialysis solution ac-f 1135-g part a, 5 litres. Medical product labelling. Ref 750 2883 801.
- Ge, Q., Ling, M., and Chung, T.-S. (2013). Draw solutions for forward osmosis processes: developments, challenges, and prospects for the future. *Journal of Membrane Science*, 442:225–237.
- Genco, N., Johnson, D., Holtta-Otto, K., and Seepersad, C. C. (2011). A study of the effectiveness of empathic experience design as a creativity technique. In *ASME 2011 International Design Engineering Technical Conferences and Computers and Information in Engineering Conference*, pages 131–139. American Society of Mechanical Engineers.
- Gray, M. and McPherson, K. (2005). Cultural safety and professional practice in occupational therapy: A new zealand perspective. *Australian Occupational Therapy Journal*, 52(1):34–42.
- Green, G., Kennedy, P., and McGown, A. (2002). Management of multi-method engineering design research: a case study. *Journal of Engineering and Technology Management*, 19(2):131–140.
- Gruber, M., Johnson, C., Tang, C., Jensen, M. H., Yde, L., and Hélix-Nielsen, C. (2011). Computational fluid dynamics simulations of flow and concentration polarization in forward osmosis membrane systems. *Journal of Membrane Science*, 379(1):488–495.
- Gu, B., Kim, D., Kim, J., and Yang, D. (2011). Mathematical model of flat sheet membrane modules for fo process: Plate-and-frame module and spiral-wound module. *Journal of Membrane Science*, 379(1):403–415.
- Han, G., Zhang, S., Li, X., and Chung, T.-S. (2015). Progress in pressure retarded osmosis (pro) membranes for osmotic power generation. *Progress in Polymer Science*, 51:1–27.
- Hempe, E., Dickerson, T., Holland, A., and Clarkson, P. (2010). Framework for design research in health and care services. *Exploring Services Science*, pages 125–135.
- Henderson, R. and Abrahams, J. (2010). Community water conservation program guide. Online, Live & Learn Environmental Education 18 Warburton St PO Box 2796 Alice Springs, 0871 Northern Territory, Australia. PowerWater information sheet.

References

- Holloway, R. W., Maltos, R., Vanneste, J., and Cath, T. Y. (2015). Mixed draw solutions for improved forward osmosis performance. *Journal of Membrane Science*, 491:121–131.
- HTI (2014). Hydration technology innovations. Website. <http://www.htiwater.com/>; Accessed 25/09/2014.
- Hughes, J., King, V., Rodden, T., and Andersen, H. (1994). Moving out from the control room: Ethnography in system design. In *Proceedings of the 1994 ACM conference on Computer supported cooperative work*, pages 429–439. ACM.
- Hydranautics (2011). Espa1-4040 reverse osmosis membrane element technical sheet. Technical report, Hydranautics - Nitto Denko.
- Jacana (2014). Energy tariffs. PDF, online. <https://www.powerwater.com.au/>; Accessed 25/09/2014.
- Johnstone, M. and Kanitsaki, O. (2007). An exploration of the notion and nature of the construct of cultural safety and its applicability to the Australian health care context. *Journal of transcultural nursing*, 18(3):247–256.
- Jung, D. H., Lee, J., Kim, D. Y., Lee, Y. G., Park, M., Lee, S., Yang, D. R., and Kim, J. H. (2011). Simulation of forward osmosis membrane process: Effect of membrane orientation and flow direction of feed and draw solutions. *Desalination*, 277(1):83–91.
- Kansou, K., Nuttle, T., Farnsworth, K., and Bredeweg, B. (2013). How plants changed the world: Using qualitative reasoning to explain plant macroevolution's effect on the long-term carbon cycle. *Ecological Informatics*, 17:117–142.
- Kaplan, B. and Duchon, D. (1988). Combining qualitative and quantitative methods in information systems research: a case study. *MIS quarterly*, pages 571–586.
- Karlberg, M., Löfstrand, M., Sandberg, S., and Lundin, M. (2013). State of the art in simulation-driven design. *International Journal of Product Development*, 18(1):68–87.
- Kim, Y. C. and Park, S.-J. (2011). Experimental study of a 4040 spiral-wound forward-osmosis membrane module. *Environmental science & technology*, 45(18):7737–7745.
- Klaysom, C., Cath, T. Y., Depuydt, T., and Vankelecom, I. F. (2013). Forward and pressure retarded osmosis: potential solutions for global challenges in energy and water supply. *Chemical Society Reviews*, 42(16):6959–6989.
- Kooshanfar, H. (2014). Control of dialysate production for remote areas. Master's thesis, School of Computer Science, Engineering, and Mathematics. Under consideration as at November 2014.
- Koro-Ljungberg, M. and Douglas, E. (2008). State of qualitative research in engineering education: Meta-analysis of jee articles, 2005–2006. *Journal of Engineering Education*, 97(2):163.

- Kotabe, M., Parente, R., and Murray, J. (2007). Antecedents and outcomes of modular production in the Brazilian automobile industry: a grounded theory approach. *Journal of International Business Studies*, 38(1):84–106.
- Kovacic, Z. and Bogdan, S. (2005). *Fuzzy controller design: theory and applications*. CRC press.
- Kowal, E. (2006). *The proximate advocate: improving indigenous health on the post-colonial frontier*. PhD thesis, The University of Melbourne.
- Lay, W. C., Zhang, J., Tang, C., Wang, R., Liu, Y., and Fane, A. G. (2012). Factors affecting flux performance of forward osmosis systems. *Journal of Membrane Science*, 394:151–168.
- Lee, K. P., Arnot, T. C., and Mattia, D. (2011). A review of reverse osmosis membrane materials for desalination – development to date and future potential. *Journal of Membrane Science*, 370(1):1–22.
- Levy, J., Brown, E., Daley, C., and Lawrence, A. (2009). *Oxford handbook of dialysis*. Oxford University Press.
- Leys, M. (2003). Health technology assessment: the contribution of qualitative research. *International journal of technology assessment in health care*, 19(02):317–329.
- Li, D., Zhang, X., Simon, G. P., and Wang, H. (2013a). Forward osmosis desalination using polymer hydrogels as a draw agent: Influence of draw agent, feed solution and membrane on process performance. *Water research*, 47(1):209–215.
- Li, K., Yi, Z.-Z., Xu, W., Zhao, K., and Wang, L. (2013b). Research on sdg-based qualitative reasoning in conceptual design. *Advances in Mechanical Engineering*, 2013.
- Liker, J., Haddad, C., and Karlin, J. (1999). Perspectives on technology and work organization. *Annual Review of Sociology*, pages 575–596.
- Loeb, S., Titelman, L., Korngold, E., and Freiman, J. (1997). Effect of porous support fabric on osmosis through a loeb-sourirajan type asymmetric membrane. *Journal of Membrane Science*, 129(2):243–249.
- Loney, H. (2000). Society and technological control: a critical review of models of technological change in ceramic studies. *American Antiquity*, pages 646–668.
- Love, T. (1998). Social, environmental and ethical factors in engineering design theory: a post positivist approach. *Praxis Education, Perth, Western Australia*.
- Lutchmiah, K., Verliefde, A., Roest, K., Rietveld, L. C., and Cornelissen, E. R. (2014). Forward osmosis for application in wastewater treatment: a review. *Water research*, 58:179–197.
- Lynch, C. T., editor (1974). *Handbook of Materials Science; General Properties*, volume I. CRC Press Inc, Cleveland, Ohio.

References

- MacLean, A., Young, R., Bellotti, V., and Moran, T. (1991). Questions, options, and criteria: Elements of design space analysis. *Human-computer interaction*, 6(3-4):201–250.
- Mamdani, E. H. and Assilian, S. (1975). An experiment in linguistic synthesis with a fuzzy logic controller. *International journal of man-machine studies*, 7(1):1–13.
- Marshall, J. M., Mahamoudou, T., Mohamed, T., Shannon, F., and Charles, T. (2010). Perspectives of people in mali toward genetically-modified mosquitoes for malaria control. *Malaria Journal*, 9.
- Martin, J., Murphy, E., Crowe, J., and Norris, B. (2006). Capturing user requirements in medical device development: the role of ergonomics. *Physiological measurement*, 27:R49.
- Martínez, A., Villarroel, V., Seoane, J., and Del Pozo, F. (2005). Analysis of information and communication needs in rural primary health care in developing countries. *IEEE Transactions on Information Technology in Biomedicine*, 9(1):66–72.
- Masse, L., Masse, D., Pellerin, Y., and Dubreuil, J. (2010). Osmotic pressure and substrate resistance during the concentration of manure nutrients by reverse osmosis membranes. *Journal of Membrane Science*, 348:28–33.
- McCutcheon, J. R. and Elimelech, M. (2007). Modeling water flux in forward osmosis: implications for improved membrane design. *AIChE Journal*, 53(7):1736–1744.
- Neuenschwander, E. (2013). Qualitas and quantitas: two ways of thinking in science. *Quality & Quantity*, 47(5):2597–2615.
- NHMRC (2003). *Values and ethics: Guidelines for ethical conduct in Aboriginal and Torres Strait Islander health research*. The Commonwealth of Australia.
- Oates, B., Griffiths, G., Lockyer, M., and Hebborn, B. (2004). Empirical methodologies for web engineering. *Web Engineering*, pages 769–769.
- Ogilvie, L., Burgess-Pinto, E., and Caufield, C. (2008). Challenges and approaches to newcomer health research. *Journal of Transcultural Nursing*, 19(1):64–73.
- Oh, Y., Lee, S., Elimelech, M., Lee, S., and Hong, S. (2014). Effect of hydraulic pressure and membrane orientation on water flux and reverse solute flux in pressure assisted osmosis. *Journal of Membrane Science*, 465:159–166.
- Orlikowski, W. and Barley, S. (2001). Technology and institutions: what can research on information technology and research on organizations learn from each other? *MIS quarterly*, 25(2):145–165.
- Ovaska, P. and Stapleton, L. (2009). Requirements engineering during complex isd: A sensemaking approach. *Information Systems Development*, pages 195–209.
- Papps, E. and Ramsden, I. (1996). Cultural safety in nursing: The new zealand experience. *International Journal for Quality in Health Care*, 8(5):491–497.

- Park, M., Lee, J. J., Lee, S., and Kim, J. H. (2011). Determination of a constant membrane structure parameter in forward osmosis processes. *Journal of Membrane Science*, 375(1):241–248.
- Parr, E. A. (1998). *Industrial control handbook*. Industrial Press Inc.
- Parush, A., Kramer, C., Foster-Hunt, T., McMullan, A., and Momtahan, K. (2014). Exploring similarities and differences in teamwork across diverse healthcare contexts using communication analysis. *Cognition, technology & work*, 16(1):47–57.
- Passino, K. M., Yurkovich, S., and Reinfrank, M. (1998). *Fuzzy control*, volume 42. Citeseer.
- Patel, V. and Kushniruk, A. (1998). Interface design for health care environments: the role of cognitive science. In *Proceedings of the AMIA Symposium*, page 29. American Medical Informatics Association.
- Pearce, M., Willis, E., Wadham, B., and Binks, B. (2010). Attitudes to drought in outback communities in south australia. *Geographical Research*, 48(4):359–369.
- Phuntsho, S., Lotfi, F., Hong, S., Shaffer, D. L., Elimelech, M., and Shon, H. K. (2014). Membrane scaling and flux decline during fertiliser-drawn forward osmosis desalination of brackish groundwater. *Water research*, 57:172–182.
- Phuntsho, S., Vigneswaran, S., Kandasamy, J., Hong, S., Lee, S., and Shon, H. K. (2012). Influence of temperature and temperature difference in the performance of forward osmosis desalination process. *Journal of Membrane Science*, 415:734–744.
- Pilemalm, S., Lindell, P.-O., Hallberg, N., and Eriksson, H. (2007). Integrating the rational unified process and participatory design for development of socio-technical systems: a user participative approach. *Design Studies*, 28(3):263–288.
- Pilemalm, S. and Timpka, T. (2008). Third generation participatory design in health informatics-making user participation applicable to large-scale information system projects. *Journal of biomedical informatics*, 41(2):327–339.
- Pislor, E., Alignan, M., Pontalier, P.-Y., and Grange, S. (2011). Haemodialysis water production by double revers osmosis. *Desalination*, 267:88–92.
- Popovici, I., Morita, P. P., Doran, D., Lapinsky, S., Morra, D., Shier, A., Wu, R., and Cafazzo, J. A. (2015). Technological aspects of hospital communication challenges: an observational study. *International Journal for Quality in Health Care*, page mzv016.
- Porifera (2014). Website. <http://porifera.com/>; Accessed 25/09/2014.
- PowerWater (2009a). Indigenous communities of the northern territory drinking water quality annual report. online. PowerWater information sheet.
- PowerWater (2009b). Indigenous communities power, water supply and sewerage services. online. PowerWater information sheet.

References

- PowerWater (2009c). Sustainable water management report. online. PowerWater information sheet.
- PowerWater (2011). Water tariffs. online. PowerWater information sheet.
- Qin, J.-J., Liberman, B., and Kekre, K. A. (2009). Direct osmosis for reverse osmosis fouling control: principles, applications and recent developments. *The Open Chemical Engineering Journal*, 3(1):8–16.
- Rajkomar, A. and Blandford, A. (2012). Understanding infusion administration in the icu through distributed cognition. *Journal of biomedical informatics*, 45(3):580–590.
- Ramon, G., Agnon, Y., and Dosoretz, C. (2010). Dynamics of an osmotic backwash cycle. *Journal of Membrane Science*, 364(1):157–166.
- Redström, J. (2006). Towards user design? on the shift from object to user as the subject of design. *Design studies*, 27(2):123–139.
- Richter, K., Weber, B., Bojduj, B., and Bertel, S. (2010). Supporting the designer's and the user's perspectives in computer-aided architectural design. *Advanced Engineering Informatics*, 24(2):180–187.
- SA Water (2013). Drinking water quality report 2012-13.
- Sagiv, A., Avraham, N., Dosoretz, C. G., and Semiat, R. (2008). Osmotic backwash mechanism of reverse osmosis membranes. *Journal of Membrane Science*, 322(1):225–233.
- Sagiv, A. and Semiat, R. (2005). Backwash of ro spiral wound membranes. *Desalination*, 179(1):1–9.
- Sagiv, A. and Semiat, R. (2010). Parameters affecting backwash variables of ro membranes. *Desalination*, 261(3):347–353.
- Sagiv, A. and Semiat, R. (2011). Finite element analysis of forward osmosis process using nacl solutions. *Journal of Membrane Science*, 379(1):86–96.
- Samaras, G. and Horst, R. (2005). A systems engineering perspective on the human-centered design of health information systems. *Journal of Biomedical Informatics*, 38(1):61–74.
- Schultz, C., Amor, R., Lobb, B., and Guesgen, H. (2009). Qualitative design support for engineering and architecture. *Advanced Engineering Informatics*, 23(1):68–80.
- Shaffer, D. L., Werber, J. R., Jaramillo, H., Lin, S., and Elimelech, M. (2015). Forward osmosis: Where are we now? *Desalination*, 356:271–284.
- Takagi, T. and Sugeno, M. (1983). Derivation of fuzzy control rules from human operator's control actions. In *Proceedings of the IFAC symposium on fuzzy information, knowledge representation and decision analysis*, volume 6, pages 55–60.

- Talaat, K. (2009). Forward osmosis process for dialysis fluid regeneration. *Artificial Organs*, 33(12):1133–1135.
- Talaat, K. et al. (2010). Dialysis fluid regeneration by forward osmosis: A feasible option for ambulatory dialysis systems. *Saudi Journal of Kidney Diseases and Transplantation*, 21(4):748.
- Tan, C. H. and Ng, H. Y. (2008). Modified models to predict flux behavior in forward osmosis in consideration of external and internal concentration polarizations. *Journal of Membrane science*, 324(1):209–219.
- Tan, C. H. and Ng, H. Y. (2013). Revised external and internal concentration polarization models to improve flux prediction in forward osmosis process. *Desalination*, 309:125–140.
- Tan, K. K., Wang, Q.-G., Hang, C. C., and Hägglund, T. J. (1999). *Advances in PID control*. Springer London.
- Thompson, A. (2004). Gentlemanly orthodoxy: Critical race feminism, whiteness theory, and the apa manual. *Educational Theory*, 54(1):27–57.
- Tiraferri, A., Yin Yip, N., Straub, A. P., Romero-Vargas Castrillon, S., and Elimelech, M. (2013). A method for the simultaneous determination of transport and structural parameters of forward osmosis membranes. *Journal of Membrane Science*.
- Tyldesley, D. (1988). Employing usability engineering in the development of office products. *The Computer Journal*, 31(5):431–436.
- Wang, L.-X. (1997). *A Course in Fuzzy Systems and Control*. Prentice-Hall, Inc.
- Werner, C. M., Logan, B. E., Saikaly, P. E., and Amy, G. L. (2013). Wastewater treatment, energy recovery and desalination using a forward osmosis membrane in an air-cathode microbial osmotic fuel cell. *Journal of Membrane Science*, 428:116–122.
- Werner, M. and Schafer, A. (2007). Social aspects of a solar-powered desalination unit for remote Australian communities. *Desalination*, 203:375–393.
- WHO (2005). *Declaration of Alma-Ata, 1978*. World Health Organization. Regional Office for Europe.
- Wilcox, S. (2012). Commentary: Ethnographic field research for medical-device design. *Biomedical Instrumentation & Technology*, 46(2):117–121.
- Wiltgen, B. and Goel, A. K. (2015). Evaluating design concepts through functional model simulation. In *Proceedings of the Third Annual Conference on Advances in Cognitive Systems ACS*, page 21.
- Wisner, B. (1988). Gobi versus phc? some dangers of selective primary health care. *Social Science & Medicine*, 26(9):963–969.

References

- Wotherspoon, R. (2001). *Janus: the multiple faces of engineering design*. PhD thesis, Department of Management-Faculty of Commerce, University of Wollongong.
- Wriggers, P., Kultsova, M., Kapysh, A., Kultsov, A., and Zhukova, I. (2014). Intelligent decision support system for river floodplain management. In *Knowledge-Based Software Engineering*, pages 195–213. Springer.
- Xiao, D., Tang, C. Y., Zhang, J., Lay, W. C., Wang, R., and Fane, A. G. (2011). Modeling salt accumulation in osmotic membrane bioreactors: Implications for membrane selection and system operation. *Journal of Membrane Science*, 366(1):314–324.
- Yao, L., Liu, J., Wang, R., Yin, K., and Han, B. (2015). A qualitative network model for understanding regional metabolism in the context of social–economic–natural complex ecosystem theory. *Ecological Informatics*, 26:29–34.
- You, S.-J., Wang, X.-H., Zhong, M., Zhong, Y.-J., Yu, C., and Ren, N.-Q. (2012). Temperature as a factor affecting transmembrane water flux in forward osmosis: Steady-state modeling and experimental validation. *Chemical Engineering Journal*, 198:52–60.
- Zhao, S., Zou, L., Tang, C., and Mulcahy, D. (2012). Recent developments in forward osmosis: Opportunities and challenges. *Journal of Membrane Science*, 396:1–21.